A Study of the Physical Chemistry of Acyl Radicals - Formation and Reactions

By Ruth Amos

Submitted in fulfilment of the Requirements of the Degree of Doctor of Philosophy

University of Tasmania

November 2010

Declaration

This thesis contains no material which has been accepted for a degree or diploma by the University or any other institution, except by way of background information and duly acknowledged in the thesis, and to the best of the candidate's knowledge and belief no material previously published or written by another person except where due acknowledgement is made in the text of the thesis, nor does the thesis contain any material that infringes copyright.

Signed

Ruth Amos

Copyright Declaration

Publications

This is to certify that Ruth Amos was the major contributor for the publications related to this thesis.

Signed

Dr Jason Smith

Statement of ethical conduct

The research associated with this thesis abides by the international and Australian codes on human and animal experimentation, the guidelines by the Australian Government's Office of the Gene Technology Regulator and the rulings of the Safety, Ethics and Institutional Biosafety Committees of the University.

Signed

Ruth Amos

List of publications arising from this thesis

Amos, R. I. J.; Gourlay, B. S.; Schiesser, C. H.; Smith, J. A.; Yates, B. F., A mechanistic study on the oxidation of hydrazides: application to the tuberculosis drug isoniazid. *Chemical Communications* **2008**, (14), 1695-1697.

Amos, R. I. J.; Schiesser, C. H.; Smith, J. A.; Yates, B. F., Nucleophilic Acyl Substitution of Acyl Diimides. *Journal of Organic Chemistry* **2009,** 74, (15), 5707-5710.

Amos, R. I. J.; Smith, J. A.; Yates, B. F.; Schiesser, C. H., Acyl radical addition to pyridine: multiorbital interactions. *Tetrahedron* **2009,** 65, (36), 7653-7657.

Amos, R. I. J.; Smith, J. A.; Yates, B. F.; Schiesser, C. H., Acyl radical addition to benzene and related systems – a computational study. *Tetrahedron* **2010,** 66, (38), 7600-7604.

Abstract

Aryl hydrazides (including isoniazid - an antibiotic used for the treatment of Tuberculosis) are oxidized to acyl radicals through a mechanism involving diimide intermediates that are prone to nucleophilic acyl substitution. This oxidation occurs regardless of the oxidant involved; however the radical formed does not undergo further oxidation to the corresponding acylium ion, even in the presence of strong oxidants. This mechanistic information adds to the knowledge base providing clarification of conflicting mechanistic information present within the literature. It also provides potential insight into isoniazid resistance in *Mycobacterium tuberculosis*.

Through DFT calculations the nucleophilic acyl substitution of the diimide intermediate formed by the oxidation of isoniazid (and other aryl hydrazides) was found to most likely involve two methanol molecules in a six membered cyclic transition state. Calculations were performed in the gas phase and solvation effects were included both explicitly and implicitly using CPCM. These results reflected those found in the experimental oxidation of isoniazid.

The addition of an acetyl radical at the various positions in both pyridine and the pyridinium ion has been investigated computationally using DFT calculations. The energy barrier for attack at the nitrogen atom in pyridine is calculated to be lower than for the analogous attack at any other atom in pyridine, or at any position in the pyridinium ion. Simultaneous SOMO $\rightarrow \pi^*$, $LP_N \rightarrow$ SOMO and $LP_N \rightarrow \pi^*_{c=o}$ interactions are responsible for this preference.

The addition of an acetyl radical to benzene, aniline, trifluorobenzene and naphthalene has also been investigated computationally using DFT calculations. Addition to benzene is

calculated to have an energy barrier which is similar to that for attack at a carbon in pyridine but higher than for the attack at the nitrogen in pyridine. This difference is due to the involvement of the nitrogen lone pair in the latter process. In the case of benzene, this reaction is associated with simultaneous SOMO → π* and π → SOMO interactions with the latter interaction dominating, suggesting that acetyl radicals react predominantly as electrophilic radicals in the interaction with benzene.

An investigation of the McFadyen-Stevens rearrangement was performed as this rearrangment was proposed to occur through the same intermediate as the oxidation of hydrazides. The proposed mechanism for this conversion from an arylsulfonylhydrazide to an aldehyde upon reflux in alkaline solution, was found to be implausible and a more reasonable radical mechanism is proposed. The results are inconclusive; however a radical mechanism is certainly at play when the reaction is performed under oxidative conditions.

Acknowledgements

First and foremost I wish to thank my Father God, to You belongs all the glory, You have taught me so much during this time and I am eternally grateful.

Secondly I want to thank Moz for all his support. Moz, so many times on this journey I needed to know that I would still be loved even if I failed and you have provided that unconditional love to me. Thanks so much for all the support you have given me.

To my amazing supervisors, Jason, Carl and Brian, wow, what can I say? What a team! You have taught me so much and put up with so much and provided so many amazing experiences, I am so grateful for your willingness to input into my life. I feel incredibly fortunate to have such an amazing team of supervisors.

To my children, Jess and Caleb, I want to say thanks for allowing your mother to chase her dream. I hope my experience inspires you to chase your own dreams. You guys are gold!

Thanks to the wider family, Mum (Roslyn) and Dad (John), Nigel and Annette, Anthony, Catherine, Paul and Chloe, Allan, Adrian, Lilly, Georgia, Jordan and Amy. You keep me grounded and show me love. Thank you.

Special thanks to Nigel Brookes and Pete Molesworth for your advice, insight, proofreading and friendship in the office and lab, and to Jess and Dess for Monday lunchtimes.

On the research front I would like to thank Michelle Coote and Trevor Lewis for helpful discussions about redox potentials, David Brittain for help with the calculations for the McFadyen Stevens work, and Mark Taylor for his help with Eckart corrections.

Three and a half years is a long time and there have been so many who have been inspirational in my life in this time. I would really love to name everyone personally and I am sure I would forget some really important people, so, you are all included! I just want to say THANKS!

Contents

Chapter 1.

Introduction and review

1.1 Thesis aims and outline

This thesis covers research into the mode of activation of isoniazid, a frontline antibiotic for the treatment of tuberculosis (TB). Isoniazid is the hydrazide of isonicotinic acid and its activation involves oxidation of the hydrazide moiety to form an acyl radical through a diimide intermediate. Determination of the formation of the acyl radicals involved in the activation of isoniazid led to a thorough investigation of the McFadyen-Stevens rearrangement which was reported to involve a diimide intermediate and had a potential acyl radical intermediate.

The aims of this thesis include:

- A determination of the mechanism of oxidation of isoniazid in particular and aromatic hydrazides in general
- A computational investigation into the nucleophilic acyl substitution pathway available to oxidised hydrazides
- A computational study into the reactivity of acyl radicals with aromatic systems
- An experimental and computational investigation into the mechanism of the McFadyen-Stevens rearrangement

In Chapter 2 the mechanism of oxidation of hydrazides is discussed to probe the formation of acyl radicals and other reactions that can occur in the process of oxidation. A Hammett plot is constructed to look at the differing effect of functional groups on the aromatic ring on mechanistic pathways.

Chapter 3 details a computational study into the nucleophilic acyl substitution of the diimide intermediate formed by the oxidation of hydrazides. This is an intervening pathway that hinders the formation of an acyl radical from the oxidation of aryl hydrazides.

Once the presence of an acyl radical in the oxidation of hydrazides was established, the reactivity of this species was investigated. For the inhibition of *M. tuberculosis* it is necessary for the radical to covalently add to the pyridinium ring in NAD^+. Chapter 4 is a computational study on the addition of acyl radicals to nitrogen containing heterocycles and Chapter 5 extends this study to benzene and aromatic rings with varying electronic demand.

Chapter 6 is the discussion of our investigation into the McFadyen-Stevens rearrangement, a little known rearrangement from an arylsulfonylhydrazide to an aldehyde. The mechanism presented in the literature for this rearrangement is improbable and is investigated experimentally and computationally.

1.2 Tuberculosis background

Almost one third of the world's population is infected with tuberculosis (TB) and about 8 million develop the active form of the infection annually leading to almost two million deaths each year.[1] In both industrialised and developing countries the threat of TB is increasing as it becomes resistant to current antibiotic treatments.[1]

TB is a bacterial infection with the bacterium *Mycobacterium tuberculosis* which usually affects the lungs although infection can occur in other parts of the body such as the brain, spine and kidney.[2] The infection lies dormant in 95% of cases but these can reactivate during the course of a lifetime especially when the immune system is weakened.[3] The infection is spread by contact with bacteria present in airborne sputum particles from the coughing and sneezing of infected individuals.[4]

The tuberculosis bacterium is inordinately hard to kill once infection has taken place. One reason for this is the resilience of the cell wall of the bacterium which is thick and has several layers.[3] The staining of the cell wall of the bacterium using an acid fast stain is one

of the earliest tests used for the diagnosis of active tuberculosis.[4] Another reason that TB is difficult to cure is that the bacteria are relatively slow in growth and replication, therefore long treatment times are required.[3]

The treatment regime for TB initially involves four antibiotics, isoniazid, ethambutol, rifampin and pyrzinamide.[3] These are taken together for two months after which, if treatment is successful, the isoniazid and rifampin are taken for a further four months. If this treatment is unsuccessful then the infected area is surgically removed and another course of chemotherapy with several more antibiotics is undertaken for at least 2 years. [3]

1.3 Isoniazid background

Isoniazid (**1**, Scheme 1.1) has been used as a frontline treatment against the bacteria *Mycobacterium tuberculosis* for more than half a century.[3] Isoniazid acts by inhibiting the fatty acid synthesis pathway of *Mycobacterium tuberculosis*, effectively preventing the

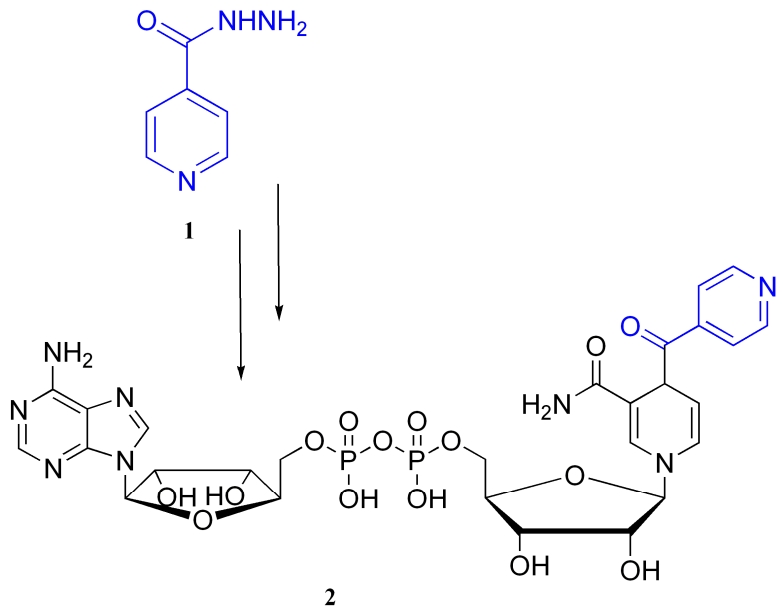

Scheme 1.1

production of mycolic acids required for synthesis of the thick cell wall.[3, 5] The target enzyme is InhA, an enoyl-acyl carrier protein reductase that is involved in elongation of the fatty acids.[5, 6] InhA utilises the coenzyme nicotinamide adenine dinucleotide (NADH) to selectively reduce a double bond at position 2 of long chain (16 carbons or more) fatty acids. By inhibiting InhA, isoniazid hinders the ability of the bacterium to produce the C_{40}-C_{60} mycolic fatty acids needed for the cell wall and thus compromises the growth of the bacterium.[6]

It is only in the latter part of the last century that studies started to elucidate the complex mode of action in which isoniazid is active against the bacterium. It was not until Sacchettini reported the crystal structure of isonicotinic acyl-NADH (**2**,Scheme 1.1) in the active site of the enzyme InhA that it was confirmed that a reactive intermediate from isoniazid and NAD^+ combined covalently to give the true inhibitor of the bacterium (Scheme 1.1).[6] Electron Spin Resonance (ESR) spin trapping studies have identified radicals as intermediates in the activation pathway of isoniazid, however these studies only provided limited structural information about the radical produced.[7, 8]

A major driving force for research into the mode of action of isonaizid was the desire to develop an understanding of the activation of the hydrazide group that could be used to combat multi-drug resistance.[9] The term “multi-drug resistant” defines strains of the tuberculosis bacteria that are resistant to isoniazid and rifampin.[10, 11] Resistance to isoniazid takes a variety of forms, as different strains of TB have different mutations in the bacterial genome. In over 50% of clinical isolates having isoniazid resistance, a mutation in the KatG catalase-peroxidase enzyme[12] is the reason for the resistance as the isoniazid adduct **2** fails to form. KatG is therefore thought to be responsible for the activation of isoniazid to form the reactive intermediate needed to give **2**, the true inhibitor of the

bacterium.[8, 13-16] One of the more interesting mutations in KatG is the S315T mutation, a single mutation of a serine residue to a threonine residue in the enzyme resulting in isoniazid resistance. Although this mutation does reduce the effectiveness of KatG as a catalase peroxidase, the isoniazid resistance is discrepantly high.[14, 15] The S315T mutation slightly decreases the diameter of the access channel leading out of the active heme site of the enzyme.[14, 16]

As KatG is a catalase-peroxidase enzyme,[13-17] the activation of isonaizid is believed to involve oxidation and it follows that the study of the oxidation of isoniazid and related hydrazides may give insight into the mechanism of the oxidative process and assist in the development of novel antibiotics which will be effective against drug resistant strains caused by a mutation in KatG.

1.4 Literature review: the oxidation of hydrazides

While the effects of various oxidants and reaction conditions on the oxidation of hydrazides have been widely explored in the literature there seems to be little elucidation of the mechanism of oxidation. Oxidants that have been used in the literature include an Anderson type hexamolybdochromate(III) catalyst,[18] thallium(III),[19] iodine(III),[20, 21] *m*-(trifluoromethyl)benzenesulfonylperoxide,[22] lead oxide,[23] lead tetra-acetate,[24] potassium ferricyanide,[23, 25] oxone ($(KHSO_5)_2.KHSO_4.K_2SO_4$),[26] cerric ammonium nitrate,[27, 28] benzeneseleninic acid and anhydride,[29] and both stoichiometric and catalytic copper(II) reagents.[30] Hydrazides are known acyl donors and the products of oxidation include esters, alcohols and N,N'-diacylhydrazines.

An early report of hydrazide oxidation was in 1894 where N,N'- diacylhydrazines (**3**,Scheme 1.2) were formed by the oxidation of hydrazides (**4**, Scheme 1.2) using iodine as the

oxidant.[31] Hypervalent iodine was used to produce the same products[20] with the mechanistic hypothesis involving the nucleophilic substitution of the starting hydrazide on a diimide intermediate (**5**, Scheme 1.2). The yields of this reaction were generally moderate with unwanted by-products observed including carboxylic acids and esters formed by trapping with the solvent. Moderate yields of the diacylhydrazide **3** were reported when various hydrazides were oxidised with *m*-(trifluoromethyl)benzenesulfonylperoxide.[22] The reaction was also proposed to proceed through nucleophilic substitution on the diimide intermediate **5** with by-products including carboxylic acids and a mixed anhydride from reaction with arenesulfonate ions present in the reaction mixture.[22] The anhydride was thought to undergo hydrolysis to the carboxylic acid during the work-up of the reaction. This seems an unlikely source of acid, however this explanation was given to explain the formation of acid in the presence of anhydrous solvents.[22]

In addition to the formation of the diacylhydrazine **3**, oxidation of **4** has been utilised to give esters and acids as products. Oxidation with thallium(III) led to the formation of methyl, ethyl, isopropyl or butyl esters when the appropriate nucleophilic alcohol was used as a solvent (Scheme 1.2).[19] However, the presence of acid as an unwanted by-product

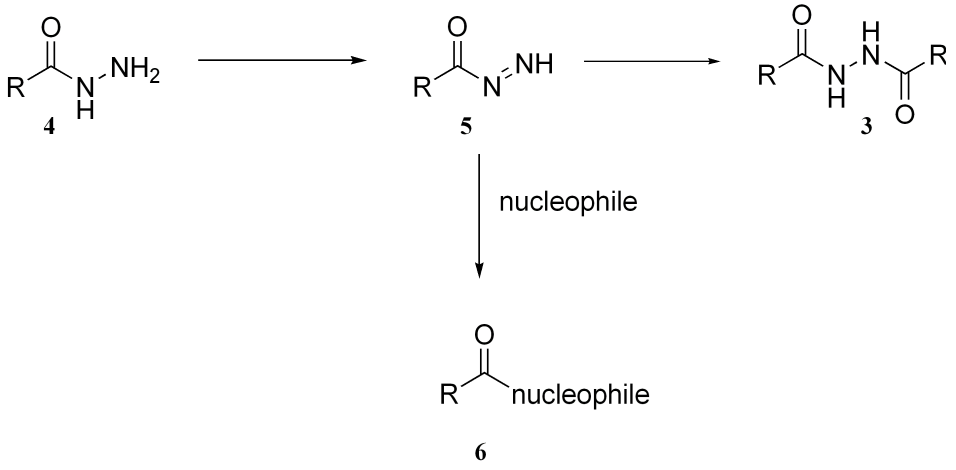

Scheme 1.2

could not be avoided. The authors proposed that the acid was formed from attack of adventitious water on the diimide – the water being unavoidable as the thallium reagent was a trihidrate. Iodine(III) oxidation in the appropriate alcoholic solvent also led to the formation of esters[20, 21] with acids also formed as by-products.[21] The acid formation was presumed to be the result of nucleophilic substitution by adventitious water on the diimide (**5,** Scheme 1.2).[20, 21]

An attempt to use less toxic, hazardous or expensive reagents for oxidation led to the oxidation of hydrazides with oxone ($(KHSO_5)_2.KHSO_4.K_2SO_4$).[26] This gave the appropriate esters when alcohols were utilised as the solvent or the carboxylic acid when water was the solvent. It is interesting to note that in the ester syntheses, the carboxylic acid was not mentioned as a by-product, but it cannot be ruled out as a base wash was employed in the workup of these syntheses, removing any acid. In these cases acid was thought to be the result of nucleophilic substitution of water on the diimide **5** (Scheme 1.2). Carboxylic acids were also formed by the oxidation of hydrazides in water with the hexamolybdochromate(III) catalyst, with the same nucleophilic substitution mechanism proposed.[18]

Oxidation of benzhydrazide with lead tetraacetate in methanol gave the carboxylic acid in 82 % yield with the methyl ester being formed in only 4% yield.[24] However, when *p*-nitrobenzhydrazide was oxidised under the same conditions the acid was the minor product, formed in 7% yield, and the ester the major product formed in 88% yield. The ester formation was thought to proceed through the diimide **5**, however the acid was thought to come from hydrolysis of a carboxylic anhydride occurring in the workup, with the anhydride being formed by the same nucleophilic substitution. Once again high energy

intermediates (in this case an anhydride) have been proposed to explain the formation of acid under anhydrous conditions.

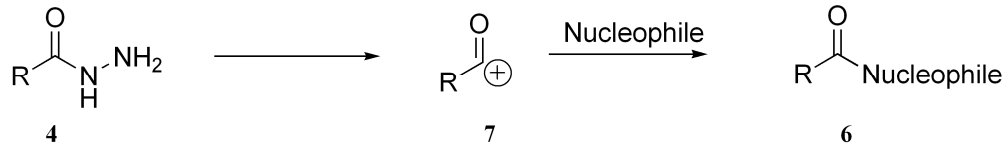

4 **7** **6**

Scheme 1.3

In contrast, when catalytic copper and oxygen was used to oxidise hydrazides the authors attributed the carboxylic acid products to the trapping of an acyl carbocation (**7**, Scheme 1.3) by the water of crystallisation present in the copper reagent. [30] The authors also found that reaction in methanol resulted in the formation of methyl esters. This was particularly evident with the reaction of *p*-nitrobenzhydrazide in methanol where the major product was methyl *p*-nitrobenzoate (76%) and the minor was *p*-nitrobenzoic acid (18%).[30]

The reaction of hydrazides with ceric ammonium nitrate (CAN) in aqueous acetonitrile gave good yields of carboxylic acids[28] while a similar oxidation of hydrazides with CAN in various alcohols gave the appropriate esters in good yields.[27] Both mechanistic possibilities (nucleophilic substitution on the diimide (Scheme 1.2) or acyl cation capture (Scheme 1.3)) were raised by the authors as likely pathways to ester formation, however the selection of substrates does not seem to support the formation of the acyl cation as only electron withdrawing groups that would promote the substitution pathway were utilised.[27] Capture of the acyl cation by the appropriate nucleophile to form acids and esters has also been suggested in the thallium mediated oxidation of hydrazides.[19]

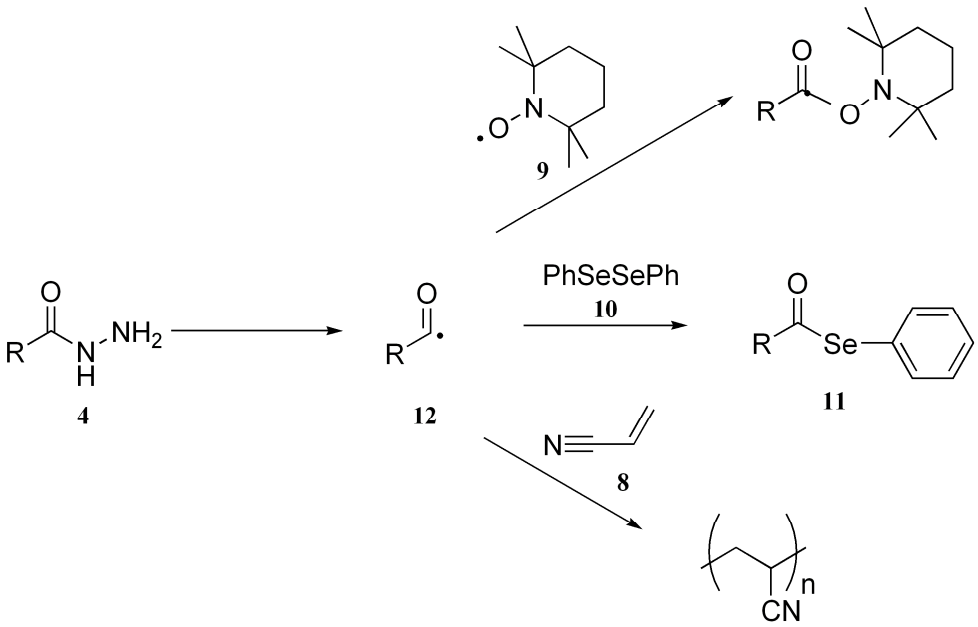

Scheme 1.4

None of the literature reviewed so far has considered the formation of a radical from the oxidation of hydrazides; however the activation of isoniazid is proposed to occur through a radical intermediate.[7, 8] While acrylonitrile polymerisation (**8**, Scheme 1.4),suggested the involvement of radicals in the oxidation of hydrazides with hexacyanoferrate(III), [25] the first report of an acyl radical from the oxidation of hydrazides involves oxidation with lead dioxide.[23] The resulting radicals were trapped using the stable nitroxide radical TEMPO[23] (**9**, Scheme 1.4). Oxidation of hydrazides with benzeneseleninic acid (or the related anhydride) produces diphenyl diselenide **10** as a by-product which is proposed to react with radicals formed by the oxidation to give the acyl selenide (**11**, Scheme 1.4).[29, 32]

It was proposed that acyl radicals formed by the oxidation of aldehydes undergo further oxidation to an acyl cation **7** when salts of cerium, chromium and manganese are used as oxidants (Scheme 1.5).[33] This could also be possible for the mechanism of hydrazide oxidation.

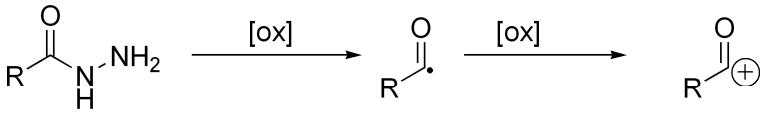

4 **12** **7**

Scheme 1.5

It is clear that the literature contains many conflicting suggestions for the mechanism of the oxidation of hydrazides. The aim of this thesis is to add to the knowledge base by clarifying the mechanistic details of this process.

1.5 Related nucleophilic substitution

Many of the previous studies of carboxylic acid and ester formation have suggested nucleophilic substitution on the diimide **5** formed from the oxidation of hydrazides (**4**) to be involved in the mechanistic pathway. To the best of our knowledge, there have not been any mechanistic studies performed that examine the details of nucleophilic acyl substitution on the acyl diimide to form the corresponding ester (Scheme 1.2). Studies on the solvolysis of hydrazides under basic[34] and acidic[35-38] conditions do not involve oxidation to the corresponding acyl diimide and are therefore not directly related to this work. However, the solvolysis of esters has been investigated both experimentally and computationally[39-45] (although for what is considered a fundamental mechanism there is surprisingly little research reported) and we expect similar mechanisms to be operating during the solvolysis of acyl diimides.

Solvent molecules are proposed to play important stabilizing roles during base and acid catalysed hydrolysis of esters.[40, 42, 44] A computational study on the decomposition of the tetrahedral intermediate in base catalysed hydrolysis determined that inclusion of solvent molecules lowered the reaction barrier by 23 kJ mol^{-1}. A representation of the proposed

transition structure from methyl acetate is displayed in Figure 1.1 showing the stabilisation of the tetrahedral intermediate by extensive solvation.[44]

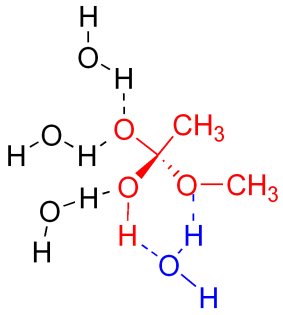

Figure 1.1

A separate theoretical study using DFT and *ab initio* methods for calculation of acid catalysed hydrolysis of methyl acetate could not find a tetrahedral intermediate on the potential energy surface until separate solvent molecules were explicitly added to the calculation.[40] This study showed that one water molecule was needed to stabilise a tetrahedral intermediate (**13**, Scheme 1.6) and that another may be involved in the decomposition of that intermediate to give the final products (**14**, Scheme 1.6).

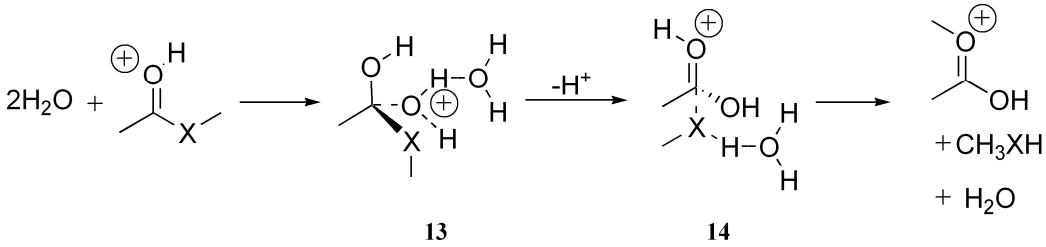

13 **14**

Scheme 1.6

Experimental[45] studies on the acid catalysed hydrolysis of esters showed the kinetics to be second order in water suggesting that two molecules of water were needed for hydrolysis. The authors suggested a transition state stabilised by water either in a linear (**15**) or a cyclic

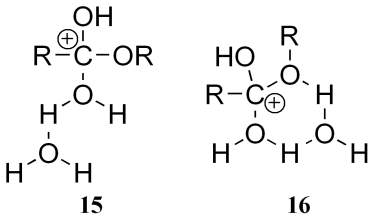

Figure 1.2 Transition states of acid catalysed hydrolysis stabilized by water molecules as represented by Lane *et al.*[45]

(**16**) orientation (Figure 1.2).[45] In the acid catalysed hydrolysis of benzamide a similar involvement of multiple solvent molecules is invoked.[46]

We would expect a similar involvement of solvent molecules during the solvolysis of acyl diimide **5**.

1.6 Reactivity of acyl radicals

The activation of isoniazid in the tuberculosis bacterium is postulated to involve oxidation of the hydrazide **4** to an acyl radical **12** (Scheme 1.5). This acyl radical, formed in the bacterium from oxidation of isoniazid by KatG, is proposed to add to the pyridinium ring in NAD^+ to give the isonicotinic acyl-NADH adduct (**2**, Scheme 1.1) that Sacchetini characterised in the active site of InhA.[6] To see whether this hypothesis is plausible we need to investigate the reactivity of acyl radicals in general and more specifically the addition of acyl radicals to aromatic ring systems. To the best of our knowledge there are no computational studies on the addition of these radicals to aromatic ring systems, however much recent research has concentrated on the related field of the addition of acyl radicals to carbon-carbon and carbon-nitrogen double bonds.[47-53]

The formation of carbon-carbon bonds is integral to organic chemistry and the use of free radicals in synthesis is now accepted as a key methodology that is particularly useful for the formation of rings through homolytic addition to carbon-carbon, carbon-nitrogen and carbon-heteroatom double bonds.

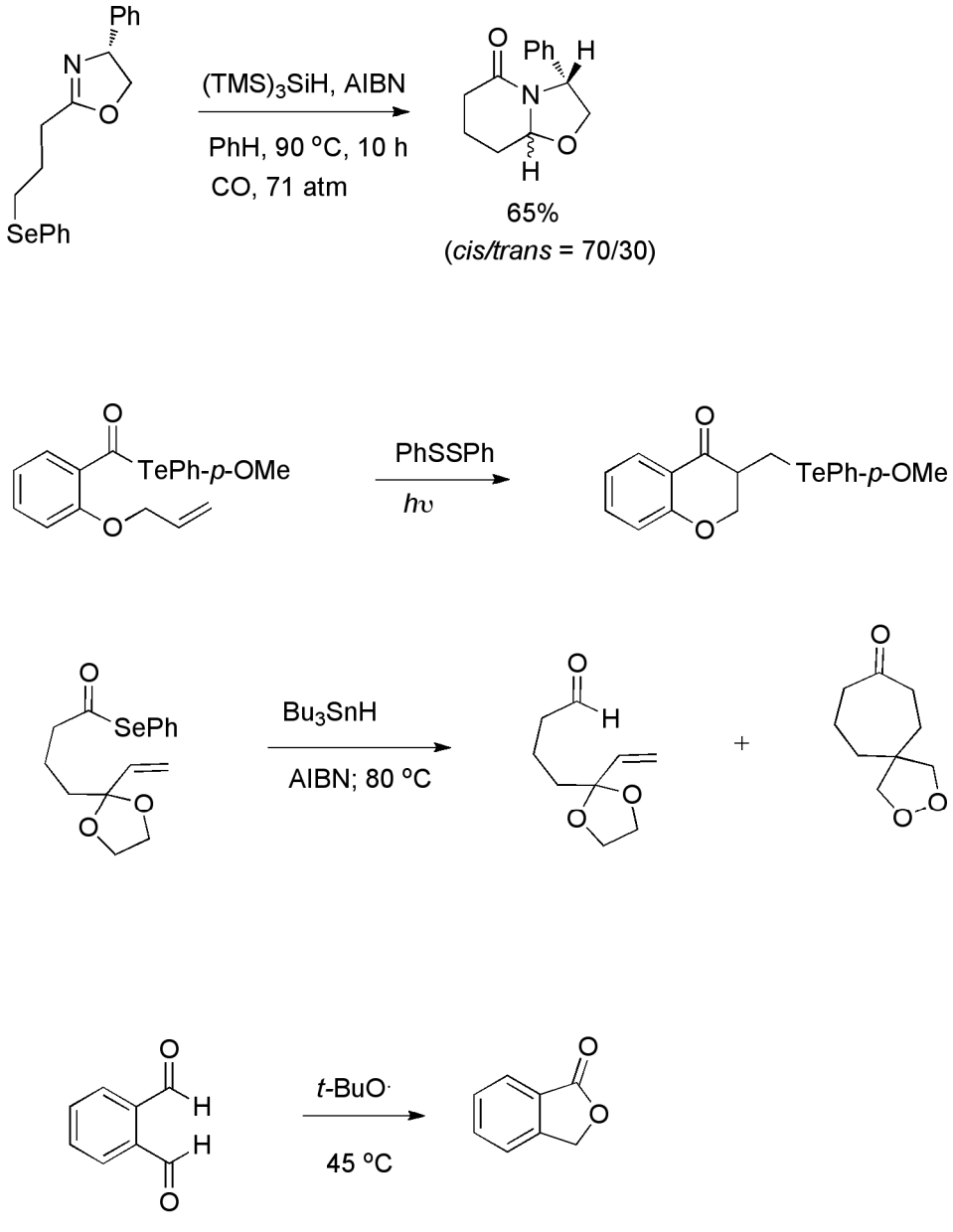

Scheme 1.7

Acyl radicals have been utilised for this chemistry as cyclisation reactions result in functionalised ring systems that include cyclic ketones, lactones and lactams.[47, 54-59] Some examples of this chemistry are depicted in Scheme 1.7.[54-59] Acyl radicals utilised for these reactions in synthesis are readily generated from seleno-[60] or telluro-ester precursors[54, 61] or through the use of the carbonylation of alkyl radicals – a methodology developed by Ryu *et al.* (Scheme 1.8).[58, 59, 62]

Acyl radicals are N-philic, that is, they prefer to attack at the electron rich nitrogen end of C=N bonds during intramolecular addition chemistry to imines,[47] sometimes defying the usual Baldwin selectivity rules.[63, 64] Alkyl radicals in contrast show little selectivity for the nitrogen end of imines in analogous chemistry.[65, 66,67, 68] In order to shed light on this

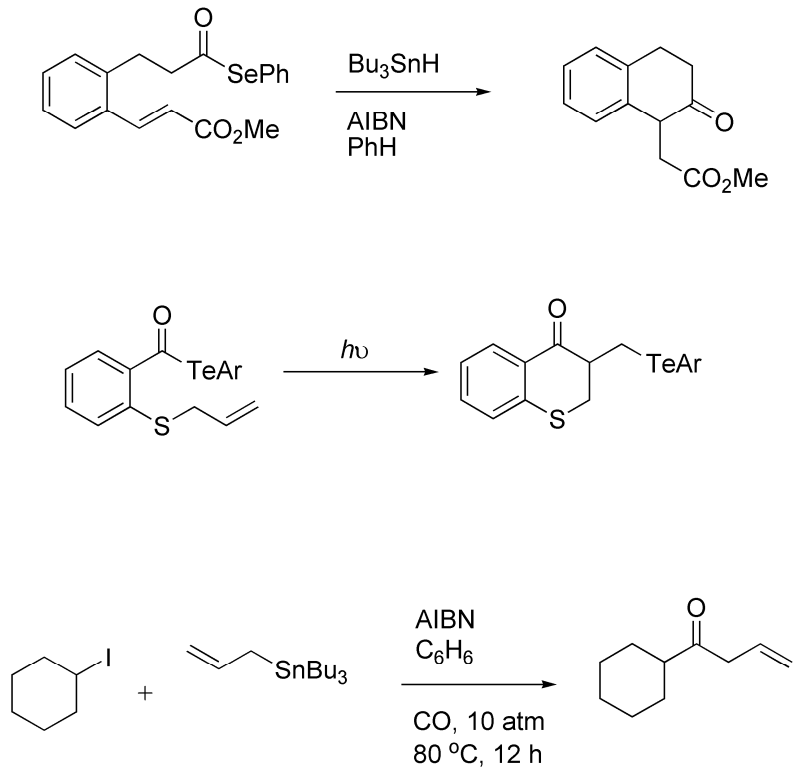

Scheme 1.8

chemistry, *ab initio* and density functional theory techniques have been used to elucidate the mechanism of the homolytic addition of acyl radicals to imines; these studies determined that simultaneous $SOMO_{radical} \rightarrow \pi^*_{imine}$ and $LP_{imine} \rightarrow \pi^*_{radical}$ interactions in the transition states for addition were responsible for the observed N-philicity of these reactions.[51, 53, 69]

Computational studies have also been conducted for reactions involving addition of acyl radicals to substituted olefins[49] and hydrazones.[48] In the case of substituted olefins, both electron withdrawing and donating groups reduced the activation energies of the reactions.[49] Calculations on the addition of the acetyl radical to aminoethylene showed a third orbital interaction in addition to the expected $SOMO \rightarrow \pi^*_{alkene}$ and $\pi_{alkene} \rightarrow SOMO$ interactions. This third $\pi_{alkene} \rightarrow \pi^*_{C=O}$ interaction contributed to the stabilisation of the transition state and the lowering of the activation energy barrier.[49] Similar additional orbital interactions were present in the reaction of the acetyl radical with the nitrogen of the hydrazone *N*-aminomethanamine (CH_2=N-NH_2).[48] It was proposed that the nature of the acetyl radical (electrophilic or nucleophilic) is determined by the π system that the radical is reacting with rather than the radical itself.[48]

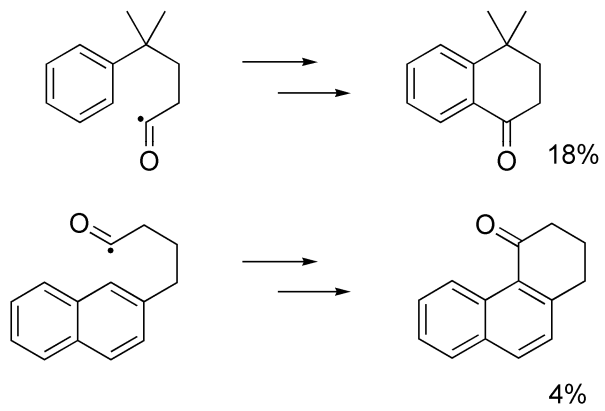

Scheme 1.9

Very little experimental work has been reported utilising the addition of acyl radicals to aromatic rings. The addition of an acyl radical to protonated benzothiazole has been utilised as a diagnostic test for the presence of acyl radicals formed from the oxidation of aldehydes.[33, 70] Minisci *et al.* have also investigated the addition of acyl radicals formed from α-keto acids to protonated heteroaromatic bases and have found that a two phase system is necessary to allow monoacylation as after one acyl group is added a second will add more readily.[71] Addition of acyl radicals to benzene and naphthalene is rare but examples include the intramolecular addition of acyl radicals to benzene[72] and to naphthalene [73] (Scheme 1.9) in relatively low yield.

1.7 McFadyen – Stevens rearrangement background

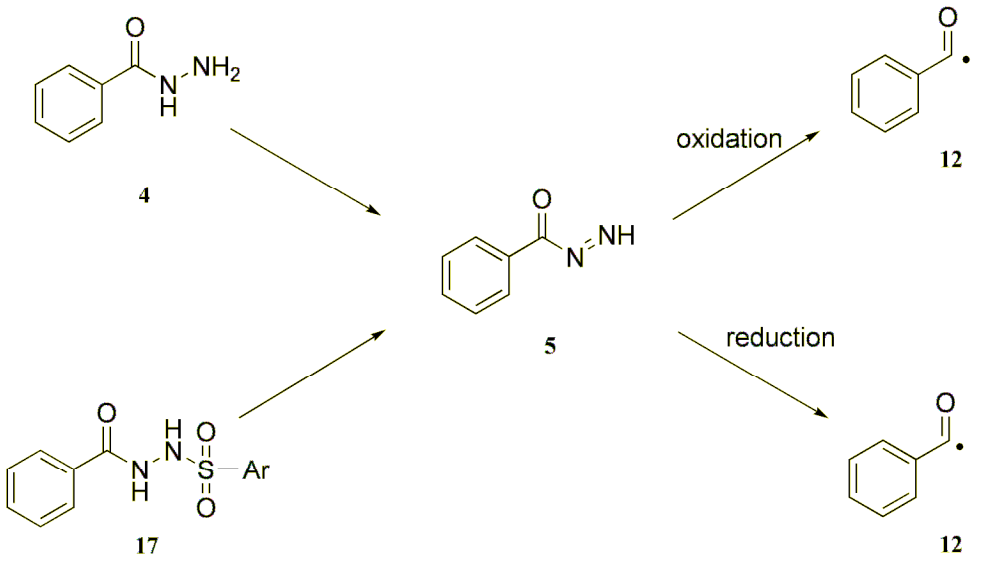

Scheme 1.10

The McFadyen-Stevens rearrangement is the conversion of an arylsulfonylhydrazide (**17**, Scheme 1.10) to an aldehyde upon reflux in an alkaline solution.[74] It has been proposed that the reaction proceeds through a complex mechanism that includes the formation and subsequent rearrangement of a diimide intermediate (**5**, Scheme 1.10) .[75] This intermediate **5** is also proposed to form upon oxidation of hydrazides such as **4** (Scheme 1.10).[76] During the course of the study of oxidation of hydrazides we required a method for the non-oxidative formation of the diimide **5** to see if a reducing agent could then form **12** (Scheme 1.10) the same acyl radical formed from the oxidation of **4**. This would mimic the possible involvement of NADH in the activation of isonaizid. We propose an alternative pathway for the activation of isonaizid: that KatG oxidises isoniazid only as far as the diimide intermediate **5**, then this intermediate can be reduced to form the acyl radical **12** by NADH, before addition to the resulting radical cation ($NAD^{+\cdot}$) (Scheme 1.12). A non-

oxidative method of forming the diimide **5** is required to investigate this proposed hypothesis.

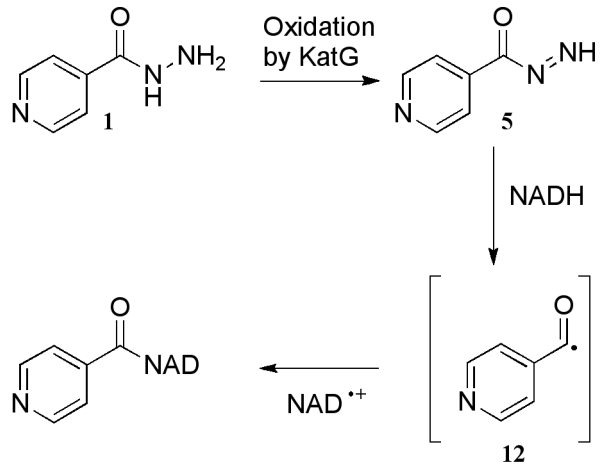

Scheme 1.12

There is some contradiction in the literature about the mechanism of the McFadyen-Stevens rearrangement. While some authors invoke the base promoted proton abstraction from the nitrogen nearest the carbonyl to give the anion **18** (Scheme 1.11) [77, 78] others suggest that the proton on the nitrogen nearest the sulfonyl group is more acidic which

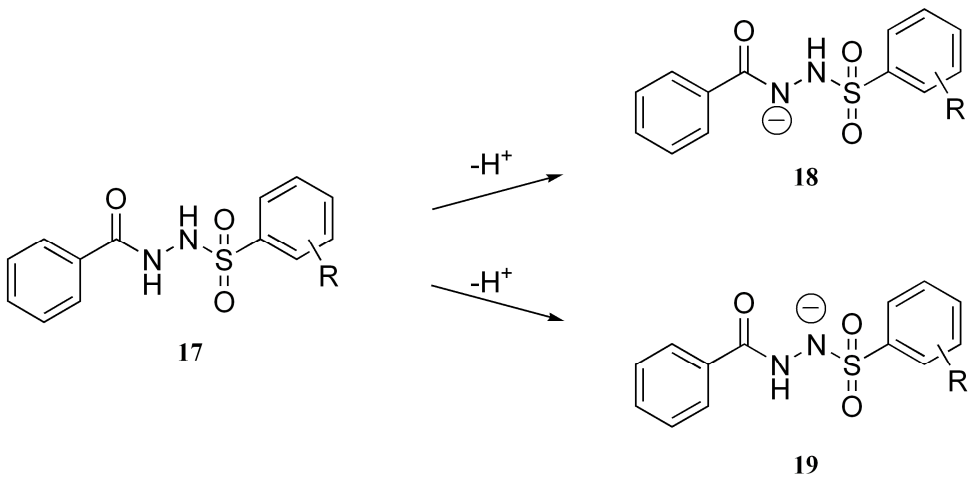

Scheme 1.11

would lead to **19** (Scheme 1.11).[75] E1cB type elimination from **18** would lead directly to the diimide **5** whereas **19** would need to undergo rearrangement to give the same product. [75]

Decomposition of **5** is the next step for formation of the aldehyde but the actual mechanism of the decomposition is also in doubt. Matin, Craig and Chan propose that the decomposition occurs through an unusual carbene intermediate (**20**, Scheme 1.13). [75] Another possibility is a radical mechanism. The related work of Myers on alkyl diazenes proposes that the reaction in this case proceeds through a radical intermediate and this hypothesis was supported by cyclisation and ring opening of cyclopropyl diazenes.[79, 80] Similar work by Zard on hydrazones and hydrazides also invokes a radical mechanism with the radical resulting from the thermal decomposition of an N-alkyl diimide.[23, 32, 81]

Depending on the functional group on the aromatic ring, some authors have found that esters, alcohols and acids form in reactions that are in competition with the McFadyen-Stevens rearrangement.[82, 83] While this could be the result of a subsequent Cannizaro type reaction, heating aldehydes under the same conditions did not result in the formation of

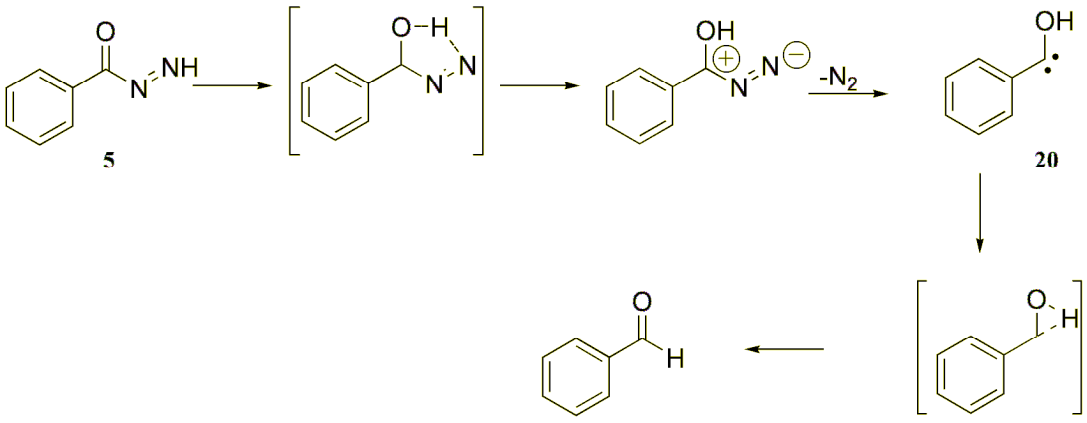

Scheme 1.13

esters and alcohols.[83] It is possible that any ester found in the reaction results from substitution of the solvent (ethanol) on the diimide **5**.[83]

McFadyen and Stevens originally used the *p*-tolylsulfonyl group for these rearrangments[74] which required very harsh conditions such as reflux in ethylene glycol, but it has since been found that much milder conditions can be used if the *o*-nitrosulfonyl group is used instead[23, 84] raising the possibility that the rate limiting step in this reaction is the separation of the sulfonyl group from the imide.

1.8 Summary of project aims

This project aims to elucidate the mechanism of oxidation of hydrazides with particular emphasis on the hydrazide of isonicotinic acid – isoniazid, a frontline antibiotic used against TB. The presence of an acyl radical in the oxidation process will be established and subsequent computational studies on the reactivity of acyl radicals with aromatic rings will be performed. The nucleophilic acyl substitution of the diimide intermediate formed from the oxidation of hydrazides will also be investigated. Finally a computational and experimental investigation of the McFadyen-Stevens rearrangement will elucidate further the mechanism of this reaction.

Chapter 2.

The oxidation of hydrazides

The tuberculosis (TB) drug isoniazid (**1**, Scheme 2.1) has been used as a frontline treatment against the bacteria *Mycobacterium tuberculosis* for almost half a century.[3] It is only in the latter part of this period that studies have started to elucidate the complex mode of action in which isoniazid is active against the bacterium. A major driving force for this was the desire to develop an understanding of the mechanism of activation that could aid in the fight to combat multi-drug resistance.[9]

It has been well established that isoniazid itself is not the 'true drug' but that it is activated by oxidation to the active species. Electron spin resonance (ESR) studies have identified radicals as intermediates in the activation but provided limited structural information.[8] It was not until Sacchettini reported the crystal structure of an isonicotinic acyl-NADH adduct (**2**, Scheme 2.1) in the active site of the enzyme InhA which is part of the fatty acid synthesis

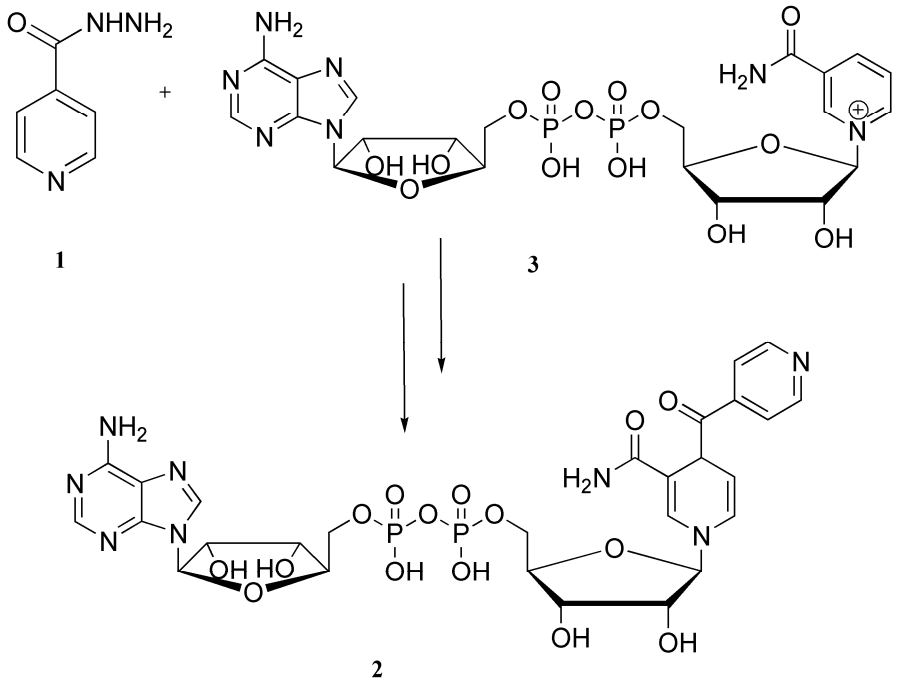

Scheme 2.1 Isoniazid (**1**) combines with NAD^+ under oxidative conditions to form the true inhibitor of InhA **2**.

II (FASII) pathway involved in building the bacterial cell wall that it was confirmed that a reactive intermediate from isoniazid and NAD^+ (**3**, Scheme 2.1) combined to give the true inhibitor of the bacterium (**2**, Scheme 2.1).[6] The true inhibiter **2** has also been synthesised using Mn(III) pyrophosphate mediated oxidation of isoniazid as a KatG mimic with some success, with yields of up to 40%.[85, 86] Unfortunately, this synthesis was not stereoselective and yielded a mix of diastereomers of which only one was biologically active.[85, 86] It has been postulated that an acyl radical is the key intermediate[87, 88] in the oxidation of isoniazid but to date this has not been verified.

When we first began this work little was known about the mechanism for the oxidation of hydrazides, although it was well established that an electrophilic species is generated and that the oxidation of hydrazides has been exploited for nucleophilic acyl substitution reactions.[25, 27, 30] The oxidation of hydrazides to give carboxylic acids in water, and esters in the presence of alcohols is well known, but there would appear to be some inconsistencies

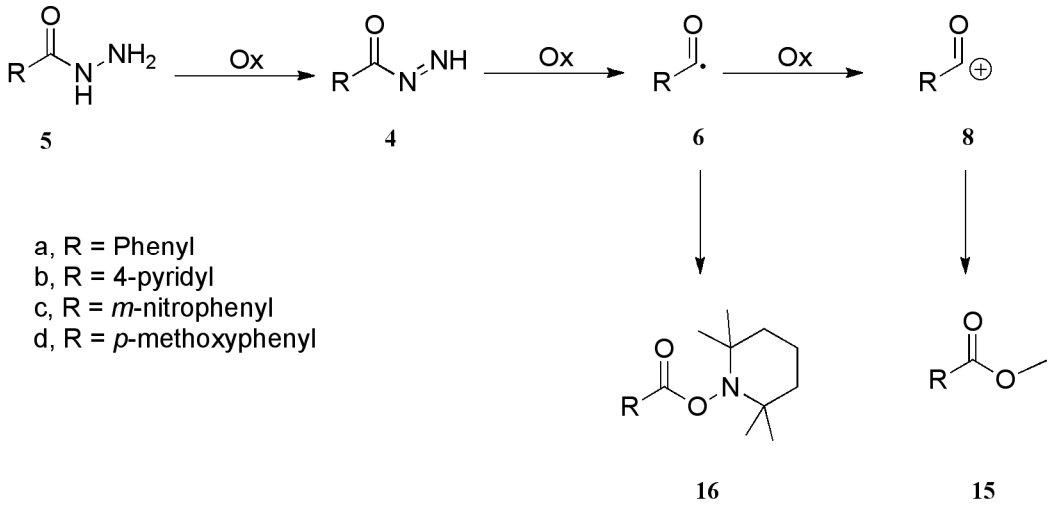

Scheme 2.2 Proposed intermediates in the oxidation of hydrazides. Competitive trapping of radical with TEMPO resulting in a TEMPO adduct, and cation with methanol, resulting in a methyl ester.

surrounding the mechanism of this transformation.[23, 27, 30, 88] Some studies invoke the presence of diimide intermediates (**4,** Scheme 2.2) during the oxidation of hydrazides (**5**, Scheme 2.2)[23, 27] and the possibility of nucleophilic acyl substitution of this intermediate.[27] Only recently, when Braslau oxidized aryl and aliphatic hydrazides with PbO_2 in the presence of the radical trap 2,2,6,6-tetramethylpiperidine-1-oxyl (TEMPO, **7**, Figure 2.1), was it reported that the oxidation of hydrazides with transition metal oxidants involves the formation of acyl radical intermediates (**6**, Scheme 2.2).[23] However, it seems generally accepted in the literature that an acyl radical could be further oxidized to the acyl cation (**8**, Scheme 2.2). [27, 30, 33] The following results support the observation that acyl radicals are formed when hydrazides are oxidised by most oxidants and that the corresponding acyl cations are not formed by further oxidation, or involved in nucleophilic acyl substitution.

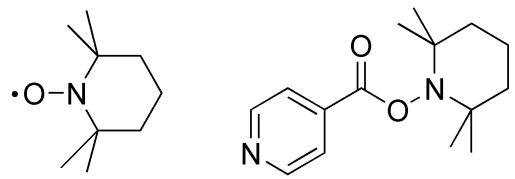

7 **13**

Figure 2.1 The stable radical 2,2,6,6-tetramethylpiperidine-1-oxyl (TEMPO) (**7**), and the resulting trapped product O-isonicotinoylhydroxylamine (**13**)

2.1 Trapping of acyl radicals

Initial experiments on the oxidation of the phenyl derivative of isoniazid – benzhydrazide (**9**, Scheme 2.3) used the benzothiazolium ion that has been reported by Minisci as a diagnostic probe for the presence of acyl radicals in the permanganate oxidation of alcohols to carboxylic acids.[33] When the hydrazide **9** was oxidised with potassium permanganate in the presence of the benzothiazolium ion (formed by adding benzthiazole to 5 M H_2SO_4), 2-benzoyl benzothiazole **10** was obtained in 16 % yield (Scheme 2.3) indicating that acyl radicals are formed under oxidative conditions. This result also supports the hypothesis that the isoniazid-NADH adduct **2** is formed by radical trapping with NAD^+ **3**, which is similar in that it is the trapping of an acyl radical with an electron deficient heterocycle. However, no such product was observed with the oxidation of isoniazid which could be attributed to

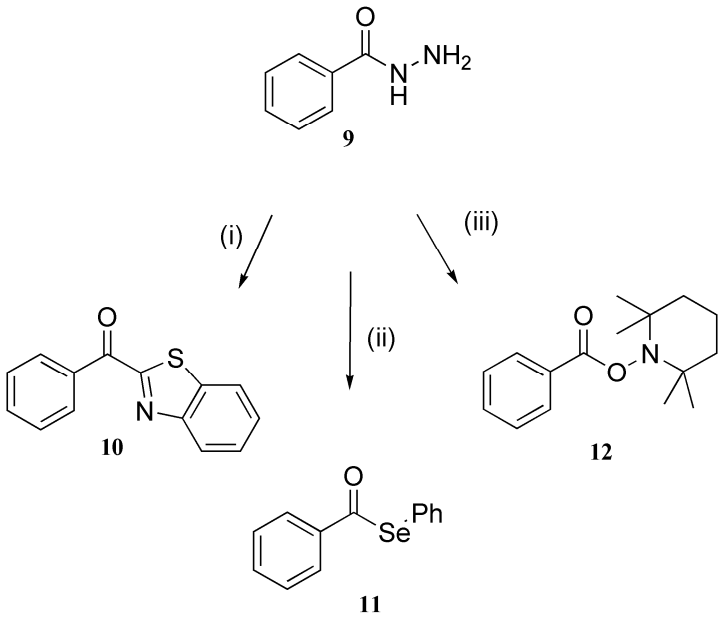

Scheme 2.3 Reagents; (i) benzothiazole, AcOH. 5M H_2SO_4, $KMnO_4$; (ii) Ph_2Se_2, CH_3CN/H_2O, $KMnO_4$; (iii) TEMPO, CH_3CN/H_2O, $KMnO_4$.

nucleophilic acyl substitution under the aqueous conditions (*vide infra*). Diphenyldiselenide has also been used as a trap for acyl radicals[54] and oxidation of benzhydrazide with potassium permanganate in the presence of diphenyldiselenide afforded phenyl selenobenzoate **11** in 34 % yield, supporting the first observation (Scheme 2.3).[61, 89] The seleno ester was confirmed by ^{1}H NMR and IR spectroscopy which shows the C=O stretch at 1683 cm^{-1} consistent with that reported.[90] Again no seleno ester was observed upon oxidation of isoniazid, therefore the common radical trap TEMPO (**7**), which reacts with carbon centred radicals at near diffusion control with a rate constant of 1 x 10^{9} M^{-1} s^{-1} at a temperature of 298 K,[91] was trialled.

In initial unpublished work by Smith and Gourlay[90] both benzhydrazide and isoniazid were reacted with various oxidants in the presence of TEMPO (**7**) under aqueous conditions; O-benzoylhydroxylamine 12 and O-isonicotinoyl hydroxylamine **13** were formed respectively (Figure 2.1, Scheme 2.3).[92] These products are the consequence of acyl radical generation (**6a**, **6b,** Scheme 2.2) and trapping, as supported by Braslau.[23] The yields appeared to vary depending on the strength of the oxidant (Table 2.1, 8-84%). Significantly, these results suggest that acyl radicals are formed when either typical single electron oxidants (such as potassium ferricyanide) or potential two electron oxidants were used.[93] These results support the previous hypothesis for isoniazid activation. Confirmation of the structure of O-benzoylhydroxylamine **12** was by comparison with the literature,[23] while O-isonicotinoylhydroxylamine **13** was a novel compound identified by NMR and IR spectroscopy and mass spectrometry. The other products formed in these reactions were the corresponding carboxylic acids, benzoic and isonicotinic acid, which were previously believed to result from acyl cation formation (**8a**, **8b** Scheme 2.2) followed by reaction with water. The yields of **13** are much lower than for the corresponding benzoyl derivative **12** (Table 2.1). This result was initially believed to indicate that the acyl radical from isoniazid

(**6b**) is much less stable than that derived from benzhydrazide (**6a**) and was most likely oxidised further to the cation (**8b**, Scheme 2.2).

Table 2.1 Yields of trapped benzoyl and isonicotinoyl radical formed by various oxidants.

Oxidant	Yield (%) **12**	Yield (%) **13**
$Mn(OAc)_3$	20	9
MnO_2	81	8
K_2MnO_4	67	10
$KMnO_4$	41	15
$[Mn_2(\mu\text{-}O)_3L_2](PF_6)_2/H_2O_2$	35	14
$[Mn_2(\mu\text{-}O)_3L_2](PF_6)_2/H_5IO_6$	21	58[a]
$K_3[Fe(CN)_6]$	84	20

[a] Nitrogen continuously bubbled through reaction mixture.

For our further investigations the manganese catalyst, $[MnIV\text{-}MnIV(\mu\text{-}O)_3L_2](PF_6)_2$ (L=1,4,7-trimethyl-1,4,7-triazacyclononane) which forms a MnV=O species as an active oxidant, was utilised as it was hypothesized to be a mimic for oxidation by the KatG enzyme as it has catalase activity.[94, 95] Under a nitrogen atmosphere with periodic acid as a co-oxidant, only a modest yield of **13** was observed (9-20%), however, when the reaction solution was purged with nitrogen throughout the reaction, the yield was dramatically increased to 58% (See Table 2.1). One reason for this increased yield may be that as the manganese catalyst is a mimic for the oxygen evolving centre of photosystem II[95] it could generate a low concentration of oxygen in the presence of periodic acid,[94,96] resulting in the formation of the carboxylic acid by the trapping of a radical with O_2.[97] Purging the reaction mixture with nitrogen gas removed oxygen, thereby reducing this competing radical reaction[97] such that **13** was now the major product. These experiments demonstrate that,

under the conditions described above, the major oxidation pathway most likely involves formation of the acyl radical **6** (Scheme 2.2).

Oxygen is known to react with radicals in a diffusion controlled manner to produce peroxides – or in the case of acyl radicals, peroxyacids.[97] Under our reaction conditions the peroxyacid formed is assumed to react with the manganese (or other metal) present to form the corresponding acid (**14**, Scheme 2.4). The carboxylic acid was an observed by-product in all hydrazide oxidations performed. The increased yield of radical product observed when purging with nitrogen suggests that acid formation is largely due to the trapping of a radical by oxygen; however this explanation is contrary to the literature which suggests that the trapping of an acyl cation by water forms the acid.[30, 88] In the initial experimental design oxidations with metal salts were carried out in an aqueous medium under an atmosphere of air, therefore acid could be formed from either pathway.

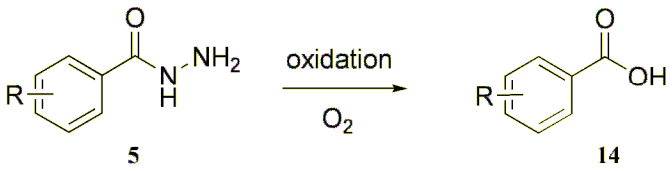

5 **14**

Scheme 2.4 Acid resulting from oxidation of hydrazides

2.2 Competitive trapping

A competitive trapping experiment (Scheme 2.2) was devised in an attempt to provide a more detailed picture of the stability of the acyl radical formed by oxidation and also whether the acyl radical was oxidised further to the acyl cation. Methanol was used as the solvent which would be able to act as a nucleophile to trap any cation once it was formed. The ratio of methyl ester **15** to *O*-acylhydroxylamine **16** (found by comparison of integration in ^{1}H NMR) was used to give an indication of the stability of the acyl radical with more *O*-acylhydroxylamine and less methyl ester indicating a more stable radical.

Table 2.2 Ratio of methyl ester **15** to TEMPO adduct **16** formed with either 5 mL methanol or 50 µL methanol in acetonitrile.

	Ratio of **15**:**16**	
hydrazide	5ml of methanol	50 µL methanol in acetonitrile
isoniazid	6:1	1:9
benzhydrazide	0.7:1	1:8
p-methoxybenzhydrazide	4:1	1:9
p-methylbenzhydrazide	2:1	1:8
p-chlorobenzhydrazide	2:1	1:4
m-bromobenzhydrazide	4:1	1:2
m-nitrobenzhydrazide	3:1	1:1

Oxidation of hydrazides (0.4 mmol) in methanol (5 mL) with the manganese catalyst and periodic acid in the presence of one molar equivalent of TEMPO showed that the methyl ester **15** (Scheme 2.2) was formed as the major product for most hydrazides (Table 2.2). Initially we interpreted this as evidence that the acyl radicals were unstable and easily oxidised further to form acyl cations. However, the low yield of the TEMPO adduct **13** was not more than 10% which is in contrast to the results when the reaction was performed in a non-nucleophilic solvent (acetonitrile) where the yield of **13** was close to 60% under similar conditions (Table 2.1). If an acyl cation is the source of methyl ester then it seems odd that the cation is not formed as readily in acetonitrile. It appears, rather, that the methyl ester is formed from a precursor to the acyl radical rather than from a further oxidation product. If this were the case then reducing the amount of methanol should give increased radical – derived product.

Therefore, the amount of methanol was reduced to three molar equivalents with respect to the hydrazide and TEMPO, and acetonitrile was used as a non-nucleophilic solvent. The results of these experiments are listed in Table 2.2. The reduction in the amount of methanol led to the formation of the TEMPO adduct (**16**, Scheme 2.2) as the major product for both isoniazid and benzhydrazide. This supports the hypothesis that that the diimide intermediate (**4**, Scheme 2.2) undergoes nucleophilic acyl substitution to yield the corresponding ester, therefore its interception reduces the yield of acyl radical products.

Nucleophilic acyl substitution is a bimolecular reaction and as such its rate is dependent on the concentration of reactants. Where there is a large concentration of a nucleophile, such as when methanol is used as the solvent, the rate of nucleophilic attack on the carbonyl carbon (Scheme 2.5, k_4) competes favourably with the rate of oxidation to the radical (Scheme 2.5, k_2). This also explains why the formation of diacylhydrazine dominates when the concentration of oxidant is kept low by the slow addition of oxidant, a well known

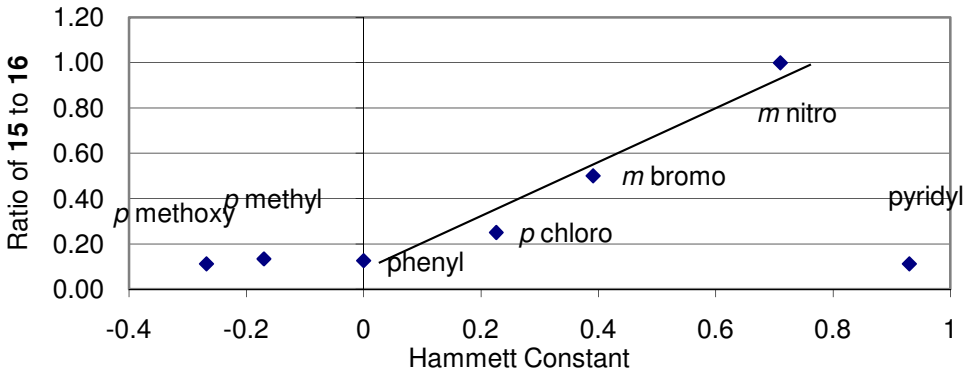

Chart 2.1 Hammett plot for ratio of products **15**:**16** vs Hammett constant for reaction in acetonitrile with three equivalents of methanol.

transformation which exploits the formation of a low concentration of the diimide in the presence of the nucleophilic hydrazide.[23, 30]

This propensity to undergo nucleophilic acyl substitution was not seen equally for all functional groups and isoniazid showed the greatest tendency to this pathway.

The increasing ratio of ester **15** to radical product **16** with the increasing electron withdrawing ability is also consistent with favouring nucleophilic acyl substitution (see Hammett plot of product ratio vs Hammet constant; Chart 2.1). Also consistent is the outcome that electron donation has little effect with the methyl and methoxy benzhydrazides essentially having the same ratio of products as the parent benzhydrazide. The one exception is isoniazid (**1**) which is less susceptible to solvolysis under these conditions. This result is in contrast to the outcome using the higher concentration of methanol. However, our experimental results are supported by calculations (reported in Chapter 3) that predict that bulk solvent is required for the stabilisation of the transition state during nucleophilic acyl substitution of the diimide, more for isoniazid than for other aryl hydrazides.[98]

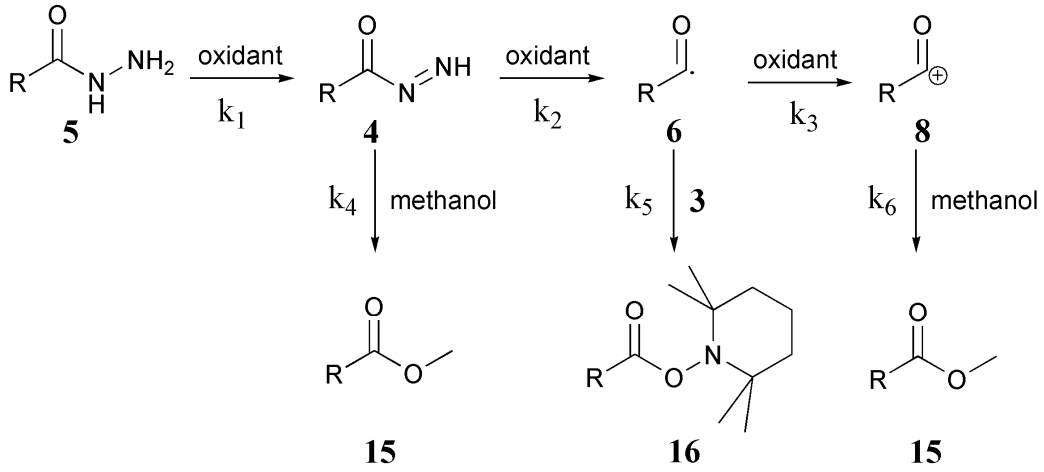

Scheme 2.5 Revised mechanism for the oxidation of hydrazides, proceeding through diimide, radical and cation intermediates

2.3 Computational investigations

Initially we had proposed (as supported by the literature) [27, 30, 88] that the formation of the ester **15** may be due to trapping of an acyl cation (**8,** Scheme 2.2) formed from further oxidation of the radical (**4**, Scheme 2.2). However, the competitive trapping experiments described above do not support this hypothesis.

To investigate the possibility that ester formation is related to radical stability we turned to computational chemistry. Providing that the radicals are similar in nature, bond dissociation enthalpies (BDEs) can be used as a measure of radical stability as they indicate the amount of energy required to homolyse the bond leading to the radicals in question.[99] We performed calculations on the isodesmic reaction mechanism shown in Scheme 2.6. The resulting BDEs were close in value, within 9 kJ mol^{-1}, showing that the stability of the radical is effectively not affected by the substitution on the aromatic ring and therefore supports the hypothesis that interception of a precursor to the radical is a more likely

Table 2.3 Standard reduction potential of cations resulting from hydrazide oxidation calculated at B3LYP/6-311+G(2d,2p)//B3LYP/6-31G(d)

	Gas phase ionisation energy (eV)	Solvated ionisation energy (eV)	Eº vs NHE (V)
isoniazid	7.28	4.75	0.47
benzhydrazide	6.75	4.47	0.19
m-nitrobenzhydrazide	7.32	4.73	0.43
p-methoxybenzhydrazide	6.32	4.28	0.00

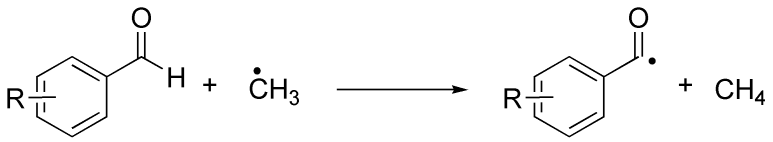

Scheme 2.6 Isodesmic scheme used for calculating BDEs.

mechanism for ester formation. (For full table of BDEs and geometries of molecules see Appendix A.)

In order to provide additional support for the hypothesis that the acyl radical is not further oxidised to the cation the ionisation energies for the acyl radicals in this study were investigated using computational techniques.[100] Geometries of radicals and cations (**6** and **8 a-d**, Scheme 2.2) were optimized using B3LYP/6-31G(d) and single point energies calculated using B3LYP/6-311+G(2d,2p). The calculations indicated gas phase adiabatic ionization energies from the radical to the cation (**6-8** Scheme 2.2) ranging from 6.3 eV to 7.3 eV (Table 2.3). These data were then converted into reduction potentials for the cations (**8a-d** Scheme 2.2) following a modification of the method of Fu *et al.* which has been shown to yield excellent agreement with experimental results.[101] Reduction potentials for the acyl cations relative to the normal hydrogen electrode (NHE) were determined to lie in the range: 0.00 V to 0.47 V (Table 2.3). These values are substantial in comparison with a reduction potential of 0.36 V for a typical oxidant such as potassium ferricyanide,[102] however they do not rule out the further oxidation of the acyl radical to the cation for all functional groups investigated.

2.4 Evidence against the formation of the acyl cation

To maximise the production of acyl radical and further potential oxidation products we used the bulky alcohol isopropanol, in place of methanol, which would be expected to react

with an acyl cation, but would slow the nucleophilic acyl substitution process due to steric bulk. For this study we utilised the four hydrazides **5 a-d** in Scheme 2.2. The formation of a trace of the isopropyl ester was only observed in the oxidation of *m*-nitrobenzhydrazide **5c** (Scheme 2.2), and was not observed for the other hydrazides. We deduced that the electron withdrawing nitro group promoted the nucleophilic substitution to a small extent in this case and that the acyl cation **8** was not formed by oxidation of the acyl radical as it would be trapped readily. In addition, for all substrates, a trace of aldehyde (determined by ^{1}H NMR) was formed consistent with hydrogen transfer to the acyl radical **6a-d** from the hydrogen donor isopropanol.

To further test the hypothesis that the acyl cation is in fact not formed from the oxidation of an acyl radical, the hydrazides were oxidised in the presence of five equivalents of methanol with acetonitrile as solvent in the absence of TEMPO. Formation of the cation **8** (Scheme 2.2) would result in an increased yield of methyl ester (**15**, Scheme 2.2), however the yield of the ester in all cases was not increased and remained low with no other identifiable product formed, indicating that the acyl radical is not a precursor for any product formed by nucleophilic acyl substitution.

In addition, the oxidation of benzyhydrazide (**9**) or isoniazid (**1**) in a non-nucleophilic solvent in the presence of anisole as a nucleophile failed to yield any Friedel-Crafts product that would be expected to form if an acyl cation were indeed generated (Scheme 2.7). This is further supporting evidence that the oxidation of the acyl radical to an acyl cation is unlikely and supports the computational results for the investigation of the oxidation of the radical to the cation.

On the balance of evidence provided by this work we suggest that nucleophilic acyl substitution is likely to be the major mechanism operating during the facile formation of esters by the oxidation of hydrazides in the presence of alcohols.

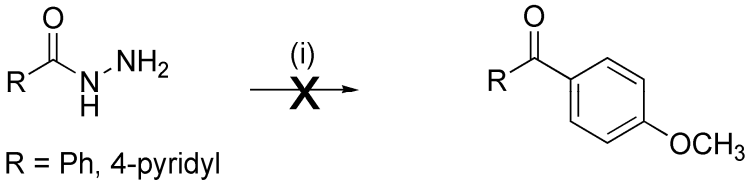

Scheme 2.7 (i) anisole (10 equiv), ceric ammonium nitrate (4equiv),acetonitrile, N_2 bubbled through reaction mixture.

2.5 Comparison with the literature

This proposed mechanism is consistent with previous observations of hydrazide oxidation such as the oxidation with catalytic Cu^{2+} in methanol in which mostly carboxylic acids were formed. This acid formation was attributed to attack of adventitious water on the acyl cation even with anhydrous methanol whereas our calculations would suggest that the cation is unlikely to form and that trapping the acyl radical with oxygen would produce this result.[30, 97] In addition, the oxidation of hydrazides with ceric ammonium nitrate in various alcohols reported by Polanc *et al.* showed good yields for those hydrazides with electron withdrawing groups which encourage the nucleophilic substitution of the diimide, but no results for electron donating groups or even benzhydrazide were reported indicating no major contribution from the cation pathway.[27] When we repeated the oxidation of benzhydrazide under Polanc's conditions the yield of methyl benzoate was a low 32% consistent with the current hypothesis. The reaction pathway proposed can also be used to

rationalise the products formed from the oxidation of isoniazid in the presence of $H_2{}^{18}O$ and $^{18}O_2$ as reported by Bernadou and Meunier.[88] Though this paper suggests incorporation of $H_2{}^{18}O$ through the cationic pathway, we would instead postulate the interception of the diimide by the labelled water, however we would agree with the trapping of the acyl radical with labelled dioxygen.

Based upon our work and prior work in the literature we now propose that the oxidation of hydrazides proceeds through a diimide intermediate (which can undergo nucleophilic acyl substitution) to an acyl radical and we find no experimental evidence to support the formation of an acyl cation for these substrates (Scheme 2.8).

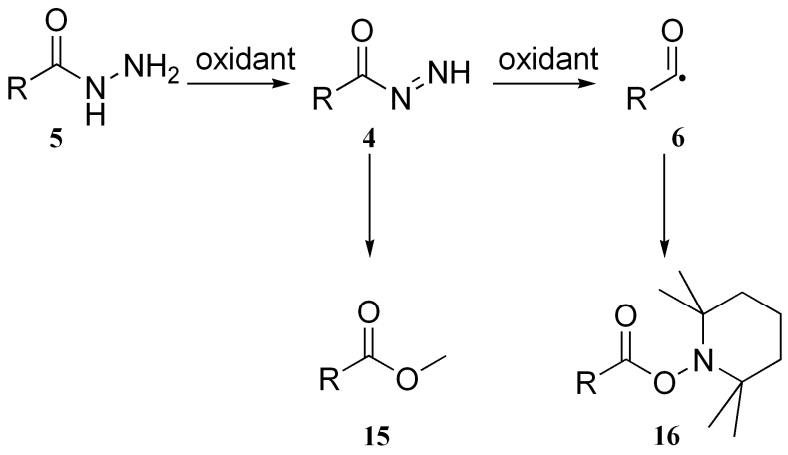

Scheme 2.8

2.6 Insight into isoniazid resistance

The clarification of the mechanism of oxidation of isoniazid could assist in understanding why a single base pair mutation in the KatG enzyme in *Mycobacterium tuberculosis* confers resistance to isoniazid.[14] This change, from a serine to a threonine in the access channel to the heme active site,[14, 17] is analogous to the change in the alcohol used for trapping from methanol to isopropanol. Our isopropanol trapping experiments yielded some additional

information, as in addition to the TEMPO ester, small amounts of aldehyde (consistent with hydrogen transfer from the isopropanol to the acyl radical) were formed. The secondary alcohol moiety in the threonine side chain may be having a similar effect and may be trapping the intermediate radical thus conferring resistance to isoniazid.

In addition, resistance to isoniazid may be caused by the mutation in KatG favouring the nucleophilic acyl substitution pathway in preference to radical formation. This competition is particularly relevant for isoniazid activation in an aqueous medium which is similar to our experiments in methanol which hindered the formation of the acyl radical.

2.7 Conclusions

In conclusion, radical trapping and competitive trapping experiments have led to a mechanistic understanding that supports and unites all experimental data available for the oxidation of hydrazides. The oxidation of hydrazides occurs through a more complex mechanism than first thought, which is dependent on reaction conditions including strength of oxidant, concentration of reactants and nucleophilicity of solvents and reactants and and we find no experimental evidence to support the formation of the cation from these substrates. We have also shown that isoniazid gives an acyl radical when oxidised, but the intermediate diimide is highly susceptible to nucleophilic attack. As a result of these investigations we speculate that the resistance conferred by the single base pair change in mutant KatG could be explained by premature reaction of the acyl radical or interception of the acyl radical precursor. This information may be of benefit in the understanding of mechanisms of drug resistance with TB and also in the development of synthetic methods involving hydrazides.

Chapter 3.

An intervening pathway

As mentioned previously, isoniazid is activated by the catalase-peroxidase enzyme, KatG in *Mycobacterium tuberculosis*.[8, 12, 14, 15, 17, 103, 104] Once activated, isoniazid forms a reactive intermediate that adds to NAD^+ to form the "true" drug (**2**, Scheme 3.1).[6] The postulated reactive intermediate is a radical (**3**, Scheme 3.2)[8, 23, 76] formed through an acyl diimide intermediate (**4**, Scheme 3.2).[23, 27]

Experimental investigations in Chapter 2 have shown that **4** is more prone to nucleophilic acyl substitution under neutral conditions than other aryl hydrazides (Scheme 3.2).[76] This substitution diverts the chemistry of isoniazid away from the formation of the acyl radical **3** and could therefore, under the right conditions, hinder the formation of **2** (Scheme 3.1).

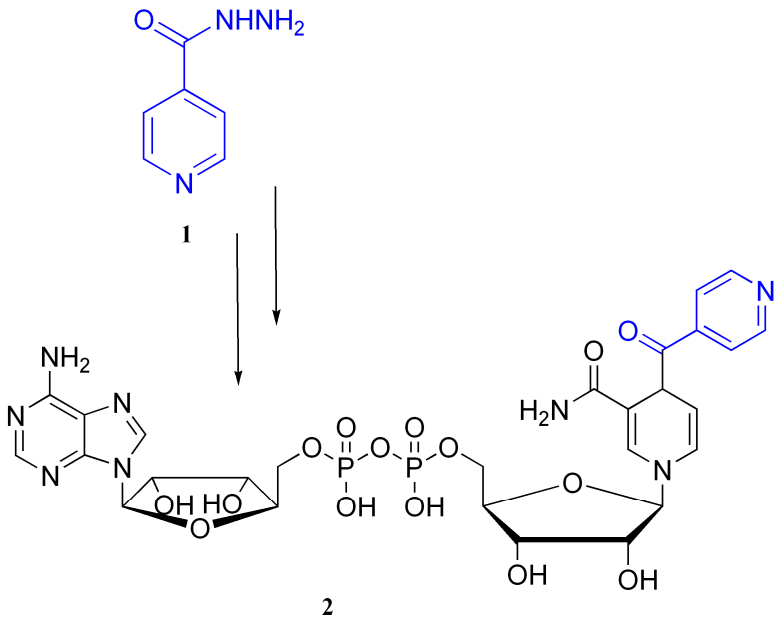

Scheme 3.1 Activation of isoniazid **1** to form the 'true drug' **2.**

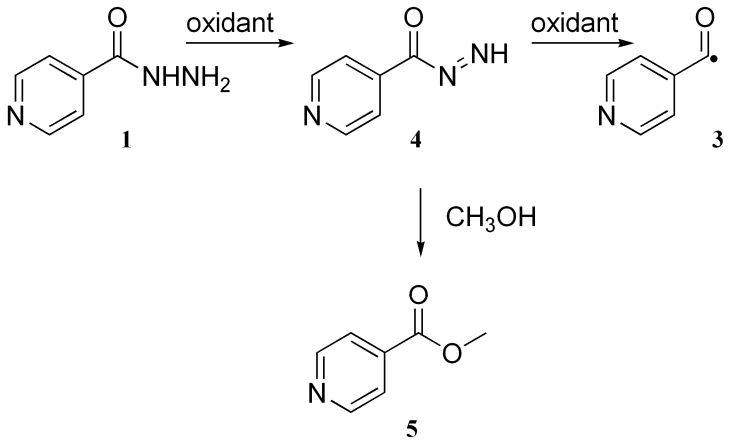

Scheme 3.2 Formation of the reactive intermediate **3** *via* the diimide

To the best of our knowledge, there have not been any mechanistic studies performed that examine the details of nucleophilic acyl substitution on the acyl diimide **4** to form the ester **5** (Scheme 3.2). Studies on the solvolysis of hydrazides under basic[34] and acidic[35, 37, 38] conditions do not involve oxidation to the corresponding acyl diimide and are therefore not directly related to this work.

The formation of esters as desired or unwanted products during the oxidation of hydrazides has been documented,[27, 29, 30] however these studies did not provide any real insight into the mechanism of their formation. In contrast, the solvolysis of esters has been investigated both experimentally and computationally[39-45] and we would expect similar mechanisms to be operating during the solvolysis of acyl diimides.

Solvent molecules play important stabilizing roles during base catalysed hydrolysis of esters[40, 42, 44, 45] and experimental[45] as well as computational[40] studies of acid catalysed solvolysis of esters suggest the involvement of solvent molecules in tetrahedral or cyclic intermediates.[40, 45] On this basis, we would expect a similar involvement of solvent molecules during the solvolysis of acyl diimide **4**.

We now present the results of a comprehensive study into the mechanism of nucleophilic acyl substitution of the acyl diimide formed by the oxidation of isoniazid, using computational chemistry. This study reveals that solvent molecules also play important roles in this process, providing the means for the cyclic transition state necessary for substitution to occur.

3.1 Stable intermediate

We began this investigation by examining the reaction of acyl diimide **4**, formed from isoniazid, with methanol. A range of pathways was explored including various oxidation and protonation states (see Appendix A) however many of these did not give stable intermediates as energy minima on their respective potential energy surfaces.

In exploring the various potential energy surfaces it was found that the tetrahedral species **6** (Figure 3.1) was a stable intermediate in that it proved to correspond to an energy minimum by frequency analysis. To investigate the mechanism for the formation of **6** a relaxed potential energy surface scan was performed in which the oxygen of a methanol molecule approached the carbonyl carbon of acyl diimide **4**.[105] During this approach a proton shift from methanol to the carbonyl oxygen was observed which led to the formation of tetrahedral intermediate **6** (Figure 3.1). We believe that this proton shift is responsible for the absence of any ionic or zwitterionic intermediates. The transition

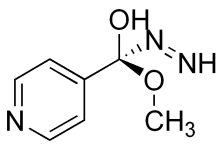

6

Figure 3.1 The stable intermediate formed by a proton shift during the methanol attack on the acyl diimide.

structure **7** (Figure 3.2, Figure 3.3) for this process was located and proved to correspond to a saddle point on the potential energy surface.

The energy of activation (E_a) for the formation of **7** is predicted to be 150.1 kJ mol^{-1} which, under the experimental conditions, would be expected to be prohibitive. As experimental studies suggest that this process is highly dependent on the amount of solvent present[76] a second methanol molecule was included to give the six-membered cyclic transition structure **8** (Figure 3.2, Figure 3.3). This proved to have a dramatic effect on the activation energy (E_a), which was calculated to be 84.1 kJ mol^{-1} for the reaction involving **8**, some 66 kJ

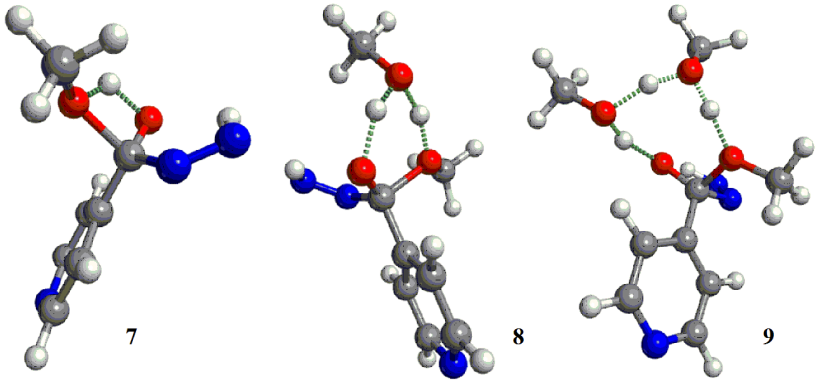

Figure 3.2 Optimized geometries of cyclic transition structures using one (**7**) , two (**8**) and three (**9**) methanol molecules.

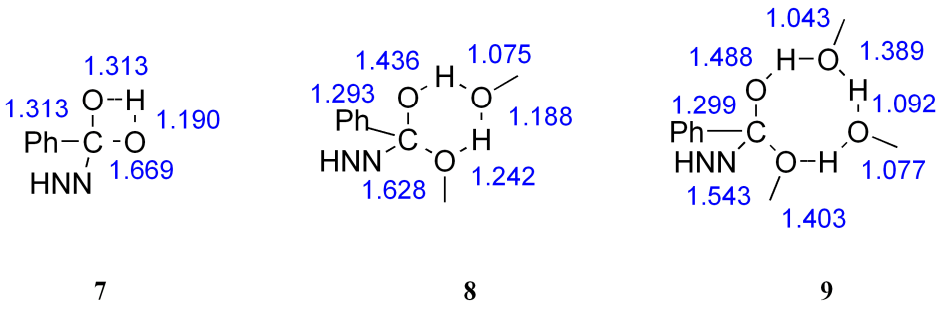

Figure 3.3 Bond lengths (Å) for transition structures **7**, **8** and **9**

Table 3.1 Transition structure energy barriers (kJ mol^{-1}), imaginary frequencies (cm^{-1}) and energies of the overall reaction (kJ mol^{-1})

Transition Structure	E_a	υ^i	ΔE
7	150.1	1648	12.4
8	84.1	1024	9.7
9	81.9	211	17.5

mol^{-1} lower than that calculated for **7**. Inclusion of a third methanol molecule to give an eight membered cycle (**9**, Figure 3.2, Figure 3.3) only reduced E_a by a further 2 kJ mol^{-1}. (See Table 3.1 for reaction barriers, imaginary frequencies and exothermicity.)

3.2 Quantum tunnelling

It is possible that the proton shift depicted in Scheme 3.3 is assisted by quantum tunnelling. Therefore we chose to use Eckart's[106] method to explore this possibility as it has been reported to give more accurate tunnelling correction coefficients than the method of Wigner.[107] The tunnelling coefficient is related to the energy of activation by Equation 3.1 where E_a* is the corrected activation energy, E_a the activation energy in the absence of

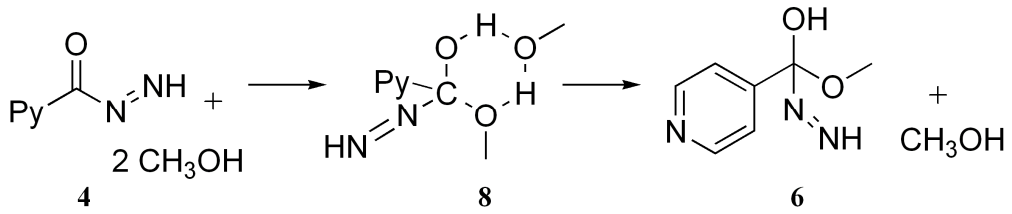

Scheme 3.3 The formation of intermediate **6** *via* a cyclic transition state **8**

tunnelling and κ the Eckart tunnelling coefficient.[108] The inclusion of the Eckart coefficient reduced the activation energy for the single solvent molecule process (**7**) by 9.1 kJ mol^{-1} and did not affect the result for the two and three methanol molecules by any significant amount (Table 3.2).[109] This strongly suggests that although tunnelling may occur it is not predicted to reduce the energy barrier of the process involving the four-membered transition structure **7** enough to allow it to be competitive. In the processes involving the six- and eight-membered transition structures, **8** and **9** there is very little lowering of the activation energy predicted by proton tunnelling calculations.

Equation 3.1

$$E_a^* = E_a - RT \ln \kappa$$

3.3 Reaction pathway to the final product

The experimentally observed product of the substitution reaction is methyl isonicotinate **5** (Scheme 3.2). The possibilities for the formation of **5** from the tetrahedral intermediate **6** include the loss of an $HN{=}N^-$ ion, addition of a proton to the imide portion followed by loss of imide, or fragmentation to lose H_2 and N_2. All of these options were investigated using gas phase calculations.

Table 3.2. Eckart tunneling coefficients and their effect on the activation energy of the hydrogen shifts

Transition structure	κ	E_a* (kJ mol^{-1})
7	94.9	141.0
8	2.3	83.8
9	1.2	81.6

Protonation of the imide portion of **6** was explored and calculations predict that this is the favoured pathway, as once protonation takes place at the nitrogen adjacent to the carbonyl, imide formation is a spontaneous process (**C** – **D** Figure 3.4 and Figure 3.5).

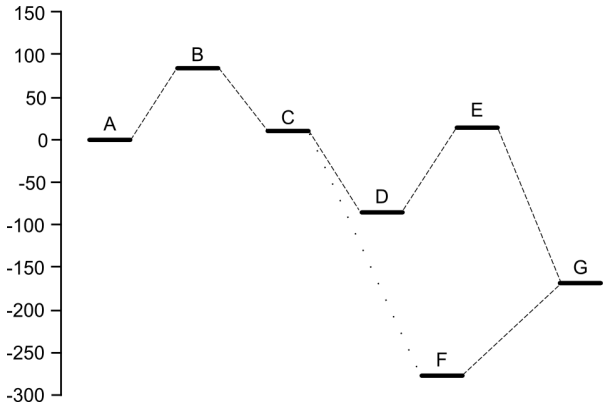

Figure 3.4 Energy diagram for the complete substitution mechanism in the gas phase, finishing with a loss of N_2(g) and H_2(g).

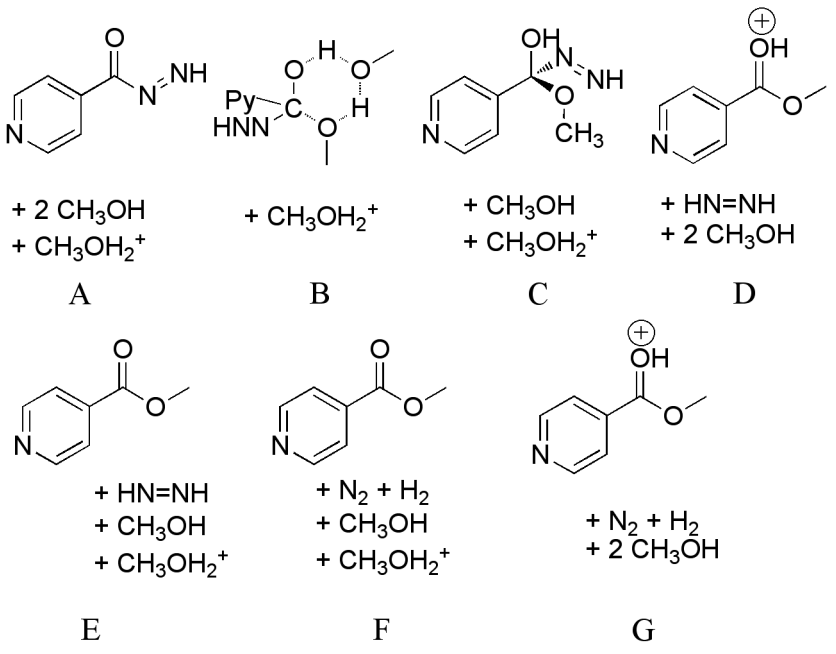

Figure 3.5 Explanatory figures relating to energy diagrams in Figures 3.4 and 3.6

Protonation at the nitrogen further from the carbonyl led to products that were 87 kJ mol^{-1} higher in energy than those in **D**.

The loss of the imide anion ($HN=N^-$) was found to correspond to a high energy pathway with a final energy of 1566 kJ mol^{-1} relative to the starting structure **A**. Although fragmentation to N_2 and H_2 led to a lower energy minimum (**F**), extensive searching of the potential energy surface did not locate a pathway which would lead to these products from the intermediate structure **6** (**C**).

Table 3.3 Relative energies of intermediates A – G as presented in Figures 3.4 and 3.6 in kJ mol^{-1}

	Figure 3.4	Figure 3.6
A	0.0	0.0
B	84.0	23.3
C	9.6	6.9
D	-82.7	-11.5
E	13.9	-60.6
F	-277.5	-204.1
G	-178.1	-

3.4 Addition of bulk solvent

The addition of a proton followed by loss of imide is not predicted to occur in the gas phase due to thermodynamic considerations (**E**, Figure 3.4 and Figure 3.5). This reaction is, however, solvent dependent and therefore bulk solvation calculations[110, 111] were performed to see if there was a stabilizing effect throughout the reaction. The resulting potential energy diagram showing the lowest energy pathway found is shown in Figure 3.6.[112] It can be seen that the inclusion of the bulk solvent has a stabilizing effect on the reaction pathway and that loss of imide is now predicted to be a thermodynamically favourable mechanism. The transition structure (**B**) in particular is stabilized relative to the reactants and products by the inclusion of the solvent and the energy barrier for this reaction is predicted to be reduced to 23.3 kJ mol^{-1} (Table 3.4).

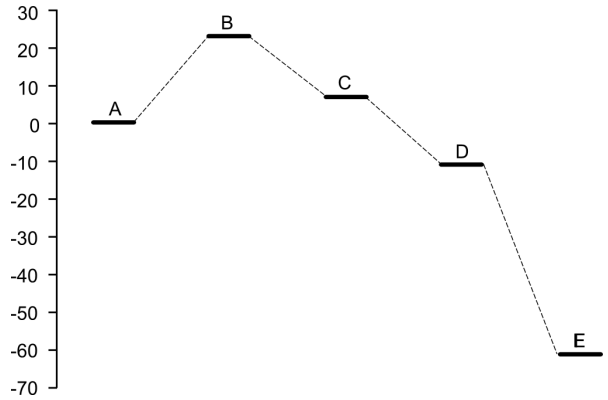

Figure 3.6 Energy diagram (kJ mol^{-1}) including CPCM calculations of solvent stabilizing effects, for the nucleophilic substitution by methanol of the diimide formed by oxidation of isoniazid.[107]

3.5 Electron donating and withdrawing effects

In experimental reactions, different aromatic groups show differing susceptibility to nucleophilic acyl substitution during the oxidation of hydrazides. Gas phase calculations for the two-solvent-molecule nucleophilic acyl substitution process were repeated to investigate the effect of electron withdrawing and donating effects. The results (in Table 3.4) indicate a typical Hammett susceptibility with the electron withdrawing *p*-nitro substituent enabling, and the electron donating *p*-methoxy substituent hindering, the process of substitution. While this is consistent with experimental results[76] to a point, it does not explain why a greater amount of substitution is observed experimentally with the pyridyl hydrazide (isoniazid, **1**).[76] However, when the bulk solvent effect is added it can be seen that the energy barrier for the transition state is less for isoniazid (**8**) than for all of the other substrates. This finding is consistent with experimental results which show that isoniazid is more prone to solvolysis by polar solvents than other hydrazides studied.[76]

These results may provide some insight into why some strains of *Mycobacterium*

Table 3.4. Calculated energy barriers for the formation of transition structures with various R groups (kJ mol^{-1}), and related imaginary frequencies (cm^{-1}) without and with CPCM solvation

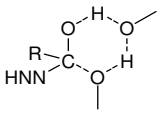

				With Solvent	
R=	E_a	ΔE	υi	E_a	ΔE
phenyl	94.1	20.1	1102	30.9	14.6
p-methoxyphenyl	102.5	29.4	1137	42.0	26.3
p-nitrophenyl	84.1	11.1	993	24.7	7.4
4-pyridyl (**8**)	84.1	9.7	1024	23.3	6.9

tuberculosis are resistant to isoniazid. It might be possible that as isoniazid undergoes oxidation in the bacterium, drug resistant strains are able to promote the solvolysis pathway, effectively interfering with the formation of the required acyl radical precursor and ultimately the 'true drug' **2**.

3.6 Conclusions

In conclusion, the nucleophilic acyl substitution of hydrazides under oxidative conditions was found to proceed through a six membered cyclic transition structure. This is a solvent dependent process requiring at least two solvent molecules in the transition state. The inclusion of the effect of various groups with differing electron demand showed that, in comparison, isoniazid is predicted to undergo this reaction in a facile manner. This computational outcome is supported by experimental results and may have implications in the understanding of resistance to isoniazid found in resistant strains of TB. As the imide formed from the oxidation (or activation) of isoniazid is prone to undergo nucleophilic acyl substitution it may be that resistant strains of TB promote this process in competition with the further oxidation to the free radical and therefore the formation of the 'true drug' (**2**). An understanding of the reactivity of isoniazid could play a role in future drug design.

Chapter 4.

Radical addition to pyridine and derivatives

As mentioned in Chapter 2, isoniazid **1** is a prodrug which is activated to form a reactive intermediate which then adds to the biological cofactor NAD^+ **3** to form the 'true drug' (**2**, Scheme 4.1).[6] This activation is carried out in the bacterium by the catalase-peroxidase enzyme KatG.[8, 12, 14, 15, 17, 103] Electron spin resonance (ESR) studies have suggested that free radical intermediates are involved in this process but limited structural information was obtained by these studies.[8] Chapter 2 reported studies supporting the hypothesis that the reactive intermediate formed is the acyl radical produced by oxidation of isoniazid.[76] An important step in the chemistry of isoniazid as a tuberculosis agent is the addition of this intermediate radical to the pyridinium ion in NAD^+ (**3**) to form the adduct **2** (Scheme 4.1) that is the true inhibitor of the bacterium.

Acyl radicals have traditionally been thought to be nucleophilic in their addition chemistry to alkenes.[47] Recent results, however, suggest that acyl radicals can also act as electrophilic

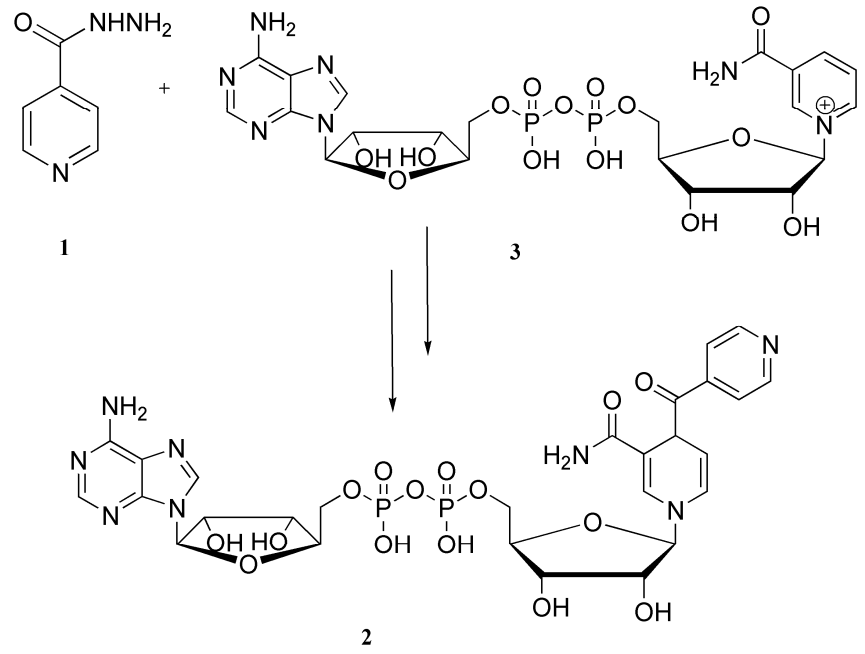

Scheme 4.1 The addition of isoniazid (**1**) to NAD^+ (**3**) to form the 'true drug' (**2**)

radicals depending on the electronic demand of the π-system undergoing addition, as well as deriving assistance during addition chemistry by masquerading as electrophiles.[49] We were interested in determining whether or not these interactions are also important in the reaction of acyl radicals generated from isoniazid described above. To that end, this chapter details our computational results for the addition of acetyl radicals (a model for the acyl radicals derived from isoniazid) to the pyridinium ion and pyridine (models for NAD^+ and its derivatives).

4.1 Reaction of an acetyl radical with the pyridinium ion

We began by examining the potential energy surfaces for the addition of acetyl radicals to the pyridinium ion. Structures **4 – 7** are the lowest energy transition structures found at the BHandHLYP/6-311G(d,p) level of theory for the reaction of the acetyl radical at the N1, C2, C3 and C4 positions of the pyridinium ring respectively (Figure 4.1). Separations (**r**, Figure 4.1) of the reacting units in these transition structures are predicted to be larger for

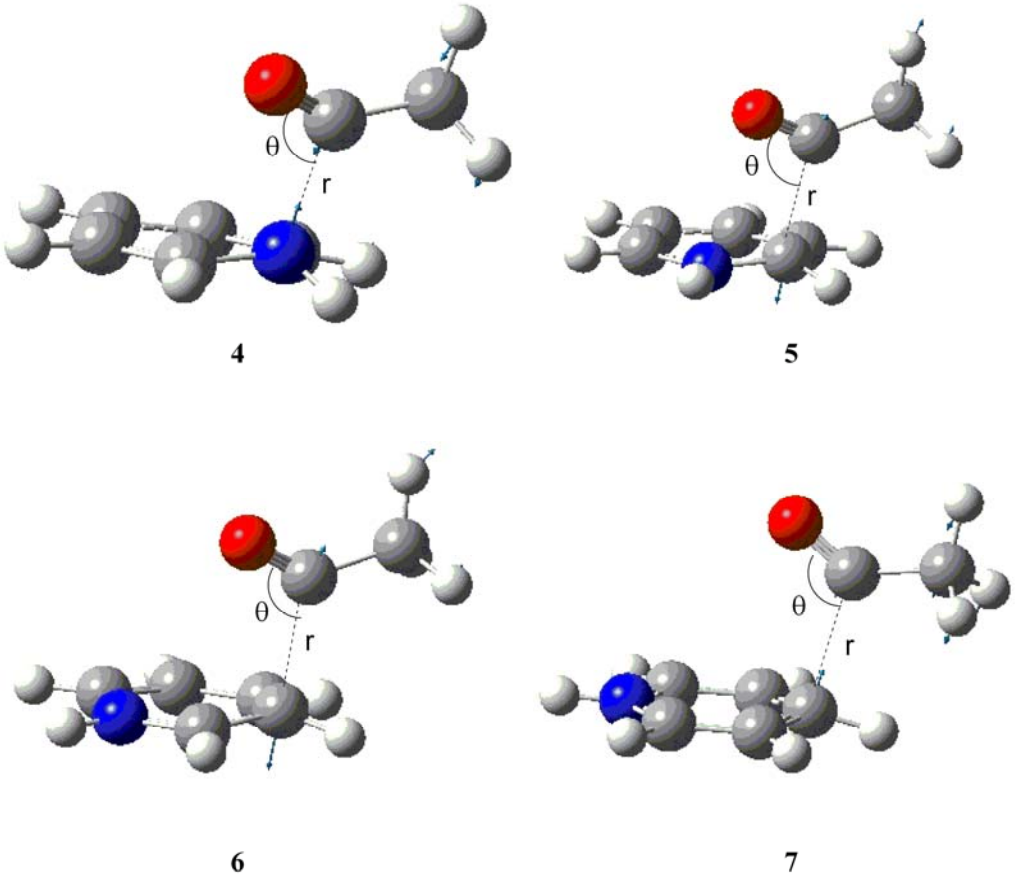

	r	θ
4	2.001Å	109.8°
5	2.161Å	110.3°
6	2.114Å	114.0°
7	2.215Å	112.1°

Figure 4.1 BHandHLYP/6-311G(d,p) optimized structures of transition states **3**, **4**, **5** and **6** for the homolytic addition of the acetyl radical to the pyridinium ion at the N1, C2, C3 and C4 positions.

attack on the carbon than on the nitrogen. For example, the attack on C2 (**5,** Figure 4.1) is predicted to have a separation, **r,** of 2.161 Å which is larger than 2.001 Å for the attack at the nitrogen (**4**, Figure 4.1). The angles (θ) around the carbonyl bond are predicted to change according to the electron density on the ring. The angle of attack is 109.8° for the nitrogen (**4**, Figure 4.1) where electron density is low as compared to 114.0° at C3 (**6**, Figure 4.1) where there is the greatest electron density.

Table 4.1 lists the energy barriers for the forward ($E_1^{\ddagger}$) and reverse ($E_2^{\ddagger}$) reactions of addition of the acetyl radical to a simple pyridinium ion (that is, protonated pyridine). Examination of these results reveals that the addition of the acetyl radical to the pyridinium ion is thermodynamically unfavourable.

Table 4.1 Calculated energy barriers in kJ mol^{-1} for the forward ($E_1^{\ddagger}$) and reverse ($E_2^{\ddagger}$) reactions of the acetyl radical with the pyridinium ion.

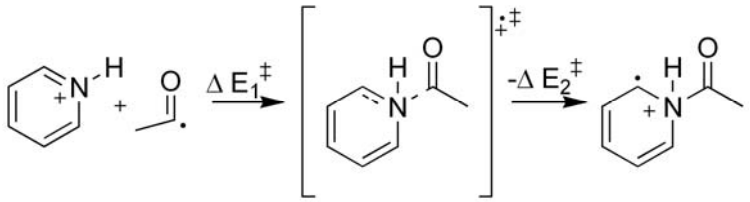

Transition Structure	$\Delta E_1^{\ddagger}$	$\Delta E_1^{\ddagger}$ + ZPVE	$\Delta E_2^{\ddagger}$	$\Delta E_2^{\ddagger}$ + ZPVE	ν_i
4	138.1	134.9	8.2	4.9	231*i*
5	72.4	72.2	46.3	41.7	262*i*
6	99.0	97.5	38.6	35.1	355*i*
7	68.9	69.1	19.0	16.6	182*i*

Inspection of the natural bond orbital (NBO) analysis data for the attack of the acetyl radical at the C2 position of the pyridinium ion (**5**) reveals an interaction between the radical (SOMO) and the π* system of the aromatic ring worth 264 kJ mol^{-1} (Table 4.2, Figure 4.3, **a**), evident in the set of *α* spin orbitals. An interaction worth 171 kJ mol^{-1} between the π system in the aromatic ring and the unoccupied *β* component of the SOMO of the radical is evident in the *β* spin set (Table 4.2, Figure 4.3, **b**).

Similar interactions are found in all positions on the pyridinium ring (Table 4.2, Figure 4.3, **a** and **b**) indicating that the acetyl radical is more nucleophilic than electrophilic in character when attacking this system. Figure 4.2 depicts representative transition state orbitals involved during the attack of the acetyl radical at the N1 and C2 positions at this level of theory.[113]

Table 4.2 Energies of interactions in kJ mol^{-1} between molecular orbitals for attack at the various positions on both the pyridinium ion and pyridine

Attack via transition state	**Fig 2** a **SOMO-π***	**Fig 2** b **π-SOMO**	**Fig 2** c **π_{ar}-$\pi^*_{C=O}$**
4	816	295	59
5	264	171	-[a]
6	274	252	-[a]
7	534	346	-[a]
9	506	600	-[a]
10	492	617	-[a]
11	294	319	-[a]

[a]Not observed in this transition structure.

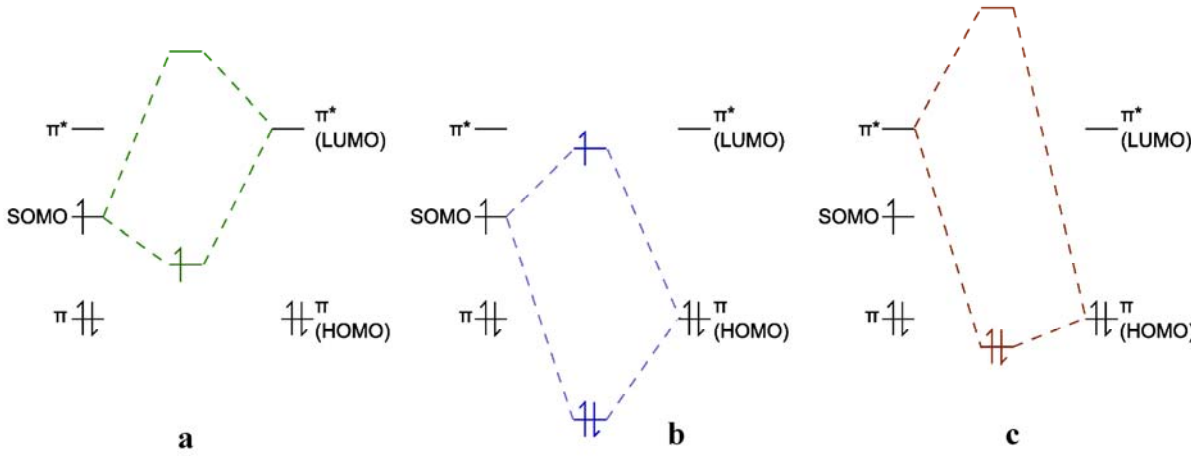

Figure 4.3 Representative energy diagrams for orbital interactions involved in the homolytic addition of the acetyl radical to the pyridinium ion through transition states **4**, (a, b and c) and **5**, **6** and **7** (a and b only). The attacks on pyridine through transition states **9**, **10** and **11** are also represented by a and b.

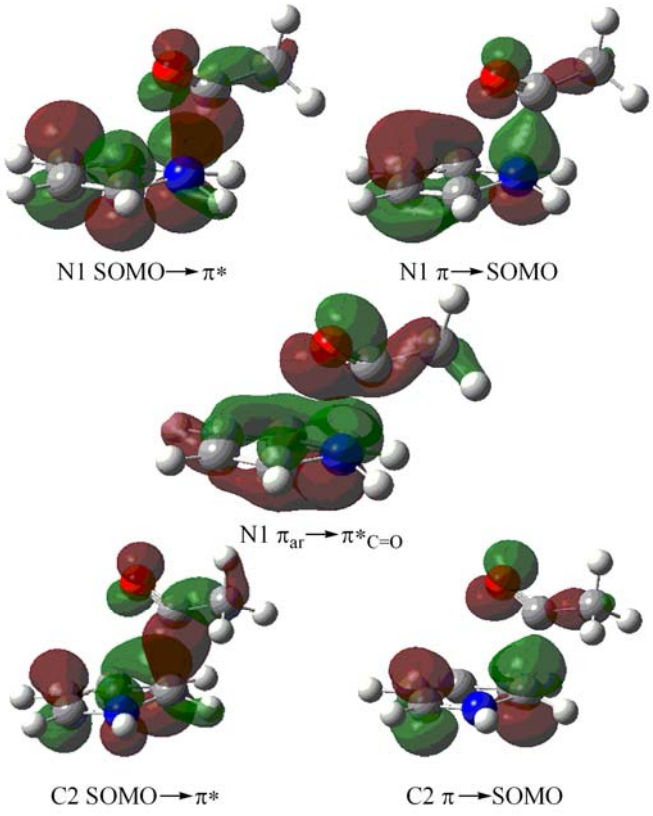

Figure 4.2 Key BHandHLYP/6-311G(d,p) generated molecular orbitals involved in the homolytic addition of the acetyl radical to the N1 and C2 positions of the pyridinium ion.[110]

When the acetyl radical attacks at the nitrogen of the pyridinium ion (**4**, Figure 4.1) there is a slightly more complex interaction pattern found in the NBO analysis. The SOMO→π* interaction in the set of α spin orbitals is worth 816 kJ mol^{-1} (Table 4.2, Figure 4.3**a**) and is the most significant interaction indicating again the nucleophilic nature of the radical in this circumstance. The π→SOMO interaction is evident in both the *α* (109 kJ mol-1) and *β* (187 kJ mol-1) spin sets (Table 4.2, Figure 4.3, **b**) and a further small $\pi_{aromatic}$→π*C=O interaction worth 42 kJ mol^{-1} (*α*) and 17 kJ mol^{-1} (*β*) is also present (Table 4.2, Figure 4.3, **c**).

4.2 Reaction of an acetyl radical with pyridine

Structures **8**, **9**, **10** and **11** (Figure 4.4) are the lowest energy transition structures found for the reaction of the acetyl radical at the N1, C2, C3 and C4 positions on the pyridine ring respectively. Once again the separation (**r**, Figure 4.4) of the reactants in the transition state is shorter for attack on the nitrogen (1.817 Å for **8** vs 2.087 Å for attack at the C2 position, **9**) and in this case the angle of attack is quite different (109.4 ° for **8** vs 119.6 ° for **9**). The angles of attack for the carbons follow the electron density of pyridine with the largest angle on the C2 and smallest on the C3 position.

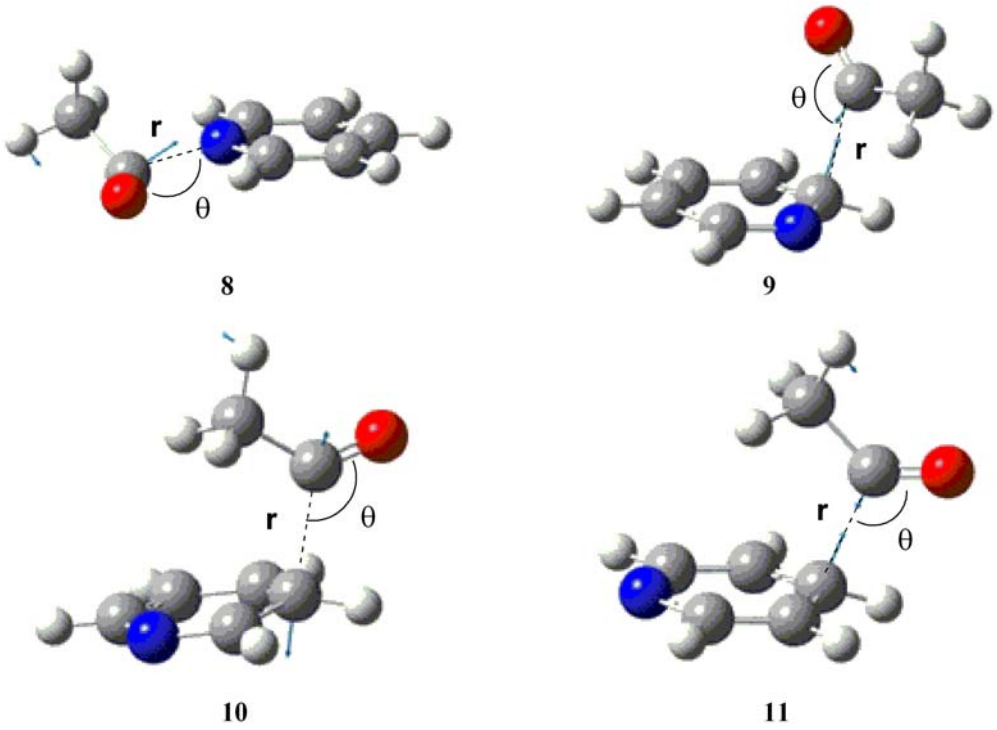

	r	θ
8	1.817Å	109.4°
9	2.087Å	119.6°
10	2.093Å	115.9°
11	2.087Å	116.0°

Figure 4.4 BHandHLYP/6-311G(d,p) optimized structures of transition states **8**, **9**, **10** and **11** for the homolytic addition of the acetyl radical to pyridine at the N1, C2, C3 and C4 positions respectively.

Table 4.3 Calculated energy barriers in kJ mol^{-1} for the forward ($E_1^{\ddagger}$) and reverse ($E_2^{\ddagger}$) reactions of the acetyl radical with pyridine.

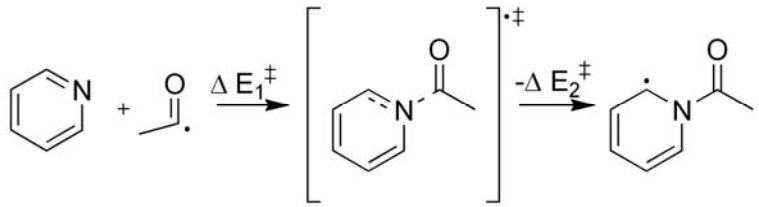

Transition Structure	$\Delta E_1^{\ddagger}$	$\Delta E_1^{\ddagger}$ + ZPVE	$\Delta E_2^{\ddagger}$	$\Delta E_2^{\ddagger}$ + ZPVE	ν_i
8	50.5	53.5	137.7	132.5	494*i*
9	64.4	63.0	73.2	68.6	479*i*
10	65.0	64.5	69.3	64.9	514*i*
11	58.5	59.0	61.6	57.4	461*i*

Table 4.3 lists the energy barriers for the forward and reverse reactions for addition of the acetyl radical to pyridine. Inspection of these data reveals that the forward reaction for addition of the radical to the nitrogen in pyridine ($\Delta E_1^{\ddagger}$, **8**) is 5.5 kJ mol^{-1} more favourable than addition at any other part of the ring, in that it has a calculated energy barrier of 53.5 kJ mol^{-1} compared to 59.0 kJ mol^{-1} for the nearest neighbour. The calculated energy barriers for the reverse reactions are similar to the forward barriers and it is only the

addition to the nitrogen on the pyridine that there is a significant preference for the forward reaction ($\Delta E_2^{\ddagger}$ **8** = 132.5 kJ mol^{-1}).[114]

Insight into the attack trajectory of the acetyl radical is found by investigating the transition state vector; this information is included as motion arrows in Figure 4.4. Whilst the vectors for the transition structures associated with addition at the C2, C3 and C4 are as expected for homolytic addition to a π-system (Figure 4.4), the vector for transition structure **8** is unusual in that it shows movement that corresponds to a rocking motion when visualized using a program such as GaussView (see Appendix A for avi file of this rocking motion). This signifies a more complex set of orbital interactions (Figure 4.4, Figure 4.5) and is similar to motion vectors associated with attack of the acetyl radical and the oxyacyl radical at the nitrogen end of imines.[49, 50]

The NBO data for attack of the acetyl radical at the C2 (**9**), C3 (**10**) and C4 (**11**) positions of pyridine reveals that the radical is now electrophilic in character. The C2 attack (**9**) gives a SOMO→π* interaction worth 121 kJ mol^{-1} in the set of α spin orbitals, while the β spin set furnishes a π→SOMO interaction worth 143 kJ mol^{-1}. Attack on the C3 (**10**) and C4 (**11**) positions show a similar effect (Figure 4.3, Table 4.2).

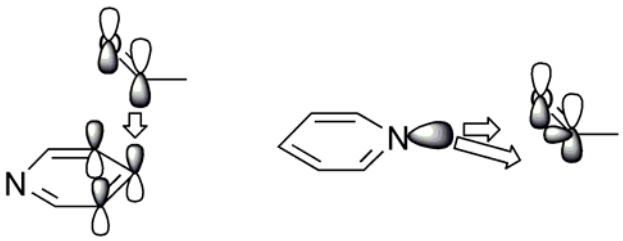

Figure 4.5 Alignment of orbitals for addition to pyridine. Arrows show interaction between the orbitals.

4.3 Multi-orbital interactions

The NBO data for the attack on the nitrogen of the pyridine ring (**9**) also shows the electrophilic character of this radical, and in addition indicates a reason for the rocking motion found in the transition state. In this case the lone pair of the nitrogen is involved in the bonding rather than the π system of the aromatic ring (Figure 4.6). The LP→ SOMO interactions are worth 377 kJ mol^{-1} (β spin set) and LP→LUMO interactions are 205 kJ mol^{-1} (α spin set) and 71 kJ mol^{-1} (β spin set), while the SOMO→π* interaction is only worth 75 kJ mol^{-1} (Figure 4.6). It is the combination of interactions that maximizes the energy gain from orbital interactions and is responsible for the rocking motion as described in Figure 4.4 and Figure 4.5. Figure 4.7 depicts the orbitals involved in these transition states for the attacks on pyridine.[115]

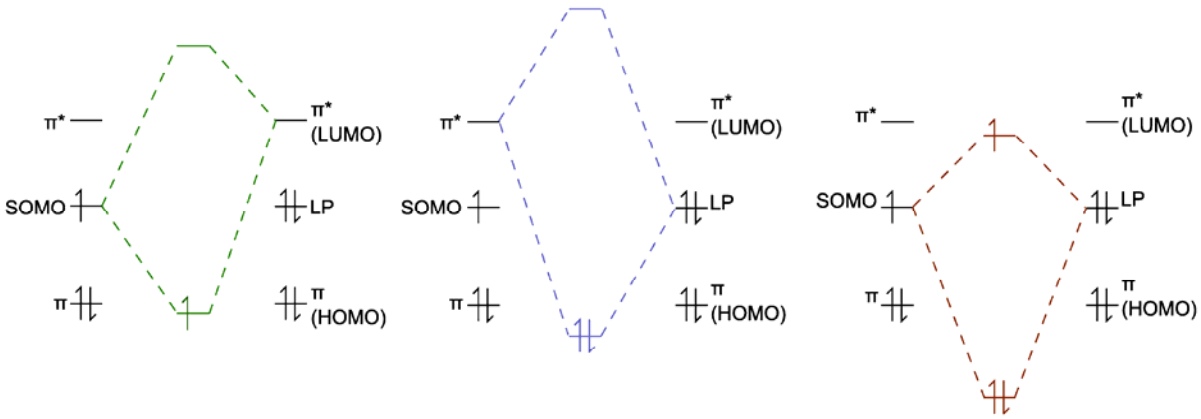

Figure 4.6 Representation of the orbital interactions between the acetyl radical and pyridine at the nitrogen

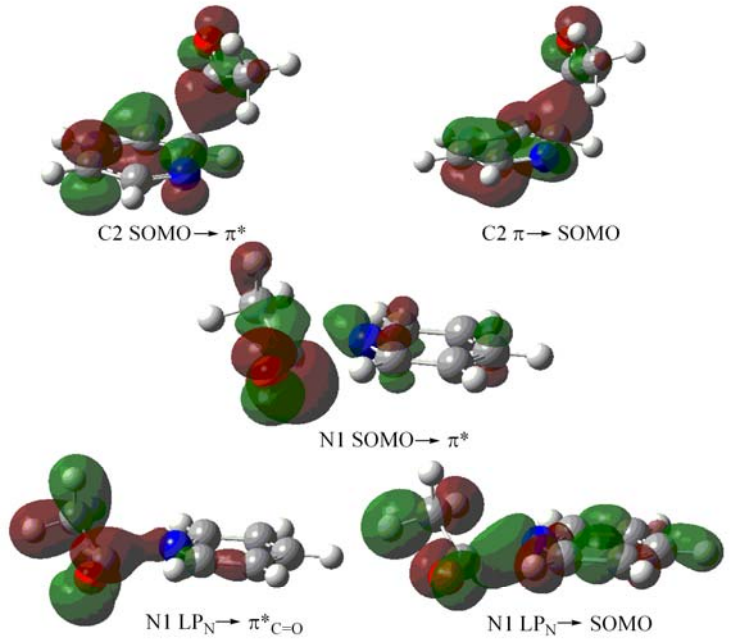

Figure 4.7 Key BHandHLYP/6-311G(d,p) generated molecular orbitals involved in the homolytic addition of the acetyl radical to the N1 and C2 positions of pyridine.[16]

4.4 NAD+ model

The calculated barriers for the addition of acetyl radical to pyridinium suggest that this reaction is endothermic. In order to model the formation of **2** more closely, we chose to examine the addition of an acetyl radical to the N-methylnicotinamide ion (**12**). This model (Scheme 4.2) was chosen as it more closely resembles the pyridinium ring system in NAD^+. These calculations reveal that this chemistry is predicted to be exothermic by 27.0 kJ mol^{-1}

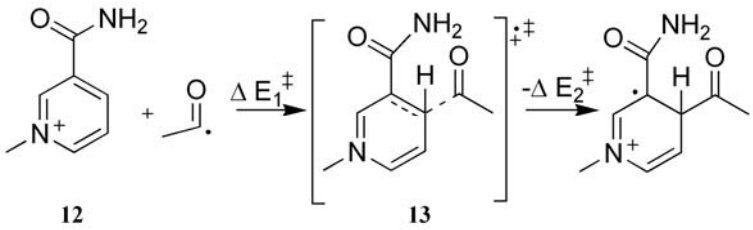

Scheme 4.2 The model for addition to NAD^+

compared to the reaction of protonated pyridine which is calculated to be endothermic by 52.3 kJ mol^{-1}. In addition, the energy barrier ($\Delta E_1^{\ddagger}$) is reduced to 21.4 kJ mol^{-1} for the reaction involving **12** (from 69.1 kJ mol^{-1} for the parent **7**). It is clear that the increased electron withdrawing ability afforded by the carbonyl of the amide group on the pyridinium ring is necessary for homolytic addition to occur readily. This observation is in agreement with the observation that the acetyl radical behaves in a nucleophilic manner with pyridinium ions (*vide supra*). It is also consistent with the data of Minisci and co-workers who report that the addition of an acyl radical to a pyridinium ring strongly activates the system for further substitution.[71]

4.5 Conclusions

In agreement with earlier calculations, the acetyl radical is calculated to be ambiphilic in nature, reacting as a nucleophilic radical with pyridinium ions, and as an electrophilic radical with pyridine. Interestingly, attack at the nitrogen atom in pyridine involves multiorbital interactions that are responsible for the unusual motion vectors associated with the transition state for this reaction. Incorporation of an electron-withdrawing amide functionality on the pyridinium ring accelerates these reactions and is likely to be responsible for the chemistry observed for NAD^+.

Chapter 5.

Radical addition to benzene and derivatives

5.1 Introduction

The formation of carbon-carbon bonds is integral to organic chemistry and the use of free radicals in synthesis is now accepted as key methodology that is particularly useful for preparing rings through homolytic addition to carbon-carbon double bonds. While alkyl radicals have been extensively explored in this regard,[116-119] acyl radicals are especially useful as cyclisation reactions can result in functionalized ring systems that include cyclic ketones, lactones and lactams.[47, 54-59] An example of this chemistry is depicted in Scheme 5.1.[90]

While acyl radicals can be generated readily from seleno-[60] or telluro-esters,[54, 61] the use of the free radical carbonylation methodology developed by Ryu and coworkers offers a convenient alternative starting from the usual suite of precursors, an example of which is provided in Scheme 5.2.[58, 59, 62]

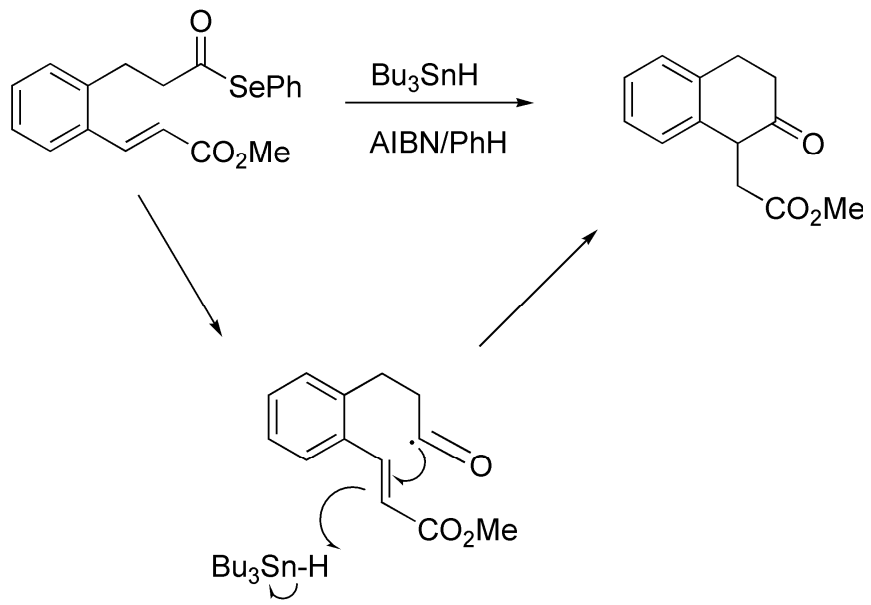

Scheme 5.1

In addition to the results reported in Chapter 4 from the investigation of the reactions of acetyl radicals with pyridine and derivatives, we now report the results of a computational investigation into the reactions of acetyl radicals with benzene, naphthalene and substituted benzenes with varying electron demand.

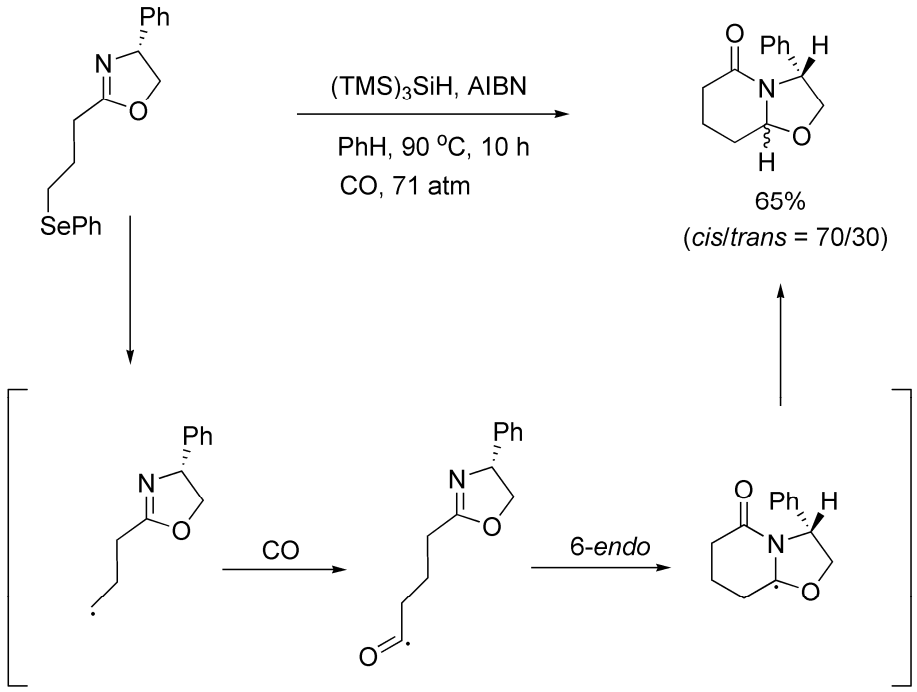

Scheme 5.2

Table 5.1 Calculated energy barriers[a] in kJ mol^{-1} and transition structure frequencies[b] for the reaction of an acetyl radical with substituted benzenes (**2**) and naphthalene (Scheme 5.3).

Transition state	Level of Theory	$\Delta E_1^{\ddagger a}$	$\Delta E_1^{\ddagger}$ + ZPVE[a]	$\Delta E_2^{\ddagger a}$	$\Delta E_2^{\ddagger}$ + ZPVE[a]	ν_{TS}[b]
2 (R=H)	HF/6-311G(d,p)	60.6	55.4	-87.9	-87.0	512i
	B3LYP/6-311G(d,p)	53.7	54.3	-46.3	-41.9	416i
	BHandHLYP/6-311G(d,p)	63.6	63.6	-70.4	-65.6	514i
	QCISD/6-311G(d,p)[c]	62.0	-	-79.1	-	-
	CCSD(t)/6-311G(d,p)[d]	56.6	-	-68.1	-	-
	CCSD(t)/6-311+G(d,p)[e]	54.2	-	-67.8	-	-
3	BHandHLYP/6-311G(d,p)	50.8	50.3	91.6	85.3	486i
4	BHandHLYP/6-311G(d,p)	57.1	56.5	78.3	72.2	487i
2 (R=*o*-NH_2)	BHandHLYP/6-311G(d,p)	65.3	64.8	85.3	78.1	578i
2 (R=*m*-NH_2)	BHandHLYP/6-311G(d,p)	63.1	63.1	69.7	65	511i
2 (R=*p*-NH_2)	BHandHLYP/6-311G(d,p)	71.3	69.6	75.8	70.2	565i
2 (R=*o*-CF_3)	BHandHLYP/6-311G(d,p)	58.5	58.9	73	66.9	461i
2 (R=*m*-CF_3)	BHandHLYP/6-311G(d,p)	62	61.9	66.2	61.4	487i
2 (R=*p*-CF_3)	BHandHLYP/6-311G(d,p)	58.2	58.6	71.9	66.5	473i

[a]Energies in kJ mol^{-1}. $\Delta E_1^{\ddagger}$ and $\Delta E_2^{\ddagger}$ are the "forward" and "reverse" energy barriers as depicted in Scheme 5.3.
[b]Frequencies in cm^{-1}.
[c]QCISD/6-311G(d,p)//BHandHLYP/6-311G(d,p)

5.2 Reaction of an acetyl radical with benzene and naphthalene

We began by examining the potential energy surface for the addition of an acetyl radical to benzene. Table 5.1 lists the calculated energy barriers at the levels of theory employed in this study for the homolytic addition of the acetyl radical to benzene (**1**, R = H) according to the reaction shown in Scheme 5.3. The barrier ($\Delta E_1^{\ddagger}$) for the forward reaction is predicted to be in the range of 52 – 64 kJ mol^{-1} depending on the level of theory. Except at the B3LYP/6-311G(d,p) level, the overall process is predicted to be slightly exothermic ($\Delta E_2^{\ddagger}$ = 65 – 88 kJ mol^{-1}). On the basis of the data provided in Table 5.1, we are confident that the BHandHLYP/6-311G(d,p) is a reliable DFT level of theory for the study of the reactions in this work, as it provides energy data for $\Delta E_1^{\ddagger}$ and $\Delta E_2^{\ddagger}$ most consistent with the highest (CCSD(T)) level of theory.

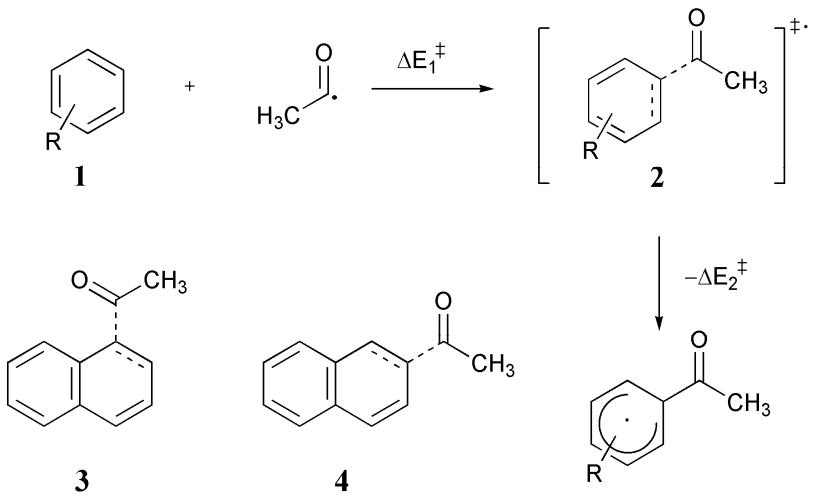

Scheme 5.3

Figure 5.1 depicts the structure of the transition state (**2**, R = H) for the addition of an acetyl radical to benzene calculated at the BHandHLYP/6-311G(d,p) level of theory. Inspection of Figure 5.1 reveals a distance for the forming bond in the transition structure of 2.089 Å associated with the attack trajectory, with a corresponding angle of 116.3˚. These data can

be compared with similar data obtained for the addition of an acetyl radical to pyridine (see Chapter 4) where separations of between 2.114 and 2.215 Å in the transition structures were obtained at the same level of theory, depending on the position of attack. Structural details for **2** at the remaining levels of theory can be found in Appendix A.

NBO analysis of transition structure **2** (R = H) reveals a $SOMO_{radical} \rightarrow \pi^*_{aromatic}$ interaction worth 273 kJ mol^{-1} evident in the α spin set, and a $\pi_{aromatic} \rightarrow SOMO_{radical}$ interaction worth 383 kJ mol^{-1} in the β spin set. These interactions are depicted in Figure 5.2 and listed in Table 5.2 together with others calculated as part of this study, and indicate that the acetyl radical is acting essentially as an ambiphilic radical in its reaction with benzene, with the electrophilic and nucleophilic components approximately equally contributing (58% and 42% respectively) to the overall transition state interaction energy.

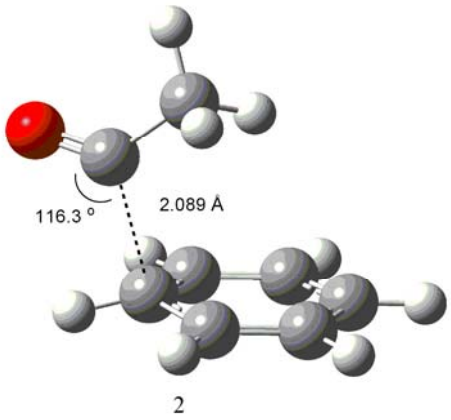

Figure 5.1 BHandHLYP/6-311G(d,p) Optimized structure for the transition state (**2**) involved in the reaction of acetyl radical with benzene

Table 5.2 BHandHLYP/6-311G(d,p) calculated NBO orbital interaction energies in kJ mol^{-1} for transition states **2**, **3** and **4**.

Transition State	SOMO-π*	π-SOMO
2 (R = H)	273	383
3	219	261
4	272	304
2 (R = *o*-NH_2)	231	399
2 (R = *m*-NH_2)	303	324
2 (R = *p*-NH_2)	262	398
2 (R = *o*-CF_3)	295	262
2 (R = *m*-CF_3)	289	324
2 (R = *p*-CF_3)	269	334

The reaction of an acetyl radical with naphthalene is calculated to be more favourable than the corresponding reaction with benzene, with BHandHLYP/6-311G(d,p) calculated energy barriers ($\Delta E_1^{\ddagger}$) of about 50 and 57 kJ mol^{-1} (ZPVE included) for attack at the C1 and C2 positions respectively. In addition, these reactions are also calculated to be more exothermic, with energy barriers ($\Delta E_2^{\ddagger}$) for the fragmentation of the adduct radical of 85

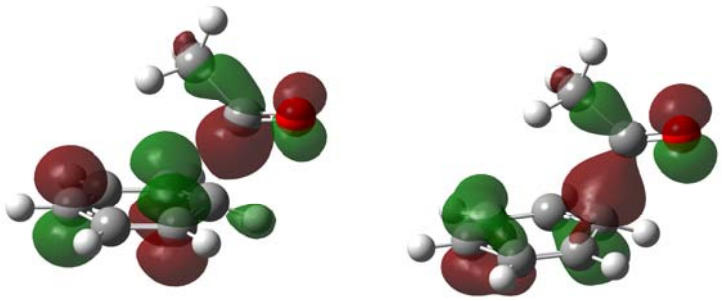

Figure 5.2 Key BHandHLYP/6-311G(d,p) generated molecular orbitals involved in the homolytic addition of acetyl radical to benzene.

and 72 kJ mol^{-1} (ZPVE included) (Table 5.1). This is not surprising given the inherent aromaticity differences between benzene and naphthalene.[120] Once the transition structure is formed the naphthalene will still have a 6π aromatic system remaining whereas the transition structure for the addition to benzene completely disrupts the aromatic structure (Scheme 5.3).

Figure 5.3 depicts the structures of transition states (**3**, **4**) for the addition of an acetyl radical to the C1 and C2 positions of naphthalene, respectively. Inspection of Figure 5.3 reveals a transition state separation for the forming bond of 2.164 Å in the transition structure for the C1 position and 2.129 Å in the transition structure for the C2 position, with corresponding angles of 116 ° and 117°. NBO analysis of transition structures **3** and **4** reveals that the acetyl radical also reacts predominantly as an ambiphilic radical at both positions of naphthalene, but the contribution of the π → SOMO interaction is somewhat less (54% for attack at C1 and 53% for attack on C2 of the total interaction energy) than that observed in the case of benzene (Table 5.2).

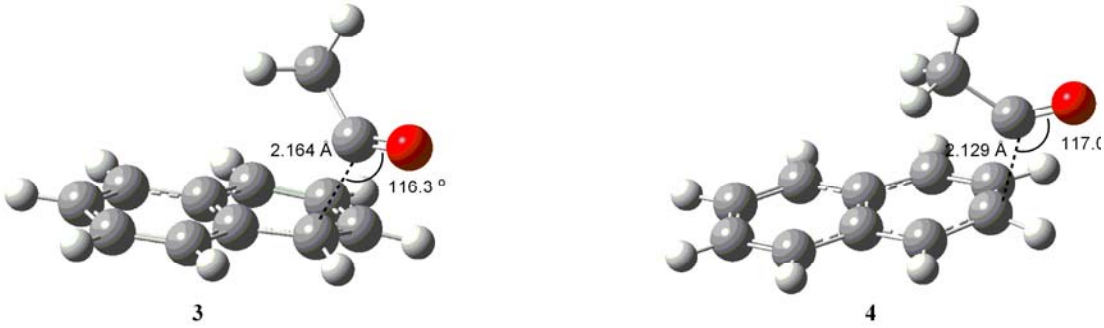

Figure 5.3 BHandHLYP/6-311G(d,p) optimized structures for transition states **3** and **4** involved in the reaction of acetyl radical with naphthalene**.**

We are only aware of one example in which an acyl radical undergoes homolytic addition to a benzene ring (**5**), and one example involving a naphthalene ring (**6**) (Scheme 5.4). Both examples involve intramolecular addition and both transformations proceed in low yield.[72, 73] Consistent with this, BHandHLYP/6-311G(d,p) + ZPVE calculations predict that the ring-closure of **5** proceeds with a lower energy barrier than that predicted for the intermolecular addition of an acetyl radical to benzene. The energy barrier is about 54 kJ mol^{-1}, compared to 64 kJ mol^{-1} for benzene, and the exothermicity is also increased by about 20 kJ mol^{-1} to 22 kJ mol^{-1}; the transition structure (**7**) involved in the cyclization of **5** is depicted in Figure 5.4.

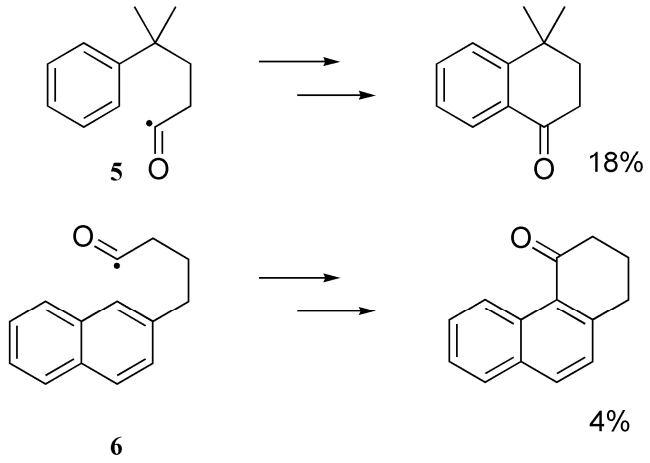

Scheme 5.4

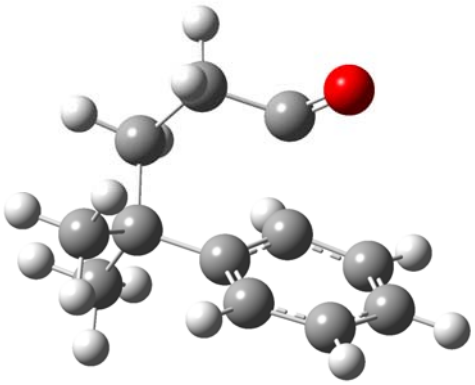

Figure 5.4 BHandHLYP/6-311G(d,p) optimized structure for the transition state (**7**) involved in the cyclization of radical **5.**

5.3 Reaction of an acetyl radical with aniline and trifluoromethylbenzene

We next chose to explore the effect of electron-donating (-NH_2) and electron-withdrawing (-CF_3) substituents on the overall chemistry described above. To that end, the potential energy surfaces for the reaction of an acetyl radical at the *ortho*, *meta* and *para* positions in aniline and trifluoromethylbenzene were examined. Figure 5.5 depicts the structures of transition states **2** (R = *p*-NH_2, *p*-CF_3) for the attack at the *para* positions in both molecules; the remaining structures **2** can be found in Figure A1 of Appendix A and are similar to those shown in Figure 5.5. Inspection of Figure 5.5 reveals separations and angles of the forming bond in the transition structures similar to those observed for the other transition structures in this study (**2**, R = H; **3**, **4**) at about 2.1 Å and 116 ° respectively.

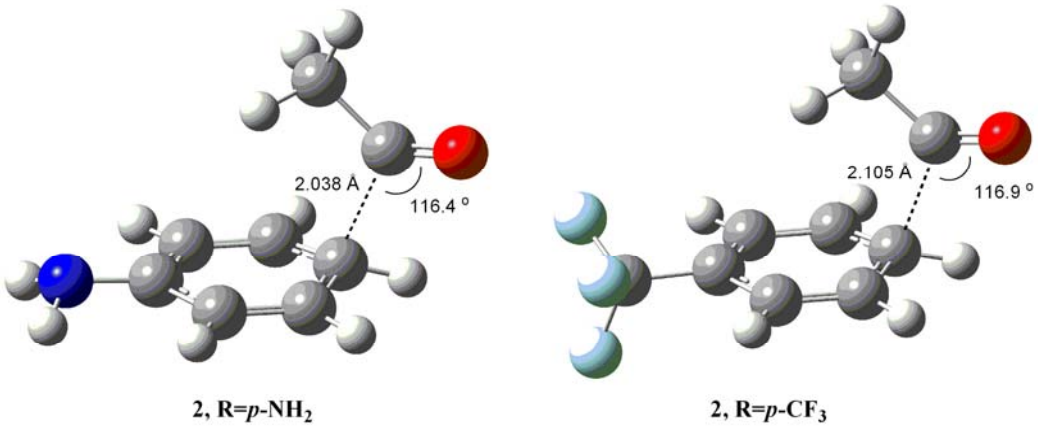

Figure 5.5 BHandHLYP/6-311G(d,p) optimized structures for the transition states **2**, R = *p*-NH_2 and R = *p*-CF_3 involved in the reaction of acetyl radical with aniline and trifluoromethylbenzene.

Table 5.1 lists the energy barriers for the forward ($\Delta E_1^{\ddagger}$) and reverse ($\Delta E_2^{\ddagger}$) reactions for attack at each position in both systems (R = NH_2, CF_3). It is interesting to note that in the case of the electron-rich system, aniline, the energy barriers for the attack at the *ortho* and

meta positions are very similar to that of the parent system, benzene, with attack at the *para* position slightly less favoured by about 7 kJ mol^{-1}. In contrast, the electron-deficient system, trifluoromethylbenzene appears to benefit slightly from inclusion of the withdrawing group at the *ortho* and *para* positions, with barriers ($\Delta E_1^{\ddagger}$) for the forward reaction some 5 kJ mol^{-1} lower than that for the reaction with benzene itself. Once again, the *meta* position is unaffected.

Not surprisingly, the data in Table 5.2 reveal that the acetyl radical is a more electrophilic radical when it reacts at the *ortho* and *para* positions in aniline than in its reaction with benzene, while in its reaction with the electron-deficient system (R = CF_3), the radical begins to prefer to react in a slightly nucleophilic manner at the *ortho* position, with E(SOMO → π*) > E(π→ SOMO). Despite these trends, the acetyl radical is still predominantly ambiphilic in nature toward the substituted benzenes in this study. The electrophilic and nucleophilic components of the overall interaction energy for reaction at the *meta* positions in both aniline and trifluoromethylbenzene are essentially equal.

5.4 Multi-orbital interactions

As we have been interested in multi-component orbital interactions during reactions involving acyl and related radicals,[48-51, 58, 121-124] we were keen to observe such interactions in the chemistry discussed above. NBO analysis at the BHandHLYP/6-311G(d,p) level of theory of each transition state (**2** – **4**) failed to locate the typical $\pi_{aromatic} \rightarrow \pi^*_{acyl}$ or LP → π^*_{acyl} interaction usually observed when the acetyl radical masquerades as an electrophile. It should be noted that this interaction is observed when the acetyl radical reacts with aminoethylene;[49] the lack of this interaction in the reaction involving aniline is attributed to the aromatic nature of the π-system undergoing reaction.

5.5 Conclusion

The acetyl radical is calculated to react as an ambiphilic radical in its reactions with benzene, naphthalene, aniline and trifluoromethylbenzene. Energy barriers for homolytic addition range from 50.3 kJ mol^{-1} for attack at C1 of naphthalene, to 69.6 kJ mol^{-1} for attack at the *para* position in aniline. NBO analysis reveals that the acetyl radical is most electrophilic (63%) in its reaction at the *ortho* position in aniline, and least (47%) in its reaction at the *ortho* position in trifluoromethylbenzene, compared with benzene (58%). Somewhat surprisingly, in none of the reactions in this study did the NBO analysis reveal any multi-component orbital interactions. This work could be extended to investigation of the addition of acyl radicals to aromatic rings of varying electron demand through tethered systems such as **5** using hydrazides as acyl radical precursors.

Chapter 6.

Investigation of the mechanism of the McFadyen-Stevens rearrangement

6.1 Introduction

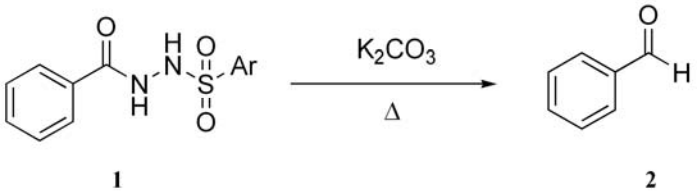

Scheme 6.2

As mentioned previously, the McFadyen-Stevens rearrangement is the conversion of an arylsulfonylhydrazide **1** to an aldehyde **2** under alkaline conditions (Scheme 6.2) .[74] This is an unusual reaction leading to an overall reduction and has been proposed to occur through a multi-step mechanism that includes the involvement of a diimide intermediate (**3**, Scheme 6.1, Scheme 6.4) .[75] This diimide intermediate is also postulated to form upon oxidation of the corresponding hydrazide (Scheme 6.1) and is the precursor for the formation of acyl radicals.[76] We wished to exploit the McFadyen-Stevens reaction for the

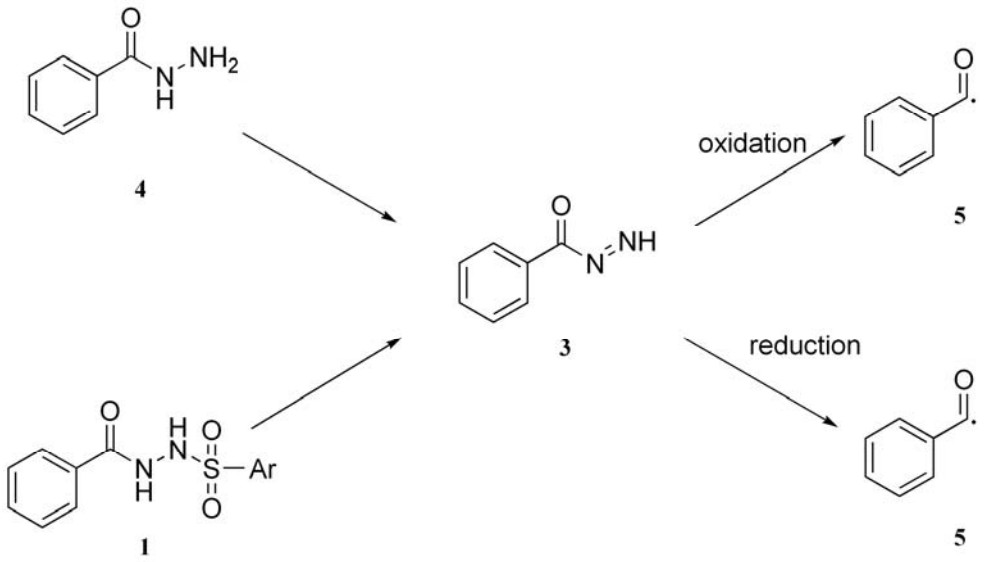

Scheme 6.1

formation of the diimide intermediate (**3**) by non-oxidative means to investigate if a reducing agent could then form the same acyl radical intermediate (**5**, Scheme 6.1). This would mimic the possible involvement of NADH in the activation of isonaizid. We propose an alternative activation pathway for isoniazid: that KatG oxidises isoniazid only as far as the diimide intermediate **3**, then this intermediate can be reduced to form the acyl radical **5** by NADH, before addition to the resulting radical cation ($NAD^{\cdot+}$) (Scheme 6.3). However, before attempting such experiments we decided to investigate the mechanism of the McFadyen-Stevens rearrangement because of the unusual mechanism proposed in the literature. Herein we report our results elucidating further the McFadyen-Stevens mechanism.

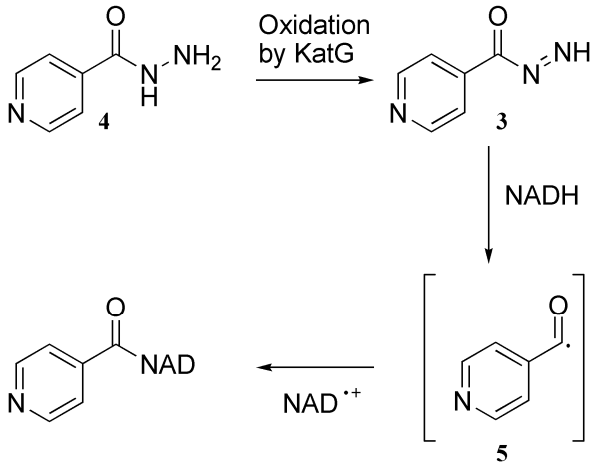

Scheme 6.3

6.2 Investigation of the existing mechanism in the literature.

To the best of our knowledge, the most recent mechanism proposed for the McFadyen-Stevens rearrangement in the literature was that outlined by Matin, Craig and Chan[75] (Scheme 6.4) that built on the work of Brown *et al.*[125] and Campaigne *et al.*[126] The mechanism is complex, proceeding through nine separate intermediates or transition

states. Two of these transition states are highly strained three co-ordinate structures (**6** and **7**, Scheme 6.4) that we would envisage would be very high in energy due to ring strain.

The first step in the proposed mechanism (shown in Scheme 6.4) involves the deprotonation of the nitrogen adjacent to the sulfur group on the sulfonyl hydrazide **8** to give the corresponding anion (**9**). This proton was chosen by the authors as the most acidic proton following solubility experiments involving diacylhydrazides and bis(benzenesulfonylhydrazides) in alkaline solutions.[75] The resulting anion **9** is proposed to fragment to form the nitrene **10** and an aryl sulfonyl anion. Proton transfer through transition state **6,** the first of the highly strained three-centred transition states, leads to the diimide intermediate **3,** which again undergoes proton transfer through **11** to give a zwitterion **12**. Loss of N_2 is proposed to give the hydroxycarbene intermediate **13** which abstracts the proton from the oxygen via the sterically strained transition state **7** finally resulting in the aldehyde **2**.

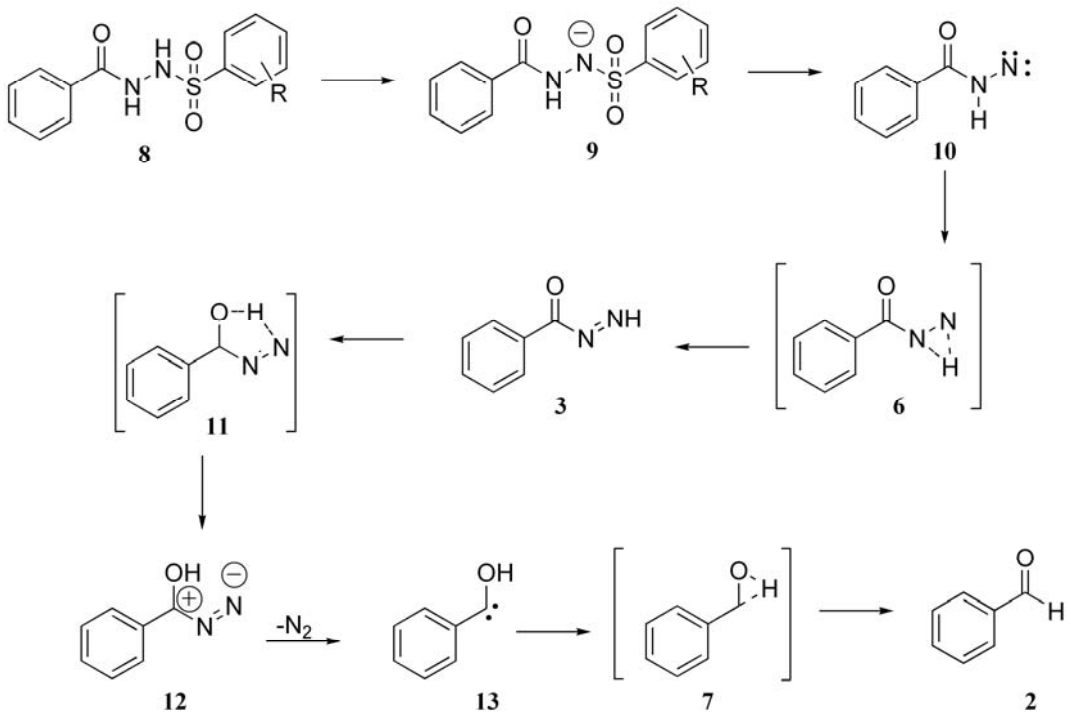

Scheme 6.4

As several highly strained intermediates are proposed in the mechanism outlined above we decided to investigate its plausibility using computational chemistry. For our calculations on this mechanism we used the *o*-nitrophenyl group as the aromatic group on the sulfonyl. This aromatic group has been utilised experimentally and it has been demonstrated to react at a much lower temperature than the toluene sulfonyl group (80 °C as opposed to 170 °C).[23]

Calculations were performed at several levels of theory (see Table 6.1). Geometry optimisations and vibrational frequencies were calculated for each level of theory using a 6-31G(d) basis set, followed by single point calculations using a 6-311+G(d,p) basis set. A strong dependency on level of theory was observed. Some structures for transition states were not able to be found at some levels of theory, and in addition, the relative energies vary greatly between levels of theory (see Table 6.1). Benchmarking (see Chapter 7)

Table 6.1 Results of **c**alculations for the mechanism of Matin Craig and Chan[75] as outlined in Scheme 6.4 E in kJ mol^{-1}

	Reaction Coordinate	B3LYP	M05	B97D	ωB97XD	MP2
A	Anion **9**	0.0	0	0.0	0.0	0.0
B	Fragmentation to give **10**	96.5	134.9	120.9	138.7	228.8
C	hydrogen shift – nitrogens (ts **6**)	304.7	331.6	322.8	354.9	415.2
D	Diimide **3**	18.9	60.3	48.9	59.4	115.2
E	hydrogen shift to oxygen (ts **11**)	170.1	-[a]	-[a]	228.3	-[a]
F	Zwitterion **12**	61.6	89.2	79.1	109.2	159.5
G	Carbene **13**	184.5	64.6	56.7	68.0	97.2
H	hydrogen shift to carbon (ts **7**)	304.5	174.8	159.7	190.7	205.7
I	Aldehyde **2**	-27.2	-147.1	-158.6	-143.7	-127.8

[a]Transition structure not found at this level of theory

suggested B3LYP and M05 to be the best levels of theory to use for these calculations and the results from these levels of theory will be discussed more fully in this chapter.

The resulting calculations confirmed the high energy of transition structures **6** and **7** (Table 6.1, Figure 6.1). B3LYP puts the barrier for the formation of **6** at 304.7 kJ mol^{-1} compared to **9,** M05 has a similar barrier of 331.6 kJ mol^{-1} for the formation of **6**. Again, transition structure **7** was also high in energy at the two levels of theory; B3LYP gave an energy for **7** of 304.5 kJ mol^{-1} relative to **9** where the M05 barrier was lower at 174.8 kJ mol^{-1}. These barriers are far too high for this reaction to proceed under the experimentally relevant reaction conditions. Therefore the reaction mechanism proposed by Matin, Craig and Chan[75] is very much in doubt.

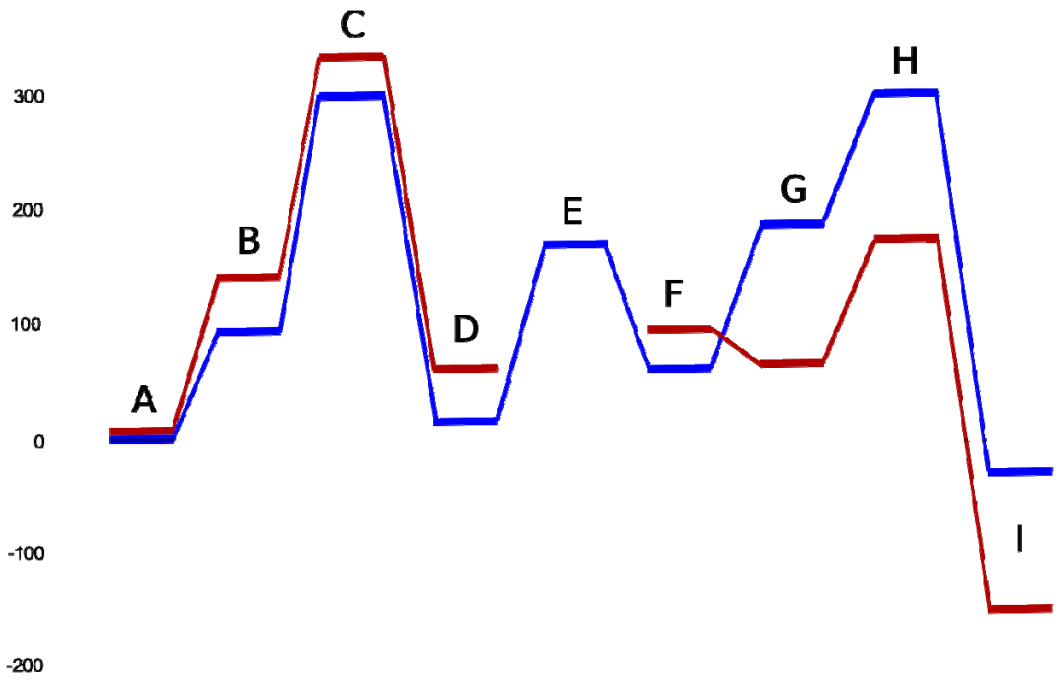

Figure 6.1 Results of calculations on the mechanism proposed by Matin Craig and Chan[75] outlined in Scheme 6.4. Colour scheme: B3LYP = blue and M05= red. Values (in kJ mol^{-1}) are found in Table 6.1

Calculations at both B3LYP and M05 predict that this reaction is exothermic, however B3LYP gives a final energy for the reaction products aldehyde **2**, N_2, and the sulfonyl anion as -27.2 kJ mol^{-1} relative to the starting anion **9** whereas M05 has a much lower final energy at -147.1 kJ mol^{-1} and compares better to other levels of theory used (see Table 6.1). While there is some difference in the outcome of calculations between the levels of theory, all our calculations for the Matin Craig and Chan[75] mechanism at all levels of theory have barriers to reaction that are too high for the reaction to proceed.

6.3 Exploration of hydrogen tunnelling

It is possible that hydrogen tunnelling would occur at transition states **6** and **7** to give a lowering of these high barriers. We chose to use Eckart's[106] method to explore this possibility as it has been reported to give more accurate tunnelling correction coefficients than the method of Wigner.[107] Truhlar's MPW1K functional[127, 128] was utilised for the tunneling calculations as it is reported to give more accurate vibrational frequencies.[129] Accordingly the geometries of **6** and **7** were reoptimized and frequencies calculated at the MPW1K/6-31+G(d,p) level of theory.[129]

The tunnelling coefficient is related to the energy of activation by Equation 6.1 where E_a^* is the corrected activation energy, E_a the activation energy in the absence of tunnelling and κ the Eckart tunnelling coefficient.[108] The lowering of the transition state barriers due to tunnelling was 40 kJ mol^{-1} for **6** and 25 kJ mol^{-1} for **7**. This is significant but does not lower barriers enough for this mechanism to be plausible.

Equation 6.1

$$E_a^* = E_a - RT \ln \kappa$$

6.4 Postulated nitrene intermediate

Another step of the Matin, Craig and Chan mechanism[75] requiring additional focus was the initial fragmentation of the anion (**9**) to form the nitrene (**10**) (see Scheme 6.4). For nitrenes the singlet state is often higher in energy than the triplet.[130, 131] Our calculations of both the singlet and triplet state of the nitrene **10** show that it is more stable in the singlet state (Table 6.2). The highest level of theory used for this investigation was CCSD(T)[132] where the singlet is more stable by 33.8 kJ mol^{-1} than the triplet (Table 6.2). Computational and experimental studies by Autrey *et al*. suggest that benzoyl nitrene (PhCON:), a nitrene closely related to **10**, also has a singlet ground state.[130]

Table 6.2 Results of calculations on the nitrene intermediate (**10**, Scheme 6.4) showing the difference in stability between the singlet and triplet states.

Singlet more favourable	B3LYP	MP2	CCSD(T)	B97D
by kJ mol^{-1}	29.3	50.5	33.8	29.4

6.5 Solvation calculations

As the McFadyen-Stevens rearrangement is performed in a polar solvent (ethanol) it is possible that the solvent may have a stabilizing effect on intermediates in the reaction. A conductor-like polarizable continuum model (CPCM)[110, 111] was used to evaluate the electrostatic effect of the bulk solvent on the energies of intermediates in the mechanism outlined in Scheme 6.4. Ethanol was specified as the solvent to complement the use of ethanol in the experimental work.

Table 6.3 Results of calculations for the reaction mechanism proposed by Matin, Craig and Chan,[75] as outlined in Scheme 6.4, at the B3LYP and M05 levels of theory, with added CPCM calculations to include the electrostatic effect of ethanol as solvent. E in kJ mol^{-1}

	Reaction Coordinate	B3LYP	B3LYP with solvent	M05	M05 with solvent
A	Anion **9**	0.0	0.0	0.0	0.0
B	Fragmentation to give **10**	96.5	61.3	134.9	108.1
C	hydrogen shift – nitrogens (ts **6**)	304.7	259.0	331.6	293.8
D	Diimide **3**	18.9	-14.7	60.3	35.0
E	hydrogen shift to oxygen (ts **11**)	170.1	133.4	-[a]	-[a]
F	Zwitterion **12**	61.6	27.6	89.2	63.2
G	Carbene **13**	184.5	-48.8	64.6	36.1
H	hydrogen shift to carbon (ts **7**)	304.5	109.4	174.8	154.1
I	Aldehyde **2**	-27.2	-227.5	-147.1	-173.3

[a]transition structure not found at this level of theory

The solvation calculations gave results that lowered the energies of intermediates by up to 200 kJ mol^{-1} at the B3LYP level of theory and approximately 30 kJ mol^{-1} for all intermediates and transition structures at the M05 level of theory. However, the reaction barriers to transition states **6** and **7** remained too high regardless of level of theory for the mechanism to be plausible under the relevant experimental conditions (Table 6.3).

6.6 E1cB type elimination

In searching for an alternative pathway to allow lower barriers for the formation of the aldehyde **2** from the hydrazide **8** (Scheme 6.4), we investigated the anion **14** (Scheme 6.5) which would be formed by deprotonation of the nitrogen closer to the carbonyl group. The formation of **14** would allow the reaction to proceed to the diimide **3** by an E1cB (conjugate base – that is an elimination from the anion) type elimination through transition state **15** (Scheme 6.5). This pathway was calculated at the relevant levels of theory and results are displayed in Table 6.4, Scheme 6.5 and Figure 6.2.

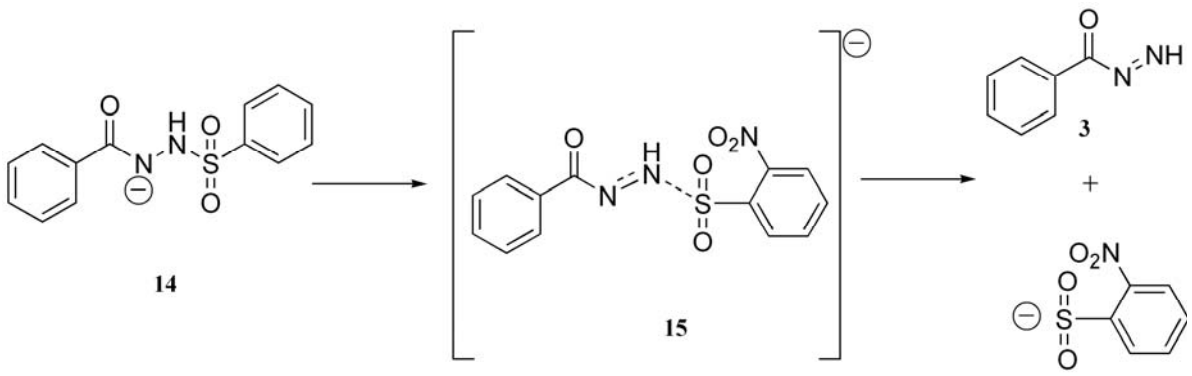

Scheme 6.5

Table 6.4 Results of **c**alculations for E1cB elimination outlined in Scheme 6.5. E in kJ mol^{-1}

	E1cB Elimination Pathway	B3LYP	B3LYP with solvent	M05	B97D	ωB97XD	MP2
J	anion **14**	0.0	0.0	0.0	0.0	0.0	0.0
K	E1cB transition structure **15**	30.9	26.0	57.0	11.4	63.7	65.4
L	Diimide **3** + sulfate anion	29.1	-1.1	67.7	41.6	77.6	106.8

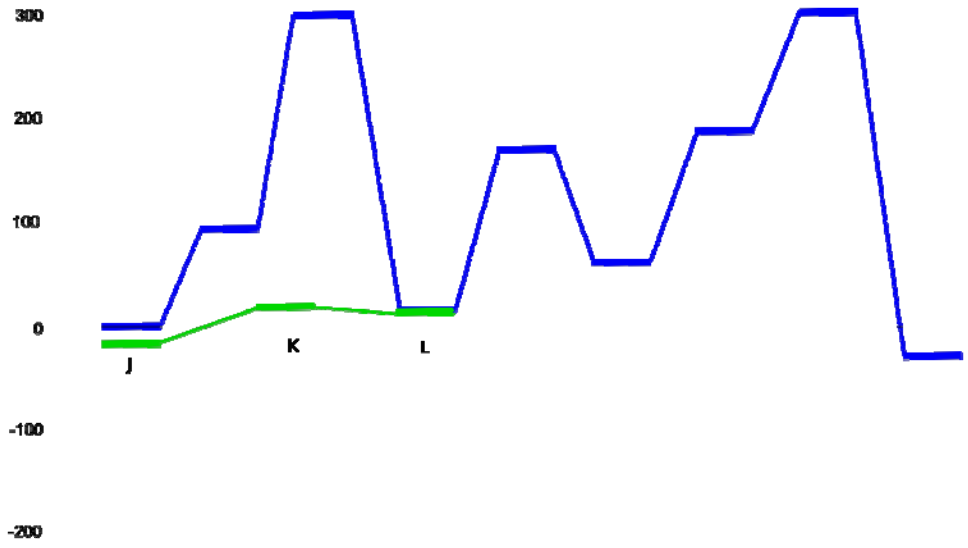

Figure 6.2 Graph of the results of B3LYP calculations on the E1cB elimination pathway outlined in Scheme 6.5 with a comparison to the results of B3LYP calculations on the Matin, Craig and Chan pathway[75] outlined in Scheme 6.4. Values (in kJ mol^{-1}) are found in Table 6.4

The E1cB type elimination lowered the barriers for the formation of the diimide **3** by significant amounts – from 233 kJ mol^{-1} to 350 kJ mol^{-1} depending on the level of theory (Table 6.4). The low barriers for diimide formation make it plausible that the mechanism for the McFadyen Stevens rearrangement does involve the diimide **3** as an intermediate.

However, the mechanism for the formation of the aldehyde **2** from the diimide **3** still involves transition structures **7** and **11** (Scheme 6.4), and barriers to these transition states remain unchanged and insurmountable under the relevant reaction conditions.

6.7 Initial experimental work

Given our interest in the mechanism of activation of isoniazid, in which a diimide is also formed as an intermediate(see Chapter 2), we next considered the possibility that the McFadyen Stevens rearrangement involved radical chemistry. Braslau *et al.* proposed that the diimide intermediate **3** could be oxidised to form the acyl radical **5** (Scheme 6.1),[23] however we were interested in the possibility that the formation of the radical could proceed in the absence of oxidant. To that end we performed the reaction depicted in Scheme 6.6 – that is, the McFadyen-Stevens rearrangement with the addition of the common radical trap TEMPO (2,2,6,6-tetramethylpiperidine-1-oxyl, **15**). The result of this reaction was the formation of the TEMPO adduct **16** (Scheme 6.6) in 25% yield, in addition to the formation of the expected aldehyde **2**. The presence of **16** strongly suggested the incidence of an acyl radical as an intermediate in the rearrangement.

Radicals have not been proposed before in this chemistry, except by the interception of the diimide under oxidative conditions, but their presence in sulfonyl hydrazide chemistry is not without precedent. The work of Myers *et al.* on N,N-disubstituted alkyl hydrazines

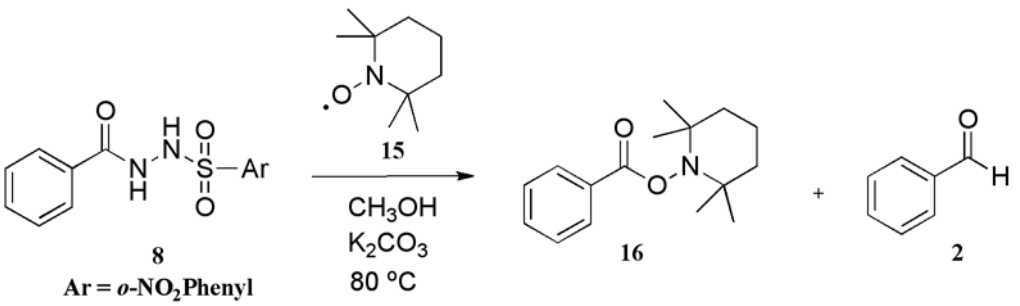

Scheme 6.6

($RCH_2N(NH_2)SO_2Ar$) found that alkyl hydrazines substituted with *o*-nitrosulfonyl groups rearrange to alkanes through radical mechanisms.[79, 80] Myers'system is very similar to the McFadyen-Stevens system, however, the McFadyen-Stevens system concerns an N,N' substituted hydrazide (**8**) which may react through a different mechanism to an N,N disubstituted hydrazine. We confirmed the structure of **8** by X-ray crystallography; the structure is displayed in Figure 6.3.

When one molar equivalent of TEMPO **15** was added to a mixture of **8** and potassium carbonate and refluxed in ethanol for 2.5 h, the resulting ratio of aldehyde **2** to TEMPO adduct **16** (found by a comparison of integration in ^{1}H NMR spectroscopy of the crude reaction mixture) was 1:1 and the yield of TEMPO adduct **16** was 25%, when four equivalents of TEMPO were used the yield of isolated acyl radical adduct **16** increased to 53% and the amount of aldehyde, as evidenced by ^{1}H NMR spectroscopy, was negligible,

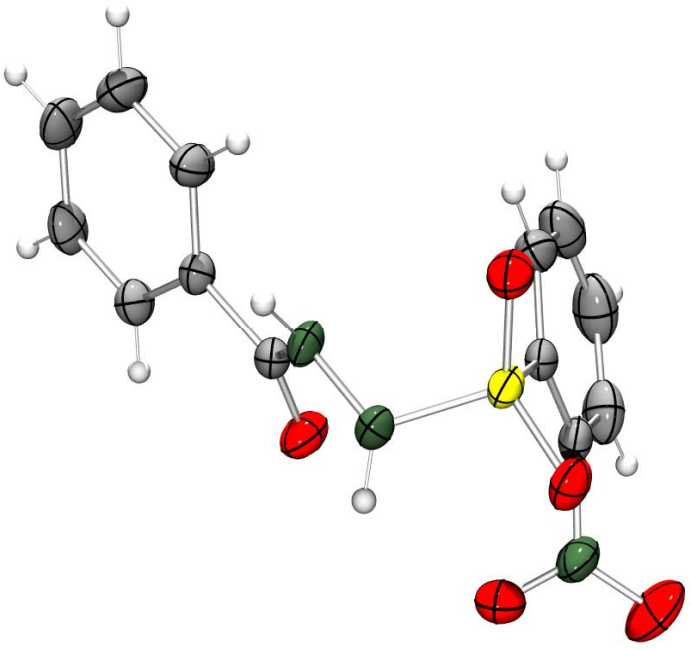

Figure 6.3 Crystal Structure of hydrazide **8**, atom colour scheme red = O, green = N, grey = C, white = H.

suggesting that an acyl radical as an intermediate in the rearrangement was intercepted by the radical trap (**15**) and was unable to complete the reaction to give benzaldehyde **2**.

To investigate the possibility of a radical based mechanism we turned again to computational chemistry. Most radical reactions are chain reactions and we would expect this reaction also to be a chain reaction involving hydrogen abstraction by the benzoyl radical **21** (Scheme 6.8) to give benzaldehyde **2**. However, for a chain reaction to occur a hydrogen atom donor is necessary for hydrogen abstraction to complete the radical chain reaction. Several possibilities for this donor could be found, including the diimide **3**, the sulfonyl hydrazide **8** and the anion **9**.

The presence of ethyl benzoate as one of the products of the McFadyen-Stevens rearrangement would indicate that the diimide (**3,** Scheme 6.1) is a reaction intermediate, as previous studies on the oxidation of hydrazides have shown the diimide to be prone to nucleophilic substitution by alcohols present in the reaction (see Chapter 3). [76, 98] The diimide **3** could easily be formed by E1cB elimination (*vide supra*). Reaction of **8** (R = *o*-NO_2) with potassium carbonate in refluxing ethanol led to the formation of ethyl benzoate and benzaldehyde in a 1:4 ratio as evidenced by ^{1}H NMR spectroscopy. The presence of ethyl benzoate and benzaldehyde was confirmed by GCMS. This result suggests the presence of the diimide **3** as an intermediate in the McFadyen- Stevens rearrangement and therefore indicates the possibility of the diimide **3** as a hydrogen atom donor.

However, when one molar equivalent of TEMPO was added to the reaction mixture described above there were no signals corresponding to ethyl benzoate in the resulting ^{1}H NMR spectrum of the crude reaction mixture. When the hydrazide **8** was refluxed in ethanol in the presence of potassium carbonate and four molar equivalents of TEMPO, column chromatography resulted in the isolation of the TEMPO adduct **16** (Scheme 6.6) and

no other products. This observation suggests that the diimide is not being formed in high enough concentration to be the hydrogen atom donor, as a high concentration of **3** would lead to the presence of ethyl benzoate.

Matin, Craig and Chan have established that if deuterated hydrazide is used as the starting material (**17**, Scheme 6.7) then the result is the formation of the corresponding deuterated aldehyde[75] (**18**, Scheme 6.7) implying that the hydrogen atom donor is likely to be either the starting material – the hydrazide **8** or an intermediate formed from **8**. We eliminated the possibility that the benzoic N-(2-nitrobenzenesulfonyl) hydrazide (**8**, Scheme 6.4) was the hydrogen atom donor by reacting it with a radical initiator (benzoyl peroxide), expecting the formation of benzaldehyde **2** from reaction of **8** with radicals formed from the decomposition of benzoyl peroxide (or subsequent radical species in the reaction mixture). The outcome of this was quantitative retrieval of the starting material - no reaction, suggesting that **8** is not the hydrogen atom donor.

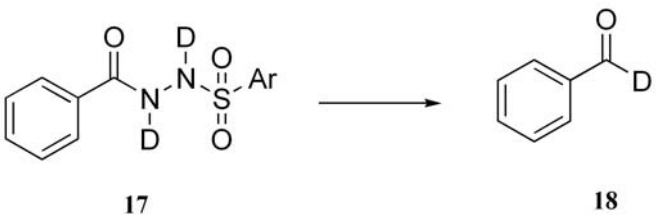

17 18

Scheme 6.7

We have also confirmed that the presence of a base is essential to the formation of the aldehyde, as when benzoic N-(2-nitrobenzenesulfonyl) hydrazide (**8**, Scheme 6.4) was refluxed in ethanol for 2.5 h in the absence of potassium carbonate no reaction occurred and **8** was retrieved quantitatively. This also suggests that **8** is not the hydrogen atom donor as alkaline conditions are essential for reaction.

This line of reasoning suggested that an anion, formed from the starting hydrazide **8**, may be the hydrogen atom donor for the radical reaction in question. As we have shown, *vide supra*, the anions formed by deprotonation of either nitrogen in the hydrazide **8** are very similar in energy; the difference between the two anions (**9** and **14**, Scheme 6.4 and Scheme 6.5) within a given level of theory is calculated to be very small (18 kJ mol^{-1} for ωB97XD[133] is the largest difference calculated). As a result of this, we chose to use both anions (**9** and **14**) as starting points in subsequent calculations. Calculations were performed at several levels of theory, however as benchmarking (see Chapter 7) suggests the most accurate levels of theory are B3LYP and M05 (in comparison to CBS-QB3 as our high level of theory), we therefore concentrated on these levels of theory in the investigation.

An alternative radical mechanism is now proposed that is quite simple. Hydrogen abstraction from anion **9** leads to radical anion **19** which is resonance stabilised, with radical anion **20** representing an alternative canonical form. Alternatively, hydrogen abstraction from anion **14** would lead directly to the canonical structure **20**. The radical anion **20** can fragment to give the benzoyl radical **21**, N_2 and the aryl sulfonyl anion. The

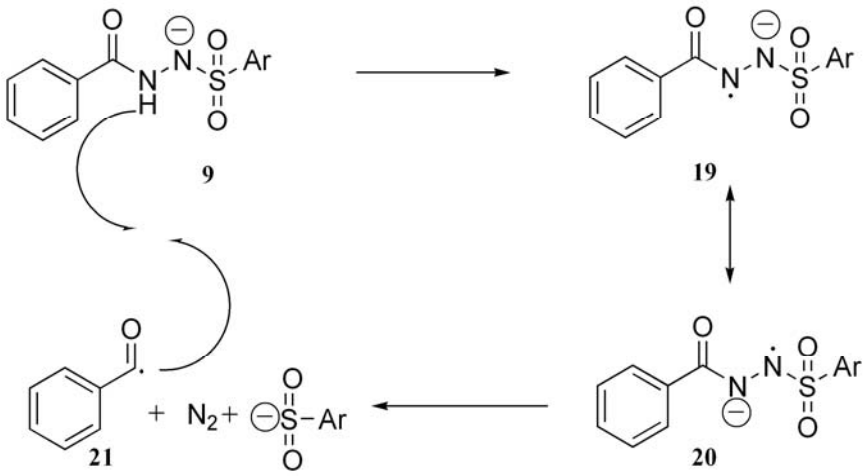

Scheme 6.8

benzoyl radical (**21**) can then abstract a hydrogen from either **9** or **14** to allow the chain reaction to proceed (Scheme 6.8, Scheme 6.9).

Our calculations on the radical mechanism outlined in Scheme 6.9 suggest that it is a very plausible mechanism as the reaction barriers are low in every step (regardless of the level of theory used) and overall the process is exothermic by 193 kJ mol^{-1} at the B3LYP level of theory and 147 kJ mol^{-1} at the M05 level of theory. The difference in barrier between hydrogen abstraction from each of the two anions is very small and thus makes no difference to the outcome (Table 6.5, Figure 6.4). The highest barrier (rate determining step) corresponds to the loss of the sulfinate anion with a value of 18 kJ mol^{-1} at the B3LYP level of theory and 35 kJ mol^{-1} at the M05 level of theory. These results are in agreement with experimental findings that the nature of the aryl group affects the observed rate of reaction.[23]

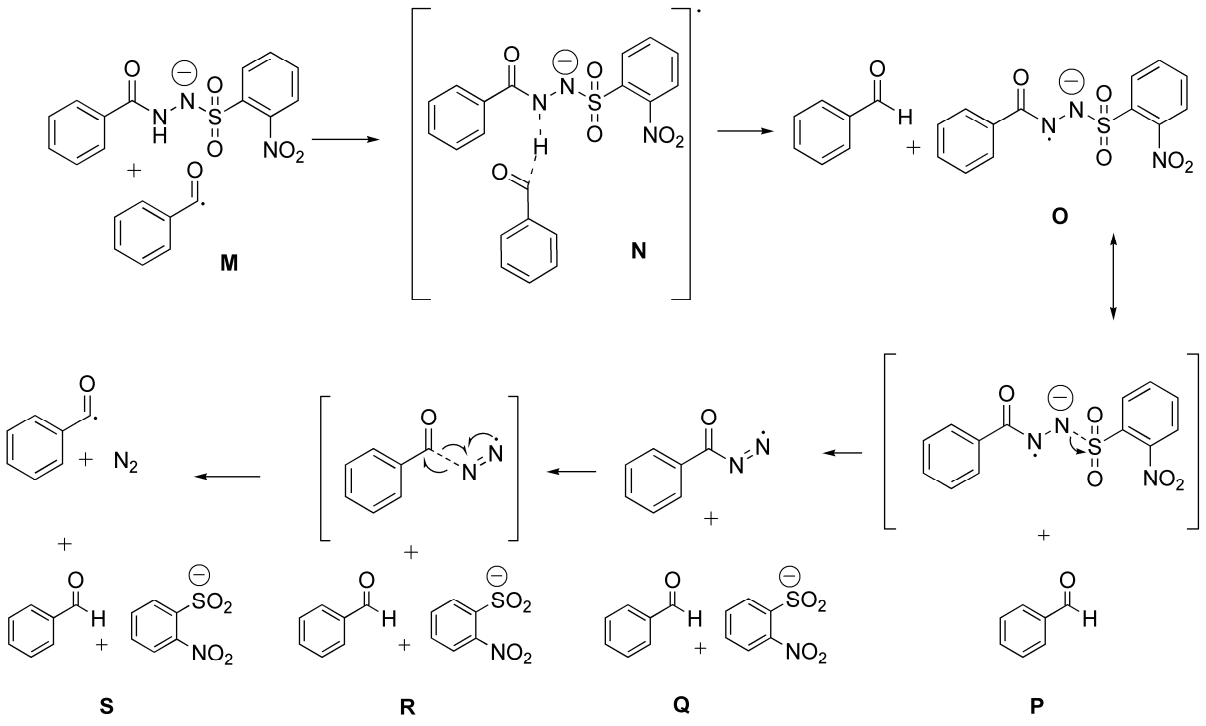

Scheme 6.9

As loss of the sulfate anion appears to be the rate determining step in the mechanism outlined in Scheme 6.9, bulk solvent stabilization also may affect the outcome of the reaction and should therefore be involved in the calculations. Calculations including a bulk

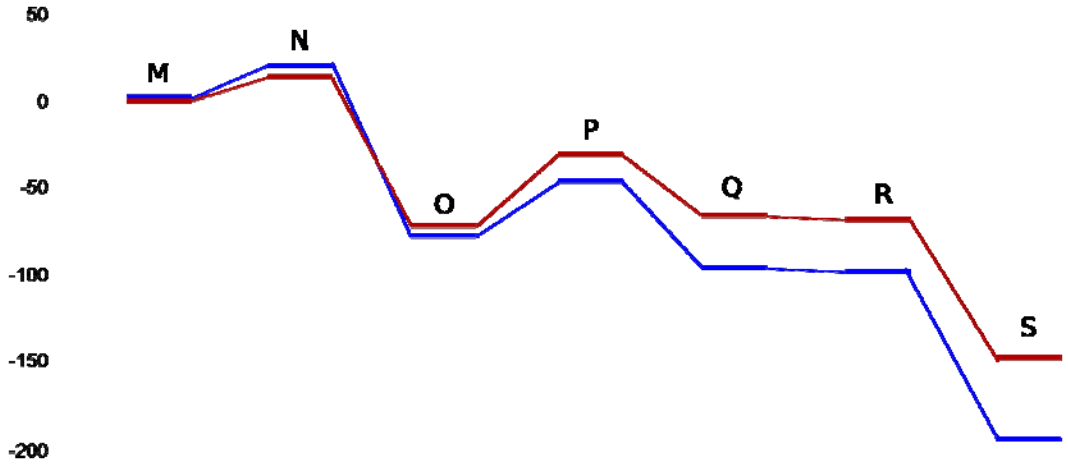

Figure 6.4 Graph of results of calculations for the reaction mechanism outlined in Scheme 6.9. Values (in kJ mol^{-1}) for the mechanism starting from anion **9** are found in Table 6.5. Colour scheme: B3LYP = blue and M05 = red

Table 6.5 Results from calculations for the radical reaction outlined in Scheme 6.9 starting at anions **9** and **14**. E in kJ mol^{-1}

	Anion **9**					Anion **14**				
	B3LYP	M05	MP2	B97D	ωB97XD	B3LYP	M05	MP2	B97D	ωB97XD
M	0.0	0.0	0	0	0	0	0	0	0	0
N	16.7	14.0	-[a]	-20.5	1.1	17.4	13.3	-[a]	-22.2	9.8
O	-76.9	-74.5	-22.6	-65.8	-79.9	-66.7	-67.0	-31.0	-73.0	-61.7
P	-48.3	-32.2	-[b]	-66.2	-23.8	-48.3	-32.2	-[b]	-66.2	-23.8
Q	-96.9	-66.2	40.5	-[b]	-55.0	-96.9	-66.2	40.5	-[b]	-55.0
R	-98.9	-69.0	42.2	-[b]	-52.8	-98.9	-69.0	42.2	-[b]	-52.8
S	-193.4	-147.1	-127.8	-158.6	-143.7	-193.4	-147.1	-127.8	-158.6	-143.7

[a]transition structure unable to be found due to computational restraints
[b]structure not found at this level of theory

solvent effect (Table 6.6) show the further stabilization of intermediates in the reaction outlined in Scheme 6.9 making this a very plausible reaction mechanism. The initiation step of the proposed radical mechanism is discussed below.

6.8 Cyclisation experiments

Homolytic cyclization chemistry can be used as a test for the presence of carbon-centred radicals, including acyl radicals.[54] Braslau and co-workers utilised this test to support the proposal for formation of an acyl radical by oxidative processes.[23] Inspired by Braslau we have performed a similar experiment in order to make a direct comparison between oxidative and non-oxidative processes. When hydrazide **22** was reacted with potassium carbonate and the oxidant potassium ferricyanide in refluxing ethanol, for 2.5 h, products **23** and **24** formed (in 75% yield, in a 1:1 ratio as evidenced by ^{1}H NMR spectroscopy). This result compares favourably with Braslau's yields.[23] Cyclisation was evidenced by the presence of doublets consistent with diastereotopic methylene protons at 4.2 and 4.0 ppm

Table 6.6 Results of calculations for the radical reaction as outlined in Scheme 6.9, at the B3LYP and M05 levels of theory, with added CPCM calculations to include the electrostatic effect of ethanol as solvent. E in kJ mol^{-1}

	Anion **9**	B3LYP	M05
M	starting anion **9** and radical **21**	0	0
N	transition structure for H abstraction	33.2	35.4
O	products of H abstraction	-92.2	-84.2
P	transition structure for loss of sulfate	-53.6	-34.2
Q	product for loss of sulfate	-133.5	-96.8
R	transition structure for loss of nitrogen	-136.4	-99.6
S	final products	-227.4	-173.3

in the ^{1}H NMR spectrum. In addition, a signal at 1692 cm^{-1} in the infra-red spectrum of the crude reaction mixture is consistent with the formation of an aromatic ketone, and therefore cyclisation. Similar results were observed under the same oxidative conditions when TEMPO was replaced with diphenyl diselenide as the radical trap which resulted in the formation of the cyclised product **25** (Scheme 6.11), in 17% yield, (identified by comparison of the ^{1}H NMR spectrum to the literature[134]) and ethyl 2-(2-methallyloxy)benzoate in a 26% yield. As no ethyl 2-(2-methallyloxy) benzoate is observed when TEMPO is utilised as a radical trap we surmised that the seleno ester **26** is formed initially by the capture of the acyl radical with diphenyldiselenide, then transesterification by ethanol affords the ethyl ester.

In contrast, when hydrazide **22** was reacted with potassium carbonate in refluxing ethanol, for 2.5 h, in the absence of potassium ferricyanide, cyclisation did not occur, which casts doubt on the proposal that the mechanism of the McFadyen-Stevens reaction is radical based. However, in the absence of potassium ferricyanide direct trapping with four molar equivalents of TEMPO (**15**) did occur to give **24** (Scheme 6.10).

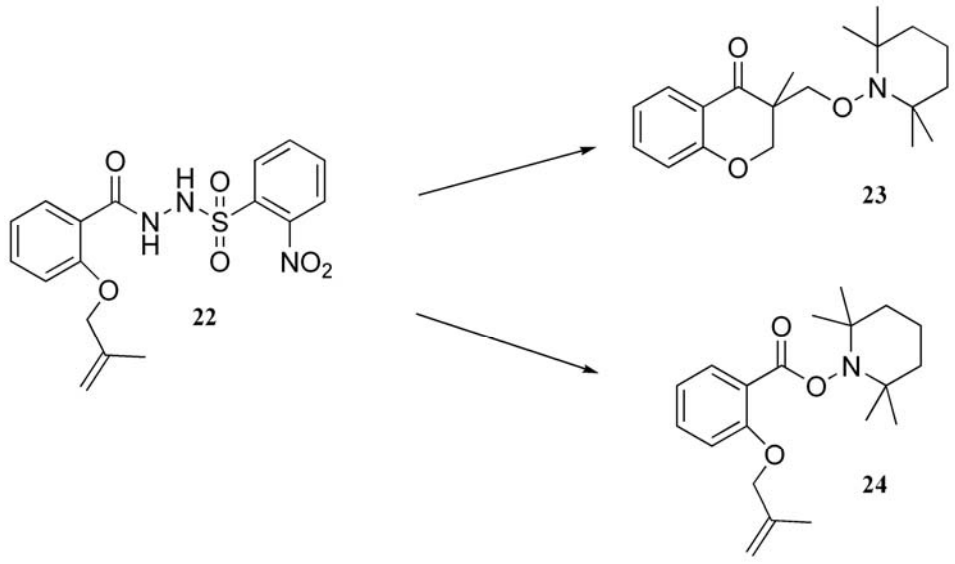

Scheme 6.10

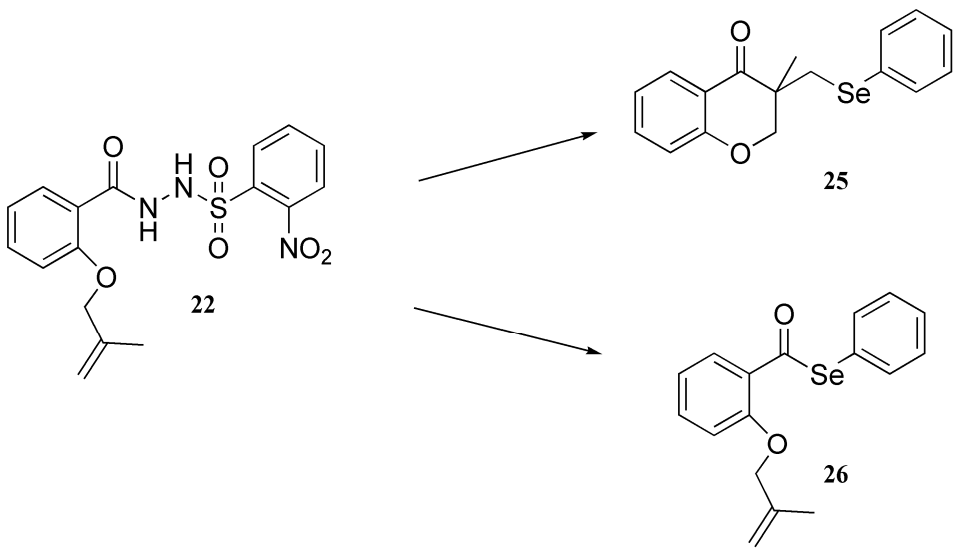

Scheme 6.11

There are several reasons why cyclisation may not occur in the absence of potassium ferricyanide. One is that the cyclisation step itself is too slow to compete with trapping by TEMPO (**15**). This is a strong possibility as the result of cyclisation is an unstabilised primary radical and TEMPO traps radicals at near diffusion control with a rate constant of 1 x 10^9 M^{-1} s^{-1}at a temperature of 298 K.[91] The possibility of trapping before cyclisation is supported by Crich and co-workers who report that an acyl radical generated by the photolysis of an acyl telluride was unable to cyclise before being trapped by TEMPO (Scheme 6.12).[54] We speculate that the presence of a metallic oxidant such as iron may

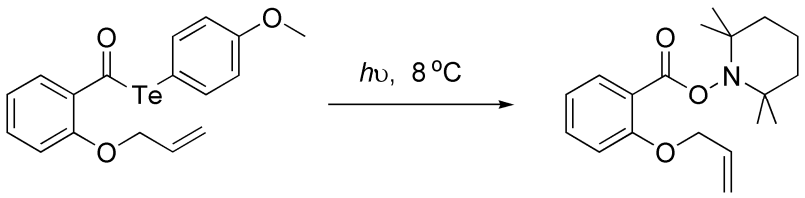

Scheme 6.12

stabilise intermediates to allow cyclisation to occur before trapping with TEMPO. It may be the absence of metal coordination to the acyl group that is responsible for the lack of observed cyclisation, rather than the absence of a radical. It is also possible that TEMPO itself is acting as an oxidant in this reaction. TEMPO can act as a one electron oxidant[135-140] that could oxidise the diimide intermediate (**3**) postulated to be involved in the McFadyen-Stevens rearrangement to give a radical that it immediately traps. The immediate trapping of the acyl radical by TEMPO could explain the formation of trapped product **24** in the absence of a metallic oxidant. The oxidative action of TEMPO could also explain the increase in yield of the radical adduct **16** (Scheme 6.6) from 25%, when one equivalent of TEMPO was present, to 53% when the amount of TEMPO was increased to four molar equivalents.

6.9 Initiation of the radical chain reaction

Up to this point the radical based reaction mechanism (Scheme 6.8, Scheme 6.9) has failed to explain the step required for the formation of the benzoyl radical **21** to initiate the chain reaction. It is possible that the anion formed in the early stages of the reaction (either **9** or **14**) is oxidised to give a radical (**27**, Scheme 6.13). This radical could react in two ways – either by abstracting a hydrogen from another anion to give the radical anion **20** and the hydrazide **1**, or by formation of the radical anion **19** or **20** through loss of a proton (Scheme 6.13). This explanation fits well with experimental observations as this would bypass the need for the formation of the diimide intermediate (**3**) and provide an explanation for why there is no ester formed under oxidative conditions (in contrast to the hydrazide oxidation results in Chapters 2 and 3 where substitution by the solvent on the diimide intermediate leads to formation of ester). The outcome would be similar with either an oxidant such as potassium ferricyanide or TEMPO which can act as an oxidant[135-140] and is also consistent with the outcome of increased yields of TEMPO adduct observed when the concentration

of TEMPO was increased. Myers' work indicates the possibility that TEMPO is involved as a hydrogen transfer agent in the mechanism of decomposition of the alkyl diazenes, rather than passively trapping the radical resulting from decomposition. It is possible in our case that TEMPO is also having an active role, changing the reaction mechanism.[80] The proposal of oxidative formation of the radical (**27**) from the anion (**14**, Scheme 6.13) is also consistent with experimental outcomes in Braslau's work where there is no mention of the presence of the expected ethyl benzoate that would be formed from nucleophilic acyl substitution by ethanol on the diimide intermediate **3**.[23] This newly proposed radical mechanism is quite plausible for oxidative reactions, however it does not lead to an alternative explanation for the formation of an aldehyde under non-oxidative conditions.

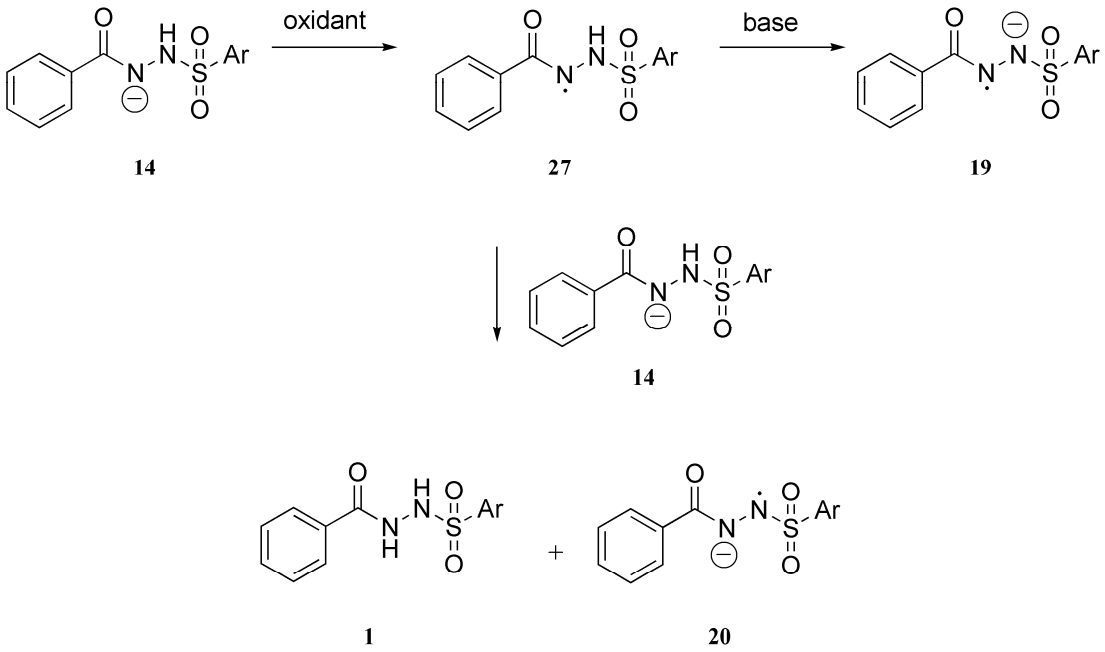

Scheme 6.13

6.10 HERON

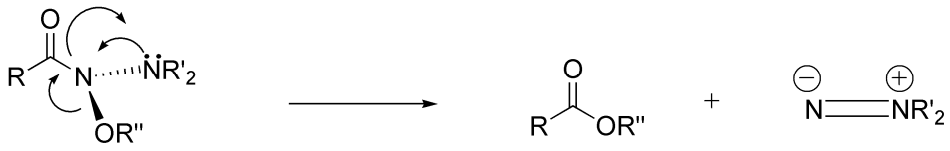

Scheme 6.14

Another possibility that must be considered for the mechanism of the McFadyen-Stevens rearrangement is a process similar to the HERON process, a concerted rearrangement of N-acyloxy-N-alkoxyamides as outlined in Scheme 6.14.[141, 142] The possibility of a similar rearrangement was investigated computationally and the results are displayed in Scheme 6.15. The three centred transition structure has a very high reaction barrier in the gas phase (and also with inclusion of bulk solvent effects), and it would seem unlikely that this process is occurring in the McFadyen-Stevens reaction.

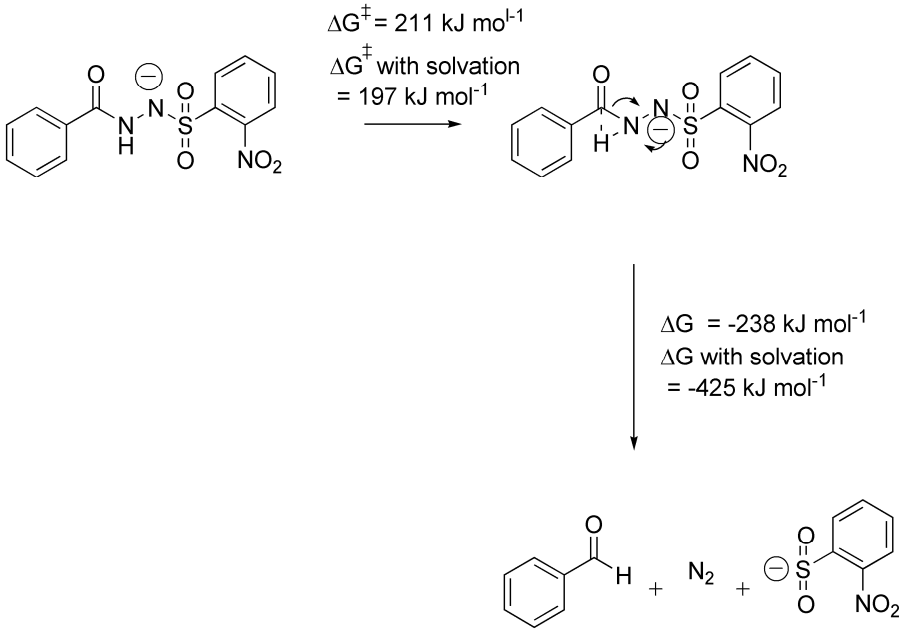

Scheme 6.15

6.11 Conclusions and future work

We have carefully investigated the original mechanism for the McFadyen-Stevens rearrangement as proposed by Matin, Craig and Chan[75] and outlined in Scheme 6.4. We find that it has high barriers for the formation of key intermediates, even when solvent stabilization is included, and cannot be considered a realistic mechanism. An alternate free radical mechanism (Scheme 6.8, Scheme 6.9) is proposed which calculations suggest would be more favourable. However, experimental results neither confirm nor deny the radical mechanism under non-oxidative conditions. Despite our alternative proposal we are unable to account for the facile formation of aldehyde under non-oxidative conditions. However, it is confirmed experimentally that the reaction proceeds through a radical mechanism under oxidative conditions.

The possibility that a direct transfer of a proton from the imide to the carbonyl carbon through a transition state such as **28** shown in Figure 6.5 was investigated however the barrier to this process at the B3LYP/6-311+G(d,p) level of theory was 239 kJ mol^{-1} so again this is not a plausible explanation. As unimolecular proton transfer seems unlikely, there is a possibility that this is a bimolecular reaction proceeding through a transition state such as **29** in Figure 6.5. This possibility has not yet been examined computationally or through laboratory based experiments.

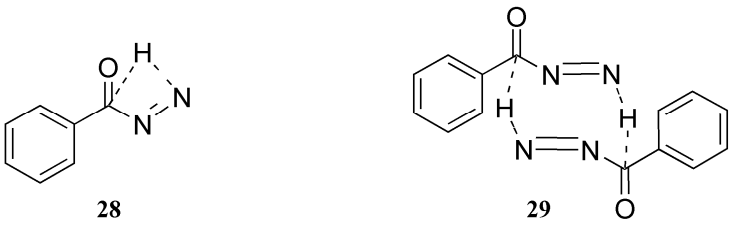

28 **29**

Figure 6.5

Future investigation to elucidate the mechanism further could involve a cyclopropyl 'radical clock' type reaction[143] using an analogue of the McFadyen-Stevens starting material. If ring opening occurred this would provide extra support for the formation of the radical, whereas if the aldehyde is formed by a rearrangement process, we would not expect ring opening to occur (Scheme 6.17).[144]

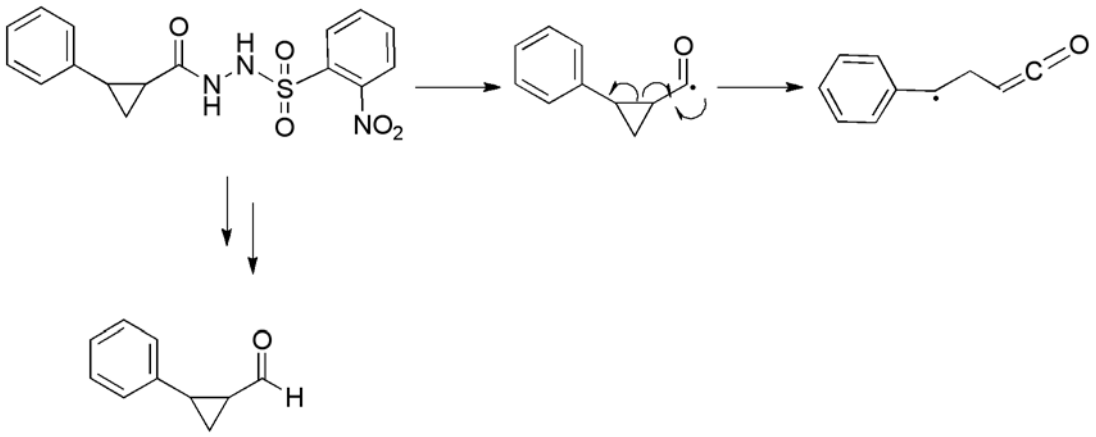

Scheme 6.17

The outcome of our cyclisation experiments was inconclusive due in part to the difference between the rate of cyclisation and the rate of trapping with TEMPO. It is possible that a modified cyclisation precursor that would yield a more stable radical intermediate from cyclisation, such as depicted in Scheme 6.16, would favour ring closure over the competing reaction of trapping of the initial acyl radical with TEMPO.

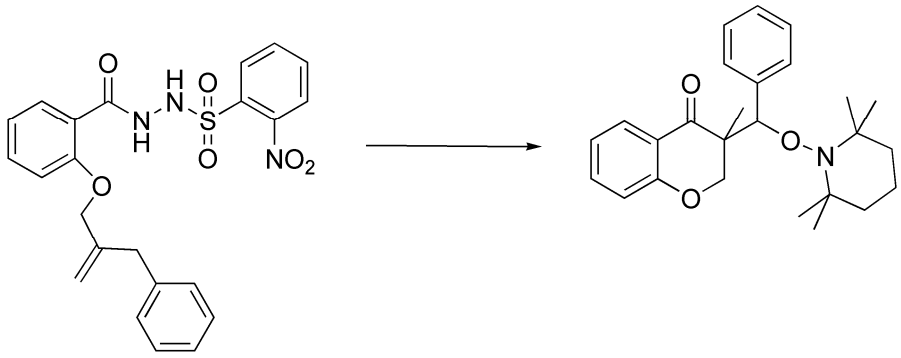

Scheme 6.16

In our experiments ring closure did occur in the presence of the oxidant potassium ferricyanide. It is possible that this is due to stabilisation of the transition state by the metal centre and this could be investigated further computationally.

While computational and experimental investigations have not comprehensively explained the mechanism for the formation of aldehyde in the McFadyen – Stevens rearrangement under non-oxidative conditions, the presence of an oxidant, whether a metallic oxidant such as potassium ferricyanide or an oxidant such as TEMPO, changes the mechanism of this reaction and we have proposed a plausible mechanism involving acyl radicals for the reaction that occurs under oxidative conditions.

Chapter 7.

Experimental and computational methods

7.1 General experimental

7.1.1 Nuclear magnetic resonance spectroscopy

Proton (^{1}H) and carbon (^{13}C) nuclear magnetic resonance spectra were recorded in deuterated chloroform ($CDCl_3$) unless otherwise stated, on a Varian Mercury 2000 at 300 MHz and 75 MHz respectively. Chemical shifts were recorded as δ values in parts per million (ppm) and referenced to the solvent used. The following abbreviations are used in assigning ^{1}H spectra; s = singlet; d = doublet; ad = apparent doublet; t = triplet; at = apparent triplet; q = quartet; m = multiplet; bs = broad singlet; dd = doublet of doublets; *J* = coupling constant (Hz).

7.1.2 Infrared spectroscopy

Infrared spectra were recorded on a Shimadzu FTIR 8400s spectrometer as a thin film (from $CDCl_3$ or CH_2Cl_2) on NaCl plates.

7.1.3 Gas chromatography / mass spectrometry

Mass spectrometry and Hi-Resolution mass spectrometry were performed on a Kratos Concept ISQ mass spectrometer using electron ionisation mass spectrometry. Sample mixtures were analysed using a Varian CP – 3800 Gas Chromtagraph loaded with a Varian FactorFour: CC. VF – 5 ms, 0.25 mm, 0.25 μm, 30 m column. This fed directly into a Varian 1200 Triple Quadrapole mass spectrometer recording the mass spectrum using electron ionisation mass spectrometry (EI).

Analytical analyses were performed by The Central Sciences Laboratory at the University of Tasmania. The molecular ion and mass fragments are quoted, with relative intensities of the peaks referenced to the most intense taken as 100%.

7.1.4 Column chromatography

Merck flash grade Silica Gel (32 – 63 μm) was used for column and flash chromatography and were performed according to the method of Still *et al.*[145]

7.1.5 Thin layer chromatography

Merck silica gel 60 F254 aluminium backed sheets were used for analytical thin layer chromatography. TLC plates were visualized under 254 nm UV lamp and / or by treatment with phosphoric acid / ceric sulfate dip, followed by heating. (phosphomolybdic acid (37.5 g), ceric sulfate (7.5 g), sulfuric acid (37.5 mL, water 720 mL).

7.1.6 Microwave assisted reactions

Microwave assisted reactions were undertaken in a sealed tube and heated using a CEM Discover Microwave reactor.

7.1.7 Solvents and reagents

Reagents were used as received from their suppliers (unless otherwise stated). Isoniazid, benzhydrazide, periodic acid and TEMPO were purchased from Sigma-Aldrich and used as received. The manganese catalyst, $[Mn^{IV}\text{-}Mn^{IV}(\mu\text{-}O)_3L_2](PF_6)_2$ (L = 1,4,7-trimethyl-1,4,7-triazacyclononane) was available in the group and prepared by the method of Wieghardt.[95] Anhydrous tetrahydrofuran, was dried using an Innovative Technology SPS400-7 solvent drying machine fitted with activated alumina and copper catalyst columns. Anhydrous dichloromethane was obtained by distillation from calcium hydride. Ethanol and methanol were dried using fresh 4 Å molecular sieves for a minimum of 24 h before use.

Anhydrous magnesium sulfate was used for drying of solvent extracts, and solvents removed under reduced pressure on a rotary evaporator.

7.1.8 Melting point

Melting points were obtained with a Reichert melting point apparatus, equipped with a Reichert microscope, and are uncorrected.

7.1.9 Crystal structure

Data were collected at 193 K for crystals of compound (**8,R = *o*NO_2**) mounted on a glass fibre using an Enraf-Nonius CAD4 diffractometer with a graphite single crystal monochromated molybdenum radiation source at the University of Tasmania (λ = 0.71073 Å (K_α) by Dr. Roderick Jones (University of Tasmania) on behalf of the author using CAD4 Express[146] and XCAD4[147] software. The structure was solved by direct methods with SHELXS-97, refined using full-matrix least squares routines against F^2 with SHELX-97,[148] and visualised using X-SEED.[149] All non-hydrogen atoms were refined anisotropically, and hydrogen atoms were placed in calculated positions and refined using a riding model with fixed C-H distances of 0.95 Å (sp^2C-H) and 0.98 Å (CH_3), and U_{iso}(H) = 1.2U_{eq}(C) (sp^2) and 1.5U_{eq}(C) (sp^3), except for H6 and H7 (amide protons) which were found in difference maps and subsequently refined in x, y, z and Uiso.

7.2 Experimental methods for Chapter 2

7.2.1 Oxidation of benzhydrazide in the presence of protonated benzothiazole:

A 3:2 ratio of glacial acetic acid and 5 M sulfuric acid (2.5 mL) at 0 °C was degassed by bubbling $N_{2(g)}$ through it for 15 min. To this was added benzothiazole (67 mg, 85 µL, 0.5 mmol) and benzhydrazide (610 mg, 4.5 mmol). Potassium permanganate (711 mg, 4.5 mmol) was added slowly and the solution stirred for 15 min. The reaction was quenched by the addition of water (5 mL) followed by a saturated solution of potassium hydrogen sulfate, and sodium sulfite until a clear solution was obtained. The resulting solution was

neutralized by the careful addition of sodium hydrogen carbonate and extracted with dichloromethane (3 x 15 mL). The combined extracts were dried and evaporated under reduced pressure to leave a yellow solid which was purified by column chromatography on silica gel (eluent 15% ethyl acetate/ 85% hexanes) to give a mixture of 2-benzoyl benzothiazole **10** and benzoic anhydride. This mixture was dissolved in ethanol (5 mL) and stirred overnight with 2 M sodium hydroxide (5 mL). The resulting solution was extracted with dichloromethane (3 x 15 mL) and the combined extracts dried and evaporated under reduced pressure to give 2-benzoyl benzothiazole **10** (27 mg, 16%) as a white solid. Spectral data is consistent with that previously reported.[150]

^{1}H NMR $\delta_H(CDCl_3)$ 7.50-7.68 (m,5H), 8.00 (m,1H), 8.16 (m,1H), 8.26 (m,1H), 8.57 (m,1H)

^{13}C NMR $\delta_C(CDCl_3)$ 122.2, 125.7, 127.0, 127.6, 128.5, 131.3, 133.9, 135.0, 137.0, 153.9, 167.1, 185.4

ν_{MAX} (cm^{-1}): 1645 (C=O)

7.2.2 Oxidation of benzhydrazide in the presence of diphenyldiselenide:

A 4:1 ratio of acetonitrile and water (5 mL) was degassed by bubbling $N_{2(g)}$ through it for 10 min. Benzhydrazide (285 mg, 2.1 mmol) and diphenyl diselenide (94 mg, 0.3 mmol) were added followed by the slow addition of potassium permanganate (332 mg, 2.1 mmol) and the resulting mixture was stirred for 15 min at room temperature. The reaction was quenched by the addition of water (5 mL) followed by a saturated solution of potassium hydrogen sulfate, and sodium sulfite until a clear solution was obtained. The resulting solution was neutralized by the careful addition of solid sodium hydrogen carbonate and extracted with dichloromethane (3 x 15 mL) and the combined extracts dried and evaporated under reduced pressure to leave a yellow solid which was purified by column chromatography on silica gel (eluent 10% ethyl acetate/90% hexanes) to give 77 mg of a

mixture of the phenylseleno ester **11** and diphenyl diselenide in a 4:1 ratio by nmr. This data was extrapolated to give a 34% yield of **11**. Spectroscopic data is consistent with that previously reported.[90]

^{1}H NMR $\delta_H(CDCl_3)$ 7.43-7.52 (m,5H), 7.60-7.65 (m,3H), 7.93-7.97 (m,2H)

^{13}C NMR $\delta_C(CDCl_3)$ 126.1, 127.6, 129.2, 129.7, 133.2, 136.6, 138.9, 193.7

ν_{MAX} (cm^{-1}): 1683 (C=O)

7.2.3 General procedure for trapping with TEMPO

TEMPO (**7**) (62.5 mg, 0.4 mmol) was added to a solution of isoniazid (**1**) (164.5 mg, 1.2 mmol) in degassed (with $N_{2(g)}$) aqueous acetonitrile (4:1 MeCN: H_2O, 5 mL) at 0 ˚C. Potassium permanganate (190 mg, 1.2 mmol) was added in small portions and the solution stirred for 5 min before being warmed to room temperature.

The reaction was quenched by adding 1M sulfuric acid (1 mL), 0.5M potassium hydrogen sulfate (1 mL) and saturated sodium sulfite solution (1 mL). The mixture was made alkaline with sodium carbonate and extracted with dichloromethane (3x20 mL). The organic extract was dried and evaporated to give a solid which was passed through a short plug of silica gel eluting with 20% ethyl acetate/80% hexanes to give the TEMPO adduct (2,2,6,6-tetramethyl-1-piperidinyloxy)-isonicotinoate **13** as a clear solid in 41% yield.

M.P.: 60-61 ˚C

^{1}H NMR δ_H(acetone-d_6) 1.10 (s, 6H), 1.27 (s, 6H), 1.42-1.77 (m, 6H), 7.9 (m, 2H), 8.8 (m, 2H).

^{13}C NMR δ_C(acetone-d_6) 17.0, 21.0, 32.1, 39.2, 60.9, 123.7, 138.1, 149.7, 164.7

LRMS: 262 (M^+, 1), 247(84), 156(32), 139(13), 125(65), 123(100), 106(50), 97(27), 83(76), 77(37), 69(60), 55(76), 51(31), 41(50)

HRMS: $M^{+\cdot}$ For ($C_{15}H_{22}N_2O_2$) predicted 262.1681, found 262.1682.

ν_{MAX} (cm^{-1}): 1755 (C=O)

7.2.4 Spectral data for novel compounds

7.2.4.1 2,2,6,6-tetramethylpiperidin-1-yl 3-nitrobenzoate

^{1}H NMR δ_H($CDCl_3$) 1.18 (s, 6H), 1.49 (s, 6H), 1.69-2.10 (m, 6H), 7.7 (t, 1H, *J*=8Hz), 8.4 (m, 2H), 8.8 (s, 1H).

^{13}C NMR δ_C($CDCl_3$) 16.9, 20.9, 32.0, 39.1, 60.7, 124.4, 127.4, 129.8, 131.5, 135.3, 148.3, 164.4

LRMS: 306 (M^+, 1), 291(100), 167(12), 156(37), 150(36), 123(20), 104(7), 69(24), 55(42), 41(50).

HRMS: $M^{+\cdot}$ For ($C_{16}H_{22}N_2O_4$) predicted 306.1580, found 306.1580

ν_{MAX} (cm^{-1}): 1752 (C=O), 1534, 1351

7.2.4.2 2,2,6,6-tetramethylpiperidin-1-yl 4-methylbenzoate

^{1}H NMR δ_H($CDCl_3$) 1.11 (s, 6H), 1.26 (s, 6H), 1.40-1.73 (m, 21H), 7.3 (d, 2H *J*=7Hz), 8.0 (d, 2H, *J*=7Hz).

^{13}C NMR δ_C($CDCl_3$) 17.2, 21.1, 21.9, 32.2, 39.3, 60.6, 127.1, 129.4, 129.8, 143.7, 166.7

LRMS: 275 (M^+, 1), 260 (15), 136 (5), 120 (12), 119 (100), 91 (17), 83 (5), 69 (5), 55 (7), 41 (4)

HRMS: $M^{+\cdot}$ For ($C_{17}H_{25}NO_2$) predicted 275.1885, found 275.1883

v_{MAX} (cm^{-1}): 1742

7.2.4.3 2,2,6,6-tetramethylpiperidin-1-yl 4-chlorobenzoate

^{1}H NMR $\delta_H(CDCl_3)$1.09 (s, 6H), 1.25 (s, 6H), 1.55-1.72 (m, 6H), 7.4 (m, 2H), 8.0 (m, 2H).

^{13}C NMR $\delta_C(CDCl_3)$ 17.2, 21.1, 32.2, 39.3, 60.7, 128.3, 129.0, 131.2, 139.5, 165.8

LRMS: 295 (M^+, 4), 280 (50), 245 (6), 199 (4), 156 (12), 139 (100), 125 (12), 111 (15), 89 (5), 75 (8), 69 (8), 55 (10), 41 (5).

HRMS: $M^{+\cdot}$ For ($C_{16}H_{22}{}^{35}ClNO_2$) predicted 295.1339, found 295.1331

v_{MAX} (cm^{-1}): 1752 (C=O)

7.2.4.4 2,2,6,6-tetramethylpiperidin-1-yl 3-bromobenzoate

^{1}H NMR $\delta_H(CDCl_3)$ 1.11 (s, 6H), 1.27 (s, 6H), 1.40-1.80 (m, 6H), 7.3 (m, 1H), 7.7 (m, 1H), 8.0 (m, 1H), 8.2 (m, 1H).

^{13}C NMR $\delta_C(CDCl_3)$ 17.2, 21.1, 32.2, 39.3, 60.8, 122.8, 128.4, 130.3, 131.9, 132.7, 136.1, 165.4

LRMS 341 (M^+, 1), 324 (58), 183(100), 156(19), 124(10), 76(11), 69(20), 55(38), 41(17).

HRMS: $M^{+\cdot}$ For ($C_{16}H_{22}{}^{79}BrNO_2$) predicted 339.0834, found 339.0832

v_{MAX} (cm^{-1}): 1749 (C=O)

7.2.5 General procedure for competitive trapping – methanol as solvent

Performed in Duplicate.

To degassed methanol (5 mL) was added TEMPO (**7**) (62.5 mg, 0.4 mmol), isoniazid (**1**) (54.9 mg, 0.4 mmol) and Mn catalyst ($[Mn^{IV}\text{-}Mn^{IV}(\mu\text{-}O)_3L_2](PF_6)_2$ (L=1,4,7-trimethyl-1,4,7-triazacyclononane)) (5mg, 6 x 10^{-3} mmol, 1.6 mol%). Periodic acid (180 mg, 0.8 mmol) was added slowly in small portions and the reaction mixture stirred for a further 15 min. The reaction was quenched by adding 1M sulfuric acid (1 mL), 0.5M potassium hydrogen sulfate (1 mL) and saturated sodium sulfite solution (1 mL). The mixture was made alkaline with sodium carbonate and extracted with dichloromethane (3x20 mL). The organic extract was dried and evaporated and the product mixture was determined by comparison of the integration of the singlet for the methyl protons of methyl isonicotinoate at 3.99 ppm (3H) and the singlet for the TEMPO protons of (2,2,6,6-tetramethyl-1-piperidinyloxy)-isonicotinoate at 1.10 ppm (6H).

7.2.6 General procedure for competitive trapping – acetonitrile as solvent

Performed in duplicate

To a solution of Mn catalyst ($[Mn^{IV}\text{-}Mn^{IV}(\mu\text{-}O)_3L_2](PF_6)_2$ (L=1,4,7-trimethyl-1,4,7-triazacyclononane)) (5 mg, 6 x10^{-3} mmoles, 1.6 mol%) in degassed acetonitrile (4.5 mL) and pyridine (0.5 mL), was added TEMPO (62.5 mg, 0.4 mmol), methanol (0.5 µL, 2 mmol) and isoniazid (54.9 mg, 0.4 mmol). To this was added dropwise a solution of periodic acid (180 mg, 0.8 mmol), in 3:1 acetonitrile/pyridine (1 mL) and the reaction mixture stirred for a further 15 min. The reaction was quenched by adding 1M sulfuric acid (1 mL), 0.5M potassium hydrogen sulfate (1 mL) and saturated sodium sulfite solution (1 mL). The mixture was made alkaline with sodium carbonate and extracted with dichloromethane (3x20 mL). The organic extract was dried and evaporated. The resulting ratio of methyl ester to TEMPO adduct was determined by ^{1}H NMR integration as detailed above.

7.2.7 General procedure for cation trapping

A solution of anisole (497 mg, 4.6 mmol) in acetonitrile (4.5 mL) was degassed by bubbling $N_{2(g)}$ through it for 10 min. Light was excluded and benzhydrazide (63 mg, 0.46 mmol) and ceric ammonium nitrate (891 mg, 1.62 mmol) was added. The mixture was stirred for 3.5 h. The reaction was quenched by the addition of water (5 mL) and solid sodium hydrogen carbonate and the mixture extracted with 3 x 20 mL dichloromethane, the extracts dried and solvent removed under reduced pressure to give a red residue. GCMS analysis of this residue showed no ketone formation, only the presence of nitroanisole.

7.3 Computational methods for Chapter 2

All calculations were performed using the Gaussian 03[100] program.

7.3.1 Bond dissociation benchmarking

B3LYP: Geometries were optimized and frequency calculations performed at B3LYP/6-31G(d), single point calculations on those geometries were performed at B3LYP/6-311+G(2d,2p).[151-153]

BHandHLYP: Geometries were optimized and frequency calculations performed at BHandHLYP/6-31G(d), single point calculations on those geometries were performed at BHandHLYP/6-311+G(2d,2p).[152]

QB3: All calculations performed at the CBS-QB3 level of theory.[154] Geometries were optimized and frequency calculations performed at B3LYP/CBS-B7.[154]

HF,[155, 156] MP2,[157-161] MP4,[162] MPWB1K,[128] BMK[163]: Geometries were optimized and frequency calculations performed at B3LYP/CBS-B7. Single point calculations on those geometries were performed with a 6-311+G(2d,2p) basis set.

7.3.2 Bond dissociation MPWB1K calculations

Geometries optimized and frequency calculations performed at MPWB1K/6-31G(d). Single point calculations on those geometries at MPWB1K/6-311+G(2d,2p).

7.3.3 General procedure for the calculation of redox potentials

B3LYP: Geometries were optimized and frequency calculations performed at B3LYP/6-31G(d), single point calculations on those geometries were performed at B3LYP/6-311+G(2d,2p).

MPWB1K and CCSD(T):[132] single point calculations with a 6-311+G(2d,2p) basis set were performed on B3LYP optimized geometries.

Enthalpy corrections for MPWB1K and CCSD(T) were used from frequency calculations performed at B3LYP/6-31G(d).

CBS-QB3 calculations were performed separately.

The value of 4.28 V was used for the absolute potential of the normal hydrogen electrode in water.[164]

Redox potentials were calculated using a modified version of the method by Fu *et al.*[101] as follows:

$$E^{o}\ (\text{versus NHE}) = IP + (1/96.48)(-T\Delta S + \Delta G_{solvation,cation} - \Delta G_{solvation,radical}) - 4.28$$

IP was calculated at ROB3LYP/6-311+G(2d,2p)//B3LYP/6-31G(d) and 0.28V added to correct for the systematic underestimation found by Fu *et al*.[101]

Solvation calculations were performed using the D-PCM formulation developed by Tomasi *et al.*[165-167] at the B3LYP/6-31G(d) level using the following G03 keywords cavity=pentakisdodecahedra, Icomp=4, TSNUM=60, TSARE=0.4, radii=bondi, alpha = 1.20.

Solvation calculations were performed using water as the solvent to allow comparison with values of experimental aqueous redox potentials.

Optimized geometries and energies for all structures are found in Appendix A.

7.4 Computational methods for Chapter 3

Calculations were performed using the Gaussian 03 [100] program at the B3LYP/6-311+G(2d,p)//B3LYP/6-31G(d) level of theory.[151-153] Zero point vibrational energy corrections were used from frequency calculations performed at B3LYP/6-31G(d).

Truhlar's MPW1K functional[127, 128] was utilized for the tunneling calculations as it is reported to give more accurate vibrational frequencies.[129] Accordingly the geometries of **7-9** were reoptimized and frequencies calculated at the MPW1K/6-31+G(d,p) level of theory.[168]

A conductor-like polarizable continuum model (CPCM)[110, 111] was used to evaluate the electrostatic effect of the bulk solvent. Methanol was specified as the solvent to complement the explicit use of methanol molecules in the gas phase calculation (**B-C** Figures 4 and 5) and the use of methanol in the experimental work.[76] The united atom topological model[165] was used to define the radii of the solvent spheres.

Optimized geometries and energies for all structures are found in Appendix A.

7.5 Computational methods for Chapter 4

Previous benchmarking studies[49, 53] established that BHandHLYP/6-311G(d,p)[152] is a reliable level of theory for the study of the reactions of acyl radicals with π-bonds, so we chose to use this method in this study. Benchmarking performed for the addition of acyl radicals to aromatic rings also supports this choice (see Chapter 5).

Geometry optimizations were performed using the Gaussian 03 program[100] at BHandHLYP/6-311G(d,p). An unrestricted method was used for the open-shell systems. Ground and transition state structures were verified using vibrational frequency analysis, also at the BHandHLYP/6-311G(d,p) level of theory. Zero point vibrational energy corrections have been applied to all structures.

Natural Bond Orbital (NBO) analyses were carried out using NBO 5.0[169] linked through the Gaussian 03 program.

Optimized geometries and energies for all transition structures as well as an Audio Video Interleave (avi) file of the interesting transition structure vector are available in Appendix A.

7.6 Computational methods for Chapter 5

Geometry optimizations for the stationary points involved in the reaction of acetyl radical with benzene were performed using the 6-311G(d,p) basis set at the HF,[155, 156] B3LYP[151-153] and BHandHLYP[152] levels of theory, with higher-level single-point calculations performed at QCISD/6-311G(d,p),[132] CCSD(T)/6-311G(d,p) and CCSD(T)/6-311+G(d,p)[132] on BHandHLYP/6-311G(d,p) optimized geometries. This study (*vide supra*), as well as previous benchmarking studies[48-50, 53] have established that the BHandHLYP/6-311G(d,p) is a reliable level of theory for the study of the reactions of acyl and related radicals with a variety of π-systems.

Consequently, geometry optimizations were performed for the majority of systems in this study using the Gaussian 03 program[100] using that level of theory. Unrestricted methods (UHF, UB3LYP, UBHandHLYP) were used for open-shell systems. All optimized stationary points were verified as corresponding to ground or transition state structures using vibrational frequency analysis. Zero-point vibrational energy (ZPVE) corrections have been applied to all structures. Natural Bond Orbital (NBO) analyses were carried out using the NBO 5.0 software[169] linked through the Gaussian 03 program.

Optimized geometries and energies for all transition structures are available in Appendix A.

7.7 Experimental methods for Chapter 6

7.7.1 Synthesis of benzoic (N'-(2-nitrobenzenesulfonyl)) hydrazide (8,R=*o*-NO_2)

Synthesis of benzoic (N'-(2-nitrobenzenesulfonyl)) hydrazide was performed according to the method of Cacchi and Paolucci.[84]

Tetrahydrofuran (5 mL) was washed with 2 M sodium hydroxide (2 x 5 mL), and 2-nitrosulfonyl chloride (2.2 g, 10 mmol)was added. This solution was added to a solution of benzhydrazide (1.36 g, 10 mmol) in tetrahydrofuran (5 mL). The reaction mixture was stirred for 30 min at room temperature before water (10 mL) was added and solution extracted with dichloromethane (3 x 15 mL). The extracts were dried and the solvent removed under reduced pressure to yield a yellow solid that was recrystallised from dichloromethane/hexanes to give the product as a crystalline white solid in 64% yield. The spectral data for the product was consistent with that previously reported.[23]

M.P.: 164-169 °C, literature M.P.: 156-158 °C[23]

$\delta_H(CDCl_3)$ 7.44 (t, 2H, J=7.2 Hz), 7.56 (t, 1H, J=7.2 Hz), 7.67 (m, 3H), 7.77 (dt, 1H, J=1.3, 7.6 Hz), 8.04 (dd, 1H, J=1.3,7.6 Hz), 8.20 (d, 1H, J=4.5Hz), 8.63 (d, 1H, J=5.7Hz)

ν_{MAX}/cm^{-1} 3258, 1668 (C=O), 1541, 1403, 1354

7.7.1.1 Crystal data for benzoic (N'-(2-nitrobenzenesulfonyl)) hydrazide (8,R=oNO$_2$)

$C_{14}H_{13}N_3O_5S_1C_{l2}$, *M* = 406.24, *T* = 193 K, triclinic, space group *P*-1, *a* = 8.022(16), *b* = 9.3736(19), *c* = 11.9312(24) Å, α = 98.473(3), β = 93.134(3), γ = 94.378(3)°, *V* = 882.81(3)Å^3, *Z* = 2, *D*c = 1.528 g cm^{-3}, specimen: colourless block, 0.30 x 0.30 x 0.2 mm, 3276 measured

reflections, R_{int} = 0.0182, R = 0.0596 for 3112 'observed' data ((I) >2σ(I)), wR = 0.1859, and GOOF = 1.136 for all data '2848'.

7.7.2 Repeat of the McFadyen-Stevens rearrangement

Benzoic (N'-(2-nitrobenzenesulfonyl)) hydrazide (**8**,R=oNO_2) (55 mg, 0.17 mmol) was placed into 2 mL absolute ethanol under an atmosphere of $N_{2(g)}$. Potassium carbonate (180 mg, 1.3 mmol) was added and the mixture refluxed for 2.5 h. Water was added and reaction mixture extracted with dichloromethane (3 x 15 mL). Extracts were dried and the solvent removed under reduced pressure giving 17 mg (87 % yield) of a mixture of benzaldehyde and ethylbenzoate in a 5:1 ratio as determined by ^{1}H NMR.

7.7.3 Repeat of the McFadyen-Stevens rearrangement with one equivalent TEMPO

Benzoic (N'-(2-nitrobenzenesulfonyl)) hydrazide (**8**,R=oNO_2) (55 mg, 0.17 mmol) was added to absolute ethanol (2 mL) under an atmosphere of $N_{2(g)}$. TEMPO (2,2,6,6-tetramethyl-1-piperidinyloxy) **15** (19 mg, 0.12 mmol) and potassium carbonate (180 mg, 1.3 mmol) were added and the mixture refluxed for 1.5 h. Water (5 mL) was added and the reaction mixture extracted with dichloromethane (3 x 15 mL). The extracts were dried and the solvent removed under reduced pressureto give a 1:1 mixture of benzaldehyde and (2,2,6,6-tetramethyl-1-piperidinyloxy)-benzoate **16** (48% combined yield) by ^{1}H NMR.

7.7.4 Repeat of the McFadyen-Stevens rearrangement with four equivalents TEMPO

Benzoic (N'-(2-Nitrobenzenesulfonyl)) hydrazide (**8**,R=oNO_2) (96 mg, 0.3 mmol) was added to absolute ethanol (2 mL) under an atmosphere of $N_{2(g)}$. TEMPO (2,2,6,6-tetramethyl-1-piperidinyloxy) **15** (190 mg, 1.2 mmol) and potassium carbonate (442 mg, 3.2 mmol) was added and the mixture was refluxed for 2 h Water (5 mL) was added and the reaction mixture extracted with dichloromethane (3 x 15 mL). The extracts were dried and the

solvent removed under reduced pressure to give a yellow solid which was purified by column chromatography on silica gel (eluent 30% ethyl acetate/ 70% hexanes) to give (2,2,6,6-tetramethyl-1-piperidinyloxy)-benzoate **16** in 53% yield.

7.7.5 Reaction of benzoic (N'-(2-nitrobenzenesulfonyl)) hydrazide with benzoyl peroxide

Oxygen was purged from ethanol (5 mL) by bubbling through with $N_{2(g)}$ for 10 min after which an atmosphere of $N_{2(g)}$ was maintained. Benzoic (N'-(2-nitrobenzenesulfonyl)) hydrazide (**8**,R=oNO_2) (193 mg, 0.6 mmol) and benzoyl peroxide (7 mg , 0.03 mmol)was added and solution heated to reflux. Three further additions of benzoyl peroxide(7 mg , 0.03 mmol) were added at 15 minute intervals and the solution was then refluxed a further hour (2h total). Water (5 mL) was added and reaction extracted with dichloromethane (3 x 15 mL). The extracts were dried and the solvent removed resulting in a quantitative retrieval of unreacted starting material.

7.7.6 Synthesis of 2-(2-methallyloxy) benzoic (N'-(2-nitrobenzenesulfonyl)) hydrazide (22)

Methyl salicylate (4.7 mL, 26.3 mmol) and 3-chloro-2-methylpropene (3.2 mL, 39.5 mmol) were added to acetone (50 mL). Potassium carbonate (7.3 g, 52.6 mmol) and sodium iodide (0.5 g, 3.3 mmol) were added. The reaction mixture was refluxed for 12 h and further 3-chloro-2-methylpropene (1.5 mL, 18 mmol) was added and reaction refluxed a further 12 h. The solvent was removed under reduced pressure, water added and mixture extracted with diethyl ether (3 x 20 mL). The extracts were washed with 2M sodium hydroxide (4x, 10 mL), and brine (2x, 10 mL), dried and then the solvent removed to give methyl 2-(2-methallyloxy) benzoate in quantitative yield that was used in the next step without further

purification. The spectral data for the product was consistent with that previously reported.[170]

$\delta_H(CDCl_3)$ 1.84 (d, 3H, *J*=0.6 Hz), 3.88 (s, 3H), 4.48 (s, 2H), 4.99(t, 1H, *J*=1.4 Hz), 5.19 (d, 1H, *J*=1 Hz), 6.91-6.98 (m, 2H), 7.41 (m, 1H), 7.79 (dd, 1H, *J*=8, 2 Hz)

Methyl 2-(2-methallyloxy) benzoate (5.5 g, 26 mmol) was refluxed for 1 h in 2M sodium hydroxide (100 mL). The solution was then extracted with dichloromethane (2 x 25 mL) before being made acidic to ~pH 1 with 32% hydrochloric acid. The acidic solution was extracted with dichloromethane (3 x 25 mL) and combined extracts dried and the solvent removed under reduced pressure to yield 2-(2-methallyloxy) benzoic acid in 88% yield that was used in the next step without further purification. The spectral data for the product was consistent with that previously reported.[170]

$\delta_H(CDCl_3)$ 1.85 (s, 3H), 4.68 (s, 2H), 5.09-5.13 (m, 2H), 7.02-7.13 (m, 2H), 7.49-7.55 (m, 1H), 8.14 (dd, 1H, *J*=8, 2 Hz), 10.8 (bs, 1H)

2-(2-Methallyloxy) benzoic acid (0.275 g, 1.43 mmol) was added to dry dichloromethane (5 mL) and carbonyl diimidazole (CDI) (0.255 g, 1.57 mmol) added. The solution was stirred 2 h before washing with water (2 x 10 mL). The organic phase was dried and the solvent removed under reduced pressure to yield the N-acyl imidazole which was reacted with an ethanolic solution of hydrazine hydrate (0.1 mL in 3 mL ethanol). The solution was stirred overnight at room temperature and water was added and solution extracted with dichloromethane (3 x 10 mL). The combined extracts were dried and the solvent removed under reduced pressure to give the benzoic 2-(2-methallyloxy) hydrazide in 92% yield that was used in the next step without further purification. The spectral data for the product was consistent with that previously reported.[23]

$\delta_H(CDCl_3)$ 1.86 (s, 3H), 4.57(s, 2H), 4.81(bs, 2H), 5.05 (s, 1H), 5.07 (s, 1H), 6.93-6.96 (m, 1H), 7.05-7.11 (m, 1H), 7.39-7.45 (m, 1H), 8.16-8.21 (m, 1H), 8.994 (bs, 1H)

Tetrahydrofuran (5 mL) was washed with 2 M sodium hydroxide (2 x 5 mL), and 2-nitrosulfonyl chloride (293 mg, 1.32 mmol) was added. This solution was added to a solution of benzoic 2-(2-methallyloxy) hydrazide (273 mg, 1.32 mmol) in tetrahydrofuran (5 mL) and the reaction stirred for 30 min. Water (10 mL) was added and the solution extracted with dichloromethane (3 x 10 mL). The extracts were dried and the solvent removed under reduced pressure yielding a yellow solid that was purified by column chromatography on silica gel (eluent 40% ethyl acetate/ 60% hexanes) to give 2-(2-methallyloxy) benzoic (N'-(2-nitrobenzenesulfonyl)) hydrazide as a white solid in 62% yield. (50% yield over 5 steps). The spectral data is consistent with that reported by Braslau[23]

M.P.: 144-146 °C Literature M.P.: 108-110 °C

$\delta_H(CDCl_3)$ 1.94 (s, 3H), 4.66 (s, 2H), 5.16(s, 1H), 5.17(s, 1H), 7.01 (m, 2H), 7.44 (dt, 2H, *J*=0.9,7.2 Hz), 7.64 (dt, 1H, *J*=1.5, 7.5 Hz), 7.74 (dt, 1H, *J*=1.5,7.8 Hz), 7.80(d, 1H, *J*=1.8 Hz), 8.02(t, 2H, *J*=6 Hz), 8.72 (d, 1H, *J*=6.3 Hz), 9.83 (d, 1H, *J*=6 Hz)

$\delta_C(CDCl_3)$ 19.8, 73.4, 113.0, 115.3, 118.4, 121.8, 126.5, 132.0, 132.5, 132.7, 133.1, 134.4, 134.6, 139.3, 148.0, 157.0, 164.5

LRMS: 391(M^+, 1), 361(1), 205(5), 175(100), 161(15), 147(18), 121(68), 91(13), 77(19), 65(15), 55(24), 39(12)

HRMS: $M^{+\cdot}$ For ($C_{17}H_{17}N_3O_6S$) predicted 391.0838, found 391.0839

ν_{MAX}/cm^{-1} 3373, 1665 (C=O), 1601, 1540, 1479, 1397

7.7.7 Cyclisation of 2-(2-methallyloxy) benzoic (N'-(2-nitrobenzenesulfonyl)) hydrazide (22) with TEMPO (4equiv)

Into dry ethanol (5 mL) was placed 2-(2-methallyloxy) benzoic (N'-(2-Nitrobenzenesulfonyl)) hydrazide (**22**) (37 mg, 0.1mmol) and TEMPO (58 mg, 0.4 mmol). Potassium carbonate (179 mg, 1.3 mmol) was added and the mixture heated at reflux for 2.5 h. Water, saturated potassium hydrogen sulfate solution and solid sodium sulfite were added until a clear, light coloured solution was obtained, and the mixture was extracted with dichloromethane (3 x 10 mL). Combined extracts were dried and the solvent removed under reduced pressure to give 50 mg of a gold solid. The products were purified using column chromatography on silica gel (eluent 10% ethyl acetate/ 90% hexanes) to give a mixture of 2-(2methallyloxy) benzaldehyde and ethyl 2-(2methallyloxy) benzoate in a 2:3 ratio (28mg, 51% combined yield) with a trace of the directly trapped TEMPO adduct **24**. These products were confirmed by ^{1}H NMR and GCMS.

7.7.7.1 Spectroscopic data for 24

$\delta_H(CDCl_3)$ 1.19-1.48 (m, 18H), 1.87 (s,3H), 4.51 (s, 2H), 5.02 (s, 1H), 5.13 (s, 1H) 6.92-7.00 (m, 2H), 7.45-7.48 (m,1H), 7.81 (d, 1H, *J*=9 Hz)

LRMS: 331 (M^+,3), 316(73), 248(7), 175(37), 157(8), 142(21), 133(15), 126(8), 120(3), 92(8), 83(30), 69(15), 55 (100), 41(52)

ν_{MAX}/cm^{-1} 1759 (C=O)

7.7.7.2 Spectroscopic data for 2-(2methallyloxy)benzaldehyde

$\delta_H(CDCl_3)$ 1.86 (s, 3H), 4.56 (s, 2H), 5.04 (s, 1H), 5.13 (s, 1H), 6.96-7.06 (m, 2H), 7.49-7.57(m, 1H), 7.85 (dd, 1H, *J*=7.6,2 Hz), 10.55 (s, 1H)

LRMS: 176(M^+, 2), 161(10), 147(4), 133(4), 120(55), 105(5), 92(12), 77(5), 65(13), 63(5), 55(100), 39(68)

ν_{MAX}/cm^{-1} 1692(C=O)

7.7.7.3 Spectroscopic data for ethyl 2-(2methallyloxy)benzoate

$\delta_H(CDCl_3)$ 1.37 (t, 3H, *J*=6 Hz), 1.85 (s, 3H), 4.37 (q, 2H, *J*=6 Hz), 5.00 (s, 1H), 5.20 (s, 1H), 6.95 (m, 2H), 7.42 (t, 1H, *J*=1 Hz), 7.80 (m, 1H)

$\delta_C(CDCl_3)$ 14.6, 19.6, 61.1, 72.4, 112.9, 113.5, 120.5, 128.6, 131.9, 133.4, 136.1, 140.6, 166.8

LRMS: 220(M^+, 22), 175(19), 159(10), 146(20), 134(5), 131(15), 121(52), 105(12), 100(35), 92(30), 77(6), 65(18), 55(100), 43(7), 39(48)

LRMS:220 (M^+, 28), 206(2), 191(3), 175(24), 166(7), 159(13), 149(48), 131(20), 121(72), 100(42), 92(47), 77(14), 65(21), 55(100), 39(40)

HRMS: $M^{+\cdot}$ For ($C_{13}H_{16}O_3$) predicted 220.1099, found 220.1099

ν_{MAX}/cm^{-1} 1729(C=O)

7.7.8 Cyclisation of 2-(2-methallyloxy) benzoic (N'-(2-nitrobenzenesulfonyl)) hydrazide (22) with TEMPO (1equiv)

Into dry THF (1 mL) was placed 2-(2-methallyloxy) benzoic (N'-(2-nitrobenzenesulfonyl)) hydrazide (**22**) (105 mg, 0.27 mmol) and TEMPO (49 mg, 0.3 mmol). Dry ethanol (14 mL) was added along with potassium carbonate (335 mg, 2.5 mmol) and the mixture heated at reflux for 3 h. Water, saturated potassium hydrogen sulfate and solid sodium sulfite were added until a clear, light coloured solution was obtained, and the mixture extracted with dichloromethane (3 x 10 mL). The combined extracts were dried and the solvent removed under reduced pressure to give a red oil that was identified as containing a trace of 2-

(2methallyloxy) benzaldehyde, ethyl 2-(2methallyloxy) benzoate and directly trapped TEMPO adduct (**24**) along with the recovered starting material **22**.

7.7.9 Cyclisation of 2-(2-methallyloxy) benzoic (N'-(2-nitrobenzenesulfonyl)) hydrazide (22) with diphenyldiselenide (1equiv)

Into dry ethanol (5 mL) was placed 2-(2-methallyloxy) benzoic (N'-(2-nitrobenzenesulfonyl)) hydrazide (100 mg, 0.255 mmol) and diphenyldiselenide (39.9 mg, 0.128 mmol). Potassium carbonate (351 mg, 2.55 mmol) was added and the mixture heated at reflux for 2.5 h. Water was added and mixture extracted with dichloromethane (3 x 10 mL). The combined extracts were dried and the solvent removed under reduced pressure to give a yellow solid which was were purified using column chromatography on silica gel (eluent 7% ethyl acetate/ 93% hexanes) to give the 2-(2methallyloxy) benzaldehyde (31% yield) and traces of ethyl 2-(2methallyloxy) benzoate and cyclised seleno ester **25**. Compound **25** was identified by comparison of the spectral details to that reported by Chen *et al.*[134]

7.7.9.1 Spectroscopic data for 25

$\delta_H(CDCl_3)$ 1.25 (s, 3H), 3.12 (d, 1H, *J*=13 Hz), 3.29 (d, 1H, *J*=13 Hz), 4.14 (d, 1H, *J*=11 Hz), 4.50 (s, 2H), 6.99-7.60 (m, 9H)

LRMS: 332(M^+, 25), 175(100), 161(10), 147(17), 133(22), 121(25), 105(6), 91(26), 77(12), 65(10), 55(71), 39(20)

ν_{MAX}/cm^{-1} 1690 (C=O)

7.7.10 Cyclisation of 2-(2-methallyloxy) benzoic (N'-(2-Nitrobenzenesulfonyl)) hydrazide (22) with TEMPO (1equiv) and 10 eq potassium ferricyanide.

Into dry THF (1 mL)was placed 2-(2-methallyloxy) benzoic (N'-(2-nitrobenzenesulfonyl)) hydrazide (98 mg, 0.27 mmol) and TEMPO (52 mg, 0.3 mmol). Dry ethanol (14 mL) was added along with potassium carbonate (381 mg, 2.8 mmol) and potassium ferricyanide (17 mg, 0.05 mmol) and the mixture heated at reflux for 3 h. Water was added and mixture extracted with dichloromethane (3 x 10 mL). The combined extracts were dried and the solvent removed under reduced pressure to give 46 mg of a mixture of cyclised TEMPO adduct **23** and 2-(2methallyloxy) benzaldehyde in a 2: 5 ratio and a 21% yield.

7.7.10.1 Spectroscopic data for 23

$\delta_H(CDCl_3)$ 1.00-1.85 (m, 18H), 3.76 (d, 1H, *J*=8.5 Hz), 4.08 (d, 1H, *J*=8.5 Hz), 4.24 (d, 1H, *J*=11 Hz), 4.59 (d, 1H, *J*=11 Hz), 6.98-7.00 (m, 2H), 7.40-7.45 (m, 1H), 7.92 (dd, 1H, *J*=7.5, 1.5 Hz)

LRMS: 331 (M^+,0.04), 316(0.5), 261(0.05), 175(100), 133(32), 129(5), 91(13), 55 (40), 41(13)

ν_{MAX}/cm^{-1} 1693 (C=O), 1602

7.7.11 Cyclisation of 2-(2-methallyloxy) benzoic (N'-(2-Nitrobenzenesulfonyl)) hydrazide (22) with diphenyldiselenide (1equiv) and $K_3Fe(CN)_6$

Into dry THF (1 mL) was placed 2-(2-methallyloxy) benzoic (N'-(2-Nitrobenzenesulfonyl)) hydrazide (90 mg, 0.23 mmol) and diphenyldiselenide (78 mg, 0.25 mmol). Dry ethanol (14 mL) was added along with potassium carbonate (335 mg, 2.5 mmol) and potassium ferricyanide (804 mg, 2.4 mmol) and the mixture heated at reflux for 4 h. Water was added and mixture extracted with dichloromethane (3 x 10 mL). The combined extracts were dried and the solvent removed under reduced pressure to give a yellow solid which was purified using column chromatography on silica gel (eluent 7% ethyl acetate/ 93% hexanes)

to give ethyl 2-(2methallyloxy) benzoate (26% yield), cyclised selenide (**25**, 17% yield) and 2-(2methallyloxy) benzamide (24 % yield).

7.7.11.1 Spectroscopic data for 2-(2methallyloxy)benzamide

$\delta_H(CDCl_3)$ 1.86 (s,3H), 4.59 (s, 2H), 5.07 (s, 1H), 5.11 (s, 1H), 6.0 (bs, 1H), 6.96 (d, 1H, *J*=8), 7.10 (m, 1H), 7.44 (m, 1H), 7.8 (bs, 1H), 8.20 (m, 1H)

LRMS: 191(M^+, 10), 174(22), 161(38), 146(24), 133(25), 121(92), 105(44), 91(42), 83(22), 77(10), 72(76), 65(17), 55(100), 43(10), 39(25)

HRMS: $M^{+\cdot}$ For ($C_{11}H_{13}NO_2$) predicted 191.0946, found 191.0943

ν_{MAX}/cm^{-1} 1668 (C=O)

7.8 Computational methods for Chapter 6

Geometry optimizations, vibrational frequency calculations and single point energy calculations were performed using the Gaussian 03 software package.

A model (see Scheme 7.1) was utilised for benchmarking calculations and the outcome is shown in Table 7.1. Benchmarking was performed at B3LYP,[151-153] BHandHLYP,[152] BMK,[163] MPW1K,[128] M05,[171, 172] and G3(MP2)RAD[173] levels of theory and results compared to CBS-QB3[154, 174] as our high level. B3LYP and M05 were chosen as the best density functional methods for calculations.

For the full structures B3LYP and M05 were utilised as levels of theory. As there are two aromatic rings in the fuller structure it was thought that dispersion effects may change the outcome of reactions, therefore structures were reoptimized at B97D[175] and ωB97XD[133] to give dispersion corrections. As there was quite a difference in results depending on the level of theory utilised, MP2 calculations were also performed however due to computational restrictions some structures were unable to be calculated.

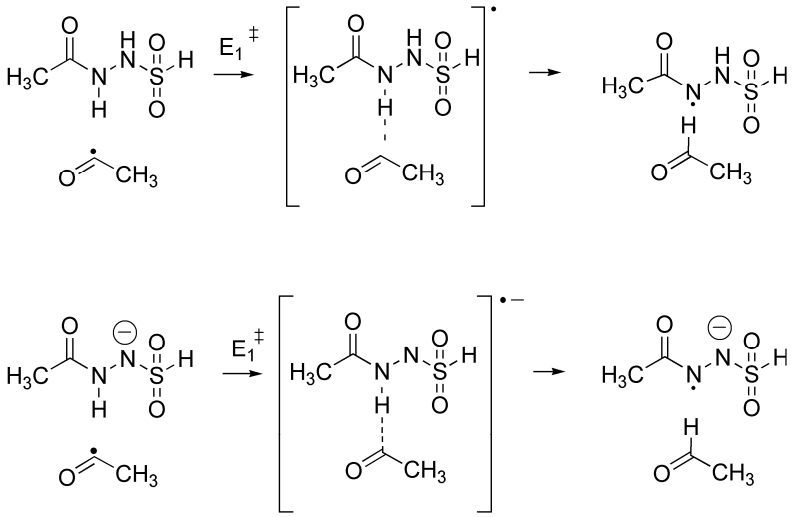

Scheme 7.1

Table 7.1 Results of calculations of barriers ($E_1^{\ddagger}$) and exothermicities of reactions outlined in Scheme 7.1. E in kJ mol^{-1}.

	Neutral reaction		Anionic reaction	
	$E_1^{\ddagger}$	ΔE	$E_1^{\ddagger}$	ΔE
B3LYP	58	-13	7	-80
BHandHLYP	87	-10	39	-74
BMK	73	-5	19	-73
MPW1K	74	-8	24	-71
M05	58	-13	6	-77
G3(MP2)RAD	59	-9	-15	-69
CBS-QB3	67	-11	16	-66

Geometry optimizations were performed at the five levels of theory using a 6-31G(d) basis set. Single point calculations were then performed on those geometries using a 6-311+G(d,p) basis set.[151-153] Zero point vibrational energy corrections were used from frequency calculations performed with the 6-31G(d) basis set. Unrestricted methods (UB3LYP, UM05, UB97D and UωB97XD) were used for open-shell systems. All optimized stationary points were verified as corresponding to ground or transition state structures using vibrational frequency analysis.

7.8.1 Tunnelling calculations

Truhlar's MPW1K functional[127, 128] was utilized for the tunneling calculations as it is reported to give more accurate vibrational frequencies.[129] Accordingly the geometries of **6** and **7** were reoptimized and frequencies calculated at the MPW1K/6-31+G(d,p) level of theory.[127]

7.8.2 Solvation calculations

Solvation calculations were performed using the Gaussian09[176] software package. A conductor-like polarizable continuum model (CPCM)[110, 111] was used to evaluate the electrostatic effect of the bulk solvent. Ethanol was specified as the solvent to complement the use of ethanol in the experimental work.[76]

Optimized geometries and energies for all transition structures are available in Appendix A.

References

1. Frieden, T. R.; Sterling, T. R.; Munsiff, S. S.; Watt, C. J.; Dye, C., Tuberculosis. *The Lancet* **2003,** 362, (9387), 887-899.
2. http://www.cdc.gov/tb/topic/basics/default.htm Centre for Disease control and prevention Basic Tuberculosis facts. http://www.cdc.gov/tb/topic/basics/default.htm (23 march),
3. Rouhi, A. M., Tuberculosis: A tough adversary. *Chemical and Engineering News* **1999,** 77, (20), 52-69.
4. Konstantinos, A., Testing for Tuberculosis. *Australian Prescriber* **2010,** 33, (1), 12-18.
5. Sullivan, T. J.; Truglio, J. J.; Boyne, M. E.; Novichenok, P.; Zhang, X.; Stratton, C. F.; Li, H.; Kaur, T.; Amin, A.; Johnson, F.; Slayden, R. A.; Kisker, C.; Tonge, P. J., High affinity InhA inhibitors with activity against drug-resistant strains of *Mycobacterium tuberculosis. ACS Chemical Biology* **2005,** 1, (1), 43-53.
6. Rozwarski, D. A.; Grant, G. A.; Barton, D. H. R.; Jacobs Jr., W. R.; Sacchettini, J. C., Modification of the NADH of the Isoniazid Target (InhA) from Mycobacterium tuberculosis. *Science* **1998,** 279, 98-102.
7. Singh, R.; Switala, J.; Loewen, P. C.; Ivancich, A., Two [Fe(IV):O Trp.bul.] Intermediates in M. tuberculosis Catalase-Peroxidase Discriminated by Multifrequency (9-285 GHz) EPR Spectroscopy: Reactivity toward Isoniazid. *Journal of the American Chemical Society* **2007,** 129, (51), 15954-15963.
8. Wengenack, N.; Rusnak, F., Evidence for isoniazid-dependant free radical generation catalyzed by *Mycobacterium tuberculosis* KatG and the isoniazid resistant mutant KatG(S315T). *Biochemistry* **2001,** 40, 8990-8996.
9. Bloom, B. R.; Murray, C. J., Tuberculosis: commentary on a reemergent killer. *Science* **1992,** 257, (5073), 1055-64.
10. http://www.mayoclinic.com/health/tuberculosis/DS00372/DSECTION=causes http://www.mayoclinic.com/health/tuberculosis/DS00372/DSECTION=causes (23 March),
11. Jasmer Robert, M.; Nahid, P.; Hopewell Philip, C. *Clinical practice. Latent tuberculosis infection*; Division of Pulmonary and Critical Care Medicine, San Francisco General Hospital, San Francisco, CA 94110, USA.: United States, 2002; pp 1860-6.
12. Ghiladi, R. A.; Medzihradszky, K. F.; Rusnak, F. M.; Ortiz de Montellano, P. R., Correlation between Isoniazid Resistance and Superoxide Reactivity in Mycobacterium tuberculosis KatG. *Journal of the American Chemical Society* **2005,** 127, (38), 13428-13442.
13. Bellei, M.; Jakopitsch, C.; Battistuzzi, G.; Sola, M.; Obinger, C., Redox Thermodynamics of the Ferric-Ferrous Couple of Wild-Type Synechocystis KatG and KatG(Y249F). *Biochemistry* **2006,** 45, (15), 4768-4774.
14. Saint-Joanis, B.; Souchon, H.; Wilming, M.; Johnsson, K.; Alzari, P. M.; Cole, S. T., Use of site-directed mutagenesis to probe the structure, function and isoniazid activation of the catalase/peroxidase, KatG, from Mycobacterium tuberculosis. *Biochemical Journal* **1999,** 338, (3), 753-760.
15. Wengenack, N.; Hoard, H. M.; Rusnak, F., Isoniazid oxidation by *Mycobacterium tuberculosis* KatG: A role for superoxide which correlates with isoniazid susceptibility. *Journal of the American Chemical Society* **1999,** 121, 9748-9749.

16. Zhao, X.; Yu, S.; Magliozzo, R. S., Characterization of the Binding of Isoniazid and Analogues to Mycobacterium tuberculosis Catalase-Peroxidase. *Biochemistry* **2007,** 46, (11), 3161-3170.
17. Zhao, X.; Yu, H.; Yu, S.; Wang, F.; Sacchettini, J. C.; Magliozzo, R. S., Hydrogen Peroxide-Mediated Isoniazid Activation Catalyzed by Mycobacterium tuberculosis Catalase-Peroxidase (KatG) and Its S315T Mutant. *Biochemistry* **2006,** 45, (13), 4131-4140.
18. Kadam, S. D.; Supale, A. R.; Gokavi, G. S., Kinetics and mechanism of oxidation of benzoic acid hydrazide by bromate catalyzed by Anderson type hexamolybdochromate(III) in aqueous acidic medium. *Zeitschrift fuer Physikalische Chemie (Muenchen, Germany)* **2008,** 222, (4), 635-646.
19. Kocevar, M.; Mihorko, P.; Polanc, S., An Efficient and Simple Thallium(III)-Induced Cleavage of the Hydrazino Moiety. *Journal of Organic Chemistry* **1995,** 60, (5), 1466-9.
20. Prakash, O.; Sharma, V.; Sadana, A., Hypervalent iodine oxidation of acid hydrazides: a new synthesis of N,N'-diacylhydrazines. *Synthetic Communications* **1997,** 27, (19), 3371-3377.
21. Prakash, O.; Sharma, V.; Sadana, A., A new and facile iodine(III)-mediated method for the cleavage of hydrazides. *Journal of Chemical Research, Synopses* **1996**, (2), 100-1.
22. Hoffman, R. V.; Kumar, A., Oxidation of hydrazine derivatives with arylsulfonyl peroxides. *Journal of Organic Chemistry* **1984,** 49, (21), 4014-17.
23. Braslau, R.; Anderson, M. O.; Rivera, F.; Jimenez, A.; Haddad, T.; Axon, J. R., Acyl hydrazines and precursors to acyl radicals. *Tetrahedron* **2002,** 58, 5513-5523.
24. Aylward, J. B.; Norman, R. O. C., Reactions of lead tetraacetate. XVI. The oxidation of mono-acylhydrazines. *J. Chem. Soc., C* **1968**, (18), 2399-402.
25. Hongekar, M. L.; Patil, J. B., Hexacyanoferrate(III) oxidation of b-valeric and iso-valeric acid hydrazides in perchloric acid. *Transition Metal Chemistry* **1994,** 19, 509-512.
26. Srivinvas, R.; Reddy, B. V. S.; Yadav, J. S.; Ramalingam, T., An efficient and selective conversion of hydrazides into esters and acids. *Journal of Chemical Research, Synopses* **2000**, (8), 376-377.
27. Stefane, B.; Kocevar, M.; Polanc, S., Ceric(IV) ammonium nitrate in the selective conversion of hydrazides to esters. *Tetrahedron Letters* **1999,** 40, 4429-4432.
28. Ho, T.-L.; Ho, H. C.; Wong, C. M., Ceric ammonium nitrate oxidation of carboxylic acid hydrazides. *Synthesis* **1972**, (10), 562-3.
29. Back, T. G.; Collins, S.; Kerr, R. G., Oxidation of hydrazines with benzeneseleninic acid and anhydride. *Journal of Organic Chemistry* **1981,** 46, (8), 1564-70.
30. Tsuji, J.; Nagashima, T.; Qui, N. T.; Takayanagi, H., Facile oxidative conversion of hydrazides of carboxylic acids to corresponding acids, esters and amides using copper compounds. *Tetrahedron* **1980,** 36, 1311-1315.
31. Curtius, T., Hydrazide und Azide organischer Säuren I. Abhandlung. *Journal fur Praktische Chemie* **1894,** 50, (1), 275-294.
32. Bath, S.; Laso, N. M.; Lopez-Ruiz, H.; Quiclet-Sire, B.; Zard, S. Z., A practical acess to acyl radicals from acyl hydrazides. *Chemical Communications* **2003,** 2, 204-205.
33. Caronna, T.; Galli, R.; Malatesta, V.; Minisci, F., Homolytic acylation of benzothiazole. A diagnostic criterion for the presence of acyl radicals. *Journal of the Chemical Society (C)* **1971**, 1747-1750.
34. Jagdale, M. H.; Nimbalkar, A. Y.; Mane, J. D.; Gidde, P. A., Kinetics and mechanism of base catalyzed hydrolysis of m-methoxybenzoic acid hydrazide. *Journal of the Indian Chemical Society* **1984,** 61, (8), 680-2.
35. Jagdale, M. H.; Nimbalkar, A. Y., Kinetics and mechanism of the acid hydrolysis of p-methoxybenzoic acid hydrazide. *Acta Ciencia Indica* **1977,** 3, (4), 299-302.

36. Jagdale, M. H.; Nimbalkar, A. Y., Kinetics and mechanism of acid hydrolysis of m-methoxybenzoic acid hydrazide. *Acta Ciencia Indica, Chemistry* **1981,** 7, (1-4), 59-62A.
37. Jagdale, M. H.; Nimbalkar, A. Y., Kinetics and mechanism of the acid hydrolysis of p-methoxybenzoic acid hydrazide. *Acta Ciencia Indica* **1976,** 2, (4), 336-40.
38. Jagdale, M. H.; Nimbalkar, A. Y.; Mane, J. D.; Gidde, P. A.; Mali, M. D., Kinetics and mechanism of acid hydrolysis of nitrobenzoic acid hydrazides. *Journal of the Indian Chemical Society* **1987,** 64, (2), 122-4.
39. DeTar, D. F.; Binzet, S.; Darba, P., Theoretical calculation of effects of steric hindrance on rates of esterification and of acid-catalyzed hydrolysis. *Journal of Organic Chemistry* **1987,** 52, (10), 2074-82.
40. Hori, K.; Ikenaga, Y.; Arata, K.; Takahashi, T.; Kasai, K.; Noguchi, Y.; Sumimoto, M.; Yamamoto, H., Theoretical study on the reaction mechanism for the hydrolysis of esters and amides under acidic conditions. *Tetrahedron* **2007,** 63, (5), 1264-1269.
41. Lesutis, H. P.; Glaser, R.; Liotta, C. L.; Eckert, C. A., Acid/base-catalyzed ester hydrolysis in near-critical water. *Chemical Communications* **1999**, (20), 2063-2064.
42. Zhan, C.-G.; Landry, D. W.; Ornstein, R. L., Theoretical Studies of Fundamental Pathways for Alkaline Hydrolysis of Carboxylic Acid Esters in Gas Phase. *Journal of the American Chemical Society* **2000,** 122, (7), 1522-1530.
43. Zhan, C.-G.; Landry, D. W.; Ornstein, R. L., Energy Barriers for Alkaline Hydrolysis of Carboxylic Acid Esters in Aqueous Solution by Reaction Field Calculations. *Journal of Physical Chemistry A* **2000,** 104, (32), 7672-7678.
44. Zhan, C.-G.; Landry, D. W.; Ornstein, R. L., Reaction Pathways and Energy Barriers for Alkaline Hydrolysis of Carboxylic Acid Esters in Water Studied by a Hybrid Supermolecule-Polarizable Continuum Approach. *Journal of the American Chemical Society* **2000,** 122, (11), 2621-2627.
45. Lane, C. A.; Cheung, M. F.; Dorsey, G. F., The possibility of a cyclic mechanism for acid-catalyzed ester hydrolysis. *Journal of the American Chemical Society* **1968,** 90, (23), 6492-4.
46. Moodie, R. B.; Wale, P. D.; Whaite, T. J., Transition state in the acid-catalyzed hydrolysis of benzamide. *Journal of the Chemical Society* **1963**, (Aug.), 4273-4.
47. Chatgilialoglu, C.; Crich, D.; Komatsu, M.; Ryu, I., Chemistry of Acyl Radicals. *Chemical Reviews* **1999,** 99, (8), 1991-2069.
48. Kyne, S. H.; Schiesser, C. H., Ab Initio Studies of Carbonyl Radical Additions to Hydrazone Systems. *Australian Journal of Chemistry* **2009,** 62, (7), 728-733.
49. Kyne, S. H.; Schiesser, C. H.; Matsubara, H., Multiorbital Interactions during Acyl Radical Addition Reactions Involving Imines and Electron-Rich Olefins. *Journal of Organic Chemistry* **2008,** 73, (2), 427-434.
50. Kyne, S. H.; Schiesser, C. H.; Matsubara, H., Multi-component orbital interactions during oxyacyl radical addition reactions involving imines and electron-rich olefins. *Organic & Biomolecular Chemistry* **2007,** 5, (24), 3938-3943.
51. Matsubara, H.; Falzon, C. T.; Ryu, I.; Schiesser, C. H., Radicals masquerading as electrophiles: a computational study of the intramolecular addition reactions of acyl radicals to imines. *Organic & Biomolecular Chemistry* **2006,** 4, (10), 1920-1926.
52. Schiesser, C. H., Taming the free radical shrew - learning to control homolytic reactions at higher heteroatoms. *Chemical Communications* **2006**, (39), 4055-4065.
53. Schiesser, C. H.; Matsubara, H.; Ritsner, I.; Wille, U., Unexpected dual orbital effects in radical addition reactions involving acyl, silyl and related radicals. *Chemical Communications* **2006**, (10), 1067-1069.
54. Crich, D.; Chen, C.; Hwang, J.-T.; Yuan, H.; Papadatos, A.; Walter, R. I., Photoinduced Free Radical Chemistry of the Acyl Tellurides: Generation, Inter- and Intramolecular

Trapping, and ESR Spectroscopic Identification of Acyl Radicals. *Journal of the American Chemical Society* **1994,** 116, (20), 8937-51.
55. Crich, D.; Quintero, L., Radical chemistry associated with the thiocarbonyl group. *Chemical Reviews* **1989,** 89, (7), 1413-32.
56. Mendenhall, G. D.; Protasiewicz, J. D.; Brown, C. E.; Ingold, K. U.; Lusztyk, J., 5-Endo Closure of the 2-Formylbenzoyl Radical. *Journal of the American Chemical Society* **1994,** 116, (5), 1718-24.
57. Mendenhall, G. G.; Protasiewicz, J. D.; Brown, C. E.; Ingold, K. U.; Lusztyk, J., 5-Endo closure of the 2-formylbenzoyl radical. [Erratum to document cited in CA120:190772]. *Journal of the American Chemical Society* **1994,** 116, (12), 5525.
58. Schiesser, C. H.; Wille, U.; Matsubara, H.; Ryu, I., Radicals Masquerading as Electrophiles: Dual Orbital Effects in Nitrogen-Philic Acyl Radical Cyclization and Related Addition Reactions. *Accounts of Chemical Research* **2007,** 40, (5), 303-313.
59. Ryu, I.; Miyazato, H.; Kuriyama, H.; Matsu, K.; Tojino, M.; Fukuyama, T.; Minakata, S.; Komatsu, M., Broad-Spectrum Radical Cyclizations Boosted by Polarity Matching. Carbonylative Access to alpha -Stannylmethylene Lactams from Azaenynes and CO. *Journal of the American Chemical Society* **2003,** 125, (19), 5632-5633.
60. Pfenninger, J.; Heuberger, C.; Graf, W., The radical induced stannane reduction of selenoesters and selenocarbonates: a new method for the degradation of carboxylic acids to nor-alkanes and for desoxygenation of alcohols to alkanes. *Helvetica Chimica Acta* **1980,** 63, (8), 2328-37.
61. Chen, C.; Crich, D.; Papadatos, A., The chemistry of acyl tellurides: Generation and trapping of acyl radicals, including aryltellurium group transfer. *Journal of the American Chemical Society* **1992,** 114, 8313-8314.
62. Ryu, I.; Yamazaki, H.; Ogawa, A.; Kambe, N.; Sonoda, N., Four carbon component coupling reaction based on free-radical carbonylation: an easy access to beta -functionalized delta, ε-unsaturated ketones. *Journal of the American Chemical Society* **1993,** 115, (3), 1187-9.
63. Beckwith, A. L. J.; Schiesser, C. H., Regio- and stereoselectivity of alkenyl radical ring closure: a theoretical study. *Tetrahedron* **1985,** 41, (19), 3925-41.
64. Spellmeyer, D. C.; Houk, K. N., Force-field model for intramolecular radical additions. *Journal of Organic Chemistry* **1987,** 52, (6), 959-74.
65. Tomaszewski, M. J.; Warkentin, J., Chiral induction in aryl radical cyclization to the aldimino functional group. *Journal of the Chemical Society, Chemical Communications* **1993**, (11), 966-8.
66. Tomaszewski, M. J.; Warkentin, J.; Werstiuk, N. H., Free-radical chemistry of imines. *Australian Journal of Chemistry* **1995,** 48, (2), 291-321.
67. Bowman, W. R.; Stephenson, P. T.; Terrett, N. K.; Young, A. R., Radical cyclizations of imines and hydrazones. *Tetrahedron* **1995,** 51, (29), 7959-80.
68. Bowman, W. R.; Stephenson, P. T.; Young, A. R., Synthesis of nitrogen heterocycles using tandem radical cyclization of imines. *Tetrahedron Letters* **1995,** 36, (31), 5623-6.
69. Falzon, C. T.; Ryu, I.; Schiesser, C., 5-Azahexenoyl radicals cyclize via nucleophilic addition to the acyl carbon rather than 5-exo homolytic addition at the imine. *Chemical Communications* **2002,** 2002, 2338-2339.
70. Bellatti, M.; Caronna, T.; Citterio, A.; Minisci, F., Nucleophilic character of acyl radicals. Absolute rate constant for the acylation of protonated benzothiazole by pivaloyl radical. *Journal of the Chemical Society Perkin Transactions II* **1976**, 1835-1838.
71. Fontana, F.; Minisci, F.; Nogueira Barbosa, M. C.; Vismara, E., Homolytic acylation of protonated pyridines and pyrazines with alpha -keto acids: the problem of monoacylation. *Journal of Organic Chemistry* **1991,** 56, (8), 2866-9.

72. Urry, W. H.; Trecker, D. J.; Hartzler, H. D., Free-radical rearrangements. II. Ketones and esters from the reactions of aldehydes with peroxides. *Journal of Organic Chemistry* **1964,** 29, (7), 1663-9.
73. Grissom, J. W.; Klingberg, D.; Meyenburg, S.; Stallman, B. L., Enediyne- and Tributyltin Hydride-Mediated Aryl Radical Additions onto Various Radical Acceptors. *Journal of Organic Chemistry* **1994,** 59, (25), 7876-88.
74. McFadyen, J. S.; Stevens, T. S., New method for the conversion of acids into aldehydes. *Journal of the Chemical Society* **1936**, 584-7.
75. Matin, S. B.; Craig, J. C.; Chan, R. P. K., An Investigation of the McFadyen-Stevens Reaction. *Journal of Organic Chemistry* **1974,** 39, (15), 2285-2289.
76. Amos, R. I. J.; Gourlay, B. S.; Schiesser, C. H.; Smith, J. A.; Yates, B. F., A mechanistic study on the oxidation of hydrazides: application to the tuberculosis drug isoniazid. *Chemical Communications* **2008**, (14), 1695-1697.
77. Cram, D. J.; Bradshaw, J. S., Electrophilic substitution at saturated carbon. XIX. Nitrogen as leaving group from an alkyl diimide. *Journal of the American Chemical Society* **1963,** 85, 1108-18.
78. Dhar, M. L.; Hughes, E. D.; Ingold, C. K.; Mandour, A. M. M.; Maw, G. A.; Woolf, L. I., Mechanism of elimination reactions. XVI. Constitutional influences in elimination. General discussion. *Journal of the Chemical Society* **1948**, 2093-2119.
79. Myers, A. G.; Movassaghi, M.; Zheng, B., Single-Step Process for the Reductive Deoxygenation of Unhindered Alcohols. *Journal of the American Chemical Society* **1997,** 119, (36), 8572-8573.
80. Myers, A. G.; Movassaghi, M.; Zheng, B., Mechanistic studies of the free-radical fragmentation of monoalkyl diazenes. *Tetrahedron Letters* **1997,** 38, (37), 6569-6572.
81. Miranda, L. D.; Zard, S. Z., Some mechanistic observations on the borohydride mediated reductive cyclization of tosylhydrazones. *Chemical Communications* **2001**, (12), 1068-1069.
82. Babad, H.; Herbert, W.; Stiles, A. W., McFadyen-Stevens synthesis of aliphatic aldehydes containing a-hydrogens. *Tetrahedron Letters* **1966**, (25), 2927-31.
83. Dudman, C. C.; Grice, P.; Reese, C. B., Use of 2,4,6-triisopropylbenzenesulfonylhydrazide in the McFadyen-Stevens aldehyde synthesis. *Tetrahedron Letters* **1980,** 21, (48), 4645-8.
84. Cacchi, S.; Paolucci, G., Aldehydes from carboxylic acids via acylsulfenylhydrazides. *Gazzetta Chimica Italiana* **1974,** 104, (1-2), 221-4.
85. Nguyen, M.; Quemard, A.; Broussy, S.; Bernadou, J.; Meunier, B., Mn(III) pyrophosphate as an efficient tool for studying the mode of action of isoniazid on the InhA protein of *Mycobacterium tuberculosis. Antimicrobial Agents and Chemotherapy* **2002,** 46, (7), 2137-2144.
86. Nguyen, M.; Claparols, C.; Bernadou, J.; Meunier, B., A fast and efficient metal-mediated oxidation of isoniazid and identification of isoniazid-NAD(H) adducts. *ChemBioChem* **2001,** 2, 877-883.
87. Johnsson, K.; Schultz, P. G., Mechanistic studies of the oxidation of isoniazid by the catalase peroxidase from Mycobacterium tuberculosis. *Journal of the American Chemical Society* **1994,** 116, 7425-7426.
88. Nguyen, M.; Claparols, C.; Bernadou, J.; Meunier, B., Is the isonicotinoyl radical generated during activation of isoniazid by Mn(III)-pyrophosphate? *Comptes Rendus Chimie* **2002,** 5, (4), 325-330.
89. Brown, D. H.; Cross, R. J.; Millington, D., Photochemical reactions between tertiary phosphines and organic diselenides. *Journal of the Chemical Society, Dalton Transactions: Inorganic Chemistry (1972-1999)* **1977**, (2), 159-61.

90. Boger, D. L.; Mathvink, R. J., Acyl radicals: intermolecular and intramolecular alkene addition reactions. *Journal of Organic Chemistry* **1992,** 57, (5), 1429-43.
91. Johnston, L. J.; Scaiano, J. C.; Ingold, K. U., Kinetics of cyclopropyl radical reactions. 1. Absolute rate constants for some addition and abstraction reactions. *Journal of the American Chemical Society* **1984,** 106, (17), 4877-81.
92. Smith J. A. and Gourlay B. Unpublished work, University of Tasmania
93. Similar experiments conducted with diphenyldiselenide and protonated benzothiazole give further evidence of the acyl radical with the selenoesters being formed in 8-24% yield and the benzoylbenzothiazole being formed in a 20% yield
94. Barton, D. H. R.; Choi, S. Y.; Hu, B.; Smith, J. A., Evidence for a higher oxidation state of manganese in the reaction of dinuclear manganese complexes with oxidants. Comparison with iron based gif chemistry. *Tetrahedron* **1998,** 54, 3367-3378.
95. Wieghardt, K.; Bossek, U.; Nuber, B.; Weiss, J.; Bonvoisin, J.; Corbella, M.; Vitols, S. E.; Girerd, J. J., Synthesis, crystal structures, reactivity, and magnetochemistry of a series of binuclear complexes of manganese (II), -(iii), and -(IV) of biological relevance. *Journal of the American Chemical Society* **1988,** 110, 7398-7411.
96. Although it was reported that the manganese catalyst and periodic acid gave no detectable amount of oxygen by a change of the headspace volume, other activating agents such as oxone do generate detectable levels.
97. Crich, D.; Hao, X., Generation and Cyclization of Acyl Radicals from Thiol Esters Under Nonreducing, Tin-Free Conditions. *Journal of Organic Chemistry* **1997,** 62, (17), 5982-5988.
98. Amos, R. I. J.; Schiesser, C. H.; Smith, J. A.; Yates, B. F., Nucleophilic Acyl Substitution of Acyl Diimides. *Journal of Organic Chemistry* **2009,** 74, (15), 5707-5710.
99. Feng, Y.; Huang, H.; Liu, L.; Guo, Q.-X., Homolytic bond dissociation energies associated with acyl radicals and electron demands of acyl groups. *Physical Chemistry Chemical Physics* **2003,** 5, (4), 685-690.
100. Frisch, M. J.; Trucks, G. W.; Schlegel, H. B.; Scuseria, G. E.; Robb, M. A.; J. R. Cheeseman; Montgomery Jr, J. A.; Vreven, T.; Kudin, K. N.; Burant, J. C.; Millam, J. M.; Iyengar, S. S.; Tomasi, J.; Barone, V.; Mennucci, B.; Cossi, M.; Scalmani, G.; Rega, N.; Petersson, G. A.; Nakatsuji, H.; Hada, M.; Ehara, M.; Toyota, K.; Fukuda, R.; Hasegawa, J.; Ishida, M.; Nakajima, T.; Honda, Y.; Kitao, O.; Nakai, H.; Klene, M.; Li, X.; Knox, J. E.; Hratchian, H. P.; Cross, J. B.; Bakken, V.; Adamo, C.; Jaramillo, J.; Gomperts, R.; Stratmann, R. E.; Yazyev, O.; Austin, A. J.; Cammi, R.; Pomelli, C.; Ochterski, J. W.; Ayala, P. Y.; Morokuma, K.; Voth, G. A.; Salvador, P.; Dannenberg, J. J.; Zakrzewski, V. G.; Dapprich, S.; Daniels, A. D.; Strain, M. C.; Farkas, O.; Malick, D. K.; Rabuck, A. D.; Raghavachari, K.; Foresman, J. B.; Ortiz, J. V.; Cui, Q.; Baboul, A. G.; Clifford, S.; Cioslowski, J.; Stefanov, B. B.; Liu, G.; Liashenko, A.; Piskorz, P.; Komaromi, I.; Martin, R. L.; Fox, D. J.; Keith, T.; Al-Laham, M. A.; Peng, C. Y.; Nanayakkara, A.; Challacombe, M.; Gill, P. M. W.; Johnson, B.; Chen, W.; Wong, M. W.; Gonzalez, C.; Pople, J. A., *Gaussian 03, Revision D.01,*. Gaussian, Inc., Wallingford CT: 2004.
101. Fu, Y.; Liu, L.; Yu, H.-Z.; Wang, Y.-M.; Guo, Q.-X., Quantum-Chemical Predictions of Absolute Standard Redox Potentials of Diverse Organic Molecules and Free Radicals in Acetonitrile. *Journal of the American Chemical Society* **2005,** 127, (19), 7227-7234.
102. Atkins, P. W., *Physical Chemistry* Fourth ed.; Oxford University Press: Oxford, 1990.
103. Lukat-Rodgers, G. S.; Wengenack, N. L.; Rusnak, F.; Rodgers, K. R., Carbon Monoxide Adducts of KatG and KatG(S315T) as Probes of the Heme Site and Isoniazid Binding. *Biochemistry* **2001,** 40, (24), 7149-7157.
104. Wengenack, N. L.; Lopes, H.; Kennedy, M. J.; Tavares, P.; Pereira, A. S.; Moura, I.; Moura, J. J. G.; Rusnak, F., Redox Potential Measurements of the Mycobacterium

tuberculosis Heme Protein KatG and the Isoniazid-Resistant Enzyme KatG(S315T): Insights into Isoniazid Activation. *Biochemistry* **2000,** 39, (37), 11508-11513.
105. The scan optimised the geometries with the relevent atoms 2.0 A apart and then reoptimised geometries as they were stepped 0.1 A closer for 10 steps
106. Eckart, C., The penetration of a potential barrier by electrons. *Physical Review* **1930,** 35, 1303-9.
107. Sandala, G. M.; Smith, D. M.; Coote, M. L.; Golding, B. T.; Radom, L., Insights into the Hydrogen-Abstraction Reactions of Diol Dehydratase: Relevance to the Catalytic Mechanism and Suicide Inactivation. *Journal of the American Chemical Society* **2006,** 128, (10), 3433-3444.
108. Yates, B. F.; Radom, L., Intramolecular hydrogen migration in ionized amines: a theoretical study of the gas-phase analogs of the Hofmann-Loeffler and related rearrangements. *Journal of the American Chemical Society* **1987,** 109, (10), 2910-15.
109. Many thanks to Dr Mark Taylor for helpful discussions and a spreadsheet to enable calculation of Eckart coefficients
110. Cossi, M.; Rega, N.; Scalmani, G.; Barone, V., Energies, structures, and electronic properties of molecules in solution with the C-PCM solvation model. *Journal of Computational Chemistry* **2003,** 24, (6), 669-81.
111. Barone, V.; Cossi, M., Quantum Calculation of Molecular Energies and Energy Gradients in Solution by a Conductor Solvent Model. *Journal of Physical Chemistry A* **1998,** 102, (11), 1995-2001.
112. The relevant energy for G is not shown as it is off the scale for this graph at -205 kJ mol
113. The BHandHLYP/6-311G(d,p) generated molecular orbitals for the C2 position are representative of the key orbitals generated for the C3 and C4 positions.
114. These results are consistent with our experimental results in that the formation of acyl radicals from the oxidation of hydrazides by a manganese catalyst in pyridine gave no acylated pyridine products.(See chapter 1 for details)
115. The BHandHLYP/6-311G(d,p) generated molecular orbitals for the C2 position are representative of the key orbitals generated for the C3 and C4 positions.
116. Hart, D. J., Free-radical carbon-carbon bond formation in organic synthesis. *Science* **1984,** 223, (4639), 883-7.
117. Ramaiah, M., Radical reactions in organic synthesis. *Tetrahedron* **1987,** 43, (16), 3541-676.
118. Curran, D. P., The design and application of free radical chain reactions in organic synthesis. Part 1. *Synthesis* **1988**, (6), 417-39.
119. Curran, D. P., The design and application of free radical chain reactions in organic synthesis. Part 2. *Synthesis* **1988**, (7), 489-513.
120. Mayo, F. R.; Hardy, W. B., The bromination of naphthalene. *Journal of the American Chemical Society* **1952,** 74, 911-17.
121. Amos, R. I. J.; Smith, J. A.; Yates, B. F.; Schiesser, C. H., Acyl radical addition to pyridine: multiorbital interactions. *Tetrahedron* **2009,** 65, (36), 7653-7657.
122. Horvat, S. M.; Schiesser, C. H., Ab Initio and DFT Study of Homolytic Substitution Reactions of Acyl Radicals at Silicon, Germanium, and Tin. *Organometallics* **2009,** 28, (12), 3311-3318.
123. Krenske, E. H.; Schiesser, C. H., A comparison of orbital interactions in the additions of phosphonyl and acyl radicals to double bonds. *Organic & Biomolecular Chemistry* **2008,** 6, (5), 854-859.
124. Tran, T. A.; Schiesser, C. H., Reactions of acetyl radical with acetylene - a computational study. *Bulletin of the Korean Chemical Society* 31, (3), 595-598.

125. Brown, U. M.; Carter, P. H.; Tomlinson, M., Formyl compounds. II. *J. Chem. Soc.* **1958**, 1843-9.
126. Campaigne, E.; Thompson, R. L.; Van Werth, J. E., Some heterocyclic aldehyde thiosemicarbazones possessing antiviral activity. *J. Med. Pharm. Chem.* **1959,** 1, 577-600.
127. Lynch, B. J.; Fast, P. L.; Harris, M.; Truhlar, D. G., Adiabatic Connection for Kinetics. *Journal of Physical Chemistry A* **2000,** 104, (21), 4811-4815.
128. Zhao, Y.; Truhlar, D. G., Hybrid Meta Density Functional Theory Methods for Thermochemistry, Thermochemical Kinetics, and Noncovalent Interactions: The MPW1B95 and MPWB1K Models and Comparative Assessments for Hydrogen Bonding and van der Waals Interactions. *Journal of Physical Chemistry A* **2004,** 108, (33), 6908-6918.
129. Coote, M. L.; Collins, M. A.; Radom, L., Calculation of accurate imaginary frequencies and tunnelling coefficients for hydrogen abstraction reactions using IRCmax. *Molecular Physics* **2003,** 101, (9), 1329-1338.
130. Autrey, T.; Schuster, G. B., Are aroylnitrenes ground-state singlets? Photochemistry of beta -naphthoyl azide. *Journal of the American Chemical Society* **1987,** 109, (19), 5814-20.
131. Smolinsky, G.; Wasserman, E.; Yager, W. A., Electron paramagnetic resonance (E.P.R.) of ground-state triplet nitrenes. *Journal of the American Chemical Society* **1962,** 84, 3220-1.
132. Pople, J. A.; Head-Gordon, M.; Raghavachari, K., Quadratic configuration interaction. A general technique for determining electron correlation energies. *Journal of Chemical Physics* **1987,** 87, (10), 5968-75.
133. Chai, J.-D.; Head-Gordon, M., Long-range corrected hybrid density functionals with damped atom-atom dispersion corrections. *Physical Chemistry Chemical Physics* **2008,** 10, (44), 6615-6620.
134. Chen, Z.-T.; Zhan, F.-L.; Gao, J.-W., The utilization of free-radical group-transfer cyclizations. *Heteroatom Chemistry* **1999,** 10, (1), 69-72.
135. Guin, J.; De Sarkar, S.; Grimme, S.; Studer, A., Biomimetic carbene-catalyzed oxidations of aldehydes using TEMPO. *Angewandte Chemie, International Edition* **2008,** 47, (45), 8727-8730.
136. Maji, M. S.; Pfeifer, T.; Studer, A., Oxidative homocoupling of aryl, alkenyl, and alkynyl Grignard reagents with TEMPO and dioxygen. *Angewandte Chemie, International Edition* **2008,** 47, (49), 9547-9550.
137. Maji, M. S.; Studer, A., Transition-metal-free oxidative homocoupling of aryl, alkenyl, and alkynyl Grignard reagents with TEMPO. *Synthesis* **2009**, (14), 2467-2470.
138. Pouliot, M.; Renaud, P.; Schenk, K.; Studer, A.; Vogler, T., Oxidation of Catecholboron Enolates with TEMPO. *Angewandte Chemie, International Edition* **2009,** 48, (33), 6037-6040, S6037/1-S6037/74.
139. Siegenthaler, K. O.; Schaefer, A.; Studer, A., Chemical Surface Modification via Radical C-C Bond-Forming Reactions. *Journal of the American Chemical Society* **2007,** 129, (18), 5826-5827.
140. Vogler, T.; Studer, A., Applications of TEMPO in synthesis. *Synthesis* **2008**, (13), 1979-1993.
141. Buccigross, J. M.; Glover, S. A., Molecular orbital studies of novel N to C migrations in N,N-bisheteroatom-substituted Amides - HERON rearrangements. *Journal of the Chemical Society, Perkin Transactions 2: Physical Organic Chemistry* **1995**, (3), 595-603.
142. Glover, S. A.; Rauk, A.; Buccigross, J. M.; Campbell, J. J.; Hammond, G. P.; Mo, G.; Andrews, L. E.; Gillson, A.-M. E., The HERON reaction - origin, theoretical background, and prevalence. *Canadian Journal of Chemistry* **2005,** 83, (9), 1492-1509.

143. Griller, D.; Ingold, K. U., Free-radical clocks. *Accounts of Chemical Research* **1980,** 13, (9), 317-23.
144. Newcomb, M.; Chestney, D. L., A hypersensitive mechanistic probe for distinguishing between radical and carbocation intermediates. *Journal of the American Chemical Society* **1994,** 116, 9753-9754.
145. Still, W. C.; Kahn, M.; Mitra, A., Rapid chromatographic technique for preparative separations with moderate resolution. *Journal of Organic Chemistry* **1978,** 43, (14), 2923-5.
146. *CAD4 Express Software*, Enraf-Nonius: Delft, The Netherlands, 1994.
147. Harms, K.; Wocadlo, S. *XCAD4, CAD4 Data Reduction*, University of Marburg: 1995.
148. Sheldrick, G. M. *Programs for Crystal Structure Analysis*, Universitat Gottingen: Germany, 1998.
149. Barbour, L. J., X-Seed – A Software Tool for Supramolecular Crystallography. *Journal of Supramolecular Chemistry* **2001,** 1, 189.
150. Boga, C.; Stengel, R.; Abdayem, R.; Del Vecchio, E.; Forlani, L.; Todesco, P. E., Regioselectivity in the Addition of Vinylmagnesium Bromide to Heteroarylic Ketones: C- versus O-Alkylation. *Journal of Organic Chemistry* **2004,** 69, (25), 8903-8909.
151. Becke, A. D., Density-functional exchange-energy approximation with correct asymptotic behavior. *Physical Review A: Atomic, Molecular, and Optical Physics* **1988,** 38, (6), 3098-100.
152. Becke, A. D., Density-functional thermochemistry. III. The role of exact exchange. *Journal of Chemical Physics* **1993,** 98, (7), 5648-52.
153. Lee, C.; Yang, W.; Parr, R. G., Development of the Colle-Salvetti correlation-energy formula into a functional of the electron density. *Physical Review B: Condensed Matter and Materials Physics* **1988,** 37, (2), 785-9.
154. Montgomery, J. A., Jr.; Frisch, M. J.; Ochterski, J. W.; Petersson, G. A., A complete basis set model chemistry. VII. Use of the minimum population localization method. *Journal of Chemical Physics* **2000,** 112, (15), 6532-6542.
155. McWeeny, R.; Diercksen, G., Self-consistent perturbation theory. II. Extension to open shells. *Journal of Chemical Physics* **1968,** 49, (11), 4852-6.
156. Pople, J. A.; Nesbet, R. K., Self-consistent orbitals for radicals. *Journal of Chemical Physics* **1954,** 22, 571-2.
157. Frisch, M. J.; Head-Gordon, M.; Pople, J. A., Semidirect algorithms for the MP2 energy and gradient. *Chemical Physics Letters* **1990,** 166, (3), 281-9.
158. Frisch, M. J.; Head-Gordon, M.; Pople, J. A., A direct MP2 gradient method. *Chemical Physics Letters* **1990,** 166, (3), 275-80.
159. Head-Gordon, M.; Head-Gordon, T., Analytic MP2 frequencies without fifth-order storage. Theory and application to bifurcated hydrogen bonds in the water hexamer. *Chemical Physics Letters* **1994,** 220, (1-2), 122-8.
160. Head-Gordon, M.; Pople, J. A.; Frisch, M. J., MP2 energy evaluation by direct methods. *Chemical Physics Letters* **1988,** 153, (6), 503-6.
161. Saebo, S.; Almlof, J., Avoiding the integral storage bottleneck in LCAO calculations of electron correlation. *Chemical Physics Letters* **1989,** 154, (1), 83-9.
162. Krishnan, R.; Pople, J. A., Approximate fourth-order perturbation theory of the electron correlation energy. *International Journal of Quantum Chemistry* **1978,** 14, (1), 91-100.
163. Boese, A. D.; Martin, J. M. L., Development of density functionals for thermochemical kinetics. *Journal of Chemical Physics* **2004,** 121, (8), 3405-3416.
164. Lewis, A.; Bumpus, J. A.; Truhlar, D. G.; Cramer, C. J., Molecular modeling of environmentally important processes: reduction of potentials. *Journal of Chemical Education* **2004,** 81, (4), 596-604.

165. Barone, V.; Cossi, M.; Tomasi, J., A new definition of cavities for the computation of solvation free energies by the polarizable continuum model. *Journal of Chemical Physics* **1997,** 107, (8), 3210-3221.
166. Cammi, R.; Mennucci, B.; Tomasi, J., An Attempt To Bridge the Gap between Computation and Experiment for Nonlinear Optical Properties: Macroscopic Susceptibilities in Solution. *Journal of Physical Chemistry A* **2000,** 104, (20), 4690-4698.
167. Cammi, R.; Mennucci, B.; Tomasi, J., On the Calculation of Local Field Factors for Microscopic Static Hyperpolarizabilities of Molecules in Solution with the Aid of Quantum-Mechanical Methods. *Journal of Physical Chemistry A* **1998,** 102, (5), 870-875.
168. This showed that for our system B3LYP/6-31G(d) overestimated the amount of tunneling for the one and two solvent molecule situations and underestimated for the three solvent molecule situation
169. Glendening, E. D.; Badenhoop, J. K.; Reed, A. E.; Carpenter, J. E.; Bohmann, J. A.; Morales, C. M.; Weinhold, F. *NBO5.0*, Theoretical Chemistry Institute: University of Wisconsin: Madison, WI, 2001.
170. Stanetty, P.; Koller, H.; Puerstinger, G., 2,3-Dihydro-7-benzofurancarboxylic acids. *Monatshefte fuer Chemie* **1990,** 121, (11), 883-91.
171. Zhao, Y.; Schultz, N. E.; Truhlar, D. G., Design of Density Functionals by Combining the Method of Constraint Satisfaction with Parametrization for Thermochemistry, Thermochemical Kinetics, and Noncovalent Interactions. *Journal of Chemical Theory and Computation* **2006,** 2, (2), 364-382.
172. Zhao, Y.; Schultz, N. E.; Truhlar, D. G., Exchange-correlation functional with broad accuracy for metallic and nonmetallic compounds, kinetics, and noncovalent interactions. *Journal of Chemical Physics* **2005,** 123, (16), 161103/1-161103/4.
173. Schmidt am Busch, M.; Knapp, E.-W., One-Electron Reduction Potential for Oxygen- and Sulfur-Centered Organic Radicals in Protic and Aprotic Solvents. *Journal of the American Chemical Society* **2005,** 127, (45), 15730-15737.
174. Montgomery, J. A., Jr.; Frisch, M. J.; Ochterski, J. W.; Petersson, G. A., A complete basis set model chemistry. VI. Use of density functional geometries and frequencies. *Journal of Chemical Physics* **1999,** 110, (6), 2822-2827.
175. Grimme, S., Semiempirical GGA-type density functional constructed with a long-range dispersion correction. *Journal of Computational Chemistry* **2006,** 27, (15), 1787-1799.
176. M. J. Frisch, G. W. T., H. B. Schlegel, G. E. Scuseria, ; M. A. Robb, J. R. C., G. Scalmani, V. Barone, B. Mennucci, ; G. A. Petersson, H. N., M. Caricato, X. Li, H. P. Hratchian, ; A. F. Izmaylov, J. B., G. Zheng, J. L. Sonnenberg, M. Hada, ; M. Ehara, K. T., R. Fukuda, J. Hasegawa, M. Ishida, T. Nakajima, ; Y. Honda, O. K., H. Nakai, T. Vreven, J. A. Montgomery, Jr., ; J. E. Peralta, F. O., M. Bearpark, J. J. Heyd, E. Brothers, ; K. N. Kudin, V. N. S., R. Kobayashi, J. Normand, ; K. Raghavachari, A. R., J. C. Burant, S. S. Iyengar, J. Tomasi, ; M. Cossi, N. R., J. M. Millam, M. Klene, J. E. Knox, J. B. Cross, ; V. Bakken, C. A., J. Jaramillo, R. Gomperts, R. E. Stratmann, ; O. Yazyev, A. J. A., R. Cammi, C. Pomelli, J. W. Ochterski, ; R. L. Martin, K. M., V. G. Zakrzewski, G. A. Voth, ; P. Salvador, J. J. D., S. Dapprich, A. D. Daniels, ; O. Farkas, J. B. F., J. V. Ortiz, J. Cioslowski, ; Fox, a. D. J. *Gaussian 09, Revision A.02*, Gaussian, Inc: Wallingford CT, 2009.

Table of Contents

Computational details for Chapter 2

Bond dissociation benchmarking results

Table 1Benchmarking of BDEs Enthalpies in kJ/mol

	QB3	B3LYP	BHandHLYP	MPWB1K	BMK	HF	MP2	MP4
Pyridyl	56.1	58.6	74.2	58.5	58.8	27.2	57.8	56.7
Phenyl	57.6	60.4	50.0	60.5	64.3	29.3	59.3	58.3
p-Methoxyphenyl	59.8	61.1	45.4	61.0	68.0	30.8	59.2	57.7
m-Nitrophenyl	54.1	62.1	45.7	55.7	59.4	25.0	56.1	55.2

Bond dissociation calculated at MPWB1K

Table 2BDEs (kJ/mol) for various functional groups calculated at MPWB1K

Functional group	Pyridyl	Phenyl	*p*-Methoxyphenyl	*p*-Nitrophenyl	*p*-*C*hlorophenyl	*m*-Methoxyphenyl	
BDE	58.5	60.5	61.0	57.5	59.5	63.8	
Functional group	*m*-Nitrophenyl	*m*-Bromophenyl	*m*-Methylphenyl	Tolyl	*m*-Fluorophenyl	*p*-ethoxycarbonylphenyl	*p*-Trifluoromethylphen
BDE	55.7	59.9	60.4	65.2	59.6	59.1	58.7

Oxidation of the radical to the cation

B3LYP	IP eV	Corrected IP eV	Eº V	Eº vs NHE V
isoniazid	7.00	7.28	4.78	0.50
benzhydrazide	6.47	6.75	4.49	0.21
p-methoxybenzhydrazide	6.04	6.32	4.28	0.00
m-nitrobenzhydrazide	7.04	7.32	4.74	0.46
CBS-QB3				
isoniazid	6.94	7.22	4.70	0.42
benzhydrazide	6.47	6.75	4.48	0.20
p-methoxybenzhydrazide	6.38	6.38	4.34	0.06
m-nitrobenzhydrazide	7.13	7.41	4.82	0.54
MPWB1K				
isoniazid	6.90	7.18	4.65	0.37
benzhydrazide	6.38	6.66	4.39	0.10
p-methoxybenzhydrazide	5.96	6.24	4.20	-0.08
m-nitrobenzhydrazide	6.90	7.18	4.60	0.32
CCSD(T)				
isoniazid	6.84	7.12	4.59	0.31

benzhydrazide	6.35	6.63	4.36	0.08
p-methoxybenzhydrazide	5.43	5.71	3.67	-0.61
m-nitrobenzhydrazide	6.29	6.57	3.99	-0.29

Ionisation potentials at different levels of theory (eV)

	isoniazid	benzhydrazide	*p*-methoxybenzhydrazide	*m*-nitrobenzhydrazide
B3LYP	7.00	6.47	6.04	7.04
BHandHLYP	6.96	6.42	6.02	6.96
MPW1K	7.16	6.63	6.22	7.17
BMK	6.92	6.39	6.02	6.95
MPWB1K	6.89	6.37	5.95	6.89
QB3	6.98	6.52	6.15	7.01
HF	6.48	5.89	5.50	6.46
MP2	6.70	6.24	5.90	6.75
MP4	6.73	6.25	5.87	6.74
CCSD(T)	6.84	6.34	5.43	6.29

Values are the uncorrected ΔH (cation – radical)
All calculations performed with a 6-311+G(2d,2p) basis set on geometries optimized with B3LYP/6-31G(d)
Enthalpy corrections added from a B3LYP/6-31G(d) frequency calculation

Calculations for aqueous redox potential vs the normal hydrogen electrode (NHE)

	E AUa	Enthalpy correctionb	corrected E AU	IP eV	corrected IP eVc	S J/molKb	ΔS kJ/molKb	TΔS Entropy term eVb	ΔGsolv kJ/mol	Eº V	Eº vs NHE V
Isoniazid radical	-361.061686	0.092988	-360.968698			340.92			-12.47		
Isoniazid cation	-360.805619	0.094081	-360.711538	7.00	7.28	330.83	-0.01	0.031173	-256.94	4.78	0.50
Benzhydrazide radical	-345.026130	0.105066	-344.921064			339.32			-6.23416		
Benzhydrazide cation	-344.790067	0.106639	-344.683428	6.47	6.75	331.65	-0.01	0.023712	-226.438	4.49	0.21
p-Methoxybenzhydrazide radical	-459.589673	0.140549	-459.449124			390.94			-10.5018		
p-Methoxybenzhydrazide cation	-459.369225	0.142195	-459.227030	6.04	6.32	385.43	-0.01	0.017028	-209.116	4.28	0.00
m-nitrobenzhydrazide radical	-549.5921882	0.110048	-549.482140			399.72			-17.9912		
m-nitrobenzhydrazide cation	-549.3347837	0.111213	-549.223571	7.04	7.32	390.94	-0.01	0.027152	-269.491	4.74	0.46

Footnotes

a B3LYP/6-311+G(2d,2p)//B3LYP/6-31G(d)

b From frequency calculations performed at B3LYP/6-31G(d)

c Corrected by adding 0.28V as specified by Fu *et al.*[1]

Geometries for all molecules

Methane

B3LYP

```
C      0.000000    0.000000    0.000000
H      0.631339    0.631339    0.631339
H     -0.631339   -0.631339    0.631339
H     -0.631339    0.631339   -0.631339
H      0.631339   -0.631339   -0.631339
```

E (au)= -40.536625

ZPVE correction (au)= 0.045214

BHandH

```
C      0.000000    0.000000    0.000000
H      0.626165    0.626165    0.626165
H     -0.626165   -0.626165    0.626165
H     -0.626165    0.626165   -0.626165
H      0.626165   -0.626165   -0.626165
```

E (au)= -40.500325

ZPVE correction (au)= 0.045214

CBS-QB3

```
C      0.000000    0.000000    0.000000
H      0.629729    0.629729    0.629729
H     -0.629729   -0.629729    0.629729
H     -0.629729    0.629729   -0.629729
H      0.629729   -0.629729   -0.629729
```

Zero point E (au)= -40.409999

Includes B3LYP/CBS-B7 ZPVE correction (au)= 0.044588

HF

E (au)= -40.211785

MP2

E (au)= -40.393458

MP4

E (au)= -40.419229

BMK

E (au)= -40.491778

MPWB1K

E (au)= - 40.495035

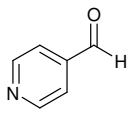

B3LYP

```
C     -1.749869    0.984890   -0.000054
C     -0.384796    1.277613   -0.000022
```

C	0.524418	0.216644	0.000013
C	0.026114	-1.091214	0.000024
C	-1.354422	-1.271511	-0.000053
H	-2.485524	1.787124	-0.000023
H	-0.039078	2.308653	-0.000049
H	0.713000	-1.931342	0.000155
H	-1.779016	-2.273582	0.000179
C	1.988877	0.475003	0.000114
O	2.834956	-0.395378	-0.000111
H	2.272346	1.550203	0.000294
N	-2.237615	-0.260940	0.000029

E (au)= -361.717234
ZPVE correction (au)= 0.098276

BHandH

C	-1.737718	0.976871	-0.000026
C	-0.382423	1.268273	-0.000063
C	0.518643	0.215335	-0.000055
C	0.026565	-1.082896	-0.000010
C	-1.344015	-1.262017	0.000012
H	-2.468057	1.771340	-0.000035
H	-0.042281	2.291584	-0.000093
H	0.706514	-1.917056	0.000000
H	-1.765360	-2.255335	0.000064
C	1.976606	0.471838	-0.000105
O	2.808448	-0.392305	0.000162
H	2.264592	1.532994	0.000169
N	-2.215563	-0.258500	0.000012

E (au)= -361.486407
ZPVE correction (au)= 0.098276

CBS-QB3

C	1.746751	0.984560	0.000040
C	0.383001	1.274549	0.000042
C	-0.523050	0.214666	0.000018
C	-0.023894	-1.089934	-0.000007
C	1.354409	-1.268932	-0.000004
H	2.479960	1.786108	0.000061
H	0.037276	2.303358	0.000063
H	-0.708586	-1.929373	-0.000027
H	1.779407	-2.268478	-0.000027
C	-1.989091	0.471667	0.000022
O	-2.830245	-0.393716	-0.000098
H	-2.269931	1.546749	-0.000067
N	2.233583	-0.258300	0.000017

Zero point E (au)= -361.013390
Includes B3LYP/CBS-B7 ZPVE correction (au)= 0.097592

HF

E (au)= -359.521101

MP2

E (au)= -360.768243

MP4

E (au)= -360.862711

MPWB1K

E (au)= -361.527605

BMK

E (au)= -361.489609

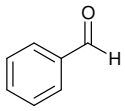

B3LYP

C	-1.735786	1.060718	0.000166
C	-0.361038	1.292088	-0.000336
C	0.534004	0.214260	-0.000521
C	0.045198	-1.101122	-0.000573
C	-1.326436	-1.331144	0.000045
H	-2.430109	1.896291	0.000690
H	0.025263	2.309452	-0.000342
H	0.758625	-1.919655	-0.000598
H	-1.707930	-2.348510	0.000424
C	1.992127	0.468649	-0.000012
O	2.847640	-0.395800	0.000521
C	-2.216822	-0.250739	0.000346
H	-3.288215	-0.433208	0.000588
H	2.273765	1.545770	0.000379

E (au)= -345.680870

ZPVE correction (au)= 0.110226

BHandH

C	-1.723442	1.053106	0.000179
C	-0.357739	1.282725	0.000078
C	0.529059	0.213250	-0.000031
C	0.045772	-1.092570	-0.000054
C	-1.316191	-1.321515	0.000049
H	-2.412233	1.881866	0.000270
H	0.023845	2.292540	0.000097
H	0.752981	-1.905005	-0.000136
H	-1.694704	-2.330630	0.000038
C	1.980991	0.465127	-0.000133
O	2.821970	-0.393277	-0.000236
C	-2.199994	-0.248646	0.000163
H	-3.262772	-0.430022	0.000242
H	2.266387	1.528611	-0.000123

E (au)= -345.46984

ZPVE correction (au)= 0.114474

QB3

C	-1.732338	1.059455	0.000184
C	-0.359505	1.288919	0.000087
C	0.532830	0.212702	-0.000046
C	0.043026	-1.099645	-0.000040
C	-1.325901	-1.327744	0.000045
H	-2.424483	1.893548	0.000267
H	0.026195	2.303907	0.000091
H	0.754532	-1.916962	-0.000138
H	-1.707829	-2.342256	0.000022
C	1.992490	0.465469	-0.000155
O	2.842673	-0.394344	-0.000225
C	-2.213818	-0.248450	0.000167

H	-3.282938	-0.429440	0.000238
H	2.272437	1.541716	-0.000133

Zero point E (au)= -344.974798

Includes B3LYP/CBS-B7 ZPVE correction (au)= 0.109513

HF

E (au)= -343.528802

MP2

E (au)= -344.744114

MP4

E (au)= -344.841808

MPWB1K

E (au)= -345.493877

BMK

E (au)= -345.450690

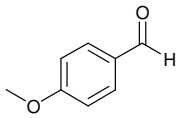

B3LYP

C	0.579549	1.466278	0.000009
C	-0.805197	1.420015	-0.000024
C	-1.483004	0.189221	-0.000016
C	0.652677	-0.968244	0.000028
H	1.119769	2.407504	-0.000022
H	-1.376479	2.346163	-0.000096
C	-2.955509	0.148330	-0.000045
O	-3.626810	-0.868399	0.000039
H	1.209512	-1.898147	-0.000012
C	1.318074	0.270140	0.000037
H	-3.444824	1.148845	-0.000171
C	-0.736987	-0.997342	0.000015
H	-1.271092	-1.942867	0.000025
O	2.667967	0.416271	0.000126
C	3.481464	-0.750318	-0.000101
H	4.512206	-0.392618	-0.000469
H	3.307923	-1.360106	0.895382
H	3.307324	-1.360230	-0.895367

E (au)= -460.244087

ZPVE correction (au)= 0.143132

BHandH

C	-0.576193	1.455392	0.000035
C	0.799141	1.409507	0.000048
C	1.470623	0.188213	0.000022
C	-0.649017	-0.959805	-0.000036
H	-1.112266	2.389017	0.000058
H	1.364480	2.329125	0.000082
C	2.936965	0.146027	0.000044
O	3.595090	-0.861535	-0.000117
H	-1.200896	-1.882589	-0.000074
C	-1.308601	0.268577	-0.000007

```
H     3.427010    1.132737   -0.000062
C     0.731922   -0.988871   -0.000021
H     1.260108   -1.927807   -0.000043
O    -2.645789    0.408739   -0.000026
C    -3.453525   -0.741691    0.000067
H    -4.476613   -0.388389    0.000138
H    -3.282126   -1.346929   -0.887870
H    -3.281983   -1.346887    0.888005
```

E (au)= -459.9691

ZPVE correction (au)= 0.148742

QB3

```
C    -0.576783    1.463128    0.000046
C     0.805293    1.415799    0.000077
C     1.481414    0.187026    0.000069
C    -0.651402   -0.965799   -0.000018
H    -1.116142    2.402167    0.000057
H     1.375432    2.339854    0.000115
C     2.954738    0.145463    0.000123
O     3.623368   -0.864563   -0.000237
H    -1.206314   -1.894024   -0.000062
C    -1.316060    0.270521   -0.000002
H     3.440800    1.146396   -0.000202
C     0.735708   -0.996176    0.000018
H     1.268071   -1.940250    0.000010
O    -2.663625    0.416295   -0.000040
C    -3.483544   -0.748390    0.000040
H    -4.509503   -0.385495    0.000094
H    -3.313298   -1.355990   -0.894638
H    -3.313184   -1.355945    0.894728
```

Zero point E (au)= -459.336038

Includes B3LYP/CBS-B7 ZPVE correction (au)= 0.141923

HF

E (au)= -457.446306

MP2

E (au)= -459.033744

MP4

E (au)= -459.157989

MPWB1K

E (au)= -460.001839

BMK

E (au)= -459.952059

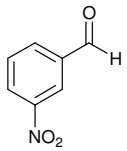

B3LYP

```
C     0.475006    2.042591   -0.000076
```

C	1.591448	1.210745	-0.000143
C	1.434210	-0.184574	0.000017
C	0.154531	-0.744830	0.000095
C	-0.946185	0.106105	-0.000007
H	0.596268	3.121416	-0.000415
H	2.598736	1.615596	-0.000272
H	0.004505	-1.819102	0.000050
C	2.626161	-1.071151	0.000159
O	3.772318	-0.670381	-0.000002
C	-0.809051	1.492997	-0.000007
H	-1.696504	2.114105	0.000368
H	2.397623	-2.158654	0.000603
N	-2.299551	-0.478511	-0.000043
O	-3.254429	0.296226	0.000330
O	-2.387950	-1.705231	-0.000360

E (au)= -550.24712

ZPVE correction (au)= 0.112782

BHandH

C	-0.468046	2.026942	0.000148
C	-1.576208	1.200330	0.000083
C	-1.420147	-0.184269	0.000026
C	-0.151569	-0.741503	0.000028
C	0.941857	0.103707	0.000093
H	-0.588606	3.097006	0.000187
H	-2.574994	1.603302	0.000079
H	-0.002972	-1.807260	-0.000015
C	-2.608546	-1.063662	-0.000034
O	-3.738502	-0.660264	-0.000086
C	0.806528	1.480238	0.000154
H	1.686380	2.097306	0.000214
H	-2.391162	-2.141436	-0.000106
N	2.279625	-0.475371	0.000099
O	3.219348	0.285807	-0.000213
O	2.365501	-1.682045	-0.000206

E (au)= -549.922228

ZPVE correction (au)= 0.117705

QB3

C	-0.477258	2.040434	0.000137
C	-1.591051	1.210056	0.000122
C	-1.433670	-0.182502	0.000048
C	-0.156093	-0.740963	-0.000010
C	0.942203	0.108614	-0.000002
H	-0.598727	3.116861	0.000195
H	-2.596599	1.613745	0.000170
H	-0.003964	-1.813025	-0.000062
C	-2.625659	-1.071093	0.000043
O	-3.766096	-0.675579	-0.000149
C	0.804973	1.492073	0.000068
H	1.691639	2.110890	0.000071
H	-2.392702	-2.156713	-0.000246
N	2.303224	-0.479229	-0.000069
O	3.251141	0.292271	-0.000091
O	2.389593	-1.698801	-0.000020

Zero point E (au)= -549.266482

Includes B3LYP/CBS-B7 ZPVE correction (au)= 0.111929

HF

E (au)= -547.058205

MP2

E (au)= -548.893255

MP4

E (au)= -549.016931

MPWB1K

E (au)= -549.973344

BMK

E (au)= -549.9209857

Methyl radical

B3LYP

C	0.000000	0.000000	0.000555
H	0.000000	1.083310	-0.001110
H	0.938174	-0.541655	-0.001110
H	-0.938174	-0.541655	-0.001110

E (au)= -39.855963

ZPVE correction (au)= 0.029815

BHandH

C	0.000000	0.000000	0.000512
H	0.000000	1.074485	-0.001025
H	0.930531	-0.537242	-0.001025
H	-0.930531	-0.537242	-0.001025

E (au)= -39.825643

ZPVE correction (au)= 0.029815

CBS-QB3

C	0.000000	0.000000	0.000526
H	0.000000	1.080395	-0.001052
H	0.935649	-0.540197	-0.001052
H	-0.935649	-0.540197	-0.001052

Zero point E (au)= -39.744794

Includes B3LYP/CBS-B7 ZPVE correction (au)= 0.029578

HF

E (au)= -39.571586

MP2

E (au)= -39.720368

MP4

E (au)= -39.743807

MPWB1K

E (au)= -39.816514

BMK

E (au)= -39.812641

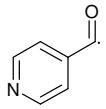

B3LYP

C	1.725123	−0.977972	0.000290
C	0.364262	−1.289502	−0.000015
C	−0.554620	−0.238001	−0.000382
C	−0.075523	1.079404	−0.000257
C	1.303894	1.275002	−0.000125
H	2.471159	−1.770247	0.000304
H	0.021082	−2.319404	−0.000079
H	−0.767745	1.915288	−0.000192
H	1.716487	2.282222	0.000391
C	−2.016641	−0.530034	−0.000596
O	−2.912296	0.257243	0.000625
N	2.196918	0.274401	0.000156

E (au)= -361.061686
ZPVE correction (au)= 0.085734
Enthalpy correction (au)= 0.092988
S (J/molK)= 340.92
ΔG solv (kJ/mol)= -12.47

BHandHLYP

C	1.713908	−0.969773	0.000151
C	0.362987	−1.280159	−0.000027
C	−0.547521	−0.236463	−0.000057
C	−0.075253	1.070913	−0.000019
C	1.293904	1.265933	0.000022
H	2.454786	−1.754061	0.000191
H	0.026011	−2.302592	−0.000109
H	−0.761299	1.900145	−0.000036
H	1.703124	2.264304	0.000077
C	−2.003453	−0.522293	−0.000219
O	−2.889647	0.252155	−0.000038
N	2.175304	0.272287	0.000154

E (au)= -360.846322
ZPVE correction (au)= 0.089344

CBS-QB3

C	1.722191	−0.975429	0.000113
C	0.363328	−1.287036	−0.000008
C	−0.553370	−0.238008	−0.000057
C	−0.076546	1.077093	−0.000016
C	1.300311	1.273957	0.000058
H	2.466962	−1.765844	0.000153
H	0.020856	−2.314936	−0.000056
H	−0.767776	1.911105	−0.000044
H	1.711299	2.279442	0.000099
C	−2.016268	−0.525793	−0.000182
O	−2.908628	0.251056	−0.000104
N	2.190492	0.274789	0.000133

Zero point E (au)= -360.369541
Includes B3LYP/CBS-B7 ZPVE correction (au)= 0.085216
Enthalpy corrected E(au)= -360.362244
S (J/molK)= 340.92
ΔG solv (kJ/mol)= -12.34

HF

E (au)= -358.898830

MP2

E (au)= -360.118475

MP4

E (au)= -360.211674

CCSD(t)

E (au)= -360.200461

Enthalpy correction (au)= 0.092467

S (J/molK)= 340.92

ΔG solv (kJ/mol)= -12.34

MPWB1K

E (au)= -360.873794

ZPVE correction (au)= 0.085734

Enthalpy correction (au)= 0.092988

S (J/molK)= 340.92

ΔG solv (kJ/mol)= -12.34

BMK

E (au)= -360.836855

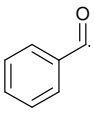

B3LYP

C	-1.711575	-1.053979	-0.000030
C	-0.340426	-1.304642	0.000012
C	0.565111	-0.236031	-0.000022
C	0.094785	1.089041	-0.000007
C	-1.274598	1.334271	0.000029
H	-2.416551	-1.880364	0.000067
H	0.043608	-2.320761	-0.000007
H	0.813544	1.903112	-0.000014
H	-1.644537	2.356006	0.000000
C	2.019024	-0.522520	0.000038
O	2.924005	0.258171	-0.000017
C	-2.176132	0.263485	-0.000002
H	-3.245235	0.458889	-0.000031

E (au)= -345.026130

ZPVE correction (au)= 0.097791

Enthalpy correction (au)= 0.092988

S (J/molK)= 339.32

ΔG solv (kJ/mol)= -6.23416

BHandHLYP

C	-1.700081	-1.046439	0.000009
C	-0.338198	-1.295155	0.000008
C	0.559068	-0.234334	0.000003
C	0.094428	1.080441	-0.000005
C	-1.265238	1.324752	-0.000008
H	-2.399703	-1.865713	0.000007
H	0.040765	-2.303730	0.000013
H	0.807326	1.887838	-0.000009
H	-1.632009	2.338050	-0.000010
C	2.006962	-0.514149	0.000001
O	2.902813	0.253454	-0.000006
C	-2.160027	0.261570	0.000000
H	-3.220364	0.455801	0.000002

E (au)= -344.81712

ZPVE correction (au)= 0.101627

CBS-QB3

C	-1.708478	-1.052151	0.000002
C	-0.339756	-1.302338	0.000012
C	0.563252	-0.235502	0.000000
C	0.093647	1.086796	-0.000007
C	-1.272959	1.331115	-0.000001
H	-2.411704	-1.876653	0.000008
H	0.044219	-2.315892	0.000018
H	0.810436	1.899485	-0.000012
H	-1.642158	2.350414	-0.000005
C	2.017928	-0.516117	0.000004
O	2.919052	0.255110	-0.000009
C	-2.172628	0.262306	0.000000
H	-3.239244	0.457111	-0.000001

Zero point E (au)= -344.331537

Includes B3LYP/CBS-B7 ZPVE correction (au)= 0.097262

Enthalpy corrected E (au)= -344.324215

S (J/molK)= 339.32

ΔG solv (kJ/mol)= -5.77

HF

E (au)= -342.907581

ZPVE correction (au)= 0.097262

MP2

E (au)= -344.094846

ZPVE correction (au)= 0.097262

MP4

E (au)= -344.191411

ZPVE correction (au)= 0.097262

CCSD(t)

E (au)= -344.181994

Enthalpy correction (au)= 0.104534

S (J/molK)= 340.92

ΔG solv (kcal/mol)= -12.34

BMK

E (au)= -344.798692

MPWB1K

E (au)= -344.840918

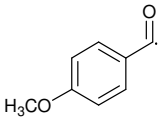

B3LYP

C	0.543884	1.468728	-0.000165
C	-0.840540	1.432115	0.000225
C	-1.522857	0.203425	-0.000107
C	0.606435	-0.967238	-0.000296
H	1.089115	2.406956	-0.000112
H	-1.415455	2.353762	0.000515
C	-2.995186	0.186123	0.000278
O	-3.729260	-0.759936	0.000177
H	1.159211	-1.899708	-0.000271
C	1.276580	0.268709	-0.000372
C	-0.783614	-0.990748	-0.000323
H	-1.315922	-1.937495	-0.000548
O	2.626002	0.408226	-0.000257
C	3.435710	-0.761476	0.000561
H	4.467522	-0.407135	0.001085
H	3.259000	-1.370090	0.896126
H	3.260116	-1.370438	-0.894960

E (au)= -459.589673

ZPVE correction (au)= 0.130782

Enthalpy correction (au)= 0.140549

S (J/molK)= 390.94

ΔG solv (kcal/mol)= -10.5018

BHandHLYP

C	0.541390	1.458301	0.000076
C	-0.833392	1.422463	0.000011
C	-1.509175	0.202940	-0.000088
C	0.603321	-0.958968	-0.000064
H	1.083236	2.388461	0.000157
H	-1.401934	2.337904	0.000042
C	-2.975321	0.179871	-0.000154
O	-3.701025	-0.752554	-0.000235
H	1.150647	-1.884481	-0.000108
C	1.267715	0.266867	0.000041
C	-0.777962	-0.981564	-0.000126
H	-1.305656	-1.920954	-0.000210
O	2.604148	0.400184	0.000089
C	3.408114	-0.753734	0.000325
H	4.432160	-0.403675	0.000535
H	3.234015	-1.357629	0.888448
H	3.234416	-1.357717	-0.887817

E (au)= -459.31671

ZPVE correction (au)= 0.135947

CBS-QB3

C	0.541228	1.466034	0.000088
C	-0.840269	1.429677	-0.000010
C	-1.520630	0.203091	-0.000089
C	0.604368	-0.964629	-0.000038
H	1.086223	2.401683	0.000163
H	-1.414886	2.348791	0.000005
C	-2.992342	0.179777	-0.000164
O	-3.724364	-0.756411	-0.000273
H	1.154461	-1.895859	-0.000091
C	1.274142	0.268811	0.000096
C	-0.783125	-0.988371	-0.000121
H	-1.314217	-1.933240	-0.000215
O	2.621100	0.407616	0.000101
C	3.436940	-0.760401	0.000308
H	4.464057	-0.401054	0.000507
H	3.264110	-1.366915	0.895142
H	3.264487	-1.366980	-0.894556

Zero point E (au)= -458.693595

Includes B3LYP/CBS-B7 ZPVE correction (au)= 0.129751

Enthalpy correction (au)= -458.683740

S (J/molK)= 390.94

ΔG solv (kcal/mol)= -10.33

HF

E (au)= -456.820834

MP2

E (au)= -458.386189

MP4

E (au)= -458.507550

MPWB1K

E (au)= -459.349150

CCSD(t)

E (au)= -458.498647

Enthalpy correction (au)= 0.139538

S (J/molK)= 390.94

ΔG solv (kcal/mol)= -10.33

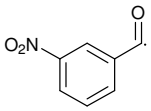

B3LYP

C	0.315000	2.240336	-0.000057
C	1.536617	1.566032	0.000020
C	1.569593	0.165451	0.000072
C	0.376242	-0.571627	0.000096
C	-0.824714	0.124351	0.000029
H	0.288682	3.325390	-0.000144
H	2.474878	2.112811	0.000014
H	0.390078	-1.654930	0.000122
C	2.884349	-0.528962	0.000062

O	3.088000	-1.703935	-0.000105
C	-0.877867	1.519833	-0.000039
H	-1.842565	2.012490	-0.000009
N	-2.091486	-0.634933	0.000005
O	-3.138635	0.009781	0.000006
O	-2.017613	-1.861311	-0.000042

E (au)= -550.24712
ZPVE correction (au)= 0.112782
Enthalpy correction (au)= 0.110048
S (J/molK)= 399.72
ΔG solv (kcal/mol)= -17.9912

BHandHLYP

C	-0.304690	2.224286	0.000045
C	-1.518768	1.556198	0.000019
C	-1.553787	0.167085	0.000001
C	-0.372628	-0.568085	0.000010
C	0.821107	0.120609	0.000030
H	-0.276740	3.300492	0.000060
H	-2.447423	2.102326	0.000010
H	-0.389387	-1.642842	-0.000002
C	-2.860699	-0.525814	-0.000031
O	-3.067108	-1.684571	-0.000039
C	0.877292	1.505817	0.000051
H	1.834876	1.993601	0.000070
N	2.071189	-0.633016	0.000029
O	3.102933	-0.001623	-0.000059
O	1.995849	-1.839186	-0.000039

E (au)= -549.267763
ZPVE correction (au)= 0.104793

CBS-QB3

C	-0.320993	2.236774	0.000044
C	-1.539085	1.561501	0.000025
C	-1.568231	0.164064	-0.000006
C	-0.375571	-0.569193	-0.000017
C	0.821262	0.127560	-0.000002
H	-0.297135	3.319467	0.000069
H	-2.476818	2.104678	0.000032
H	-0.384824	-1.650692	-0.000038
C	-2.878849	-0.537951	-0.000028
O	-3.083611	-1.703304	-0.000033
C	0.871149	1.520123	0.000028
H	1.833869	2.012311	0.000037
N	2.096240	-0.633833	-0.000020
O	3.135086	0.010339	-0.000002
O	2.022668	-1.852812	0.000007

Zero point E (au)= -548.621869
Includes B3LYP/CBS-B7 ZPVE correction (au)= 0.099572
Enthalpy corrected E (au)= -548.611825
S (J/molK)= 399.72
ΔG solv (kJ/mol)= -17.24

HF

E (au)= -546.430366

MP2

E (au)= -548.244346

MP4

E (au)= -548.365363

MPWB1K

E (au)= -549.318462

CCSD(t)

E (au)= -548.344925

Enthalpy correction (au)= 0.109397

S (J/molK)= 399.72

ΔG solv (kJ/mol)= -17.24

Methyl cation

B3LYP

C	0.000000	0.000000	0.000068
H	0.000000	1.094991	-0.000136
H	-0.948290	-0.547496	-0.000136
H	0.948290	-0.547496	-0.000136

E (au)= -39.493472

ZPVE correction (au)= 0.031596

BHandH

C	0.000000	0.000000	0.000023
H	0.000000	1.084768	-0.000047
H	-0.939437	-0.542384	-0.000047
H	0.939437	-0.542384	-0.000047

E (au)= -39.471411

ZPVE correction (au)= 0.031596

CBS-QB3

C	0.000000	0.000000	0.000005
H	0.000000	1.093498	-0.000115
H	-0.946997	-0.546749	-0.000115
H	0.946997	-0.546749	-0.000115

Zero point E (au)= -39.384653

Includes B3LYP/CBS-B7 ZPVE correction (au)= 0.031172

MPWB1K

E (au)= -39.459980

BMK

E (au)= -39.457880

HF

E (au)= -39.245950

MP2

E (au)= -39.364941

MP4

E (au)= -39.388045

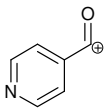

B3LYP

C	−1.542988	1.158332	0.000284
C	−0.151879	1.235966	0.000038
C	0.540431	0.000162	−0.000027
C	−0.151605	−1.235783	−0.000038
C	−1.542668	−1.158592	−0.000122
H	−2.140195	2.066279	0.000115
H	0.367689	2.188030	−0.000024
H	0.368428	−2.187600	−0.000045
H	−2.139698	−2.066635	0.000067
C	1.934029	0.000194	−0.000090
O	3.067651	−0.000069	−0.000141
N	−2.215622	−0.000171	0.000107

E (au)= -360.805619
ZPVE correction (au)= 0.087028
Enthalpy correction (au)= 0.094081
S (J/molK)= 330.83
ΔG solv (kJ/mol)= -256.94

CBS-QB3

C	1.538483	−1.156438	0.000094
C	0.150153	−1.232677	0.000014
C	−0.540491	−0.000008	−0.000031
C	0.150132	1.232668	0.000003
C	1.538469	1.156446	0.000082
H	2.134474	−2.062858	0.000132
H	−0.368063	−2.182978	−0.000011
H	−0.368091	2.182965	−0.000031
H	2.134439	2.062881	0.000113
C	−1.930360	−0.000011	−0.000110
O	−3.053885	0.000003	−0.000175
N	2.208572	0.000013	0.000127

Zero point E (au)= -360.114101
Includes B3LYP/CBS-B7 ZPVE correction (au)= 0.086626
Enthalpy corrected E (au)= -360.107028
S (J/molK)= 330.83
ΔG solv (kJ/mol)= -258.91

HF

E (au)= -358.657151

MP2

E (au)= -359.874896

MP4

E (au)= -359.965629

MPWB1K

E (au)= -360.621418

CCSD(t)

E (au)= -359.950341
Enthalpy correction (au)= 0.093653
S (J/molK)= 330.83
ΔG solv (kJ/mol)= -258.91

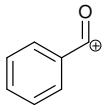

B3LYP

C	1.515414	1.225236	0.000004
C	0.132136	1.248204	0.000005
C	-0.554766	0.000280	0.000000
C	0.131730	-1.247645	-0.000010
C	1.514987	-1.225749	-0.000005
H	2.067469	2.159126	0.000009
H	-0.418714	2.182866	0.000013
H	-0.419723	-2.182011	-0.000015
H	2.066539	-2.159895	-0.000008
C	-1.937095	0.000347	0.000001
O	-3.074577	-0.000236	0.000002
C	2.200080	-0.000348	0.000001
H	3.286127	-0.000147	0.000007

E (au)= -344.790067
ZPVE correction (au)= 0.099508
Enthalpy correction (au)= 0.106639
S (J/molK)= 331.65
ΔG solv (kJ/mol)= -226.438

CBS-QB3

C	1.512573	1.222388	0.000007
C	0.132186	1.244776	0.000006
C	-0.553824	0.000215	0.000000
C	0.131773	-1.244570	-0.000007
C	1.512175	-1.222662	-0.000006
H	2.063563	2.154263	0.000012
H	-0.416966	2.177834	0.000011
H	-0.417690	-2.177448	-0.000012
H	2.062832	-2.154732	-0.000009
C	-1.932554	0.000346	0.000000
O	-3.059981	0.000279	0.000000
C	2.195829	-0.000254	0.000001
H	3.279692	-0.000407	0.000002

Zero point E (au)= -344.093523
Includes B3LYP/CBS-B7 ZPVE correction (au)= 0.099083
Enthalpy corrected E (au)= -344.086374
S (J/molK)= 340.92
ΔG solv (kJ/mol)= -12.34

HF

E (au)= -342.687588

MP2

E (au)= -343.868435

MP4

E (au)= -343.963198

MPWB1K

E (au)= -344.608200

CCSD(t)

E (au)= -343.950244

Enthalpy correction (au)= 0.106183

S (J/molK)= 331.65

ΔG solv (kcal/mol)= -226.94

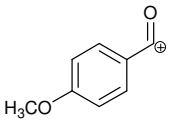

B3LYP

C	-0.446593	1.421470	0.000344
C	0.915026	1.296703	0.000411
C	1.490086	-0.017035	0.001102
C	-0.706211	-1.034370	0.001213
H	-0.921856	2.396280	0.000084
H	1.553101	2.173959	0.000060
C	2.851286	-0.164070	-0.000551
O	3.987440	-0.288143	-0.001931
H	-1.334102	-1.916610	0.002114
C	-1.279553	0.266463	0.000318
C	0.659357	-1.179559	0.001506
H	1.105748	-2.168587	0.002672
O	-2.572853	0.510405	0.000904
C	-3.541441	-0.564494	-0.002239
H	-4.509815	-0.067941	-0.011841
H	-3.423860	-1.176821	-0.900462
H	-3.437660	-1.169019	0.902966

E (au)= -459.369225

ZPVE correction (au)= 0.132468

Enthalpy correction (au)= 0.142195

S (J/molK)= 385.43

ΔG solv (kJ/mol)= -209.116

CBS-QB3

C	0.442071	1.418089	-0.000061
C	-0.915877	1.292110	0.000021
C	-1.489411	-0.019112	0.000034
C	0.703042	-1.031847	-0.000219
H	0.916354	2.390979	-0.000056
H	-1.552869	2.167483	0.000129

C	-2.846932	-0.165546	0.000088
O	-3.973441	-0.285751	0.000138
H	1.329322	-1.912571	-0.000446
C	1.276155	0.266530	-0.000091
C	-0.659379	-1.177942	-0.000149
H	-1.103073	-2.165744	-0.000243
O	2.565687	0.510126	-0.000247
C	3.540594	-0.561939	0.000369
H	4.503723	-0.060871	0.001079
H	3.432879	-1.168266	0.901150
H	3.434123	-1.168075	-0.900696

Zero point E (au)= -458.469200
Includes B3LYP/CBS-B7 ZPVE correction (au)= 0.131600
Enthalpy corrected E(au)= -458.459414
S (J/molK)= 385.43
ΔG solv (kJ/mol)= -209.33

HF

E (au)= -456.620348

MP2

E (au)= -458.171075

MP4

E (au)= -458.293658

MPWB1K

E (au)= -459.131714

CCSD(t)

E (au)= -458.300823
Enthalpy correction (au)= 0.141319
S (J/molK)= 385.43
ΔG solv (kJ/mol)= -209.33

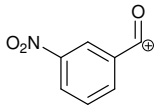

B3LYP

C	-0.385201	2.162085	0.000046
C	-1.570448	1.444259	0.000183
C	-1.495189	0.021792	0.000006
C	-0.259414	-0.676327	-0.000330
C	0.883949	0.095424	0.000034
H	-0.412275	3.246593	0.000126
H	-2.532047	1.946935	0.000129
H	-0.191613	-1.758873	-0.000072
C	-2.670416	-0.716625	-0.000059
O	-3.631802	-1.320796	-0.000055
C	0.846753	1.492660	0.000021
H	1.784689	2.038698	-0.000016
N	2.202033	-0.599384	0.000375
O	3.191842	0.116188	-0.000288
O	2.169561	-1.822551	0.000069

E (au)= -549.33478

ZPVE correction (au)= 0.101596
Enthalpy correction (au)= 0.111213
S (J/molK)= 390.94
ΔG solv (kJ/mol)= -269.491

CBS-QB3

C	−0.394462	2.156854	0.000049
C	−1.574396	1.436342	0.000031
C	−1.495648	0.017458	−0.000018
C	−0.259908	−0.674505	−0.000043
C	0.878835	0.098945	−0.000005
H	−0.425116	3.239026	0.000080
H	−2.535542	1.935378	0.000036
H	−0.186472	−1.755045	−0.000068
C	−2.665912	−0.721990	−0.000035
O	−3.617680	−1.322395	−0.000014
C	0.837211	1.492692	0.000037
H	1.772795	2.039548	0.000062
N	2.206979	−0.596156	−0.000017
O	3.187420	0.119154	0.000040
O	2.176656	−1.811832	−0.000039

Zero point E (au)= -548.365584
Includes B3LYP/CBS-B7 ZPVE correction (au)= 0.101015
Enthalpy corrected E (au)= -548.349813
S (J/molK)= 390.94
ΔG solv (kcal/mol)= -269.28

HF

E (au)= -546.194078

MP2

E (au)= -547.997598

MP4

E (au)= -548.118916

MPWB1K

E (au)= -549.065983

CCSD(t)

E (au)= -548.114889
Enthalpy correction (au)= 0.110643
S (J/molK)= 390.94
ΔG solv (kcal/mol)= -269.28

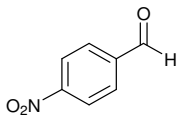

C	0.473899	1.280234	0.000148
C	−0.914875	1.376775	0.000110
C	−1.705054	0.220079	0.000056
C	−1.101063	−1.046788	0.000024
C	0.283279	−1.159263	0.000044
H	1.111715	2.155210	0.000288
H	−1.389438	2.355010	0.000151
H	−1.735829	−1.926989	0.000044

C	-3.187037	0.336840	-0.000099
O	-3.945339	-0.611238	-0.000097
C	1.046337	0.010102	0.000047
H	0.780908	-2.121085	0.000028
H	-3.572830	1.379261	-0.000138
N	2.518647	-0.102797	-0.000032
O	3.168992	0.940892	-0.000246
O	3.001601	-1.233366	0.000076

E (au)= -549.9723805

ZPVE correction (au)= 0.112667

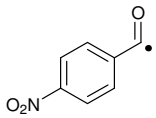

C	1.280086	0.454039	0.000000
C	1.403196	-0.932652	0.000000
C	0.258518	-1.739499	0.000000
C	-1.022291	-1.160026	0.000000
C	-1.156977	0.222987	0.000000
H	2.143451	1.107435	0.000000
H	2.382635	-1.400736	0.000000
H	-1.895819	-1.804196	0.000000
C	0.419844	-3.219452	0.000000
O	-0.442055	-4.043808	0.000000
C	0.000000	1.003613	0.000000
H	-2.126981	0.704874	0.000000
N	-0.139292	2.475437	0.000000
O	0.892630	3.143114	0.000000
O	-1.278388	2.937007	0.000000

E (au)= -549.3181748

ZPVE correction (au)= 0.100111

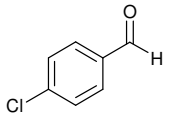

C	-0.748730	1.259663	-0.000010
C	0.640305	1.363369	-0.000002
C	1.441373	0.214939	0.000076
C	0.838255	-1.052110	0.000094
C	-0.545735	-1.171689	0.000077
H	-1.377240	2.143482	-0.000014
H	1.106873	2.346046	-0.000039
H	1.475051	-1.931411	0.000139
C	2.916248	0.339269	0.000023
O	3.687766	-0.600441	-0.000178
C	-1.326657	-0.010670	0.000024
H	-1.023784	-2.145389	0.000049
Cl	-3.074518	-0.155992	-0.000049
H	3.293434	1.386040	0.000430

E (au)= -805.1725207

ZPVE correction (au)= 0.100529

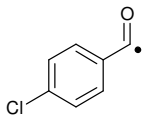

C	0.713893	1.263458	0.000113
C	-0.673858	1.377822	-0.000091
C	-1.479108	0.232137	0.000319
C	-0.884844	-1.041991	0.000133
C	0.499226	-1.167490	-0.000035
H	1.347940	2.143321	0.000285
H	-1.144674	2.356511	-0.000128
H	-1.520409	-1.922368	0.000177
C	-2.952323	0.382440	-0.000207
O	-3.779058	-0.480263	-0.000085
C	1.285049	-0.010273	0.000051
H	0.972189	-2.143813	0.000001
Cl	3.031129	-0.165187	-0.000080

E (au)= -804.5191749

ZPVE correction (au)= 0.088092

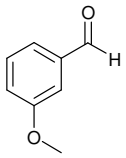

C	-0.442515	0.032226	0.378261
C	0.948596	0.118641	0.512133
C	1.585889	1.347528	0.293948
C	0.840230	2.473892	-0.053431
C	-0.556001	2.390027	-0.188486
C	-1.181947	1.170937	0.028676
H	-0.958246	-0.907241	0.542013
H	2.666189	1.402679	0.400664
H	-1.112382	3.280968	-0.459556
H	-2.260748	1.086716	-0.071109
C	1.539036	3.760890	-0.278432
O	0.991046	4.802394	-0.583877
H	2.643240	3.717196	-0.145785
O	1.765645	-0.920421	0.846916
C	1.178259	-2.191567	1.080393
H	0.663096	-2.568141	0.186900
H	2.003880	-2.860430	1.329069
H	0.471014	-2.161060	1.919646

E (au)= -459.9989795

ZPVE correction (au)= 0.143022

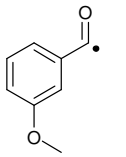

C	-0.475554	0.059965	0.471704
C	0.922736	0.148246	0.386641
C	1.516841	1.358009	0.011808
C	0.714076	2.467583	-0.274490
C	-0.683604	2.382994	-0.190553

C	-1.266227	1.176819	0.182712
H	-0.953982	-0.868959	0.760647
H	2.597474	1.428836	-0.054715
H	-1.285809	3.256967	-0.417418
H	-2.346943	1.091791	0.253337
C	1.334882	3.755134	-0.672841
O	2.495863	4.008831	-0.795813
O	1.780047	-0.878489	0.646904
C	1.237161	-2.133002	1.031439
H	0.592893	-2.551254	0.246920
H	2.092580	-2.792830	1.184931
H	0.666320	-2.056091	1.966175

E (au)= -459.3472336

ZPVE correction (au)= 0.13052

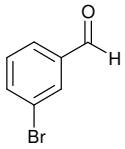

C	-0.566205	0.236248	0.000078
C	0.477690	-0.684007	0.000275
C	1.798420	-0.218978	0.000210
C	2.063594	1.158091	0.000078
C	1.008000	2.063498	0.000037
C	-0.314964	1.607975	0.000004
H	0.270313	-1.750236	0.000276
H	3.097417	1.488189	-0.000054
H	1.202463	3.132179	-0.000121
H	-1.142224	2.309690	-0.000126
C	2.914245	-1.196578	0.000107
O	4.091144	-0.894674	-0.000386
H	2.598072	-2.262918	0.000610
Br	-2.372568	-0.387343	-0.000064

E (au)= -2919.367031

ZPVE correction (au)= 0.100135

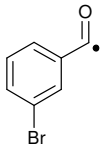

C	-0.453013	0.300135	0.000092
C	0.657241	-0.532901	0.000688
C	1.937783	0.047069	0.000294
C	2.090488	1.437863	-0.000284
C	0.961686	2.256141	0.000295
C	-0.314559	1.691342	0.000068
H	0.554688	-1.612475	0.001240
H	3.090600	1.860292	-0.001140
H	1.068119	3.336904	-0.000038
H	-1.198057	2.320629	-0.000394
C	3.145630	-0.815704	-0.000391
O	3.197344	-2.008111	-0.000081
Br	-2.207018	-0.461261	-0.000103

E (au)= -2918.713799

ZPVE correction (au)= 0.087662

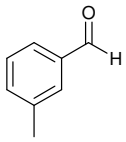

C	1.376564	-0.499101	-0.000110
C	0.011116	-0.779339	-0.000078
C	-0.939022	0.253861	0.000050
C	-0.521523	1.588903	0.000136
C	0.841593	1.884448	0.000001
C	1.776125	0.849726	-0.000162
H	-0.347571	-1.805032	-0.000203
H	-1.261051	2.386837	0.000221
H	1.177247	2.917835	-0.000048
H	2.837746	1.088414	-0.000352
C	-2.384325	-0.064294	0.000045
O	-2.849600	-1.188309	-0.000088
H	-3.053055	0.825834	0.000188
C	2.406272	-1.605066	0.000134
H	3.054888	-1.546308	0.882915
H	1.931300	-2.590558	-0.000740
H	3.056499	-1.545372	-0.881365

E (au)= -384.7982028

ZPVE correction (au)= 0.137739

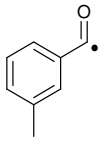

C	1.331668	-0.512020	-0.000091
C	-0.037269	-0.777745	-0.000074
C	-0.974379	0.270934	0.000013
C	-0.544331	1.601696	0.000068
C	0.822413	1.878446	0.000011
C	1.744570	0.832356	-0.000082
H	-0.401824	-1.801525	-0.000145
H	-1.281559	2.399149	0.000117
H	1.171038	2.907372	0.000006
H	2.808843	1.058766	-0.000165
C	-2.427394	-0.018187	0.000058
O	-2.968086	-1.084425	-0.000033
C	2.349161	-1.629494	0.000083
H	2.997190	-1.578445	0.883651
H	1.863913	-2.610012	-0.002213
H	3.000454	-1.575825	-0.880901

E (au)= -384.145246

ZPVE correction (au)= 0.125342

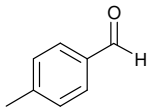

C	-1.755208	-0.064247	-0.000079
C	-0.917784	-1.195372	-0.000090
C	0.463221	-1.062608	-0.000035

C	1.047478	0.214663	0.000005
C	0.223262	1.345328	-0.000020
C	-1.163473	1.205262	-0.000072
H	1.114909	-1.931203	-0.000053
H	0.671286	2.337095	-0.000027
H	-1.795968	2.089565	-0.000121
C	2.517040	0.368584	0.000043
O	3.313294	-0.551726	0.000055
H	2.870934	1.424347	0.000068
H	-1.364152	-2.187397	-0.000156
C	-3.256015	-0.226624	0.000112
H	-3.594508	-0.782755	0.883086
H	-3.765677	0.741535	-0.002369
H	-3.594309	-0.787284	-0.880043

E (au)= -384.7990357

ZPVE correction (au)= 0.137702

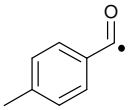

C	-1.713481	-0.067495	-0.000768
C	-0.869100	-1.193061	-0.000841
C	0.511397	-1.050991	-0.000304
C	1.083867	0.234561	0.000083
C	0.253208	1.360420	-0.000152
C	-1.131672	1.206948	-0.000674
H	1.164605	-1.918670	-0.000452
H	0.703258	2.349175	-0.000188
H	-1.771475	2.085795	-0.001088
C	2.551483	0.414497	0.000448
O	3.399750	-0.428670	0.000499
H	-1.308183	-2.188459	-0.001457
C	-3.212930	-0.241113	0.001023
H	-3.547609	-0.781003	0.895484
H	-3.729648	0.722884	-0.021924
H	-3.545585	-0.822957	-0.867260

E (au)= -384.1479025

ZPVE correction (au)= 0.125282

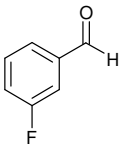

C	1.547839	-0.394868	-0.000325
C	0.295315	-0.993245	0.000092
C	-0.840685	-0.174081	0.000068
C	-0.707274	1.222424	0.000052
C	0.560995	1.795569	0.000146
C	1.702731	0.987539	-0.000175
H	0.211981	-2.076483	0.000130
H	-1.606249	1.829983	0.000078
H	0.672205	2.875970	0.000169
H	2.702049	1.410596	-0.000091
C	-2.186416	-0.797339	-0.000089
O	-3.232175	-0.178443	-0.000037
F	2.647211	-1.175404	0.000135

H	-2.182524	-1.909891	0.000182

E (au)= -444.738588

ZPVE correction (au)= 0.101933

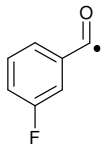

C	-1.291205	-0.620410	0.000051
C	0.078895	-0.824160	-0.000099
C	0.918064	0.303100	0.000100
C	0.378721	1.595148	0.000089
C	-1.005665	1.767435	-0.000157
C	-1.850630	0.657045	0.000095
H	0.494207	-1.826179	0.000046
H	1.050166	2.448019	-0.000036
H	-1.432182	2.765998	-0.000055
H	-2.930787	0.761969	0.000228
C	2.392780	0.136047	-0.000127
O	3.016539	-0.882089	0.000060
F	-2.115498	-1.686479	-0.000041

E (au)= -444.085295

ZPVE correction (au)= 0.089503

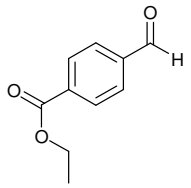

C	0.371485	-0.854410	-0.000261
C	1.743632	-1.069953	-0.000201
C	2.626439	0.020709	0.000053
C	2.121736	1.327949	0.000182
C	0.748172	1.547278	0.000094
C	-0.131818	0.457027	-0.000145
H	-0.318437	-1.690444	-0.000372
H	2.157389	-2.073580	-0.000254
H	2.810177	2.170273	0.000439
H	0.334729	2.550128	0.000270
C	4.092037	-0.204463	0.000051
O	4.621426	-1.298652	0.000070
H	4.704222	0.724438	0.000140
C	-1.598033	0.750241	-0.000127
O	-2.067327	1.871536	-0.000347
O	-2.347357	-0.371533	0.000213
C	-3.780941	-0.173267	0.000285
C	-4.431190	-1.543417	0.000009
H	-4.052580	0.413720	-0.882793
H	-4.052538	0.413354	0.883633
H	-5.521164	-1.435189	0.000027
H	-4.142417	-2.114652	-0.888096
H	-4.142437	-2.115021	0.887879

E (au)= -361.885202

ZPVE correction (au)= 0.112128

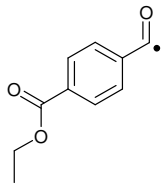

C	-0.416097	-0.853604	-0.000055
C	-1.788783	-1.069125	-0.000056
C	-2.668943	0.026931	0.000014
C	-2.166076	1.334349	0.000085
C	-0.791798	1.549210	0.000086
C	0.086463	0.457612	0.000013
H	0.273399	-1.690180	-0.000097
H	-2.197659	-2.074918	-0.000108
H	-2.861209	2.168698	0.000139
H	-0.376679	2.551299	0.000132
C	-4.139106	-0.182648	-0.000002
O	-4.730822	-1.220059	-0.000016
C	1.554181	0.748813	-0.000020
O	2.023582	1.869690	-0.000077
O	2.301175	-0.373865	-0.000003
C	3.735731	-0.178059	-0.000116
C	4.383423	-1.549268	0.000152
H	4.007704	0.408548	0.883047
H	4.007615	0.408146	-0.883577
H	5.473548	-1.442694	-0.000269
H	4.094227	-2.119851	0.888542
H	4.093611	-2.120446	-0.887656

E (au)= -361.249842

ZPVE correction (au)= 0.085734

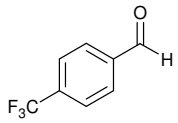

C	0.713791	0.036780	-0.038701
C	0.103612	1.293612	-0.027661
C	-1.286455	1.380196	-0.010093
C	-2.066158	0.217718	-0.003067
C	-1.445839	-1.040312	-0.015870
C	-0.060009	-1.131194	-0.033628
H	0.712070	2.191465	-0.039174
H	-1.770889	2.353960	-0.004679
H	-2.069402	-1.928743	-0.014402
H	0.428187	-2.099932	-0.051148
C	2.217115	-0.069223	0.002341
F	2.658569	-1.163949	-0.653904
F	2.668802	-0.161619	1.273733
F	2.813289	1.007947	-0.552516
C	-3.546436	0.319802	0.014322
H	-3.940408	1.359906	0.023123
O	-4.300402	-0.632792	0.019326

E (au)= -682.551575

ZPVE correction (au)= 0.114905

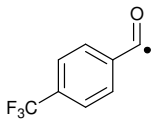

C	0.672185	0.039408	-0.038454
C	0.068670	1.299684	-0.027288
C	-1.320553	1.395966	-0.009266
C	-2.103032	0.235691	-0.002545
C	-1.491363	-1.029241	-0.015723
C	-0.105298	-1.125532	-0.033530
H	0.682166	2.194028	-0.039099
H	-1.810028	2.365166	-0.002922
H	-2.113846	-1.918600	-0.014623
H	0.378629	-2.096535	-0.051138
C	2.175895	-0.073560	0.002090
F	2.610583	-1.177132	-0.643100
F	2.626442	-0.154932	1.274305
F	2.775620	0.994733	-0.564245
C	-3.583388	0.361995	0.015950
O	-4.391179	-0.516817	0.019716

E (au)= -681.897897

ZPVE correction (au)= 0.102442

Computational Details for Chapter 3

Unsuccessful intermediates

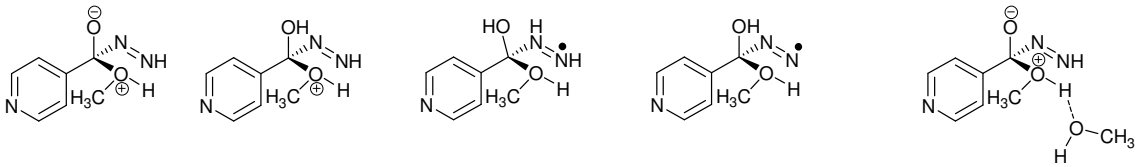

The above geometries were explored at B3LYP/6-31G(d) but no saddle points or energy minima were found for these on the potential energy surface.

Gas phase energy diagram for 7, 8 and 9

Comparison of energies for **7**, **8** and **9** in the gas phase (kJ mol^{-1}) showing the stabilizing effects of explicit solvation.

	reactants	associated reactants	transition structure	associated products	products
7	-586.807441	-586.80845	-586.75132	-586.80376	-586.803761
8	-702.523413	-702.532957	-702.500941	-702.529276	-702.519733
9	-818.239385	-818.26294	-818.23175	-818.25627	-818.235705

7	0.0	-2.6	147.3	9.7	9.7
8	0.0	-25.1	59.0	-15.4	9.7
9	0.0	-61.9	20.0	-44.3	9.7

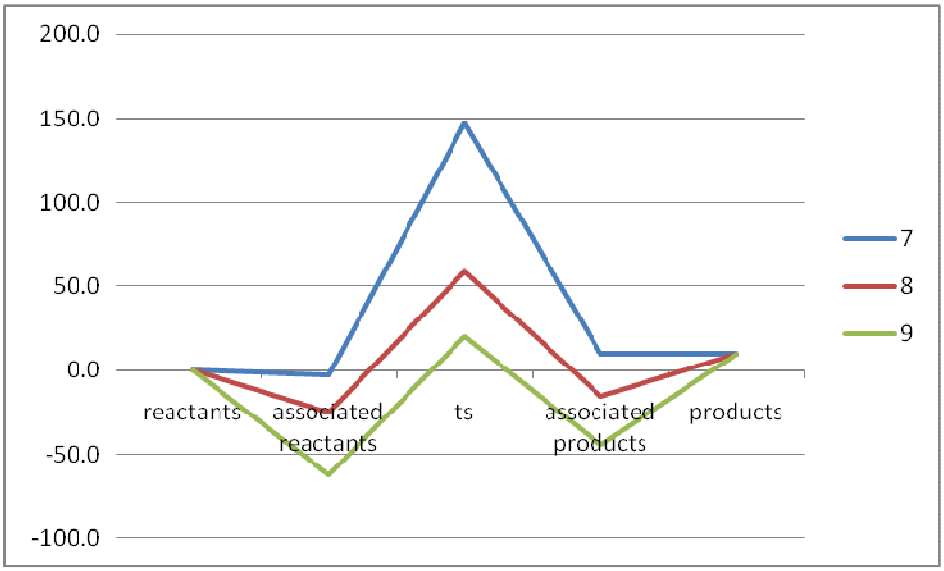

Geometries, energies and vibrational frequencies for all molecules

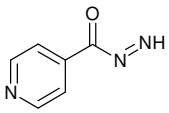

4

C	2.393694	0.964858	0.000234
C	1.025046	1.216638	-0.000226
C	0.146713	0.123699	-0.000740
C	0.684266	-1.169829	-0.000729
C	2.074345	-1.303530	0.000144
C	-1.310374	0.366815	-0.000132
O	-1.834127	1.459248	-0.000089
N	-2.148067	-0.892389	-0.000106
N	-3.368254	-0.683145	0.000630
N	2.921912	-0.268467	0.000647
H	3.104656	1.788582	0.000180
H	0.635180	2.228958	-0.000009
H	0.036155	-2.037635	-0.001685
H	2.527499	-2.292836	0.001115
H	-3.551749	0.355050	0.001615

B3LYP/6-31G(d) optimized energy = -471.057814272 au
ZPVE correction = 0.108130 au
Single point energy at B3LYP/6-311+G(2d,p) = -471.199598714
ΔG solv = -38.03 kJ mol^{-1}

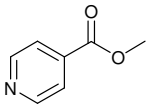

5

C	1.940063	-1.180205	-0.521429
C	0.568313	-0.945260	-0.628310

C	0.050510	0.243929	−0.104598
C	0.941643	1.143372	0.489753
C	2.289771	0.798058	0.564969
N	2.795784	−0.340678	0.072346
H	2.370890	−2.090954	−0.933894
H	−0.068371	−1.665006	−1.132915
H	0.582802	2.091582	0.875999
H	3.001769	1.471987	1.037782
C	−1.389748	0.653847	−0.254910
O	−1.690540	1.773331	−0.596066
O	−2.368226	−0.259876	−0.038609
C	−2.163692	−1.434597	0.759062
H	−1.960070	−2.302231	0.124111
H	−1.348405	−1.306497	1.475547
H	−3.100131	−1.596631	1.297130

B3LYP/6-31G(d) optimised energy = -476.141446633 au

ZPVE correction = 0.131649 au

Single point energy at B3LYP/6-311+G(2d,p) = -476.289703645 au

ΔG solv = -42.68 kJ mol^{-1}

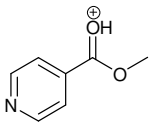

C	2.385237	0.831406	0.396938
C	1.038963	1.190022	0.339356
C	0.113757	0.210534	−0.067893
C	0.583646	−1.065056	−0.431374
C	1.957056	−1.297112	−0.357483
N	2.838744	−0.381244	0.058451
H	3.130430	1.551440	0.724700
H	0.718753	2.187329	0.618442
H	−0.071290	−1.840950	−0.808848
H	2.364033	−2.262649	−0.646589
C	−1.292983	0.576806	−0.152845
O	−1.554868	1.824821	−0.406529
O	−2.325570	−0.177585	−0.012611
C	−2.341792	−1.547233	0.525544
H	−2.334755	−2.236732	−0.318164
H	−1.492090	−1.698372	1.189991
H	−3.286236	−1.608524	1.063047
H	−2.519857	2.003082	−0.392070

B3LYP/6-31G(d) optimised energy = -476.480116009 au

ZPVE correction = 0.144600 au

Single point energy at B3LYP/6-311+G(2d,p) = -476.623004860 au

ΔG solv = -250.58 kJ mol^{-1}

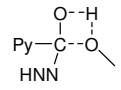

7

C	2.525372	-1.225525	0.468922
C	1.141881	-1.056821	0.535148
C	0.597791	0.142895	0.064051
C	1.465485	1.114563	-0.440970
C	2.831789	0.839339	-0.459855
N	3.368097	-0.306192	-0.018021
H	2.979747	-2.147105	0.828568
H	0.508035	-1.832179	0.950123
H	1.070862	2.059246	-0.798040
H	3.532869	1.576263	-0.847734
C	-0.872061	0.422683	0.095305
O	-1.322321	1.622690	-0.190717
N	-1.559676	-0.336167	1.203226
N	-2.353458	0.343185	1.865931
H	-2.370006	1.324977	1.481718
O	-1.544409	-0.222344	-1.289519
C	-2.507733	-1.291055	-1.278001
H	-3.334598	-1.086691	-0.591752
H	-2.879258	-1.388774	-2.301230
H	-1.999924	-2.210983	-0.981567
H	-1.853765	0.920233	-1.163757

B3LYP/6-31G(d) optimized energy =-586.722648259 au
ZPVE correction = 0.158276 au
Single point energy at B3LYP/6-311+G(2d,p) = -586.909602801 au
ν_i= 1647.6514 cm^{-1}

Associated reagents for 7

C	-2.462817	0.868394	1.122899
C	-1.155729	0.378597	1.115487
C	-0.749655	-0.401208	0.026351
C	-1.671170	-0.652958	-0.998428
C	-2.949419	-0.113820	-0.886809
N	-3.352003	0.635278	0.150431
H	-2.812122	1.479238	1.953103
H	-0.469505	0.595739	1.924553
H	-1.384361	-1.256658	-1.852894
H	-3.690104	-0.289494	-1.664551
C	0.607552	-0.978102	-0.062754
O	1.021531	-1.644254	-0.988095
N	1.469125	-0.731516	1.153787
N	2.552981	-1.329379	1.131206
H	2.630301	-1.887182	0.239897
O	1.763584	1.365776	-0.946580
C	2.900453	1.957024	-0.324568
H	3.585413	1.206605	0.094920
H	3.457211	2.603837	-1.017271
H	2.522808	2.571452	0.495971
H	2.073433	0.836040	-1.697351

B3LYP/6-31G(d) optimized energy = -586.778192379 au
ZPVE correction = 0.160975 au
Single point energy at B3LYP/6-311+G(2d,p) = -586.969478909 au

6 / **Associated products for 7**

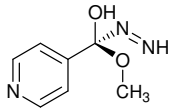

6

C	-2.408198	0.606200	1.107911
C	-1.014713	0.539418	1.035966
C	-0.432467	-0.161147	-0.024407
C	-1.282741	-0.755732	-0.961683
C	-2.660133	-0.624887	-0.794843
N	-3.231150	0.042273	0.217409
H	-2.884275	1.142054	1.927443
H	-0.402398	1.012594	1.795137
H	-0.875867	-1.317589	-1.794672
H	-3.341904	-1.081903	-1.510195
C	1.076002	-0.249941	-0.208732
O	1.405916	-1.480133	-0.776358
N	1.750624	-0.026835	1.133323
N	2.407485	-0.958435	1.607479
H	2.356701	-1.794272	0.972962
O	1.605311	0.715030	-1.089681
C	1.427116	2.097413	-0.767607
H	1.890773	2.349926	0.189781
H	1.919280	2.645516	-1.573324
H	0.364340	2.364849	-0.744831
H	2.165627	-1.307316	-1.361105

B3LYP/6-31G(d) optimized energy = -586.780075717 au
ZPVE correction = 0.160975 au
Single point energy at B3LYP/6-311+G(2d,p) = -586.967722847 au

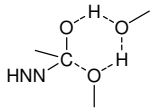

8

C	3.338744	0.860410	0.061558
C	1.962783	1.039768	-0.103263
C	1.146293	-0.092786	-0.184888
C	1.756806	-1.347961	-0.108354
C	3.137489	-1.411964	0.062497
N	3.931800	-0.334709	0.150523
H	3.996186	1.726451	0.122712
H	1.544479	2.036613	-0.185986
H	1.155434	-2.246095	-0.193730
H	3.636144	-2.377648	0.128924
C	-0.353881	-0.021458	-0.369125
O	-0.926383	-1.037109	-0.927624
N	-0.759712	1.357931	-0.911205
N	-1.439602	1.315076	-1.941678
H	-1.571986	0.302692	-2.214164
O	-0.952661	0.084906	1.140890
C	-0.810835	1.276845	1.925360

H	−1.371313	2.114059	1.501212
H	−1.176335	1.039153	2.928675
H	0.248019	1.539680	1.985100
H	−2.063071	−0.461248	1.037169
H	−2.179160	−1.297186	−0.275318
O	−2.877113	−1.164142	0.531513
C	−4.050237	−0.459205	0.082036
H	−4.658665	−0.226174	0.958234
H	−3.785050	0.464458	−0.444645
H	−4.615812	−1.113978	−0.584816

B3LYP/6-31G(d) optimized energy = -702.480129125 au
ZPVE correction = 0.212261 au
Single point energy at B3LYP/6-311+G(2d,p) = -702.713202246 au
ν_i= 1024.3621 cm^{-1}
ΔG solv = -95.52 kJ mol^{-1}

Associated reagents for 8

C	3.292292	0.415374	0.815443
C	2.074395	0.929945	0.370354
C	1.245180	0.097790	−0.391272
C	1.677822	−1.205417	−0.669277
C	2.913473	−1.613456	−0.174765
N	3.717229	−0.827111	0.555331
H	3.960640	1.033679	1.411151
H	1.769277	1.940686	0.609994
H	1.062506	−1.873915	−1.261900
H	3.279741	−2.618824	−0.372935
C	−0.048181	0.565698	−0.925612
O	−0.839331	−0.126635	−1.545121
N	−0.292462	2.039689	−0.763274
N	−1.304254	2.454292	−1.345356
H	−1.784257	1.655069	−1.835085
O	−1.135116	0.401997	1.488965
C	−2.176237	1.308074	1.809731
H	−2.820493	1.537886	0.945471
H	−2.812006	0.930380	2.624173
H	−1.711235	2.241429	2.137602
H	−1.546974	−0.453879	1.235983
H	−1.747837	−1.553087	−0.587225
O	−2.173826	−1.874140	0.229010
C	−3.562142	−2.058915	−0.030409
H	−4.024488	−2.373644	0.908392
H	−4.050669	−1.134648	−0.370262
H	−3.731227	−2.843554	−0.780262

B3LYP/6-31G(d) optimized energy = -702.511135599 au
ZPVE correction = 0.215570 au
Single point energy at B3LYP/6-311+G(2d,p) = -702.748526848 au
ΔG solv = -34.81 kJ mol^{-1}

Associated products for 8

C	3.389492	0.862874	0.053846
C	2.006478	1.059781	0.060429
C	1.172974	−0.043290	−0.142871
C	1.772741	−1.291120	−0.338176

C	3.163682	-1.375102	-0.321994
N	3.974685	-0.325402	-0.129953
H	4.059045	1.708223	0.204304
H	1.594368	2.051495	0.209993
H	1.163388	-2.170694	-0.512004
H	3.653981	-2.335249	-0.474092
C	-0.346174	0.060443	-0.128014
O	-0.872781	-0.804750	-1.059610
N	-0.752785	1.511473	-0.363531
N	-1.338574	1.765211	-1.421097
H	-1.422324	0.890836	-1.999262
O	-0.915414	-0.279648	1.138213
C	-0.444741	0.426405	2.292406
H	-0.591762	1.505020	2.189747
H	-1.038739	0.049227	3.127618
H	0.613335	0.213362	2.478000
H	-2.810079	-0.881469	0.842627
H	-1.811414	-1.016939	-0.804918
O	-3.329490	-1.159116	0.064164
C	-4.345521	-0.183830	-0.179953
H	-5.069991	-0.152418	0.643711
H	-3.928199	0.820706	-0.330250
H	-4.867003	-0.489935	-1.089578

B3LYP/6-31G(d) optimized energy = -702.514618010 au
ZPVE correction = 0.218286 au
Single point energy at B3LYP/6-311+G(2d,p) = -702.747561505 au
ΔG solv = -37.61 kJ mol^{-1}

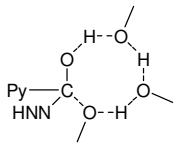

9

C	3.824222	0.131055	0.070885
C	2.663577	-0.607203	0.316050
C	1.420701	0.014536	0.161522
C	1.418015	1.354952	-0.243893
C	2.633790	1.994685	-0.473268
N	3.830744	1.409463	-0.321724
H	4.800644	-0.335349	0.195690
H	2.727715	-1.643701	0.626780
H	0.486840	1.896607	-0.374916
H	2.649957	3.035840	-0.793045
C	0.096506	-0.698392	0.435063
O	-0.812303	-0.027143	1.075574
N	0.382747	-2.088713	1.044612
N	-0.214113	-2.313893	2.100283
H	-0.785486	-1.459246	2.344547

O	-0.495372	-1.120498	-0.925936
C	0.298277	-1.834535	-1.877477
H	0.677245	-2.757970	-1.433282
H	-0.357603	-2.073245	-2.719870
H	1.135521	-1.224293	-2.233435
H	-1.717971	-0.503247	-1.230634
H	-2.522332	0.906138	-0.785162
O	-2.684959	-0.036307	-1.311484
C	-3.603478	-0.849098	-0.531080
H	-3.710679	-1.807760	-1.039821
H	-3.201013	-0.989482	0.474582
H	-4.564990	-0.334145	-0.507530
C	-2.882821	2.626001	0.918915
H	-3.543357	3.246625	0.307533
H	-3.489412	1.956403	1.542762
H	-2.290432	3.276479	1.570794
O	-2.018187	1.900493	0.043604
H	-1.416468	1.237978	0.578451

B3LYP/6-31G(d) optimized energy = -818.219989220 au
ZPVE correction = 0.267713 au
Single point energy at B3LYP/6-311+G(2d,p) = -818.499477346 au
ν_i= 211.2808cm^{-1}

Associated reagents for 9

C	-3.924597	0.211728	0.173255
C	-2.903309	-0.375345	-0.574170
C	-1.615267	0.166958	-0.482574
C	-1.414501	1.270696	0.355971
C	-2.507582	1.771544	1.060020
N	-3.745829	1.264648	0.979705
H	-4.937340	-0.183030	0.118191
H	-3.107513	-1.220061	-1.222746
H	-0.431827	1.716610	0.468448
H	-2.383736	2.624753	1.724242
C	-0.469945	-0.415893	-1.228923
O	0.589916	0.155526	-1.455280
N	-0.737206	-1.669468	-1.868420
N	-0.154877	-2.718144	-1.549162
H	0.447523	-2.554670	-0.707105
O	0.765218	-1.692935	0.980014
C	0.438429	-2.226925	2.253168
H	-0.457060	-2.844744	2.135545
H	1.242606	-2.859068	2.656591
H	0.217539	-1.436077	2.984317
H	1.599948	-1.164666	1.059416
H	2.757552	0.684513	0.832278
O	3.059344	-0.218870	1.087040
C	3.913834	-0.687779	0.047592
H	4.213480	-1.707421	0.304271
H	3.406215	-0.704654	-0.926803
H	4.820210	-0.072185	-0.033627
C	2.566715	3.161733	-0.645590
H	3.108393	3.729032	0.115331
H	3.278435	2.839548	-1.418046
H	1.819703	3.821226	-1.106510

O	1.950974	2.056628	0.009869
H	1.444979	1.528541	-0.644306

B3LYP/6-31G(d) optimized energy = -818.249913833 au
ZPVE correction = 0.270396 au
Single point energy at B3LYP/6-311+G(2d,p) = -818.533362857 au

Associated Products for 9

C	-3.840902	0.180684	-0.249777
C	-2.701762	-0.610360	-0.419868
C	-1.457586	-0.076938	-0.078172
C	-1.422422	1.227376	0.431123
C	-2.621127	1.925646	0.563351
N	-3.820928	1.427127	0.233395
H	-4.820460	-0.214802	-0.513964
H	-2.790453	-1.619633	-0.805538
H	-0.482613	1.696943	0.705640
H	-2.618297	2.941478	0.955477
C	-0.149714	-0.850794	-0.255755
O	0.713721	-0.255694	-1.142124
N	-0.450888	-2.257546	-0.711517
N	-0.000838	-2.622570	-1.803197
H	0.524003	-1.840881	-2.260899
O	0.546765	-0.993257	0.987458
C	-0.157114	-1.604665	2.078287
H	-0.474246	-2.618268	1.821768
H	0.554760	-1.634997	2.905666
H	-1.026824	-1.006285	2.369799
H	2.311226	-0.468582	1.138867
H	2.448053	1.426583	0.365344
O	3.171972	-0.001121	1.076942
C	3.986131	-0.734044	0.161539
H	4.238161	-1.725195	0.560858
H	3.493279	-0.857958	-0.811375
H	4.913167	-0.170574	0.026813
C	2.496824	2.920868	-0.952544
H	3.068195	3.622551	-0.331401
H	3.181426	2.436204	-1.662560
H	1.750297	3.484635	-1.517554
O	1.799388	1.974772	-0.147933
H	0.990155	0.655457	-0.841553

B3LYP/6-31G(d) optimized energy = -818.249301845au
ZPVE correction = 0.272462 au
Single point energy at B3LYP/6-311+G(2d,p) = -818.528775340 au

MPW1K calculations

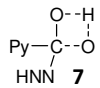

7

C	-2.481749	1.162900	0.589138
C	-1.106093	0.994868	0.615407
C	-0.575017	-0.143569	0.026217

C	-1.439382	-1.061167	-0.547155
C	-2.798121	-0.791265	-0.515333
N	-3.319269	0.296432	0.036373
H	-2.930073	2.037925	1.039338
H	-0.472292	1.723895	1.094673
H	-1.049007	-1.960613	-0.996221
H	-3.501178	-1.485876	-0.954050
C	0.894738	-0.413474	-0.004186
O	1.327314	-1.560191	-0.448610
N	1.552466	0.137258	1.206955
N	2.271391	-0.659134	1.791299
H	2.267960	-1.563749	1.278348
O	1.525423	0.404936	-1.199168
C	2.430905	1.492257	-1.030934
H	3.277531	1.209885	-0.412586
H	2.760520	1.774682	-2.024891
H	1.893826	2.314382	-0.572236
H	1.847014	-0.673684	-1.311465

MPW1K/6-31+G(d,p) optimized energy = -586.562997823 au
ZPVE correction = 0.164325 au
ν_i= 1545.7715 cm^{-1}

Associated reagents for 7

C	-2.515124	0.555760	1.241919
C	-1.265917	-0.047382	1.201381
C	-0.789458	-0.477156	-0.029373
C	-1.582673	-0.293443	-1.155011
C	-2.812557	0.318796	-0.997120
N	-3.276727	0.740150	0.174082
H	-2.919746	0.903882	2.182086
H	-0.683831	-0.186398	2.097570
H	-1.237478	-0.624868	-2.121788
H	-3.457476	0.479131	-1.849798
C	0.534277	-1.109822	-0.179257
O	0.949036	-1.580936	-1.201306
N	1.309151	-1.186870	1.055776
N	2.518052	-1.296408	0.898606
H	2.752126	-1.279922	-0.109233
O	2.226869	1.168233	-0.697076
C	2.705738	2.253001	0.060130
H	3.684857	2.587599	-0.284204
H	2.013319	3.095454	0.044785
H	2.802997	1.903942	1.083108
H	2.138939	1.426179	-1.610729

MPW1K/6-31+G(d,p) optimized energy = -586.615883321 au
ZPVE correction = 0.166158 au

Associated products for 7

C	-2.379030	0.615352	1.082637
C	-0.994417	0.558244	1.011363
C	-0.415617	-0.161700	-0.023294
C	-1.253564	-0.786006	-0.935180
C	-2.622823	-0.660037	-0.770672
N	-3.187326	0.025365	0.215192

H	-2.856441	1.165432	1.881983
H	-0.388302	1.056117	1.751309
H	-0.846457	-1.367458	-1.746432
H	-3.298893	-1.138465	-1.466000
C	1.084609	-0.242094	-0.205160
O	1.421085	-1.455507	-0.756906
N	1.731156	-0.014282	1.115308
N	2.368522	-0.930545	1.607388
H	2.333827	-1.765388	0.996875
O	1.596646	0.717104	-1.070361
C	1.338006	2.076857	-0.788539
H	1.683362	2.347406	0.205722
H	1.891757	2.638635	-1.532178
H	0.276770	2.299371	-0.886414
H	2.133078	-1.295880	-1.378875

MPW1K/6-31+G(d,p) optimized energy = -586.627624479 au
ZPVE correction = 0.169739 au

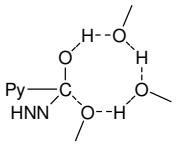

8

C	3.336733	0.745874	0.209914
C	1.982530	1.005291	0.047301
C	1.130626	-0.063530	-0.191415
C	1.678735	-1.334931	-0.266546
C	3.042562	-1.479893	-0.082124
N	3.867063	-0.466112	0.155307
H	4.025482	1.560061	0.390990
H	1.611360	2.017292	0.085712
H	1.044963	-2.180924	-0.479835
H	3.497261	-2.459854	-0.132210
C	-0.356852	0.093771	-0.383224
O	-0.951544	-0.815380	-1.066240
N	-0.670678	1.512019	-0.772099
N	-1.298103	1.617941	-1.813369
H	-1.470573	0.664383	-2.195393
O	-0.961435	0.049308	1.062525
C	-0.785154	1.100030	2.000455
H	-1.260112	2.014638	1.660558
H	-1.220803	0.761885	2.935657
H	0.277689	1.265377	2.142866
H	-1.983194	-0.477019	0.944821
H	-2.198556	-1.220726	-0.401681
O	-2.831672	-1.196889	0.415524
C	-4.093060	-0.633165	0.108136
H	-4.651745	-0.530624	1.032586
H	-3.987770	0.342500	-0.364726
H	-4.631482	-1.300923	-0.557668

MPW1K/6-31+G(d,p) optimized energy = - 702.297592063 au
ZPVE correction = 0.219634 au
ν_i = 793.3651 cm^{-1}

Associated reagents for 8

C	-3.866229	-0.407201	0.360786
C	-2.707189	-0.849792	-0.259723
C	-1.635304	0.029229	-0.341469
C	-1.770531	1.302715	0.196258
C	-2.972628	1.635593	0.794560
N	-4.004292	0.804134	0.878839
H	-4.723235	-1.061175	0.440533
H	-2.644738	-1.841167	-0.678780
H	-0.954038	2.005739	0.149629
H	-3.114429	2.616008	1.227071
C	-0.352650	-0.360492	-0.959426
O	0.534953	0.413435	-1.220500
N	-0.260220	-1.737700	-1.329422
N	0.762856	-2.352404	-1.043842
H	1.422570	-1.783921	-0.481605
O	2.393964	-0.948446	0.966177
C	3.049589	-1.420122	2.111419
H	4.132940	-1.441085	1.980379
H	2.813179	-0.816937	2.989397
H	2.709509	-2.435816	2.292746
H	2.661406	-0.039734	0.766404
H	2.028965	1.460039	-0.559220
O	2.781607	1.600113	0.019818
C	3.899925	1.990835	-0.738448
H	4.728072	2.123212	-0.049298
H	4.174602	1.234261	-1.474370
H	3.722695	2.936964	-1.249601

MPW1K/6-31+G(d,p) optimized energy = -702.326222143 au
ZPVE correction = 0.222238 au

Associated products for 8

C	3.436624	0.657531	0.076667
C	2.086277	0.977875	0.070590
C	1.167658	-0.037659	-0.147011
C	1.648070	-1.323518	-0.345740
C	3.016601	-1.531558	-0.313828
N	3.905002	-0.567476	-0.106957
H	4.174667	1.431400	0.238196
H	1.766369	1.996326	0.224004
H	0.967071	-2.137683	-0.534464
H	3.418399	-2.523865	-0.466817
C	-0.328156	0.199860	-0.140363
O	-0.919342	-0.606574	-1.063282
N	-0.581653	1.650690	-0.386681
N	-1.132582	1.954533	-1.432049
H	-1.315202	1.106113	-1.997864
O	-0.917140	-0.075688	1.102743
C	-0.361309	0.548942	2.242392
H	-0.342469	1.629916	2.130718

H	-1.005574	0.280286	3.072795
H	0.643501	0.178920	2.436645
H	-2.888077	-0.798132	0.889905
H	-1.826891	-0.833296	-0.777503
O	-3.296915	-1.128076	0.087575
C	-4.539656	-0.502150	-0.131922
H	-5.244156	-0.735916	0.665307
H	-4.439009	0.580155	-0.217420
H	-4.933478	-0.891680	-1.064694

MPW1K/6-31+G(d,p) optimized energy = -702.336241315 au
ZPVE correction = 0.225173 au

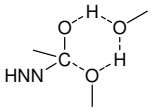

9

C	3.765641	0.228323	-0.126953
C	2.662997	-0.542719	0.215473
C	1.404455	0.039125	0.173667
C	1.320097	1.369402	-0.216680
C	2.483211	2.042028	-0.548856
N	3.692204	1.494261	-0.508521
H	4.757501	-0.202027	-0.091521
H	2.787559	-1.570585	0.516609
H	0.369457	1.878520	-0.254107
H	2.441011	3.077488	-0.858913
C	0.139492	-0.710294	0.548282
O	-0.758034	-0.057361	1.186926
N	0.510997	-2.035642	1.163225
N	-0.016278	-2.249627	2.241381
H	-0.612228	-1.429821	2.482145
O	-0.487966	-1.216010	-0.759685
C	0.305272	-1.826815	-1.762750
H	0.866132	-2.643984	-1.321649
H	-0.374476	-2.216379	-2.514762
H	0.982025	-1.106723	-2.216092
H	-1.496097	-0.628542	-1.077510
H	-2.467906	0.780474	-0.778978
O	-2.492653	-0.075859	-1.344995
C	-3.629793	-0.858928	-1.005754
H	-3.604589	-1.763354	-1.603264
H	-3.616234	-1.116262	0.050577
H	-4.527278	-0.298002	-1.245923
C	-2.957991	2.544277	1.035237
H	-3.586058	3.169257	0.406606
H	-3.594068	1.895539	1.638753
H	-2.384462	3.188442	1.699665
O	-2.098564	1.804865	0.205107
H	-1.511309	1.171548	0.726945

MPW1K/6-31+G(d,p) optimized energy = -818.014537824 au

ZPVE correction = 0.275368 au
ν_i = 393.2927cm^{-1}

Associated reagents for 9

C	-3.810241	-0.456609	-0.630634
C	-2.975073	0.142292	0.300224
C	-1.665495	-0.310760	0.391924
C	-1.252353	-1.336927	-0.447974
C	-2.171628	-1.856856	-1.342578
N	-3.426185	-1.433583	-1.438824
H	-4.837422	-0.133354	-0.726076
H	-3.338207	0.926405	0.945201
H	-0.241066	-1.711434	-0.416174
H	-1.884258	-2.651933	-2.016203
C	-0.707558	0.290339	1.341640
O	0.345032	-0.204872	1.668538
N	-1.169166	1.465245	1.996139
N	-0.498769	2.490307	1.948534
H	0.310488	2.372504	1.316765
O	0.729006	1.884030	-0.580557
C	0.277384	2.592556	-1.703015
H	-0.549384	3.224743	-1.389517
H	1.056824	3.233355	-2.118762
H	-0.079320	1.922313	-2.486379
H	1.477558	1.315163	-0.831036
H	2.667572	-0.571902	-0.725935
O	2.793102	0.238524	-1.244896
C	4.115183	0.689676	-1.108254
H	4.214131	1.607085	-1.681109
H	4.367047	0.903855	-0.068227
H	4.826205	-0.037089	-1.502654
C	2.939378	-2.770468	1.109033
H	3.594787	-3.267064	0.400176
H	3.551175	-2.273267	1.862410
H	2.322661	-3.526040	1.595514
O	2.152721	-1.854282	0.389345
H	1.543569	-1.393776	0.979428

MPW1K/6-31+G(d,p) optimized energy = -818.03644598 au
ZPVE correction = 0.277995 au

Associated products for 9

C	3.837466	0.190290	0.005896
C	2.729863	-0.603315	0.274081
C	1.468249	-0.069399	0.070029
C	1.379222	1.233809	-0.404149
C	2.549674	1.932563	-0.642760
N	3.763730	1.432518	-0.444879
H	4.833004	-0.202794	0.161527
H	2.858030	-1.613789	0.627840
H	0.421264	1.701344	-0.579524
H	2.508091	2.948383	-1.011626
C	0.191362	-0.845154	0.349332
O	-0.611780	-0.228274	1.252984
N	0.542281	-2.201054	0.833054
N	0.164881	-2.528535	1.946692

H	−0.351251	−1.755952	2.397659
O	−0.556567	−1.039660	−0.826689
C	0.105930	−1.633020	−1.929382
H	0.492519	−2.613977	−1.668662
H	−0.641361	−1.727720	−2.709839
H	0.915580	−0.998118	−2.283607
H	−2.307014	−0.501060	−1.007457
H	−2.490084	1.414018	−0.232203
O	−3.132869	−0.002995	−1.065760
C	−4.192647	−0.777624	−0.561463
H	−4.336844	−1.683081	−1.150597
H	−4.030588	−1.055940	0.480677
H	−5.096403	−0.179506	−0.627872
C	−2.444869	2.909522	1.064365
H	−2.956741	3.640028	0.438868
H	−3.156725	2.485079	1.773295
H	−1.663990	3.418512	1.620979
O	−1.832378	1.914747	0.281972
H	−0.970480	0.627499	0.930714

MPW1K/6-31+G(d,p) optimized energy = -818.046387037 au
ZPVE correction = 0.280891 au

CH_3OH

C	0.662325	−0.019545	0.000000
H	1.079718	0.991033	−0.000001
H	1.036957	−0.543658	−0.893148
H	1.036957	−0.543656	0.893149
O	−0.749169	0.122497	0.000000
H	−1.134236	−0.766420	0.000000

B3LYP/6-31G(d) optimized energy =-115.714405144 au
ZPVE correction = 0.051474 au
Single point energy at B3LYP/6-311+G(2d,p) = -115.767446192 au
ΔG solv = -26.19 kJ mol^{-1}

$CH_3OH_2^+$

C	0.802614	−0.002047	0.000100
H	1.107227	−0.513103	−0.910873
H	1.080265	1.049718	−0.002127
H	1.106999	−0.509333	0.913258
O	−0.707023	−0.000885	−0.000401
H	−1.222833	−0.831497	0.001163
H	−1.231160	0.823578	0.001188

B3LYP/6-31G(d) optimized energy = -116.012240494 au
ZPVE correction = 0.062536 au
Single point energy at B3LYP/6-311+G(2d,p) = -116.061014441 au
ΔG solv = -382.54 kJ mol^{-1}

HN=NH

N	0.593214	0.190165	−0.000049
H	1.173800	−0.672916	0.000346
N	−0.593334	−0.190241	−0.000049
H	−1.172960	0.673450	0.000346

B3LYP/6-31G(d) optimized energy = -110.637415522 au
ZPVE correction = 0.028351 au
Single point energy at B3LYP/6-311+G(2d,p) = -110.681995728 au
ΔG solv = -40.38 kJ mol^{-1}

N=NH$_2$

N	0.000013	−0.457465	0.000000
H	−0.000091	−1.053588	0.866170
N	0.000013	0.758490	0.000000
H	−0.000091	−1.053588	−0.866170

B3LYP/6-31G(d) optimized energy = -110.601669569 au
ZPVE correction = 0.026574 au
Single point energy at B3LYP/6-311+G(2d,p) = -110.647157755 au
ΔG solv = -52.22 kJ mol^{-1}

N$_2$

N	0.000000	0.000000	0.552750
N	0.000000	0.000000	−0.552750

B3LYP/6-31G(d) optimized energy = -109.524129072 au
ZPVE correction = 0.005599 au
Single point energy at B3LYP/6-311+G(2d,p) = -109.562951007 au
ΔG solv = 1.59 kJ mol^{-1}

H$_2$

H	0.000000	0.000000	0.371394
H	0.000000	0.000000	−0.371394

B3LYP/6-31G(d) optimized energy = -1.17548238770 au
ZPVE correction = 0.010145 au
Single point energy at B3LYP/6-311+G(2d,p) = -1.17956974143 au
ΔG solv = 6.49 kJ mol^{-1}

N=NH$^-$

N	0.118534	0.488644	0.000000
H	−1.659480	1.141386	0.000000
N	0.118534	−0.651699	0.000000

B3LYP/6-31G(d) optimized energy = -110.008391540 au
ZPVE correction = 0.008018 au
Single point energy at B3LYP/6-311+G(2d,p) = -110.070659182 au
ΔG solv = -280.96 kJ mol^{-1}

Phenyl analogue

C	−3.325313	−0.942996	0.013743
C	−1.941981	−1.052080	−0.147140
C	−1.144831	0.100326	−0.182689
C	−1.749020	1.358838	−0.064980
C	−3.127707	1.463609	0.100594
H	−3.936861	−1.841201	0.033362
H	−1.482846	−2.027521	−0.265852
H	−1.122264	2.242514	−0.118162
H	−3.587899	2.444041	0.191570
C	0.352630	0.043222	−0.361084
O	0.931896	1.083738	−0.871188
N	0.775442	−1.309088	−0.950412
N	1.457816	−1.224817	−1.977246

H	1.582335	-0.202914	-2.214595
O	0.963693	-0.121186	1.152723
C	0.811372	-1.336795	1.893122
H	1.373049	-2.162024	1.446469
H	1.167111	-1.137876	2.908714
H	-0.249156	-1.597682	1.932100
H	2.075004	0.413804	1.059021
H	2.164352	1.290409	-0.231872
O	2.888690	1.132658	0.565769
C	4.051531	0.441855	0.077515
H	4.677559	0.182956	0.934483
H	3.779619	-0.467468	-0.470982
H	4.607381	1.113709	-0.581250
C	-3.919716	0.312250	0.141795
H	-4.996206	0.395533	0.266917

B3LYP/6-31G(d) optimized energy = -686.444471765 au
ZPVE correction = 0.223836 au
Single point energy at B3LYP/6-311+G(2d,p) = -686.673086820 au
ν_i= -1102.3146 cm^{-1}
ΔG solv = -86.86 kJ mol^{-1}

Associated reagents for phenyl analogue

C	-3.343576	-0.628597	0.725525
C	-2.097281	-1.001471	0.228552
C	-1.288487	-0.046955	-0.411977
C	-1.741857	1.277314	-0.548531
C	-2.987188	1.641589	-0.051887
H	-3.967750	-1.364082	1.224625
H	-1.735426	-2.016599	0.333865
H	-1.108352	2.001614	-1.050299
H	-3.337372	2.664165	-0.159242
C	0.021078	-0.407619	-0.962135
O	0.809174	0.369373	-1.482650
N	0.325090	-1.882060	-0.942588
N	1.368593	-2.193888	-1.532118
H	1.825772	-1.327703	-1.920594
O	1.191046	-0.479813	1.533308
C	2.182980	-1.453443	1.801652
H	2.802326	-1.685762	0.919754
H	2.850733	-1.150109	2.622532
H	1.670099	-2.372722	2.098180
H	1.645069	0.364286	1.320419
H	1.774703	1.610719	-0.395559
O	2.313272	1.834455	0.387167
C	3.680242	1.844265	-0.009826
H	4.273893	2.051233	0.884323
H	4.000962	0.879712	-0.428645
H	3.881178	2.632102	-0.748821
C	-3.788761	0.687993	0.586105
H	-4.762443	0.974206	0.974933

B3LYP/6-31G(d) optimized energy = -686.479433823 au
ZPVE correction = 0.227462 au
Single point energy at B3LYP/6-311+G(2d,p) = -686.712562265 au
ΔG solv = -23.60 kJ mol^{-1}

Associated products for phenyl analogue

C	3.379054	0.940881	0.138853
C	1.989111	1.077787	0.154553
C	1.171125	-0.017061	-0.148677
C	1.759365	-1.250585	-0.458405
C	3.146095	-1.384943	-0.468278
H	4.005532	1.798561	0.368541
H	1.540698	2.036012	0.394370
H	1.121378	-2.093142	-0.702434
H	3.592875	-2.344859	-0.713223
C	-0.346937	0.075010	-0.122907
O	-0.872570	-0.649512	-1.171448
N	-0.774111	1.538595	-0.142409
N	-1.356367	1.940393	-1.155597
H	-1.421203	1.161168	-1.858853
O	-0.924778	-0.449746	1.079151
C	-0.439679	0.066471	2.322583
H	-0.583446	1.148599	2.390543
H	-1.025588	-0.433879	3.096918
H	0.619994	-0.173611	2.458500
H	-2.800722	-0.966604	0.701464
H	-1.810988	-0.892243	-0.951615
O	-3.340117	-1.148481	-0.092373
C	-4.349725	-0.143569	-0.198837
H	-5.054462	-0.197744	0.641107
H	-3.925238	0.868216	-0.245561
H	-4.897407	-0.339719	-1.123538
C	3.959930	-0.288672	-0.170658
H	5.041612	-0.393675	-0.182187

B3LYP/6-31G(d) optimized energy = -686.479226492 au
ZPVE correction = 0.230287 au
Single point energy at B3LYP/6-311+G(2d,p) = -686.707724498 au
ΔG solv = -29.16 kJ mol^{-1}

***p*-Nitrophenyl analogue**

C	2.285351	1.138893	-0.037767
C	0.897363	1.197484	-0.152166
C	0.144613	0.019281	-0.260054
C	0.796351	-1.221801	-0.265176
C	2.178895	-1.294678	-0.144840
H	2.887349	2.035610	0.041023
H	0.399414	2.159996	-0.177828
H	0.201806	-2.121349	-0.377176
H	2.702287	-2.242805	-0.142901
C	-1.364170	0.028526	-0.390744
O	-1.906589	-0.985427	-0.980298
N	-1.853038	1.410894	-0.851772
N	-2.572071	1.382319	-1.855526
H	-2.669453	0.378099	-2.169889
O	-1.911353	0.033532	1.141687
C	-1.810517	1.195820	1.975810
H	-2.431589	2.017154	1.609023
H	-2.127531	0.892767	2.977910
H	-0.767052	1.517869	2.015581
H	-2.994152	-0.580672	1.055702

H	-3.120528	-1.360495	-0.287096
O	-3.781910	-1.306351	0.552905
C	-5.015748	-0.654265	0.190660
H	-5.592571	-0.498059	1.104214
H	-4.829455	0.305801	-0.303252
H	-5.572553	-1.312752	-0.479495
C	2.903772	-0.108152	-0.030226
N	4.369076	-0.176429	0.097697
O	4.984549	0.884522	0.201122
O	4.891653	-1.290689	0.095635

B3LYP/6-31G(d) optimized energy = -890.945697948 au
ZPVE correction = 0.223128 au
Single point energy at B3LYP/6-311+G(2d,p) = -891.242526 au
ν_i= -1781.1078 cm^{-1}
ΔG solv = -91.76 kJ mol^{-1}

Associated reagents for *p*-nitrophenyl analogue

C	-2.266850	-1.105947	0.383275
C	-0.932753	-1.350012	0.073628
C	-0.188745	-0.388026	-0.628691
C	-0.788893	0.820116	-1.020734
C	-2.120215	1.072297	-0.716936
H	-2.865723	-1.825691	0.926923
H	-0.456267	-2.273679	0.376135
H	-0.202318	1.550634	-1.567282
H	-2.609373	1.993621	-1.006888
C	1.221127	-0.629062	-0.988298
O	1.951435	0.183789	-1.532102
N	1.693882	-2.034785	-0.748563
N	2.819428	-2.278222	-1.204452
H	3.208588	-1.417053	-1.669093
O	1.928523	-0.265698	1.536070
C	3.012788	-1.011656	2.063561
H	3.819441	-1.165282	1.328823
H	3.442750	-0.533016	2.955687
H	2.628139	-1.994144	2.349066
H	2.259129	0.632709	1.312024
H	2.547643	1.730159	-0.502553
O	2.824807	2.107438	0.352687
C	4.205563	2.448744	0.266917
H	4.500352	2.837745	1.244549
H	4.836304	1.580552	0.028881
H	4.381307	3.229844	-0.484796
C	-2.836364	0.100195	-0.018524
N	-4.253585	0.360704	0.306564
O	-4.865786	-0.511630	0.919266
O	-4.731730	1.433581	-0.057358

B3LYP/6-31G(d) optimized energy = -890.9768195 au
ZPVE correction = 0.230042 au
Single point energy at B3LYP/6-311+G(2d,p) = -891.277980 au
ΔG solv = -32.30 kJ mol^{-1}

Associated products for the *p*-nitrophenyl analogue

C	2.330795	1.147219	-0.006205
C	0.939015	1.217559	-0.025343

C	0.170879	0.049784	-0.119524
C	0.809825	-1.196504	-0.187548
C	2.197578	-1.281005	-0.164430
H	2.943095	2.037940	0.059690
H	0.449779	2.183660	0.023657
H	0.209784	-2.095216	-0.271579
H	2.710989	-2.233017	-0.218166
C	-1.352887	0.084059	-0.119319
O	-1.829821	-0.872056	-0.986012
N	-1.826806	1.492384	-0.464078
N	-2.425367	1.637002	-1.534736
H	-2.468133	0.718927	-2.045654
O	-1.915363	-0.187508	1.165579
C	-1.487990	0.624708	2.265914
H	-1.685475	1.684433	2.082976
H	-2.069377	0.282312	3.124517
H	-0.422401	0.477219	2.472151
H	-3.804286	-0.894773	0.900163
H	-2.758294	-1.114114	-0.717441
O	-4.274815	-1.266923	0.130792
C	-5.345652	-0.388103	-0.223791
H	-6.098700	-0.341563	0.572791
H	-4.991970	0.627751	-0.444792
H	-5.812265	-0.803464	-1.119647
C	2.938116	-0.103122	-0.074205
N	4.409005	-0.184528	-0.049820
O	5.037960	0.869474	0.037126
O	4.919707	-1.301946	-0.116425

B3LYP/6-31G(d) optimized energy = -890.979631740 au
ZPVE correction = 0.232626 au
Single point energy at B3LYP/6-311+G(2d,p) = -891.276348 au
ΔG solv = -35.98 kJ mol^{-1}

***p*-Methoxyphenyl analogue**

C	2.458495	1.330160	-0.009639
C	1.074234	1.312989	-0.128819
C	0.379946	0.096313	-0.238921
C	1.111079	-1.094956	-0.235831
C	2.499128	-1.091336	-0.112288
H	3.005170	2.264717	0.068328
H	0.527843	2.249514	-0.157950
H	0.575663	-2.032045	-0.344862
H	3.036411	-2.032918	-0.114328
C	-1.115445	0.019467	-0.375113
O	-1.610978	-1.038225	-0.939260
N	-1.683589	1.358817	-0.857724
N	-2.393059	1.277462	-1.866584
H	-2.431582	0.265966	-2.168754
O	-1.702813	0.023369	1.164369
C	-1.646044	1.196324	1.980816
H	-2.300556	1.989256	1.607472
H	-1.945738	0.898807	2.990583
H	-0.615629	1.559895	2.008868
H	-2.757889	-0.615225	1.058661

H	−2.785425	−1.403684	−0.291466
O	−3.506092	−1.379220	0.533453
C	−4.744699	−0.778413	0.120618
H	−5.367676	−0.637416	1.007073
H	−4.580493	0.186650	−0.372914
H	−5.252653	−1.458525	−0.567917
C	3.180716	0.128364	0.003725
O	4.533054	0.251200	0.127181
C	5.319124	−0.930571	0.135672
H	5.210067	−1.494364	−0.800005
H	6.354203	−0.599994	0.239084
H	5.060248	−1.581619	0.981020

B3LYP/6-31G(d) optimized energy = -800.968005760 au
ZPVE correction = 0.256440 au
Single point energy at B3LYP/6-311+G(2d,p) = -801.233622125 au
ν_i= -1136.5463 cm^{-1}
ΔG solv = -93.97 kJ mol^{-1}

Associated reagents for *p*-methoxyphenyl analogue

C	−2.487484	−1.281069	0.491199
C	−1.167010	−1.478959	0.132692
C	−0.461289	−0.477578	−0.567985
C	−1.121478	0.719319	−0.894160
C	−2.446841	0.926765	−0.539759
H	−3.045209	−2.036252	1.035209
H	−0.658520	−2.399016	0.392507
H	−0.578212	1.487094	−1.435803
H	−2.933616	1.857936	−0.804409
C	0.927502	−0.655546	−0.964468
O	1.625492	0.180719	−1.527864
N	1.477979	−2.032945	−0.707334
N	2.624459	−2.210937	−1.141146
H	2.965299	−1.325659	−1.599982
O	1.853729	−0.145122	1.644439
C	3.003627	−0.831702	2.100353
H	3.731765	−1.028429	1.295974
H	3.521268	−0.290160	2.907607
H	2.675386	−1.798394	2.493043
H	2.136156	0.738381	1.324167
H	2.194777	1.699682	−0.568389
O	2.573133	2.170823	0.199508
C	3.942389	2.436333	−0.081301
H	4.364909	2.923043	0.801714
H	4.514148	1.519041	−0.282822
H	4.056343	3.115101	−0.938053
C	−3.138170	−0.078592	0.160189
O	−4.428623	0.016113	0.557510
C	−5.150003	1.210974	0.277103
H	−5.232191	1.384063	−0.803001
H	−6.145466	1.059874	0.696772
H	−4.681217	2.080929	0.752887

B3LYP/6-31G(d) optimized energy = -801.005893 au
ZPVE correction = 0.260271 au
Single point energy at B3LYP/6-311+G(2d,p) = -801.276509313 au
ΔG solv = -33.39 kJ mol^{-1}

Associated products for *p*-methoxyphenyl analogue

C	2.508565	1.332814	0.054298
C	1.119643	1.333630	0.024159
C	0.404876	0.133879	-0.117313
C	1.119929	-1.062665	-0.220517
C	2.514091	-1.077378	-0.187567
H	3.068759	2.256819	0.156972
H	0.585002	2.274222	0.102125
H	0.576264	-1.993473	-0.341009
H	3.037317	-2.022694	-0.274895
C	-1.111112	0.087306	-0.130444
O	-1.541970	-0.874112	-1.021182
N	-1.660435	1.474352	-0.445174
N	-2.255997	1.613545	-1.518955
H	-2.242162	0.706459	-2.051086
O	-1.688011	-0.241645	1.142704
C	-1.292173	0.545147	2.269588
H	-1.547866	1.600051	2.133136
H	-1.843965	0.138645	3.120395
H	-0.217473	0.448879	2.456285
H	-3.488134	-0.993566	0.851950
H	-2.459227	-1.157143	-0.765419
O	-3.991919	-1.375816	0.107058
C	-5.073384	-0.498608	-0.210308
H	-5.800059	-0.449950	0.611215
H	-4.729221	0.517687	-0.444441
H	-5.572177	-0.913370	-1.089421
C	3.216697	0.127179	-0.049867
O	4.575131	0.232158	-0.007625
C	5.346951	-0.954636	-0.111246
H	5.174295	-1.466284	-1.067115
H	6.389990	-0.638200	-0.054910
H	5.133329	-1.648049	0.712768

B3LYP/6-31G(d) optimized energy = -801.002661 au
ZPVE correction = 0.263005 au
Single point energy at B3LYP/6-311+G(2d,p) = -801.268063541 au
ΔG solv = -36.40 kJ mol^{-1}

Computational Details for Chapter 4

Geometries and energies for optimised transition structures 4-11

Transition Structure **4**

C	1.79697	-1.06752	-0.05562
C	0.72449	-1.07226	0.77305
C	0.47624	1.30681	0.45481
C	1.544	1.30792	-0.37818
H	2.34966	-1.98025	-0.18509
H	0.37979	-1.93417	1.30974
H	-0.02726	2.19157	0.79356
H	1.9059	2.24891	-0.75136

O	-1.60125	-1.3837	-0.65482
C	-1.69699	-0.34001	-0.21234
C	-2.59995	0.82204	-0.2102
H	-2.8929	1.05774	0.80743
H	-2.08473	1.67442	-0.63812
H	-3.47304	0.57647	-0.80435
C	2.20252	0.11042	-0.69706
H	3.04683	0.11056	-1.36017
N	-0.08008	0.08054	0.88919
H	-0.51732	0.15607	1.79584

E (au) = -401.66972
ZPVE (au) =0.150747

Transition Structure **5**

C	1.75846	-1.03922	-0.10871
C	0.0289	0.13497	1.02295
C	0.51567	1.34147	0.47667
C	1.54649	1.31248	-0.42095
C	2.1599	0.09447	-0.75369
H	2.21438	-1.99899	-0.26642
H	-0.55801	0.13029	1.92414
H	0.0494	2.26647	0.76247
H	1.90531	2.22737	-0.85821
H	2.96017	0.04627	-1.46717
O	-1.6174	-1.35695	-0.65025
C	-1.71596	-0.3112	-0.17112
C	-2.73296	0.77051	-0.21986
H	-2.29523	1.6342	-0.7094
H	-3.5995	0.42641	-0.77345
H	-3.01325	1.05452	0.78841
N	0.77252	-0.98766	0.79859
H	0.50523	-1.83818	1.2598

E (au)= -401.694726
ZPVE (au) = 0.151838

Transition Structure **6**

C	-0.05638	0.27852	1.01173
C	0.49041	1.41059	0.33492
C	1.52509	1.2519	-0.55429
C	2.1225	0.01373	-0.69741
H	-0.67127	0.43394	1.88111
H	0.06388	2.38429	0.4976
H	1.90499	2.08233	-1.1201
H	2.93243	-0.19781	-1.36711
O	-1.43384	-1.27274	-0.85754
C	-1.66932	-0.34762	-0.20237
C	-2.84067	0.56073	-0.09163
H	-3.27059	0.45756	0.89977
H	-2.51876	1.5886	-0.21582
H	-3.57516	0.30089	-0.84574
N	1.71844	-0.99041	0.11039
C	0.73251	-0.88853	0.98251
H	0.53568	-1.74661	1.59736
H	2.21554	-1.8643	0.05979

E (au) = -401.684213
ZPVE (au) = 0.151305

Transition Structure **7**

C	-1.60909	1.16798	-0.46161
C	-0.52794	1.36148	0.33447
C	0.04537	0.26016	1.01885
C	-0.66965	-0.96234	1.00459
C	-1.74366	-1.101	0.18972
H	-2.06959	1.95284	-1.03162
H	-0.10632	2.34613	0.41631
H	0.74093	0.44871	1.81779
H	-0.35218	-1.79587	1.60276
H	-2.30346	-2.01311	0.10269
O	1.36232	-0.76574	-1.29634
C	1.72093	-0.22552	-0.3452
C	3.02372	0.26397	0.17292
H	2.94707	1.32295	0.39336
H	3.25218	-0.25942	1.09554
H	3.79825	0.08332	-0.5648
N	-2.18028	-0.05321	-0.54404
H	-2.98159	-0.17553	-1.13546

E (au) = -401.695595
ZPVE (au) = 0.151977

Transition Structure **8**

C	1.94969	1.19324	-0.14912
C	0.57489	1.18984	-0.11897
C	0.51349	-1.08878	0.18432
C	1.89011	-1.16635	0.17013
H	2.47842	2.11969	-0.28301
H	0.00864	2.09668	-0.23508
H	-0.12952	-1.94648	0.28216
H	2.37055	-2.12058	0.29052
O	-2.18704	-1.28982	-0.27775
C	-1.88577	-0.12876	-0.36195
C	-2.60464	0.99701	0.33468
H	-2.67054	0.81114	1.40637
H	-2.14653	1.96306	0.16436
H	-3.61314	1.02517	-0.06371
C	2.62592	-0.00851	-0.00075
H	3.701	-0.03828	-0.02259
N	-0.12639	0.06886	0.04755

E (au) = -401.311067
ZPVE (au) = 0.138714

Transition Structure **9**

C	1.49063	-1.30543	-0.1458
C	0.00859	0.08517	0.93061
C	0.778	1.2325	0.54158
C	1.84777	1.06221	-0.28957
C	2.20866	-0.23041	-0.67578
H	1.79672	-2.31464	-0.37891
H	-0.5363	0.15627	1.86414
H	0.46368	2.20968	0.86121
H	2.41741	1.91064	-0.62875
H	3.04562	-0.4084	-1.32653
O	-2.02988	1.32043	-0.44555
C	-1.6903	0.25275	-0.11136
C	-2.39201	-1.05495	-0.31076
H	-2.58822	-1.18239	-1.37119

H	-1.79619	-1.87296	0.06595
H	-3.34617	-1.00545	0.20627
N	0.46779	-1.18673	0.66268

E (au) = -401.304486
ZPVE (au) = 0.136536

Transition Structure **10**

C	-0.06507	0.53129	0.87877
C	0.56408	1.40197	-0.07521
C	1.62987	0.93549	-0.79625
C	2.15758	-0.3266	-0.50915
H	-0.6294	0.98167	1.68189
H	0.16563	2.38752	-0.24339
H	2.09184	1.54445	-1.55435
H	2.99793	-0.71381	-1.05916
O	-2.72853	0.52648	0.28612
C	-1.75463	-0.04229	-0.02477
C	-1.6002	-1.08708	-1.08864
H	-1.8937	-0.65608	-2.04093
H	-0.58739	-1.45808	-1.14547
H	-2.28127	-1.90235	-0.86343
N	1.7031	-1.08926	0.49799
C	0.68169	-0.66153	1.18772
H	0.36292	-1.27778	2.01502

E (au) = -401.301903
ZPVE (au) = 0.136154

Transition Structure **11**

C	-1.55636	0.97508	-0.77944
C	-0.50381	1.3777	0.00608
C	0.02486	0.47699	0.96774
C	-0.73054	-0.70435	1.18013
C	-1.772	-0.99398	0.33312
H	-1.93884	1.6323	-1.54457
H	-0.05895	2.34703	-0.13504
H	0.64377	0.86212	1.76019
H	-0.47358	-1.38366	1.97429
H	-2.32813	-1.91013	0.45689
O	2.72774	0.5744	0.23008
C	1.78671	-0.07722	-0.00466
C	1.58997	-1.14414	-1.03056
H	1.42844	-2.08755	-0.51938
H	0.69763	-0.92934	-1.60704
H	2.46044	-1.21016	-1.67401
N	-2.18368	-0.19662	-0.65520

E (au) = -401.303623
ZPVE (au) = 0.137205

Computational Details for Chapter 5

Figure A1: Remaining transition states 2

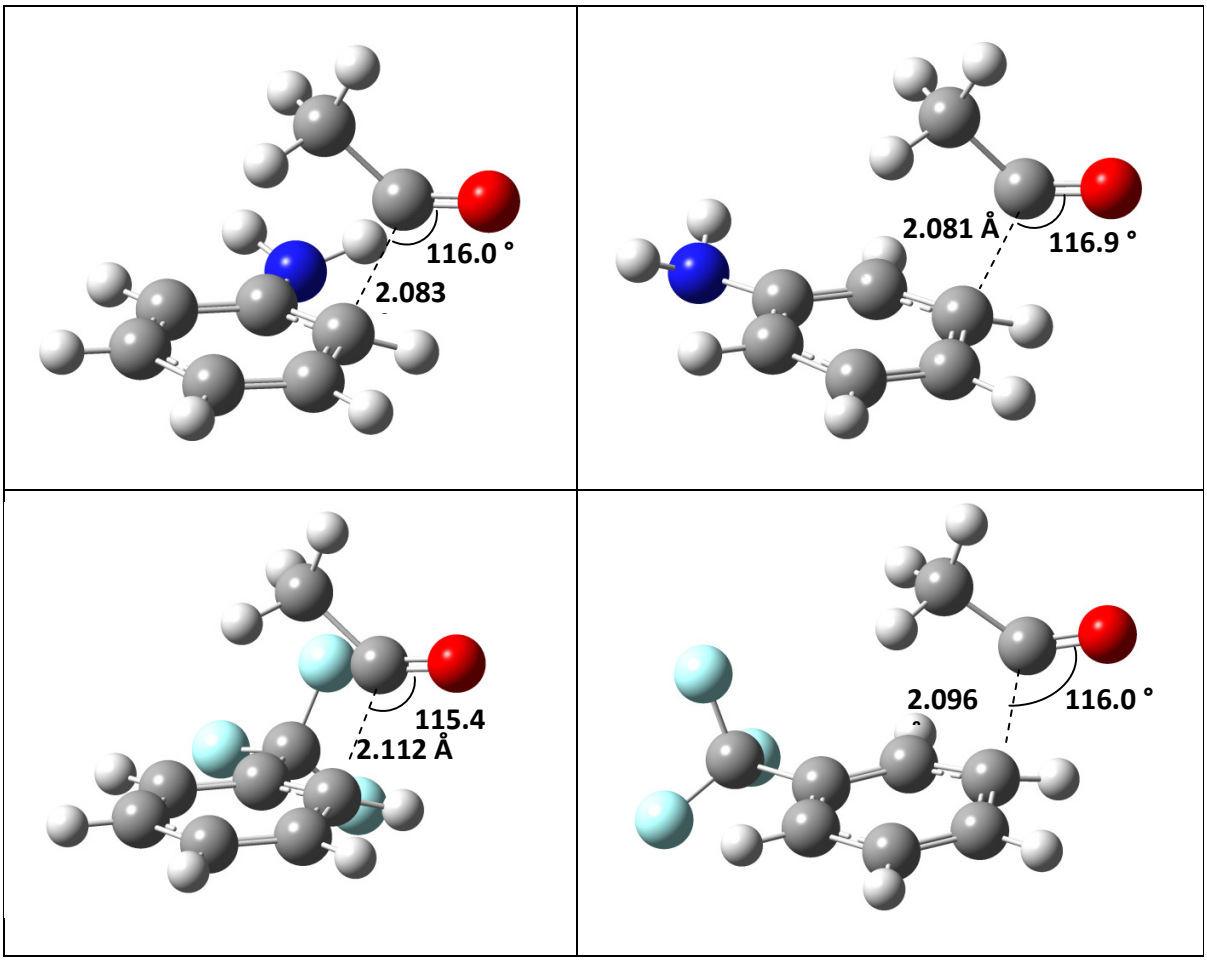

Geometries and energies for optimised transition structures

Acetyl radical addition to Benzene **2 R=H**

C	-1.51659	1.10054	-0.73063
C	-0.46191	1.39244	0.10142
C	0.03936	0.41232	1.00313
C	-0.72912	-0.77225	1.16923
C	-1.78262	-1.04432	0.33063
C	-2.17401	-0.12575	-0.64358
H	-1.85606	1.8383	-1.43821
H	0.02473	2.35096	0.04682

H	0.6621	0.7432	1.81694
H	-0.45612	-1.47329	1.93971
H	-2.33001	-1.96522	0.44362
H	-3.00484	-0.34323	-1.29141
O	2.7315	0.56573	0.20683
C	1.79302	-0.10192	-0.00861
C	1.58854	-1.12092	-1.08349
H	1.40457	-2.08494	-0.62085
H	0.70299	-0.86149	-1.65283
H	2.46055	-1.17088	-1.72706

E (au) = -385.269703
ZPVE (au) = 0.148886

Acetyl radical addition to C1 on Naphthalene **3**

C	-2.36542	-1.60612	-0.40411
C	-1.10449	-1.36725	-0.88171
C	-0.44937	-0.1554	-0.61634
C	-1.11105	0.83092	0.14986
C	-2.40467	0.55652	0.63569
C	-3.01925	-0.63448	0.36631
H	1.29132	-0.55262	-1.83828
H	-2.85707	-2.53907	-0.61938
H	-0.59749	-2.11464	-1.46972
C	0.89296	0.09244	-1.07434
C	-0.46923	2.07575	0.38356
H	-2.90858	1.30721	1.22154
H	-4.00957	-0.82767	0.74143
C	0.75975	2.33948	-0.16818
C	1.42317	1.38096	-0.93318
H	-0.97996	2.82403	0.9653
H	1.21157	3.30687	-0.02715
H	2.37447	1.61202	-1.37971
C	2.16499	-0.97268	0.31535
O	3.18356	-1.36461	-0.10824
C	1.7193	-0.82929	1.73636
H	1.46513	0.20883	1.91994
H	0.81899	-1.41557	1.88429
H	2.50257	-1.15765	2.41210

E (au) = -538.857972
ZPVE (au) = 0.197273

Acetyl radical addition to C2 Naphthalene **4**

C	-3.11018	-1.08178	0.0311
C	-1.92746	-1.35532	-0.59587
C	-0.87063	-0.41718	-0.59562
C	-1.07241	0.82839	0.05844
C	-2.29799	1.07976	0.69161
C	-3.3005	0.14515	0.68509
H	0.48588	-1.59553	-1.76944
H	-3.90324	-1.80985	0.02401
H	-1.7842	-2.29719	-1.09895
C	0.35707	-0.66891	-1.23519
C	-0.02495	1.79655	0.01761
H	-2.44401	2.02717	1.1838
H	-4.23613	0.35137	1.17512

C	1.15647	1.53079	-0.58104
C	1.42376	0.23327	-1.1426
H	-0.20223	2.76268	0.46085
H	1.93136	2.27745	-0.61328
H	2.24504	0.14278	-1.83246
C	2.7668	-0.44736	0.36216
O	3.89757	-0.1774	0.22709
C	2.07525	-1.09159	1.51983
H	1.25203	-0.46094	1.83618
H	1.65148	-2.03401	1.18919
H	2.772	-1.25533	2.33526

E (au) = -538.854752
ZPVE (au) = 0.197068

Acetyl radical addition *ortho* to aniline **2,R=*o*-NH_2**

C	-1.43132	-1.67728	-0.20097
C	-0.3898	-1.26336	-1.00222
C	0.0646	0.07831	-0.9711
C	-0.7242	1.03354	-0.25955
C	-1.76725	0.60002	0.52953
C	-2.11705	-0.74911	0.57371
H	-1.73361	-2.71023	-0.20004
H	0.12515	-1.96641	-1.63396
H	0.65226	0.43382	-1.80158
H	-2.33331	1.31828	1.10074
H	-2.93988	-1.06234	1.19233
O	2.79168	-0.36464	-0.48871
C	1.82511	-0.10521	0.12693
C	1.58524	-0.28928	1.59516
H	1.28944	0.65878	2.03167
H	0.76073	-0.98049	1.73198
H	2.48187	-0.66427	2.07756
N	-0.38948	2.36967	-0.37966
H	-0.74907	2.97969	0.32657
H	0.56735	2.55679	-0.60697

E (au) = -440.611725
ZPVE (au) =0.166201

Acetyl radical addition *meta* to aniline **2,R=*m*-NH_2**

C	0.71479	1.74509	0.58811
C	-0.33676	1.59496	-0.28289
C	-0.45013	0.39945	-1.04482
C	0.64361	-0.50253	-1.03542
C	1.69612	-0.33819	-0.1541
C	1.71816	0.78632	0.68325
H	0.77946	2.63076	1.19801
H	-1.09914	2.34945	-0.36228
H	-1.09565	0.40597	-1.90689
H	0.63994	-1.34398	-1.70901
H	2.54311	0.9297	1.3607
O	-3.10802	-0.16122	-0.31686
C	-2.02296	-0.4532	0.01758

C	-1.58439	-1.17494	1.25248
H	-1.14672	-2.12426	0.96071
H	-0.81208	-0.59789	1.74764
H	-2.42931	-1.34043	1.91279
N	2.76459	-1.22539	-0.14736
H	3.30417	-1.23631	0.69451
H	2.55768	-2.14729	-0.47493

E (au)= -440.609631
ZPVE (au) =0.166071

Acetyl radical addition *para* to aniline **2,R=*p*-NH_2**

C	-1.15068	1.0698	-0.66381
C	0.04243	1.4527	-0.10352
C	0.6415	0.69461	0.94088
C	-0.1728	-0.30971	1.53326
C	-1.36598	-0.67997	0.96904
C	-1.87204	-0.01717	-0.15717
H	-1.55611	1.63015	-1.49119
H	0.56303	2.31088	-0.49203
H	1.40101	1.1669	1.5399
H	0.17357	-0.81379	2.41959
H	-1.94131	-1.47873	1.40965
O	3.13703	0.39978	-0.3154
C	2.15958	-0.22964	-0.14505
C	1.71767	-1.46683	-0.86369
H	1.57386	-2.26382	-0.14147
H	0.75689	-1.27895	-1.33075
H	2.45389	-1.75753	-1.60611
N	-3.04587	-0.44483	-0.76858
H	-3.6743	-0.94166	-0.16808
H	-3.52379	0.25932	-1.29597

E (au) = -440.608747
ZPVE (au) = 0.165952

Acetyl radical addition *ortho* to trifluoromethylbenzene **2, R=*o*-CF_3**

C	-1.91163	1.99349	-0.29467
C	-1.74888	0.86767	-1.06336
C	-0.59065	0.05814	-0.92507
C	0.46974	0.58136	-0.13711
C	0.29205	1.71139	0.62845
C	-0.90536	2.41533	0.57459
H	-2.81443	2.57322	-0.38532
H	-2.51731	0.5613	-1.75117
H	-0.35264	-0.63707	-1.71135
H	1.09685	2.06384	1.24833
H	-1.03395	3.30371	1.16634
O	-1.95144	-2.37997	-0.55046
C	-1.43868	-1.57068	0.11767
C	-1.46588	-1.38596	1.599
H	-0.45607	-1.50621	1.97457
H	-1.78705	-0.37557	1.82523
H	-2.12934	-2.11294	2.05512
C	1.75406	-0.16951	-0.10245

F	2.72005	0.49288	0.52519
F	2.19845	-0.46038	-1.32425
F	1.62337	-1.34783	0.53236

E (au) = -722.289012
ZPVE (au) = 0.154633

Acetyl radical addition *meta* to trifluoromethylbenzene **2, R=*m*-CF_3**

C	0.65116	2.11566	-0.60197
C	1.61762	1.68488	0.27451
C	1.42418	0.50098	1.03968
C	0.12341	-0.06644	1.04182
C	-0.82321	0.37601	0.1506
C	-0.5707	1.45459	-0.69768
H	0.82739	2.99046	-1.20402
H	2.54983	2.21571	0.35886
H	2.05561	0.34048	1.89646
H	-0.10779	-0.87079	1.71695
H	-1.32989	1.79706	-1.37625
O	3.7871	-0.82647	0.28834
C	2.65794	-0.82377	-0.01622
C	1.98295	-1.45843	-1.18824
H	1.19847	-2.11877	-0.83473
H	1.50739	-0.68327	-1.77943
H	2.70309	-2.00681	-1.78571
C	-2.13377	-0.33715	0.0551
F	-2.47532	-0.92567	1.1984
F	-3.12844	0.4778	-0.28556
F	-2.09384	-1.29994	-0.87333

E (au) = -722.285813
ZPVE (au) = 0.154257

Acetyl radical addition para to trifluoromethylbenzene **2, R=*p*-CF_3**

C	0.22244	-0.93371	-0.90165
C	-1.0546	-1.37963	-0.67255
C	-1.72108	-1.07202	0.54487
C	-0.94651	-0.49356	1.58555
C	0.33001	-0.05531	1.34509
C	0.917	-0.24453	0.09267
H	0.70132	-1.1295	-1.84468
H	-1.57887	-1.92872	-1.4349
H	-2.59479	-1.64401	0.80571
H	-1.38186	-0.36864	2.5619
H	0.89351	0.4233	2.12678
O	-4.05962	0.03284	-0.57511
C	-3.03735	0.41397	-0.15578
C	-2.42178	1.77316	-0.22164
H	-2.29913	2.14893	0.78872
H	-1.43384	1.69549	-0.66107
H	-3.04961	2.44276	-0.7995
C	2.32312	0.18718	-0.13923
F	2.56421	0.4343	-1.42663
F	3.20829	-0.73851	0.24169
F	2.62225	1.2958	0.53983

E (au) =-722.286480
ZPVE (au) = 0.154398

Transition structure **7**

C	1.85654	1.02638	0.3349
C	1.54663	-0.47233	0.10718
C	0.03594	-0.65966	0.08434
C	-0.74519	0.10203	1.00979
C	-0.49852	1.84725	-0.06644
C	0.9604	1.96916	-0.45101
H	-0.07729	-1.96838	-1.59351
H	1.76214	1.26257	1.39147
C	-0.63033	-1.43278	-0.84319
C	-2.14157	-0.12669	1.08673
H	1.23154	3.00644	-0.26753
C	-2.76671	-0.90778	0.14952
C	-2.01824	-1.55408	-0.83058
H	-2.7117	0.36528	1.85521
H	-3.83532	-1.03574	0.18038
H	-2.50617	-2.16762	-1.56756
H	2.89566	1.21267	0.07919
H	1.03275	1.81281	-1.52542
O	-1.41778	2.38366	-0.55499
C	2.20677	-0.92552	-1.19578
H	3.27725	-0.74908	-1.14548
H	2.06265	-1.98692	-1.3686
H	1.81752	-0.39221	-2.05797
C	2.15084	-1.27764	1.26461
H	3.22035	-1.09398	1.34099
H	1.69581	-1.00816	2.21283
H	1.99927	-2.34178	1.11288
H	-0.26154	0.48475	1.89253

Benchmarking – archive details

HF/6-311G(d,p)


```
1\1\GINC-R1I1N4\FTS\UHF\6-311G(d,p)\C8H9O1(2)\RIJAMOS\17-May-2010\0\\#
 uHF/6-311g(d,p) opt=(ts,readfc,noeigentest)\\Addition of acetyl radica
 l to benzene\\0,2\C,1.62628,1.07287,0.724325\C,0.536563,1.405659,-0.06
 7132\C,-0.046365,0.437073,-0.957885\C,0.687879,-0.78191,-1.164554\C,1.
 777454,-1.096783,-0.36526\C,2.244455,-0.184866,0.598811\H,2.020701,1.7
 93045,1.419469\H,0.086581,2.379337,0.011871\H,-0.651279,0.806067,-1.76
 6965\H,0.359887,-1.469486,-1.924469\H,2.287873,-2.03389,-0.502704\H,3.
 093971,-0.432442,1.209264\O,-2.770695,0.53144,-0.307715\C,-1.82034,-0.
 056086,0.027795\C,-1.688672,-1.038552,1.160539\H,-1.443342,-2.012911,0
 .752816\H,-0.873932,-0.736201,1.807185\H,-2.618425,-1.089472,1.715416\
 \Version=EM64L-G09RevA.02\State=2-A\HF=-383.0726335\S2=1.389065\S2-1=0
 .\S2A=1.135941\RMSD=8.605e-09\RMSF=2.723e-06\Dipole=0.6762611,-0.60239
 22,0.459506\Quadrupole=-4.8815307,3.1095144,1.7720163,1.8377595,0.1502
 19,1.3356796\PG=C01 [X(C8H9O1)]\\@
```


B3LYP/6-311G(d,p)


```
1\1\GINC-R1I3N5\FTS\UB3LYP\6-311G(d,p)\C8H9O1(2)\RIJAMOS\11-May-2010\0
 \\#ub3lyp/6-311g(d,p) opt=(ts,readfc)\\Addition of acetyl radical to b
 enzene\\0,2\C,-1.5236212847,1.108585838,-0.7333080143\C,-0.4601838114,
 1.3978665173,0.1029335176\C,0.0453153656,0.4079646058,1.0071949084\C,-
 0.7337188468,-0.7813001205,1.173589888\C,-1.795778402,-1.0499438249,0.
 33130139\C,-2.1880738748,-0.1234750258,-0.6479817926\H,-1.8652953525,1
 .8548377821,-1.4429748078\H,0.0311558231,2.3628012748,0.0500518998\H,0
```

.6634102138,0.7423971025,1.833752079\H,-0.461030167,-1.4887876727,1.94
91925006\H,-2.3510655902,-1.9751791467,0.4457952401\H,-3.0266923207,-0
.3389338038,-1.2993135036\O,2.747688149,0.5993268636,0.1843137766\C,1.
809380005,-0.0970415889,-0.00814678\C,1.6027541755,-1.1280695085,-1.08
24648011\H,1.4143058713,-2.0964578681,-0.6126520494\H,0.7093940838,-0.
8710166163,-1.6556232004\H,2.4781539629,-1.1843168077,-1.7340022511\\V
ersion=EM64L-G09RevA.02\State=2-A\HF=-385.5173945\S2=0.777861\S2-1=0.\
S2A=0.750529\RMSD=9.848e-09\RMSF=3.839e-06\Dipole=-0.3405742,-0.604466
,-0.3655605\Quadrupole=-3.9141139,2.5134052,1.4007087,-1.6621455,0.663
5859,-1.0293108\PG=C01 [X(C8H9O1)]\\@

QCISD/6-311G(d,p)//BHandHLYP/6-311G(d,p)

1\1\GINC-R1I2N2\SP\UQCISD-FC\6-311G(d,p)\C8H9O1(2)\RIJAMOS\07-May-2010
\0\\#QCISD/6-311g(d,p)\\Addition of acetyl radical to benzene\\0,2\C,0
,-1.516585,1.100536,-0.730626\C,0,-0.461906,1.392441,0.101422\C,0,0.03
9363,0.412322,1.003129\C,0,-0.729122,-0.772252,1.169233\C,0,-1.782622,
-1.044321,0.330626\C,0,-2.174007,-0.125754,-0.643581\H,0,-1.856061,1.8
38298,-1.438213\H,0,0.024725,2.350962,0.046823\H,0,0.662099,0.743198,1
.816944\H,0,-0.456115,-1.473287,1.939708\H,0,-2.330006,-1.965224,0.443
616\H,0,-3.004838,-0.343233,-1.291412\O,0,2.731501,0.565726,0.206832\C
,0,1.79302,-0.101916,-0.008609\C,0,1.588536,-1.120923,-1.083491\H,0,1.
404573,-2.084942,-0.620851\H,0,0.702994,-0.861491,-1.652828\H,0,2.4605
49,-1.170882,-1.727064\\Version=EM64L-G09RevA.02\State=2-A\HF=-383.071
1829\MP2=-384.3245843\MP3=-384.3762986\MP4D=-384.4071739\MP4DQ=-384.37
92338\PUHF=-383.1137866\PMP2-0=-384.3630204\PMP3-0=-384.4076817\MP4SDQ
=-384.4000728\QCISD=-384.4155622\S2=1.339202\S2-1=1.188035\S2A=1.07131
6\RMSD=8.783e-09\PG=C01 [X(C8H9O1)]\\@

CCSD)(T)/6-311G(d,p)//BHandHLYP/6-311G(d,p)

1\1\GINC-R1I2N11\SP\UCCSD(T)-FC\6-311G(d,p)\C8H9O1(2)\RIJAMOS\12-May-2
010\0\\#CCSD(t)/6-311g(d,p)\\Addition of acetyl radical to benzene\\0,
2\C,0,-1.516585,1.100536,-0.730626\C,0,-0.461906,1.392441,0.101422\C,0
,0.039363,0.412322,1.003129\C,0,-0.729122,-0.772252,1.169233\C,0,-1.78
2622,-1.044321,0.330626\C,0,-2.174007,-0.125754,-0.643581\H,0,-1.85606
1,1.838298,-1.438213\H,0,0.024725,2.350962,0.046823\H,0,0.662099,0.743
198,1.816944\H,0,-0.456115,-1.473287,1.939708\H,0,-2.330006,-1.965224,
0.443616\H,0,-3.004838,-0.343233,-1.291412\O,0,2.731501,0.565726,0.206
832\C,0,1.79302,-0.101916,-0.008609\C,0,1.588536,-1.120923,-1.083491\H
,0,1.404573,-2.084942,-0.620851\H,0,0.702994,-0.861491,-1.652828\H,0,2
.460549,-1.170882,-1.727064\\Version=EM64L-G09RevA.02\State=2-A\HF=-38
3.0711829\MP2=-384.3245843\MP3=-384.3762986\MP4D=-384.4071739\MP4DQ=-3
84.3792338\PUHF=-383.1137866\PMP2-0=-384.3630204\PMP3-0=-384.4076817\M
P4SDQ=-384.4000728\CCSD=-384.4119092\CCSD(T)=-384.4730904\S2=1.339202\
S2-1=1.188035\S2A=1.071316\RMSD=8.783e-09\PG=C01 [X(C8H9O1)]\\@

CCSD(T)/6-311+G(d,p)//BHandHLYP/6-311G(d,p)

1\1\GINC-R1I2N9\SP\UCCSD(T)-FC\6-311+G(d,p)\C8H9O1(2)\RIJAMOS\12-May-2
010\0\\#CCSD(t)/6-311+g(d,p)\\Addition of acetyl radical to benzene\\0
,2\C,0,-1.516585,1.100536,-0.730626\C,0,-0.461906,1.392441,0.101422\C,
0,0.039363,0.412322,1.003129\C,0,-0.729122,-0.772252,1.169233\C,0,-1.7
82622,-1.044321,0.330626\C,0,-2.174007,-0.125754,-0.643581\H,0,-1.8560
61,1.838298,-1.438213\H,0,0.024725,2.350962,0.046823\H,0,0.662099,0.74
3198,1.816944\H,0,-0.456115,-1.473287,1.939708\H,0,-2.330006,-1.965224
,0.443616\H,0,-3.004838,-0.343233,-1.291412\O,0,2.731501,0.565726,0.20
6832\C,0,1.79302,-0.101916,-0.008609\C,0,1.588536,-1.120923,-1.083491\
H,0,1.404573,-2.084942,-0.620851\H,0,0.702994,-0.861491,-1.652828\H,0,
2.460549,-1.170882,-1.727064\\Version=EM64L-G09RevA.02\State=2-A\HF=-3
83.0764854\MP2=-384.3379899\MP3=-384.3884377\MP4D=-384.4196696\MP4DQ=-
384.3911705\PUHF=-383.1182583\PMP2-0=-384.3756328\PMP3-0=-384.4190723\
MP4SDQ=-384.412322\CCSD=-384.4237328\CCSD(T)=-384.4861663\S2=1.32935\S

2-1=1.179878\S2A=1.059299\RMSD=4.946e-09\PG=C01 [X(C8H9O1)]\\@

Computational Details for Chapter 6

Geometries and energies for all compounds

2

B3LYP

C	-1.73578600	1.06071800	0.00016600
C	-0.36103800	1.29208700	-0.00033600
C	0.53400400	0.21426000	-0.00052200
C	0.04519800	-1.10112200	-0.00057300
C	-1.32643600	-1.33114400	0.00004500
H	-2.43010900	1.89629100	0.00069100
H	0.02526300	2.30945200	-0.00034200
H	0.75862500	-1.91965500	-0.00059900
H	-1.70793000	-2.34851000	0.00042500
C	1.99212700	0.46864900	-0.00001200
O	2.84764000	-0.39580000	0.00052200
C	-2.21682200	-0.25073900	0.00034700
H	-3.28821500	-0.43320800	0.00058900
H	2.27376500	1.54577000	0.00037900

E (au) = -345.6689742
ZPVE (au) = 0.110226
solvated E (au) = -345.676122

M05

C	1.735393	1.055834	-0.000216
C	0.363848	1.290781	0.000007
C	-0.532231	0.218312	0.000180
C	-0.047961	-1.094966	0.000243
C	1.320148	-1.330047	0.000057
H	2.431890	1.888667	0.000054
H	-0.017445	2.309402	0.000199
H	-0.765627	-1.909177	0.000170
H	1.698082	-2.347990	-0.000318
C	-1.990333	0.467869	-0.000011
O	-2.839765	-0.395810	-0.000251
C	2.211202	-0.254421	-0.000091
H	3.281538	-0.439646	0.000069
H	-2.270712	1.545054	0.000823

E (au) = -345.4003473
ZPVE (au) = 0.111029
solvated E (au) = -345.407471

B97D

C	-1.74117400	1.07048500	0.00018500
C	-0.35841000	1.29732900	0.00007700
C	0.53766300	0.20963900	-0.00004300
C	0.04117700	-1.11197900	-0.00005500
C	-1.33834400	-1.33738800	0.00005000
H	-2.43620400	1.91231100	0.00027800
H	0.03825800	2.31646100	0.00008500
H	0.75701100	-1.93532800	-0.00014800
H	-1.72671700	-2.35776800	0.00003700

C	1.99980700	0.46801100	-0.00015700
O	2.86724600	-0.39527000	-0.00022200
C	-2.22965500	-0.24688700	0.00017100
H	-3.30689700	-0.42613300	0.00025600
H	2.27018900	1.55735200	-0.00010600

E (au) = -345.4173361
ZPVE (au) = 0.107156

ωB97XD

C	-1.73137000	1.05752700	0.00018100
C	-0.35995500	1.28866800	0.00008500
C	0.53033100	0.21405000	-0.00003100
C	0.04602800	-1.09737200	-0.00004400
C	-1.32227100	-1.32752400	0.00005100
H	-2.42603400	1.89173300	0.00026400
H	0.02501400	2.30625300	0.00010000
H	0.75978200	-1.91533300	-0.00013100
H	-1.70378300	-2.34403600	0.00003300
C	1.98961700	0.46832500	-0.00014600
O	2.83698900	-0.39604900	-0.00024500
C	-2.20994200	-0.25035100	0.00016500
H	-3.28058300	-0.43299100	0.00024400
H	2.27505700	1.54284000	-0.00011800

E (au) = -345.5402255
ZPVE (au) = 0.111412

MP2

C	-1.73926100	1.05537800	0.00016300
C	-0.36493400	1.29545400	0.00009900
C	0.53027100	0.21972900	0.00000000
C	0.05355200	-1.09804100	-0.00002600
C	-1.31845200	-1.33277300	0.00003900
H	-2.43825200	1.88799400	0.00025100
H	0.01549500	2.31616200	0.00011600
H	0.77182900	-1.91399900	-0.00010400
H	-1.69522000	-2.35264500	0.00002900
C	1.98733700	0.47817900	-0.00005500
O	2.84446400	-0.40023800	-0.00030500
C	-2.21536300	-0.25788100	0.00014400
H	-3.28645800	-0.44568200	0.00019700
H	2.27799700	1.54980200	-0.00023000

E (au) = -344.6655868
ZPVE (au) = 0.109983

3

B3LYP

C	2.04683900	-1.36452500	-0.00003600
C	0.66566700	-1.17875700	-0.00003500
C	0.13796200	0.12435900	-0.00004300
C	1.00483500	1.23256500	0.00003400
C	2.38038200	1.03885300	0.00008700
H	2.45621900	-2.37053700	-0.00009300
H	-0.01019700	-2.02539800	-0.00010600
H	0.57742500	2.23012900	0.00006400
H	3.04999400	1.89413400	0.00013200
C	-1.31159000	0.36513000	-0.00009400
O	-1.84733500	1.45478900	-0.00010400
N	-2.15315400	-0.89596800	0.00000500

N	-3.37268100	-0.68337300	0.00014200
H	-3.54877800	0.35640200	0.00013300
C	2.90197700	-0.26056300	0.00002700
H	3.97843900	-0.41001800	0.00003300

E (au) = -455.1518773
ZPVE (au) = 0.120169
solvated E (au) = -455.159334

M05

C	2.047386	-1.360226	0.000039
C	0.668589	-1.177746	-0.000105
C	0.138226	0.120570	-0.000115
C	1.000525	1.227691	0.000014
C	2.374275	1.038932	0.000157
H	2.458626	-2.364697	0.000050
H	-0.003629	-2.027327	-0.000205
H	0.571863	2.224232	0.000005
H	3.041028	1.895646	0.000260
C	-1.309429	0.363921	-0.000269
O	-1.843149	1.448722	-0.000189
N	-2.155131	-0.897646	-0.000274
N	-3.368393	-0.676186	0.000428
H	-3.534166	0.360688	0.000719
C	2.897508	-0.256170	0.000168
H	3.973660	-0.403324	0.000277

E (au) = -454.8216673
ZPVE (au) = 0.120822
solvated E (au) = -454.828922

B97D

C	2.05626800	-1.37565800	-0.00003700
C	0.66862800	-1.18552300	-0.00004000
C	0.13895200	0.12722700	0.00000200
C	1.01662800	1.23873800	0.00004500
C	2.39857700	1.03990400	0.00004700
H	2.46465400	-2.38765900	-0.00006800
H	-0.01032200	-2.03612100	-0.00007200
H	0.59010600	2.24222300	0.00007700
H	3.07370400	1.89748700	0.00008100
C	-1.31383200	0.37735800	0.00000300
O	-1.84860700	1.47570800	0.00003100
N	-2.17780900	-0.90556900	-0.00005600
N	-3.40148400	-0.69161300	-0.00002000
H	-3.58692200	0.35693700	0.00009000
C	2.92002800	-0.26819100	0.00000700
H	4.00119200	-0.42138600	0.00000900

E (au) = -454.8312904
ZPVE (au) = 0.116228

ωB97XD

C	-2.04589600	-1.35793700	0.00016300
C	-0.66734300	-1.17780100	0.00004500
C	-0.13933300	0.11874900	-0.00004300
C	-0.99652900	1.22713800	-0.00000100
C	-2.36987500	1.03957200	0.00011800
H	-2.45944800	-2.36138100	0.00023300
H	0.00370800	-2.02858400	0.00002900
H	-0.56634800	2.22328900	-0.00007300

H	-3.03591900	1.89662400	0.00014700
C	1.31132600	0.35798100	-0.00020200
O	1.84106000	1.44415700	-0.00028500
N	2.14840100	-0.89155700	-0.00036100
N	3.36249200	-0.67529000	0.00022000
H	3.53357600	0.36044300	0.00095900
C	-2.89402700	-0.25369100	0.00020100
H	-3.97023800	-0.39978300	0.00029700

E (au) = -454.9852374
ZPVE (au) = 0.121862

MP2

C	2.04890800	-1.36085500	0.00000200
C	0.66551600	-1.18283900	-0.00002400
C	0.14181000	0.11970000	-0.00000200
C	0.99887700	1.23219500	0.00004800
C	2.37646100	1.04022100	0.00007500
H	2.46173600	-2.36637200	-0.00001500
H	-0.00614900	-2.03457600	-0.00005900
H	0.56803600	2.22991600	0.00006400
H	3.04336900	1.89860700	0.00011400
C	-1.30811300	0.35970000	-0.00003500
O	-1.84570700	1.45709400	-0.00006200
N	-2.14615400	-0.90154900	-0.00014700
N	-3.38260800	-0.67789900	0.00004500
H	-3.54249300	0.36337900	0.00034000
C	2.90347400	-0.25614800	0.00005200
H	3.98088900	-0.40341800	0.00007400

E (au) = -453.8790143
ZPVE (au) = 0.119592

6

B3LYP

C	-2.42793100	0.99044900	0.00010300
C	-1.05911900	1.23312100	0.00009300
C	-0.15428900	0.15743700	0.00000400
C	-0.63612700	-1.16117900	-0.00007700
C	-2.00941800	-1.39819400	-0.00006700
H	-3.12685100	1.82199700	0.00017200
H	-0.66648400	2.24502500	0.00015400
H	0.06341000	-1.98905300	-0.00014700
H	-2.38214900	-2.41838600	-0.00013000
C	1.28716000	0.45521300	-0.00000900
O	1.81469700	1.53264800	0.00003800
C	-2.90367900	-0.32548800	0.00002200
H	-3.97397800	-0.51346500	0.00003000
N	2.24009500	-0.78618200	-0.00008000
N	3.49668200	-0.55383600	-0.00003800
H	2.83145300	-1.73533300	0.00002000

E (au) = -455.0364992
ZPVE (au) = 0.113658
solvated E (au) = -455.048566

M05

C	2.42797200	0.98805000	0.00016300
C	1.06166800	1.23047300	-0.00003800
C	0.15837800	0.15792200	-0.00018800
C	0.63799100	-1.15782000	-0.00016600

C	2.00819200	-1.39585100	0.00002200
H	3.12700300	1.81859200	0.00029300
H	0.66926800	2.24210400	-0.00006800
H	-0.06167100	-1.98532500	-0.00031900
H	2.38042300	-2.41550200	0.00002400
C	-1.27947400	0.45843900	-0.00034800
O	-1.81411900	1.52611600	-0.00058700
C	2.90075800	-0.32543500	0.00019500
H	3.97028100	-0.51427700	0.00035000
N	-2.25282200	-0.79631500	-0.00015300
N	-3.49532500	-0.54124500	0.00099300
H	-2.82824200	-1.72628100	0.00070100

E (au) = -454.7121498
ZPVE (au) = 0.114633
solvated E (au) = -454.724142

B97D

C	-2.31692900	0.92840900	0.36139600
C	-0.96093200	1.24860400	0.25755500
C	-0.02473200	0.26128000	-0.13090900
C	-0.46792400	-1.04919500	-0.42391100
C	-1.83079900	-1.35979800	-0.32309500
H	-3.03655400	1.69277500	0.66040300
H	-0.60070600	2.25516400	0.47346300
H	0.23834600	-1.80776000	-0.75274600
H	-2.17285300	-2.36955600	-0.55603500
C	1.39766700	0.66473700	-0.20582800
O	1.84178700	1.78260100	-0.34520400
C	-2.75250000	-0.37849500	0.07427200
H	-3.81236800	-0.62848800	0.15455300
N	2.46468500	-0.50326800	-0.02123600
N	2.24922900	-1.52092700	0.73536100
H	3.38934000	-1.12682500	0.12623500

E (au) = -454.7205989
ZPVE (au) = 0.109861

ωB97XD

C	-2.42793100	0.99044900	0.00010300
C	-1.05911900	1.23312100	0.00009300
C	-0.15428900	0.15743700	0.00000400
C	-0.63612700	-1.16117900	-0.00007700
C	-2.00941800	-1.39819400	-0.00006700
H	-3.12685100	1.82199700	0.00017200
H	-0.66648400	2.24502500	0.00015400
H	0.06341000	-1.98905300	-0.00014700
H	-2.38214900	-2.41838600	-0.00013000
C	1.28716000	0.45521300	-0.00000900
O	1.81469700	1.53264800	0.00003800
C	-2.90367900	-0.32548800	0.00002200
H	-3.97397800	-0.51346500	0.00003000
N	2.24009500	-0.78618200	-0.00008000
N	3.49668200	-0.55383600	-0.00003800
H	2.83145300	-1.73533300	0.00002000

E (au) = -454.8664708
ZPVE (au) = 0.115619

MP2

C	2.43136800	0.98918500	0.00024500

C	1.06209300	1.23723600	0.00012700
C	0.16185900	0.16042000	-0.00011100
C	0.63342000	-1.16008500	-0.00023400
C	2.00784400	-1.39684600	-0.00013300
H	3.13228400	1.82001800	0.00044000
H	0.67046300	2.25116600	0.00021200
H	-0.06673900	-1.98921000	-0.00042100
H	2.37945800	-2.41830000	-0.00023600
C	-1.27714800	0.45669000	-0.00020100
O	-1.82742300	1.52961500	-0.00036700
C	2.90586400	-0.32703000	0.00011700
H	3.97630800	-0.51770700	0.00020400
N	-2.24731700	-0.79152300	0.00011600
N	-3.50162800	-0.54997700	0.00043600
H	-2.78157900	-1.74980700	0.00001400

E (au) = -453.7593334
ZPVE (au) = 0.114175

7

B3LYP

C	1.28202600	1.34847400	0.00007500
C	-0.07838300	1.06350700	0.00001600
C	-0.51480700	-0.27313300	-0.00004500
C	0.42337200	-1.31631400	-0.00005000
C	1.78704400	-1.02964400	0.00001500
C	2.21314800	0.30137600	0.00007600
H	1.62643900	2.37923900	0.00012400
H	-0.82501100	1.85298400	0.00001900
H	0.06200700	-2.34093100	-0.00010000
H	2.51639300	-1.83478700	0.00001600
H	3.27653300	0.52698800	0.00012400
C	-1.94427000	-0.60670100	-0.00009400
O	-2.80786400	0.39934700	-0.00003500
H	-3.20222200	-0.70365100	0.00013900

E (au) = -345.5365686
ZPVE (au) = 0.104174
solvated E (au) = -345.541770

M05

C	1.27742100	1.34611700	0.00006000
C	-0.08000900	1.05875600	0.00002700
C	-0.51375500	-0.27428000	-0.00002100
C	0.42321600	-1.31389100	-0.00003600
C	1.78401200	-1.02636100	-0.00000300
C	2.20723700	0.30238900	0.00004500
H	1.62039200	2.37671500	0.00009800
H	-0.82731400	1.84691300	0.00003800
H	0.06408800	-2.33875400	-0.00007400
H	2.51349600	-1.83039700	-0.00001500
H	3.26989800	0.52870500	0.00007200
C	-1.94506200	-0.60410000	-0.00005100
O	-2.79820400	0.39909100	-0.00002800
H	-3.17329200	-0.70770100	-0.00001400

E (au) = -345.2718217
ZPVE (au) = 0.105108
solvated E (au) = -345.276852

B97D

C	-1.29490100	1.35487500	-0.00004600
C	0.07345200	1.07393300	-0.00003500
C	0.51976000	-0.26956100	0.00000200
C	-0.42232200	-1.32189500	0.00002800
C	-1.79405800	-1.03866400	0.00001700
C	-2.22784600	0.29836200	-0.00002000
H	-1.64543200	2.38927100	-0.00007500
H	0.81952700	1.87119600	-0.00005300
H	-0.05476900	-2.35008700	0.00005600
H	-2.52439900	-1.85004200	0.00003700
H	-3.29712300	0.52129900	-0.00002800
C	1.95182800	-0.61423200	0.00002200
O	2.83047100	0.40241700	0.00001400
H	3.22295000	-0.69788300	0.00014000

E (au) = -345.2902413
ZPVE (au) = 0.101276

ωB97XD

C	-1.27747700	1.34447700	-0.00004500
C	0.07991900	1.05952300	-0.00005100
C	0.51132300	-0.27266000	-0.00002000
C	-0.42124900	-1.31303100	0.00001400
C	-1.78171100	-1.02665000	0.00002400
C	-2.20544100	0.30082500	-0.00000500
H	-1.62102700	2.37460100	-0.00006600
H	0.82567500	1.84944600	-0.00007400
H	-0.06122500	-2.33778400	0.00003500
H	-2.51113600	-1.83052500	0.00005600
H	-3.26822200	0.52584700	0.00000700
C	1.94329600	-0.60255100	-0.00000100
O	2.79407800	0.39758200	0.00004300
H	3.19134500	-0.70184300	0.00019900

E (au) = -345.4068998
ZPVE (au) = 0.105444

MP2

C	-1.27334900	1.34869600	-0.00004200
C	0.08803800	1.06027000	-0.00001200
C	0.51102000	-0.27744900	0.00003000
C	-0.42494100	-1.31928400	0.00004600
C	-1.78788000	-1.02435200	0.00001000
C	-2.21063200	0.30786600	-0.00003200
H	-1.61297000	2.38176600	-0.00007300
H	0.83676300	1.84979900	-0.00002300
H	-0.06705300	-2.34640800	0.00008200
H	-2.52140400	-1.82675800	0.00001800
H	-3.27360400	0.53824600	-0.00005700
C	1.94178000	-0.62162100	0.00006200
O	2.79413300	0.40421100	-0.00005300
H	3.22098600	-0.67509100	0.00010700

E (au) = -344.5326175
ZPVE (au) = 0.104032

9

B3LYP

C	5.66503000	-1.18036800	0.06925800
C	4.40178500	-1.75916100	0.19046600
C	3.24378700	-0.99943200	0.00273800

C	3.33915000	0.36787900	-0.30622700
C	4.61755900	0.94005900	-0.42273900
C	5.76841800	0.17859800	-0.23998100
H	6.56142600	-1.78057300	0.21503800
H	4.30800300	-2.81542600	0.43377700
H	2.26635500	-1.45586300	0.08759300
H	4.66981600	1.99794400	-0.65655300
H	6.74733700	0.64452000	-0.33687400
C	2.18943500	1.33203400	-0.51425500
O	2.43458200	2.53141300	-0.73098900
N	0.89733800	0.92100100	-0.47080200
N	0.42438300	-0.40395200	-0.47919100
H	0.23060900	1.67090200	-0.63075600
O	-0.68863400	0.22028600	1.83992400
S	-0.59646400	-0.74538500	0.72336100
O	-0.45923200	-2.18516500	1.04022400
C	-2.29303200	-0.72270700	-0.03163100
C	-2.76961200	-1.93991000	-0.53746000
C	-3.17208200	0.36630300	-0.07879900
C	-4.04832200	-2.06081600	-1.07422400
H	-2.10944200	-2.79695500	-0.46542400
C	-4.47513700	0.25226800	-0.57268900
C	-4.91189400	-0.96187200	-1.08896300
H	-4.38004900	-3.02038100	-1.46373500
H	-5.12079000	1.12326900	-0.55135800
H	-5.91789200	-1.04968400	-1.49042200
N	-2.80145700	1.72424300	0.35655800
O	-1.75726500	2.20787400	-0.07114300
O	-3.61499200	2.33085600	1.05523700

E (au) = -1440.159244
ZPVE (au) = 0.22433
solvated E (au) = -1440.240936

M05

C	5.398727	-0.976139	0.600684
C	4.169747	-1.095877	1.247017
C	3.053375	-0.405782	0.779128
C	3.162525	0.425052	-0.340255
C	4.406594	0.568260	-0.961360
C	5.515758	-0.138237	-0.507574
H	6.263495	-1.527057	0.963459
H	4.074152	-1.734265	2.121392
H	2.104204	-0.492105	1.294966
H	4.484161	1.252084	-1.800616
H	6.473724	-0.027317	-1.010510
C	2.040409	1.278341	-0.861948
O	2.270511	2.418108	-1.272465
N	0.781226	0.771437	-0.872995
N	0.443073	-0.582035	-0.864930
H	0.105367	1.425969	-1.250191
O	-0.367454	-0.249580	1.608841
S	-0.500215	-1.007018	0.354172
O	-0.493566	-2.471045	0.422767
C	-2.250808	-0.683525	-0.151717
C	-2.894179	-1.699811	-0.865227
C	-3.011245	0.441960	0.160820
C	-4.222751	-1.589642	-1.257372
H	-2.321467	-2.596416	-1.076411
C	-4.357903	0.554203	-0.182567
C	-4.963584	-0.459860	-0.911581

H	-4.689169	-2.396904	-1.815894
H	-4.908832	1.437778	0.122196
H	-6.007689	-0.371231	-1.197526
N	-2.456341	1.624661	0.858555
O	-1.531144	2.204909	0.328454
O	-3.032122	1.988813	1.868614

E (au) = -1439.492331
ZPVE (au) = 0.226953
solvated E (au) = -1439.576696

B97D

C	5.57425700	-1.32838400	-0.16762100
C	4.34961700	-1.71088000	0.40265500
C	3.23445200	-0.85996600	0.34774200
C	3.33596800	0.40587900	-0.27208900
C	4.57907800	0.78908900	-0.82254200
C	5.68408100	-0.07050600	-0.78355400
H	6.43536000	-2.00214400	-0.13044300
H	4.25412500	-2.68355300	0.89265500
H	2.28571600	-1.18095500	0.77021900
H	4.65362800	1.78079800	-1.27017800
H	6.63342000	0.24281300	-1.22777400
C	2.24005500	1.45308100	-0.31958000
O	2.52958200	2.65796100	-0.48096000
N	0.93241200	1.08103400	-0.18050600
N	0.42804200	-0.22301300	-0.28753300
H	0.27017600	1.86038300	-0.19184300
O	-0.86469200	0.45777800	1.94772300
S	-0.62348800	-0.59152700	0.91657200
O	-0.37993000	-1.99277800	1.37191400
C	-2.22186900	-0.75847000	-0.01321800
C	-2.54387200	-2.03864300	-0.51011500
C	-3.17717800	0.26419800	-0.20521500
C	-3.75085300	-2.28928400	-1.17001400
H	-1.82679500	-2.84035600	-0.33586200
C	-4.41551100	0.01157000	-0.82452300
C	-4.69973700	-1.26106900	-1.32382400
H	-3.96302100	-3.29300100	-1.54661500
H	-5.12855200	0.83055300	-0.91711100
H	-5.65213600	-1.44911800	-1.82407200
N	-2.95297800	1.67574700	0.17137900
O	-1.89688300	2.21293300	-0.18432000
O	-3.88424900	2.26697300	0.74112700

E (au) = -1439.482295
ZPVE (au) = 0.217324

ωB97XD

S	-1.22260100	-1.50947800	-0.67684100
O	1.10780900	0.17092700	2.00905200
O	-0.45939400	-1.63492100	-1.93746500
O	-2.54076900	-2.13190100	-0.61405100
O	-3.20641400	-0.59027900	1.73184500
O	-4.77029500	0.37278500	0.58211700
N	0.95135600	-1.45886500	0.39249400
N	-0.36523400	-1.89662300	0.61699400
N	-3.59449200	0.13894200	0.84512400
C	3.88765500	0.36837900	1.41415900
H	3.59216000	0.49298700	2.45117800
C	5.16236300	0.70946300	0.97797400

H	5.89426800	1.08829800	1.68682200
C	5.50064300	0.57173800	-0.36750000
H	6.49581700	0.84204100	-0.71140900
C	4.55402400	0.09809200	-1.27107800
H	4.80263800	0.00634700	-2.32505100
C	3.27977300	-0.25245300	-0.83071900
H	2.53743700	-0.59531700	-1.54773600
C	2.94155400	-0.13370500	0.51981900
C	1.55862500	-0.45141000	1.05624100
C	-1.53726000	0.29032000	-0.60546600
C	-0.63890700	1.13041800	-1.26461700
H	0.16256300	0.66765700	-1.82855900
C	-0.77741200	2.51267700	-1.22973400
H	-0.05150000	3.13891700	-1.74057200
C	-1.85078500	3.08969700	-0.55889400
H	-1.97751600	4.16800300	-0.53720400
C	-2.77357500	2.27308400	0.08057200
H	-3.63513500	2.68835500	0.59156600
C	-2.59142400	0.89536600	0.07556700
H	1.46033100	-1.93271200	-0.34179400

E (au) = -1439.780253
ZPVE (au) = 0.228265

MP2

C	-3.95728100	0.27569000	-0.41015700
C	-3.41378000	-0.95640400	-0.78472500
C	-2.28811200	-1.46711900	-0.13544300
C	-1.69314900	-0.73367700	0.90218200
C	-2.25780100	0.48628900	1.29752500
C	-3.37055800	0.99876900	0.63162800
H	-4.83049600	0.66990400	-0.92786500
H	-3.87440700	-1.53001400	-1.58748500
H	-1.83798300	-2.40241800	-0.44994700
H	-1.80359700	1.01674400	2.13019600
H	-3.79027300	1.95656100	0.93532000
C	-0.52640500	-1.21250700	1.72074400
O	-0.47892600	-0.96842000	2.94048700
N	0.45431700	-1.90924400	1.09461300
N	0.49551700	-2.25353300	-0.27796800
H	1.26493300	-2.11847100	1.67651600
O	1.47970800	-1.60806500	-2.46874700
S	1.51544500	-1.26966600	-1.03351700
O	2.83455700	-1.08866700	-0.38413900
C	0.76621800	0.38693000	-0.93762200
C	-0.31898200	0.63597000	-1.78965000
C	1.12663200	1.39704900	-0.04722900
C	-1.00208100	1.84824500	-1.75798700
H	-0.59444100	-0.14255800	-2.49578900
C	0.47271900	2.63135700	-0.01523000
C	-0.61314300	2.84653600	-0.85839500
H	-1.84811900	2.01012900	-2.42173800
H	0.81346200	3.39630100	0.67819400
H	-1.14116500	3.79714400	-0.82654000
N	2.25072200	1.27609200	0.88751500
O	3.22899000	2.01491000	0.66826200
O	2.11634700	0.53091300	1.86944400

E (au) = -1436.860514
ZPVE (au) = 0.224916

10

B3LYP

C	-1.85153300	-1.41089900	0.00008600
C	-0.48543100	-1.13307500	0.00003300
C	-0.04977000	0.20478200	-0.00000900
C	-0.99816100	1.24671800	0.00000300
C	-2.35692700	0.95789300	0.00005600
C	-2.78566900	-0.37359600	0.00009800
H	-2.18638400	-2.44424700	0.00012100
H	0.24785600	-1.92917400	0.00002700
H	-0.64503400	2.27252100	-0.00003000
H	-3.08291500	1.76590200	0.00006400
H	-3.84863600	-0.60026600	0.00014000
C	1.36564800	0.62082800	-0.00006800
O	1.76530800	1.76387500	-0.00006900
N	2.50288100	-0.39714600	-0.00004800
N	2.49540300	-1.61058200	-0.00009300
H	3.37571800	0.20244900	0.00002100

E (au) = -455.1214026
ZPVE (au) = 0.119268
solvated E (au) = -455.129493

M05

C	1.84693400	-1.41019800	-0.00006900
C	0.48437000	-1.12978000	-0.00025000
C	0.05154100	0.20542800	-0.00029500
C	0.99987700	1.24279200	-0.00012000
C	2.35592100	0.95304500	0.00006200
C	2.78052800	-0.37632600	0.00008700
H	2.18003500	-2.44342100	-0.00004600
H	-0.24675900	-1.92726000	-0.00037200
H	0.64762200	2.26867300	-0.00014600
H	3.08258400	1.75945500	0.00018000
H	3.84252500	-0.60477200	0.00023200
C	-1.36025400	0.62583400	-0.00050200
O	-1.75881500	1.76360600	0.00040200
N	-2.50229900	-0.39833800	0.00005600
N	-2.50080700	-1.60628000	0.00034400
H	-3.36725800	0.20603900	0.00065800

E (au) = -454.7923243
ZPVE (au) = 0.119901
solvated E (au) = -454.800135

B97D

C	-1.83901400	-1.43528300	0.00010000
C	-0.47245400	-1.12630400	0.00000200
C	-0.06377800	0.22914500	-0.00005800
C	-1.04021700	1.25763500	-0.00001100
C	-2.39893600	0.93657300	0.00008200
C	-2.80055300	-0.41208700	0.00014200
H	-2.15368900	-2.48028600	0.00015100
H	0.28136300	-1.91033800	-0.00001000
H	-0.70829300	2.29606300	-0.00005800
H	-3.14677700	1.73157300	0.00011000
H	-3.86338600	-0.66282300	0.00022000
C	1.34861300	0.65535700	-0.00017200
O	1.76538300	1.79719700	-0.00009700
N	2.53719900	-0.41189700	-0.00004100

N	2.55780200	-1.61814500	0.00000000
H	3.40073900	0.22830600	0.00013100

E (au) = -454.8027206
ZPVE (au) = 0.115108

ωB97XD

C	-1.85464900	-1.40147100	0.00008100
C	-0.48996200	-1.13475500	0.00004300
C	-0.04727400	0.19511400	0.00000400
C	-0.98283600	1.24062900	0.00000400
C	-2.34096900	0.96369000	0.00003700
C	-2.77804700	-0.36029800	0.00007700
H	-2.19691800	-2.43158800	0.00011300
H	0.23496000	-1.93821400	0.00003600
H	-0.62293200	2.26401800	-0.00002400
H	-3.06016600	1.77655300	0.00003500
H	-3.84205900	-0.57847100	0.00010700
C	1.37135200	0.60972300	-0.00001500
O	1.76038900	1.75124500	0.00000000
N	2.49281100	-0.39072800	-0.00007700
N	2.47418400	-1.60446200	-0.00015800
H	3.36933800	0.18828900	-0.00000600

E (au) = -454.954203
ZPVE (au) = 0.121031

MP2

C	-1.85582300	-1.40582200	0.00003900
C	-0.48618100	-1.13960500	-0.00012800
C	-0.05141400	0.19709700	-0.00019400
C	-0.98877900	1.24641400	-0.00004200
C	-2.34981800	0.96220700	0.00012500
C	-2.78709600	-0.36607700	0.00017200
H	-2.19622400	-2.43816600	0.00008200
H	0.24103400	-1.94183100	-0.00023400
H	-0.63092400	2.27205800	-0.00008200
H	-3.07173400	1.77489200	0.00022100
H	-3.85159700	-0.58838000	0.00031300
C	1.36388100	0.61433300	-0.00035700
O	1.76794000	1.76494100	0.00001700
N	2.49901900	-0.39578000	0.00000900
N	2.49031800	-1.61153400	0.00023600
H	3.37194200	0.20181100	0.00015700

E (au) = -453.8355358
ZPVE (au) = 0.11937

CCSD(T)

C	-1.85153300	-1.41089900	0.00008600
C	-0.48543100	-1.13307500	0.00003300
C	-0.04977000	0.20478200	-0.00000900
C	-0.99816100	1.24671800	0.00000300
C	-2.35692700	0.95789300	0.00005600
C	-2.78566900	-0.37359600	0.00009800
H	-2.18638400	-2.44424700	0.00012100
H	0.24785600	-1.92917400	0.00002700
H	-0.64503400	2.27252100	-0.00003000
H	-3.08291500	1.76590200	0.00006400
H	-3.84863600	-0.60026600	0.00014000
C	1.36564800	0.62082800	-0.00006800

O	1.76530800	1.76387500	-0.00006900
N	2.50288100	-0.39714600	-0.00004800
N	2.49540300	-1.61058200	-0.00009300
H	3.37571800	0.20244900	0.00002100

E (au) singlet = -453.950713
E (au) triplet = -453.93573

11

B3LYP

C	-2.34892200	1.06994200	-0.09622300
C	-0.97322000	1.23645500	-0.02452700
C	-0.12968900	0.10289400	0.05720000
C	-0.70206500	-1.19037300	0.10614900
C	-2.08144700	-1.33828200	0.04236300
C	-2.90800400	-0.21398100	-0.06046800
H	-2.99381100	1.94092100	-0.17012500
H	-0.53068000	2.22675000	-0.05251400
H	-0.04924400	-2.04935900	0.21442400
H	-2.51827400	-2.33184300	0.08432500
H	-3.98678000	-0.33573900	-0.10015600
C	1.28522100	0.24989100	-0.00813800
O	1.91548700	1.35905400	0.18705500
N	2.20377500	-0.91587100	-0.02152100
N	3.37048900	-0.64218600	-0.18324800
H	2.88379700	1.08395200	-0.13714200

E (au) =-455.0895183
ZPVE (au) = 0.115418
solvated E (au) =-455.098192

M05

Not found at this level of theory

B97D

Not found at this level of theory

ωB97XD

C	-2.33334700	1.07133400	-0.09567700
C	-0.95829000	1.22819400	-0.02975200
C	-0.13120600	0.09441000	0.05397300
C	-0.70149900	-1.18881600	0.10432400
C	-2.08017000	-1.33075400	0.04128600
C	-2.89615700	-0.20538500	-0.05954200
H	-2.97282400	1.94528300	-0.16871000
H	-0.50930600	2.21531100	-0.06085400
H	-0.05271400	-2.05120600	0.21222200
H	-2.52232100	-2.32092100	0.08375500
H	-3.97482300	-0.32180200	-0.10126300
C	1.29410900	0.23686000	0.00252500
O	1.90507600	1.35436600	0.18970400
N	2.18290300	-0.89654600	-0.00973700
N	3.35566200	-0.65162600	-0.19682600
H	2.86078000	1.10055300	-0.13967200

E (au) =-454.9164103
ZPVE (au) = 0.117353
solvated E (au) =

MP2

Not found at this level of theory

12

B3LYP

C	2.33710300	0.97713500	-0.07603200
C	0.96287600	1.20755400	-0.07521200
C	0.06110500	0.13014600	0.00185900
C	0.57564500	-1.17938900	0.07407400
C	1.94935900	-1.39744900	0.06729100
C	2.84039900	-0.32261400	-0.00491300
H	3.01781300	1.82223100	-0.13864300
H	0.57588500	2.21832300	-0.15018400
H	-0.10174500	-2.02698900	0.13792000
H	2.32680500	-2.41511300	0.12264300
H	3.91233100	-0.49789900	-0.00728600
C	-1.36954600	0.40695700	0.01561100
O	-1.87868600	1.69277500	0.01175300
N	-2.25495300	-0.54885900	-0.03995600
N	-3.03186900	-1.39705000	-0.10193800
H	-1.83549000	2.04456100	0.91871200

E (au) =-455.1344065
ZPVE (au) = 0.118987
solvated E (au) =-455.142029

M05

C	2.33241700	0.97322500	-0.07567600
C	0.96142900	1.20660000	-0.07514000
C	0.05956300	0.13387900	0.00136300
C	0.56857800	-1.17373500	0.07340500
C	1.93933600	-1.39509600	0.06775100
C	2.83123100	-0.32509400	-0.00395000
H	3.01509400	1.81586800	-0.13822700
H	0.57719100	2.21829400	-0.15057500
H	-0.11054000	-2.01968400	0.13566700
H	2.31394000	-2.41307800	0.12321900
H	3.90214500	-0.50327600	-0.00590400
C	-1.36884700	0.41683600	0.01392000
O	-1.87492100	1.68891400	0.01202200
N	-2.24703900	-0.54555700	-0.03912900
N	-3.00961100	-1.40626500	-0.10191300
H	-1.84415700	2.03361900	0.91690400

E (au) =-454.8095165
ZPVE (au) = 0.119674
solvated E (au) =-454.817013

B97D

C	2.34821900	0.97877200	-0.07590900
C	0.96759100	1.21418800	-0.08510300
C	0.05736700	0.13148700	-0.01071500
C	0.57166000	-1.18756700	0.06878000
C	1.95157300	-1.40875900	0.07089800
C	2.85082100	-0.32940200	0.00211900
H	3.03418800	1.82645800	-0.13691600
H	0.58130600	2.23030400	-0.16941900
H	-0.11398400	-2.03508800	0.13196100
H	2.32825700	-2.43193700	0.13166500
H	3.92747600	-0.50783200	0.00756200

C	-1.37179100	0.41464100	-0.00176200
O	-1.89001900	1.70170500	0.02849300
N	-2.26664900	-0.54661900	-0.02956300
N	-3.04547800	-1.40272300	-0.10156900
H	-1.70483400	2.06968500	0.91528800

E (au) =-454.8191445
ZPVE (au) = 0.115594

ωB97XD

C	2.32830200	0.97443100	-0.08392300
C	0.95790900	1.20583600	-0.08052500
C	0.06056100	0.13363600	0.00437900
C	0.56793000	-1.17163200	0.08272000
C	1.93844400	-1.39221000	0.07356200
C	2.82751400	-0.32248000	-0.00678700
H	3.01100400	1.81638700	-0.15253900
H	0.57151400	2.21646300	-0.16059900
H	-0.11087900	-2.01748800	0.15276900
H	2.31493100	-2.40906800	0.13458000
H	3.89845800	-0.49944800	-0.01110800
C	-1.37206700	0.41257200	0.01993400
O	-1.87770800	1.69017900	0.02106600
N	-2.24294800	-0.54794000	-0.04521100
N	-2.99588500	-1.40937600	-0.11388300
H	-1.84310200	2.03202500	0.92586700

E (au) =-454.9650678
ZPVE (au) = 0.120639

MP2

C	2.32559100	0.98213800	-0.13109400
C	0.95338400	1.21816200	-0.06707200
C	0.05841800	0.14317600	0.07136100
C	0.56892200	-1.16555000	0.15556500
C	1.94134800	-1.38882800	0.08039900
C	2.82922100	-0.31819000	-0.05614700
H	3.00583700	1.82339900	-0.24375800
H	0.56222900	2.22823000	-0.14401100
H	-0.10742100	-2.01124600	0.27148700
H	2.31977500	-2.40670200	0.14040500
H	3.90002800	-0.49701100	-0.10900500
C	-1.36477000	0.42005700	0.17894400
O	-1.89426600	1.69108000	-0.01784800
N	-2.22683800	-0.56576200	-0.07643900
N	-2.96113800	-1.44531800	-0.21294700
H	-2.08316500	2.06646800	0.86163400

E (au) =-453.8616906
ZPVE (au) = 0.119148

13

B3LYP

C	-1.27229200	1.35148200	-0.00005100
C	0.08701300	1.06203600	-0.00010700
C	0.53132300	-0.27711500	-0.00003300
C	-0.42295800	-1.30878600	0.00010300
C	-1.78718600	-1.02136400	0.00017400
C	-2.20951000	0.30940400	0.00009200
H	-1.61238100	2.38401300	-0.00012000
H	0.82206700	1.86125500	-0.00020900

H	-0.06035600	-2.33286300	0.00014500
H	-2.51791100	-1.82551700	0.00028700
H	-3.27196900	0.54033200	0.00013700
C	1.94382700	-0.72007900	-0.00011000
O	2.72212800	0.36781000	-0.00006600
H	3.64222700	0.05683600	-0.00012600

E (au) =-345.5877972
ZPVE (au) = 0.109714
solvated E (au) =-345.622310

M05

C	-1.26690600	1.34948900	-0.00006900
C	0.08908500	1.05590700	-0.00014300
C	0.53080300	-0.27987800	-0.00007200
C	-0.42423000	-1.30654200	0.00006000
C	-1.78531700	-1.01703600	0.00020600
C	-2.20396600	0.31181500	0.00012700
H	-1.60427800	2.38224500	-0.00015100
H	0.82461900	1.85405700	-0.00026800
H	-0.06603100	-2.33165500	0.00006700
H	-2.51665100	-1.81962100	0.00035400
H	-3.26550700	0.54426300	0.00019200
C	1.94416800	-0.72166600	-0.00022900
O	2.71205700	0.36937200	0.00007000
H	3.62956300	0.06321100	-0.00004000

E (au) =-345.3189901
ZPVE (au) = 0.110283
solvated E (au) =-345.326992

B97D

C	-1.28963500	1.35625600	-0.00004600
C	0.07855900	1.07436900	-0.00009100
C	0.53789800	-0.27037100	-0.00001100
C	-0.41844700	-1.31338200	0.00011300
C	-1.79154000	-1.03294800	0.00016500
C	-2.22577200	0.30243500	0.00008300
H	-1.63847100	2.39163200	-0.00011100
H	0.80976000	1.88442400	-0.00018900
H	-0.04979800	-2.34135200	0.00016800
H	-2.52082600	-1.84558300	0.00026400
H	-3.29484400	0.52756800	0.00011800
C	1.95512300	-0.72394300	-0.00005900
O	2.74431100	0.37302500	-0.00012800
H	3.66257400	0.04461700	-0.00015300

E (au) =-345.3348029
ZPVE (au) = 0.106614

ωB97XD

C	-1.26743900	1.34772600	-0.00004500
C	0.08839700	1.05774700	-0.00008800
C	0.52761200	-0.27723500	-0.00000900
C	-0.42164900	-1.30543600	0.00011400
C	-1.78272500	-1.01778500	0.00016000
C	-2.20209100	0.30942600	0.00008000
H	-1.60610200	2.37978000	-0.00010800
H	0.82336100	1.85664100	-0.00018200
H	-0.06152600	-2.33017900	0.00017300
H	-2.51377200	-1.82041600	0.00025500

H	-3.26384000	0.54025700	0.00011500
C	1.94240900	-0.71645700	-0.00004400
O	2.71080700	0.36542800	-0.00013800
H	3.62834200	0.06258600	-0.00016300

E (au) =-345.4593904
ZPVE (au) = 0.111226

MP2

C	-1.26827200	1.35009800	-0.00004600
C	0.09297700	1.06239700	-0.00009400
C	0.52896800	-0.27653200	-0.00001500
C	-0.42030300	-1.31022700	0.00011000
C	-1.78454000	-1.02005900	0.00016400
C	-2.20763900	0.31082300	0.00008300
H	-1.60721400	2.38357400	-0.00011000
H	0.82806600	1.86289800	-0.00019200
H	-0.05927100	-2.33602500	0.00016400
H	-2.51654900	-1.82397000	0.00026400
H	-3.27042300	0.54282300	0.00012100
C	1.94165300	-0.72226900	-0.00005800
O	2.71165800	0.36894200	-0.00012000
H	3.63506700	0.05378400	-0.00015300

E (au) =-344.5796546
ZPVE (au) = 0.109753

14

B3LYP

C	4.49711200	-0.85987000	0.44181900
C	3.20204400	-1.21875200	0.06810800
C	2.40813100	-0.32713700	-0.66954300
C	2.92972600	0.92604500	-1.01432800
C	4.22612100	1.28177000	-0.63906400
C	5.01574600	0.39259300	0.09474900
H	5.10794400	-1.55966600	1.01085100
H	2.78320400	-2.18616100	0.33081600
H	2.29239100	1.59417300	-1.58749900
H	4.62157700	2.25907700	-0.91354100
H	6.02786900	0.66810400	0.38725400
C	0.99074500	-0.63912700	-1.06254200
O	0.36438100	0.16521200	-1.82187300
N	0.52946700	-1.77073900	-0.51229000
N	-0.84693400	-1.95360100	-0.90878800
S	-1.82387700	-1.59179400	0.39898000
O	-3.22399700	-1.53245100	-0.03475200
O	-1.45582900	-2.44912200	1.52819100
C	-1.27228400	0.06304700	0.85786300
C	-1.69757500	1.25379600	0.26109000
C	-0.20289100	0.12486900	1.75839300
C	-1.14268200	2.48516600	0.60646100
C	0.39852300	1.34343700	2.07232300
H	0.13607100	-0.80251100	2.20754000
C	-0.06810200	2.52368800	1.49151500
H	-1.53223300	3.38566300	0.14238000
H	1.24993600	1.36425900	2.74825300
H	0.39697200	3.47705400	1.73123200
N	-2.75312400	1.31129600	-0.75343100
O	-3.62035700	2.19491000	-0.59953800
O	-2.69521200	0.53529400	-1.71941300
H	-1.06713400	-1.24789600	-1.64140100

E (au) =-1440.162971
ZPVE (au) = 0.224149
solvated E (au) =-1440.245919

M05

S	1.55234300	-1.62344300	0.60829000
O	-1.02890600	-0.33255700	-1.94611700
O	1.22667100	-2.09782100	1.94396100
O	2.77673600	-2.07569800	-0.03555800
O	2.43981600	-0.17395000	-2.02120100
O	4.08435500	1.15220600	-1.56761900
N	-0.96751300	-1.48048700	0.07201800
N	0.27885100	-1.92035300	-0.40291800
N	3.01372900	0.62201500	-1.31071500
C	-3.55979800	0.67690400	-1.33235800
H	-3.04404100	0.95622800	-2.24551100
C	-4.82953400	1.16153400	-1.02716200
H	-5.33049700	1.84097400	-1.71375100
C	-5.46015500	0.77594600	0.15503400
H	-6.45289400	1.15036900	0.39555800
C	-4.80717000	-0.09755700	1.02710100
H	-5.29318700	-0.40600000	1.95049700
C	-3.53827800	-0.57969100	0.71946300
H	-3.01797300	-1.26247800	1.38273400
C	-2.89813300	-0.19648700	-0.46531400
C	-1.52117600	-0.68012800	-0.84586300
C	1.65491000	0.18467200	0.78493100
C	0.95826600	0.73731800	1.86116400
H	0.43184300	0.05920400	2.52181900
C	0.95574000	2.11005700	2.08736900
H	0.39376200	2.51468200	2.92389600
C	1.67722600	2.95791900	1.25198200
H	1.69069300	4.02925100	1.42860900
C	2.38058100	2.42776900	0.17701500
H	2.95506500	3.05896900	-0.49077900
C	2.33601300	1.05889200	-0.06845100
H	0.47394300	-1.51467200	-1.33159700

E (au) =-1439.494874
ZPVE (au) = 0.226671
solvated E (au) =-1439.577185

B97D

S	1.78052200	-1.65598000	0.40721200
O	-0.54053000	0.17993700	-1.87911500
O	1.35726100	-2.48678100	1.55341800
O	3.17347200	-1.74873100	-0.07855000
O	2.88635800	0.49079300	-1.70800100
O	3.96219100	2.00538600	-0.53797000
N	-0.65226000	-1.73313200	-0.52184600
N	0.68898900	-1.94026000	-0.91913300
N	3.01940900	1.21623000	-0.72152700
C	-3.14191500	0.92464500	-1.09307700
H	-2.55024100	1.55652600	-1.75707200
C	-4.43156500	1.29365600	-0.68264200
H	-4.86686800	2.23447300	-1.03367100
C	-5.16522600	0.45995400	0.17754400
H	-6.17166300	0.74493900	0.49825400
C	-4.59318100	-0.74587700	0.62314400
H	-5.15719300	-1.40195600	1.29325900

C	-3.30368900	-1.11297600	0.21378900
H	-2.84676700	-2.04158600	0.55625600
C	-2.55932800	-0.28083400	-0.65154400
C	-1.14288600	-0.59895500	-1.08421700
C	1.36953200	0.07051200	0.85559200
C	0.23619600	0.21561500	1.68042600
H	-0.20957400	-0.67932600	2.10728800
C	-0.31242300	1.48124000	1.92978800
H	-1.21747200	1.56449200	2.53435700
C	0.29205500	2.62830800	1.39814900
H	-0.12551400	3.61801300	1.59390000
C	1.43385300	2.50447400	0.59593300
H	1.92777600	3.37674400	0.16943600
C	1.93021400	1.23109400	0.28639300
H	0.95637300	-1.22647000	-1.63377100

E (au) =-1439.479536
ZPVE (au) = 0.217319

ωB97XD

S	1.75891300	-1.63049300	0.40118100
O	-0.51745700	0.08681900	-1.86252300
O	1.39525300	-2.41577500	1.57001200
O	3.12979300	-1.68700600	-0.08437700
O	2.60729900	0.38309600	-1.80448100
O	3.66494200	2.05014100	-0.92406300
N	-0.64090800	-1.73494100	-0.43008600
N	0.70792900	-1.96258700	-0.84262400
N	2.78308500	1.19659200	-0.92177600
C	-3.10584000	0.85012100	-1.16735200
H	-2.51652800	1.42346300	-1.87617700
C	-4.39174600	1.23492600	-0.79811600
H	-4.83436400	2.13123300	-1.22737600
C	-5.11202700	0.47446900	0.12006000
H	-6.11773000	0.77169200	0.40919900
C	-4.53492500	-0.67220400	0.66577300
H	-5.09237800	-1.27130700	1.38253500
C	-3.24968400	-1.05509400	0.29596500
H	-2.78174100	-1.94239500	0.70981800
C	-2.52401200	-0.29616400	-0.62661800
C	-1.11234800	-0.64640800	-1.03447200
C	1.36208600	0.08460800	0.84621100
C	0.41231600	0.24303400	1.85236500
H	0.02641300	-0.65073100	2.32717600
C	-0.03782400	1.50645500	2.21770200
H	-0.80144200	1.60265500	2.98314900
C	0.48189400	2.63667900	1.59835700
H	0.13822700	3.62762200	1.87889100
C	1.43978300	2.49842800	0.60298300
H	1.86533700	3.36042200	0.10389800
C	1.84546800	1.22872700	0.21250900
H	0.94335500	-1.32187400	-1.61736600

E (au) =-1439.787855
ZPVE (au) = 0.228937

MP2

C	4.49711	-0.85987	0.44182
C	3.20204	-1.21875	0.06811
C	2.40813	-0.32714	-0.66954
C	2.92973	0.92605	-1.01433

C	4.22612	1.28177	-0.63906
C	5.01575	0.39259	0.09475
H	5.10794	-1.55967	1.01085
H	2.7832	-2.18616	0.33082
H	2.29239	1.59417	-1.5875
H	4.62158	2.25908	-0.91354
H	6.02787	0.6681	0.38725
C	0.99075	-0.63913	-1.06254
O	0.36438	0.16521	-1.82187
N	0.52947	-1.77074	-0.51229
N	-0.84693	-1.9536	-0.90879
S	-1.82388	-1.59179	0.39898
O	-3.224	-1.53245	-0.03475
O	-1.45583	-2.44912	1.52819
C	-1.27228	0.06305	0.85786
C	-1.69758	1.2538	0.26109
C	-0.20289	0.12487	1.75839
C	-1.14268	2.48517	0.60646
C	0.39852	1.34344	2.07232
H	0.13607	-0.80251	2.20754
C	-0.0681	2.52369	1.49152
H	-1.53223	3.38566	0.14238
H	1.24994	1.36426	2.74825
H	0.39697	3.47705	1.73123
N	-2.75312	1.3113	-0.75343
O	-3.62036	2.19491	-0.59954
O	-2.69521	0.53529	-1.71941
H	-1.06713	-1.2479	-1.64140

E (au) =-1436.857616
ZPVE (au) = 0.225205

15

B3LYP

C	5.52970000	-0.39833200	0.40169600
C	4.20037400	-0.78118900	0.22396000
C	3.29021100	0.09128300	-0.39062000
C	3.73305300	1.35031000	-0.81829000
C	5.06164700	1.73238700	-0.64015400
C	5.96518100	0.85790200	-0.02972200
H	6.22881600	-1.08019400	0.88146500
H	3.83817800	-1.74748800	0.55670500
H	3.01017300	2.01043200	-1.28766100
H	5.39519200	2.71221900	-0.97621200
H	7.00261900	1.15484800	0.11109700
C	1.85376600	-0.28525900	-0.60803000
O	1.05513700	0.52470200	-1.10464100
N	1.53484500	-1.57490800	-0.20853700
N	0.32483300	-1.96227200	-0.54689000
S	-1.12915900	-1.31572600	0.97008300
O	-2.24263800	-2.29471200	1.13248500
O	-0.32052600	-0.98239300	2.18009600
C	-2.02976700	0.31334400	0.65326200
C	-2.97309000	0.56645800	-0.34843700
C	-1.75275300	1.34364500	1.55407800
C	-3.63625500	1.79310800	-0.44748600
C	-2.39818100	2.57555600	1.46451100
H	-1.02025300	1.13757900	2.32832800
C	-3.34404800	2.80379200	0.46111300
H	-4.36204800	1.93095500	-1.23989700

H	-2.16492400	3.36027300	2.18078100
H	-3.84691900	3.76397300	0.38144900
N	-3.29847100	-0.42886500	-1.38036700
O	-4.38310700	-0.31747100	-1.96419900
O	-2.46680000	-1.29528500	-1.63548300
H	-0.07831600	-1.28543600	-1.22818000

E (au) =-1440.14918
ZPVE (au) =0.222119
solvated E (au) =-1440.233995

M05

S	1.02766400	-1.11949700	0.99970000
O	-1.14116300	0.51055100	-1.18853300
O	0.03579800	-0.56317200	1.95780600
O	2.08177300	-2.00509900	1.55792100
O	2.80469400	-1.55516400	-1.31325400
O	4.81212500	-0.76177900	-1.26931200
N	-1.57212800	-1.64257100	-0.39189800
N	-0.38042600	-1.98204600	-0.73269600
N	3.62160000	-0.71560100	-0.99224600
C	-3.80999900	1.30418300	-0.77554300
H	-3.10937300	1.99537000	-1.23328800
C	-5.13217100	1.66159700	-0.53494600
H	-5.48656200	2.65215100	-0.80954000
C	-6.00317200	0.74845200	0.06014300
H	-7.03725800	1.02598400	0.25062400
C	-5.54303200	-0.51941500	0.41493200
H	-6.21803600	-1.23064300	0.88437700
C	-4.21932200	-0.87671900	0.17433300
H	-3.83483800	-1.85211800	0.44961600
C	-3.34233500	0.03321000	-0.42617900
C	-1.91726100	-0.31360000	-0.71248800
C	1.99879900	0.42999300	0.53811100
C	1.57075600	1.62357200	1.11421900
H	0.68400500	1.57821900	1.73952500
C	2.25855500	2.81439100	0.90237200
H	1.90238200	3.73303500	1.36218300
C	3.40460900	2.83304800	0.10746900
H	3.94498800	3.75994900	-0.06302600
C	3.85062800	1.65556700	-0.47771700
H	4.73631800	1.62748600	-1.10190900
C	3.13530300	0.47752400	-0.26745300
H	0.03845700	-1.22946500	-1.31643100

E (au) =-1439.470303
ZPVE (au) = 0.223827
solvated E (au) =-1439.555667

B97D

C	-4.37508500	-0.96603100	-0.57719100
C	-3.11600000	-1.25922500	-0.03502700
C	-2.42905800	-0.29977400	0.74104900
C	-3.03629500	0.95401700	0.96291000
C	-4.29477800	1.24739300	0.42003000
C	-4.97092000	0.28850800	-0.35359600
H	-4.89488600	-1.71710000	-1.17909700
H	-2.63409600	-2.22114700	-0.20835800
H	-2.48684500	1.68589100	1.55644600
H	-4.75014400	2.22640900	0.59667800
H	-5.95221700	0.51632200	-0.77975400

C	-1.03658600	-0.53370600	1.27424700
O	-0.46391400	0.34767700	1.95352400
N	-0.51438600	-1.78168800	0.93585700
N	0.74907000	-1.98556900	1.30839900
S	1.98383900	-1.61689000	-0.42838400
O	3.46533500	-1.47926000	-0.25121000
O	1.48684300	-2.53757000	-1.49849300
C	1.27465800	0.04226000	-0.87268700
C	1.69195400	1.28293800	-0.35234300
C	0.07646500	0.00679600	-1.60826500
C	0.98487800	2.46257400	-0.62113300
C	-0.67824400	1.16974200	-1.81919700
H	-0.25952400	-0.95417100	-1.99327200
C	-0.21962500	2.40139900	-1.33405500
H	1.37104200	3.40550000	-0.23552800
H	-1.63355200	1.10446100	-2.34318600
H	-0.80097800	3.31201100	-1.49240600
N	2.85049900	1.43951800	0.56138800
O	3.61227200	2.39836600	0.34465800
O	2.94646700	0.66654200	1.51608000
H	1.09928900	-1.14113900	1.82818900

E (au) =-1439.47343
ZPVE (au) = 0.215564

ωB97XD

S	2.34963800	-1.22778600	0.36011200
O	-0.23572000	0.21410800	-2.33194800
O	2.09956900	-2.34647600	1.30210200
O	3.66555500	-0.55583500	0.48860800
O	2.38995200	1.17840900	-1.31753300
O	2.00023400	3.14446500	-0.51502900
N	0.00857700	-1.82235200	-1.22231900
N	1.26384000	-1.85271500	-1.55690600
N	1.85552600	1.92488300	-0.52228200
C	-2.71896100	0.68047300	-1.12450800
H	-2.28438500	1.43420900	-1.77335400
C	-3.93841000	0.88541200	-0.48868300
H	-4.48043400	1.81530000	-0.64129500
C	-4.46011900	-0.09828300	0.34871700
H	-5.41299700	0.06017400	0.84803700
C	-3.75807100	-1.28644800	0.54496900
H	-4.16135200	-2.05464800	1.19990600
C	-2.53602300	-1.48958300	-0.08734000
H	-1.96070900	-2.39638800	0.06404400
C	-2.00988200	-0.50466600	-0.92665800
C	-0.66234400	-0.64847100	-1.56631900
C	1.08020600	0.03461600	0.92960000
C	0.14927200	-0.42139500	1.85743500
H	0.25110200	-1.44988300	2.18932000
C	-0.87393200	0.39828200	2.32065100
H	-1.60741000	0.00518300	3.01872800
C	-0.97818200	1.70799400	1.86472200
H	-1.78723600	2.34829400	2.20235800
C	-0.04997400	2.19331400	0.95410000
H	-0.09883400	3.20850100	0.58037100
C	0.95420300	1.35077200	0.48838100
H	1.50901900	-0.96434800	-2.03936100

E (au) =-1439.760846
ZPVE (au) = 0.226206

MP2

C	3.64713000	-1.39772800	0.44429500
C	2.40238300	-1.55475700	-0.16549100
C	1.87257100	-0.51417700	-0.94257200
C	2.59377100	0.67743600	-1.09507300
C	3.83275000	0.83038800	-0.47511400
C	4.36332700	-0.20602200	0.29855800
H	4.05899800	-2.20785700	1.04350900
H	1.82604100	-2.46775900	-0.05324100
H	2.16238500	1.46714300	-1.70496600
H	4.38618100	1.76058000	-0.59153800
H	5.33216300	-0.08757900	0.78079300
C	0.54000300	-0.62742500	-1.60299400
O	0.15776800	0.20753500	-2.43346400
N	-0.17901500	-1.79921600	-1.23892100
N	-1.42755200	-1.82381300	-1.62137800
S	-2.49455600	-1.07001900	0.32956700
O	-3.64937900	-0.15328000	0.60088000
O	-2.35458600	-2.23392400	1.26418500
C	-0.96690700	-0.02780900	0.84659300
C	-0.72343900	1.30785000	0.52076300
C	-0.12841300	-0.60981300	1.79822500
C	0.32125400	2.04512200	1.08038700
C	0.93609200	0.09384700	2.36530900
H	-0.34763600	-1.64009900	2.07371500
C	1.16147400	1.42362100	2.00326800
H	0.45680400	3.08204800	0.79019100
H	1.59241400	-0.39426800	3.08367200
H	1.99504600	1.97779000	2.42933700
N	-1.55679900	2.00825800	-0.46281400
O	-1.60161100	3.25380500	-0.39847800
O	-2.16264000	1.32921300	-1.30621200
H	-1.63433800	-0.93630100	-2.13496700

E (au) =-1436.829199
ZPVE (au) = 0.221703

sulfate anion

B3LYP

C	0.203110	1.841009	-0.121394
C	0.187385	0.445113	-0.181272
C	-1.060990	-0.167559	-0.067210
C	-2.253725	0.550274	0.101242
C	-2.202775	1.938005	0.141853
C	-0.964877	2.585279	0.026676
H	1.186549	2.306949	-0.198804
H	-3.190143	0.011584	0.190589
H	-3.120007	2.511105	0.258110
H	-0.921273	3.673640	0.055424
N	-1.194281	-1.632658	-0.158413
O	-2.249151	-2.148457	0.241214
O	-0.266381	-2.276318	-0.643085
O	2.057231	-0.730186	1.334640
O	2.806903	0.871747	-0.489391
S	2.010454	-0.372605	-0.133927

E (au) =-984.995486
ZPVE (au) = 0.099464
solvated E (au) =-985.082500

M05

C	0.173064	1.849310	-0.109478
C	0.183863	0.456517	-0.173920
C	-1.052215	-0.174407	-0.065921
C	-2.255979	0.519683	0.094947
C	-2.230647	1.905869	0.138898
C	-1.005683	2.572293	0.035179
H	1.148143	2.333223	-0.176925
H	-3.183469	-0.035024	0.178333
H	-3.158281	2.461685	0.250478
H	-0.979955	3.660297	0.070998
N	-1.161451	-1.650875	-0.152131
O	-2.208132	-2.171263	0.220729
O	-0.221190	-2.272680	-0.607018
O	2.050579	-0.777219	1.273451
O	2.786837	0.930377	-0.421350
S	2.010284	-0.332086	-0.156418

E (au) =-984.6424064
ZPVE (au) = 0.100841
solvated E (au) =-984.729159

B97D

C	0.21999600	1.83403700	-0.18233000
C	0.17350000	0.43129000	-0.23122800
C	-1.08720600	-0.16184500	-0.07645800
C	-2.26824900	0.58219700	0.13053100
C	-2.19027300	1.97722700	0.13902300
C	-0.93924300	2.60627400	-0.03043400
H	1.20907000	2.29748400	-0.28105600
H	-3.21679100	0.06330600	0.26961900
H	-3.09807000	2.57191500	0.27322400
H	-0.88027300	3.70017300	-0.03860600
N	-1.23733200	-1.63747000	-0.17167800
O	-2.25991900	-2.15845500	0.31970900
O	-0.34286500	-2.28352400	-0.73422900
O	2.06309900	-0.47617100	1.47611900
O	2.87748800	0.68436000	-0.65650500
S	2.03086400	-0.43220900	-0.04730000

E (au) =-984.6272659
ZPVE (au) = 0.095966

ωB97XD

C	0.09084400	1.88309000	-0.11101800
C	0.18009900	0.49429700	-0.17573700
C	-1.01572000	-0.20766700	-0.07531100
C	-2.25528300	0.41265000	0.08112000
C	-2.31148400	1.79771700	0.12260400
C	-1.12931300	2.53386900	0.02682400
H	1.03803400	2.41942400	-0.16091000
H	-3.14887100	-0.19496400	0.16569700
H	-3.27010400	2.29789100	0.23138700
H	-1.16615600	3.62076500	0.06736400
N	-1.03856000	-1.67552600	-0.15955800
O	-1.97742400	-2.26486400	0.37204600
O	-0.15116200	-2.23288300	-0.78036300
O	1.97436100	-0.85743400	1.19254600
O	2.74043900	1.07457300	-0.24558400
S	1.98577800	-0.22833100	-0.16916900

E (au) =-984.7676325

ZPVE (au) = 0.101659

MP2

C	0.173064	1.849310	-0.109478
C	0.183863	0.456517	-0.173920
C	-1.052215	-0.174407	-0.065921
C	-2.255979	0.519683	0.094947
C	-2.230647	1.905869	0.138898
C	-1.005683	2.572293	0.035179
H	1.148143	2.333223	-0.176925
H	-3.183469	-0.035024	0.178333
H	-3.158281	2.461685	0.250478
H	-0.979955	3.660297	0.070998
N	-1.161451	-1.650875	-0.152131
O	-2.208132	-2.171263	0.220729
O	-0.221190	-2.272680	-0.607018
O	2.050579	-0.777219	1.273451
O	2.786837	0.930377	-0.421350
S	2.010284	-0.332086	-0.156418

E (au) =-982.9326699
ZPVE (au) = 0.100366

N_2

B3LYP

N	0.000000	0.000000	0.552779
N	0.000000	0.000000	-0.552779

E (au) =-109.4960962
ZPVE (au) = 0.005577
solvated E (au) =0.005577

M05

N	0.000000	0.000000	0.554059
N	0.000000	0.000000	-0.554059

E (au) =-109.4960962
ZPVE (au) = 0.005577
solvated E (au) =-109.496554

B97D

N	0.00000000	0.00000000	0.55658700
N	0.00000000	0.00000000	-0.55658700

E (au) =-109.4892981
ZPVE (au) = 0.005413

ωB97XD

N	0.00000000	0.00000000	0.55087000
N	0.00000000	0.00000000	-0.55087000

E (au) =-109.5176409
ZPVE (au) = 0.005708

MP2

N	0.00000000	0.00000000	0.56536200
N	0.00000000	0.00000000	-0.56536200

E (au) =-109.3013183
ZPVE (au) = 0.004954

19

B3LYP

C	-5.283759	0.420600	0.569777
C	-4.308888	-0.575436	0.571758
C	-2.999426	-0.301762	0.148711
C	-2.688753	0.999577	-0.277204
C	-3.664021	1.996675	-0.278611
C	-4.966150	1.713353	0.144006
H	-6.294709	0.190282	0.901286
H	-4.528999	-1.586950	0.898566
H	-1.675871	1.208842	-0.602560
H	-3.407587	3.000997	-0.610966
H	-5.725544	2.492905	0.141960
C	-1.994932	-1.426020	0.175436
O	-2.330464	-2.550738	0.575476
N	-0.751900	-1.041446	-0.282576
N	0.155895	-2.007787	-0.232315
S	1.580983	-1.449354	-0.948106
O	2.732647	-2.118400	-0.325758
O	1.483912	-1.484099	-2.423405
C	1.758300	0.359426	-0.577028
C	2.283317	0.904708	0.598751
C	1.493320	1.231190	-1.635651
C	2.552059	2.269298	0.717965
C	1.721916	2.601761	-1.518098
H	1.120526	0.799815	-2.557519
C	2.256357	3.124010	-0.339311
H	2.982077	2.636346	1.642440
H	1.491994	3.259339	-2.352609
H	2.447367	4.189308	-0.241927
N	2.557560	0.096261	1.803444
O	3.546892	0.414293	2.472868
O	1.768022	-0.790395	2.091840

E (au) =-1439.534849
ZPVE (au) = 0.21117
solvated E (au) =-1439.620514

M05

C	-5.258582	0.396331	0.514985
C	-4.282321	-0.594818	0.521510
C	-2.965719	-0.310996	0.140735
C	-2.647659	0.997592	-0.245122
C	-3.622840	1.991414	-0.250561
C	-4.932967	1.696283	0.127905
H	-6.277040	0.156507	0.812797
H	-4.506479	-1.614032	0.820101
H	-1.626679	1.217069	-0.537938
H	-3.359837	3.002978	-0.552086
H	-5.693539	2.473605	0.121785
C	-1.964434	-1.436721	0.168950
O	-2.304526	-2.560124	0.544772
N	-0.717616	-1.039487	-0.268337
N	0.185219	-1.996576	-0.210994
S	1.608875	-1.468721	-0.900716
O	2.737390	-2.100499	-0.226764
O	1.549829	-1.562104	-2.362879
C	1.755287	0.340671	-0.592140
C	2.237443	0.929215	0.577047

C	1.492152	1.177452	-1.675720
C	2.470427	2.299156	0.666433
C	1.680599	2.553372	-1.588991
H	1.148506	0.714860	-2.593651
C	2.175178	3.117883	-0.415834
H	2.872725	2.700300	1.589440
H	1.449955	3.182672	-2.444058
H	2.336255	4.189355	-0.341894
N	2.499684	0.161848	1.818956
O	3.483189	0.492137	2.465157
O	1.699585	-0.687568	2.137764

E (au) =-1438.869089
ZPVE (au) = 0.213582
solvated E (au) =-1438.954436

B97D

S	-1.99652000	-1.46756800	-0.61880400
O	2.11111700	-2.86500800	0.40084600
O	-2.24285500	-1.78531200	-2.05359200
O	-3.09973800	-1.72414100	0.33702700
O	-1.20351200	-0.37700600	2.19570600
O	-2.51426800	1.30912200	2.73237600
N	0.42336800	-1.32620200	-0.21507800
N	-0.50850100	-2.23722100	-0.08986400
N	-1.82350400	0.65392400	1.92788600
C	4.04765300	-0.79515600	0.30170300
H	4.34107200	-1.81580900	0.55208600
C	4.98563000	0.24424600	0.25444600
H	6.03809000	0.03730200	0.47069700
C	4.57967900	1.55085000	-0.06837100
H	5.31086800	2.36354000	-0.10418900
C	3.22288100	1.80263400	-0.34267800
H	2.89396500	2.81558500	-0.59301100
C	2.28350900	0.76446900	-0.29607800
H	1.23296500	0.95842300	-0.50771200
C	2.68227900	-0.55507000	0.02700200
C	1.72316200	-1.71714400	0.10141100
C	-1.62772900	0.38227800	-0.58732300
C	-1.45661700	0.99893300	-1.83564700
H	-1.43083300	0.36444400	-2.72103200
C	-1.31614800	2.38943000	-1.94218400
H	-1.15323500	2.84360700	-2.92226800
C	-1.38782300	3.19371300	-0.79294300
H	-1.28402300	4.27840100	-0.86559100
C	-1.59943400	2.59825600	0.45469800
H	-1.67510500	3.19172400	1.36478900
C	-1.69953400	1.20075100	0.55389700

E (au) =-1438.852974
ZPVE (au) = 0.203836

ωB97XD

S	-1.77696800	-1.48493400	-0.75887400
O	2.17683000	-2.68721500	0.52489100
O	-1.85076100	-1.71660500	-2.20377700
O	-2.91755800	-1.90306900	0.04842900
O	-1.53273000	-0.46818300	2.19131300
O	-3.15878300	0.93178100	2.49269000
N	0.56570700	-1.17022100	-0.22529800
N	-0.36214100	-2.10864900	-0.12976100

N	-2.24905700	0.44199600	1.83166400
C	4.14547900	-0.70173700	0.41175500
H	4.40447200	-1.72515200	0.66466800
C	5.10252900	0.30669500	0.38242500
H	6.14020500	0.07727000	0.61342000
C	4.73375100	1.61068900	0.05796500
H	5.48002300	2.40127600	0.03630800
C	3.40129400	1.89429100	-0.23668900
H	3.10486100	2.91036900	-0.48680900
C	2.44481700	0.88442500	-0.21014700
H	1.40482700	1.09379600	-0.43681300
C	2.80902900	-0.42674200	0.11441300
C	1.81686300	-1.56380800	0.16706400
C	-1.65990300	0.33854600	-0.60956400
C	-1.36451700	1.04131200	-1.77450600
H	-1.14726700	0.46629000	-2.66723300
C	-1.35191300	2.43079200	-1.79035900
H	-1.10013000	2.95525300	-2.70742800
C	-1.66987400	3.14571900	-0.63906800
H	-1.67041300	4.23150800	-0.64460600
C	-1.99539000	2.46230500	0.52381200
H	-2.26325300	2.98659400	1.43355200
C	-1.96872700	1.07187700	0.53161900

E (au) =-1439.155004
ZPVE (au) = 0.214999

MP2

C	-3.57407500	1.87940700	-0.23278200
C	-2.57752200	0.90272100	-0.22330400
C	-2.88209200	-0.40808300	0.17519500
C	-4.19141900	-0.71906600	0.56426600
C	-5.18490000	0.25930900	0.55195400
C	-4.88042800	1.56385600	0.15277900
H	-3.33016400	2.89498900	-0.54084600
H	-1.55911100	1.13631100	-0.51922700
H	-4.39605100	-1.74006100	0.87515800
H	-6.19986000	0.00665100	0.85471100
H	-5.65457500	2.32935400	0.14347300
C	-1.85295300	-1.51018100	0.21723900
O	-2.15052500	-2.62672200	0.66239200
N	-0.64212700	-1.08710100	-0.28967000
N	0.31854700	-2.02968000	-0.18784200
S	1.65562900	-1.38898700	-0.94793000
O	2.87634800	-1.91674400	-0.32159700
O	1.54049800	-1.45769600	-2.41860200
C	1.62483900	0.39727400	-0.59594000
C	2.15109300	0.97977200	0.55749200
C	1.17551400	1.25072100	-1.60835700
C	2.24393600	2.36277400	0.71593800
C	1.22680600	2.63607800	-1.45610100
H	0.79624800	0.79466300	-2.51760100
C	1.76573600	3.19452500	-0.29358900
H	2.68166600	2.76171700	1.62610400
H	0.85583400	3.28017600	-2.25031500
H	1.81774600	4.27403500	-0.17269100
N	2.59773800	0.17943300	1.69914000
O	3.69466800	0.48706700	2.20412700
O	1.82799700	-0.69681100	2.11967600

E (au) =-1436.222219
ZPVE (au) = 0.21242

21

B3LYP

C	1.711552	-1.053994	-0.000041
C	0.340376	-1.304631	0.000046
C	-0.565102	-0.235989	0.000074
C	-0.094767	1.089086	0.000102
C	1.274598	1.334265	0.000081
H	2.416478	-1.880434	-0.000098
H	-0.043637	-2.320752	0.000068
H	-0.813480	1.903190	0.000138
H	1.644626	2.355979	0.000111
C	-2.018998	-0.522513	0.000179
O	-2.924016	0.258155	-0.000349
C	2.176157	0.263427	-0.000007
H	3.245241	0.458874	-0.000037

E (au) =-345.0160044
ZPVE (au) = 0.097791
solvated E (au) =-345.021322

M05

C	-1.523112	-1.212768	0.000007
C	-0.146500	-1.242769	0.000006
C	0.588334	-0.000112	0.000000
C	-0.146369	1.242694	-0.000006
C	-1.522909	1.212900	-0.000006
H	-2.064970	-2.154076	0.000011
H	0.392777	-2.183302	0.000011
H	0.393174	2.183079	-0.000011
H	-2.064743	2.154220	-0.000010
C	1.941302	-0.000076	0.000000
O	3.114813	0.000027	-0.000001
C	-2.233571	0.000074	0.000001
H	-3.317793	0.000204	0.000001

E (au) =-344.7477902
ZPVE (au) = 0.096701
solvated E (au) =-344.752178

B97D

C	1.72009600	-1.06018800	-0.00001900
C	0.34173100	-1.31229800	-0.00002000
C	-0.56971400	-0.23697000	-0.00000400
C	-0.09526400	1.09620600	0.00002700
C	1.28135500	1.34205000	0.00004300
H	2.42874600	-1.89037100	-0.00004100
H	-0.04511800	-2.33320900	-0.00003500
H	-0.81902500	1.91282100	0.00003600
H	1.65410400	2.36851700	0.00007300
C	-2.02752100	-0.52760400	0.00001600
O	-2.93898900	0.26074100	-0.00005200
C	2.18783500	0.26472900	0.00001700
H	3.26209900	0.46076200	0.00002800

E (au) =-344.764222
ZPVE (au) = 0.094942

ωB97XD

C	1.70778700	-1.05028100	-0.00001900

C	0.34027800	-1.30131100	-0.00001600
C	-0.56115900	-0.23604200	0.00000100
C	-0.09587600	1.08509500	0.00003100
C	1.26990200	1.33082500	0.00004300
H	2.41350100	-1.87493200	-0.00004300
H	-0.04213000	-2.31766600	-0.00002700
H	-0.81460900	1.89863500	0.00004000
H	1.63906800	2.35189400	0.00007500
C	-2.01665400	-0.52253900	0.00000800
O	-2.91429200	0.25810700	-0.00005600
C	2.16922900	0.26382500	0.00001500
H	3.23746200	0.45977700	0.00002200

E (au) =-344.885294
ZPVE (au) = 0.098906

MP2

C	1.71367400	-1.04963900	-0.00002300
C	0.34256000	-1.30790600	-0.00001000
C	-0.56128000	-0.23985300	0.00000200
C	-0.10238900	1.08682900	0.00004000
C	1.26832600	1.33541600	0.00004400
H	2.42230900	-1.87389200	-0.00004600
H	-0.03731500	-2.32663100	-0.00002200
H	-0.82529600	1.89902900	0.00004700
H	1.63413300	2.35930500	0.00007700
C	-2.01476000	-0.53079700	0.00003000
O	-2.92084700	0.26156200	-0.00008400
C	2.17532200	0.26942200	0.00001600
H	3.24423700	0.46886500	0.00001800

E (au) =-344.0187601
ZPVE (au) = 0.097571

Radical from reaction coordinate Q

B3LYP

C	1.871399	-1.410549	-0.074182
C	0.507008	-1.138695	-0.142182
C	0.056370	0.188037	-0.068077
C	0.980104	1.236999	0.074306
C	2.340805	0.957892	0.142763
C	2.787290	-0.365244	0.068232
H	2.220605	-2.437062	-0.135027
H	-0.204972	-1.948698	-0.261292
H	0.610769	2.255776	0.130783
H	3.055009	1.768765	0.252808
H	3.850843	-0.581406	0.120420
C	-1.375412	0.537138	-0.096081
O	-1.862965	1.637625	-0.121065
N	-2.292394	-0.662375	-0.278843
N	-3.083880	-1.079318	0.483438

E (au) =-454.5418467
ZPVE (au) = 0.10658
solvated E (au) =-454.548631

M05

C	1.858491	-1.411209	-0.076096
C	0.498250	-1.133933	-0.142648
C	0.053487	0.191667	-0.069891
C	0.980012	1.233511	0.072258

C	2.337320	0.949858	0.140063
C	2.777051	-0.371887	0.065576
H	2.203344	-2.438534	-0.136919
H	-0.215135	-1.942911	-0.261055
H	0.614122	2.253119	0.128937
H	3.054265	1.757555	0.250089
H	3.839123	-0.592283	0.116892
C	-1.372622	0.554532	-0.081734
O	-1.857974	1.653089	-0.111015
N	-2.295300	-0.630834	-0.274168
N	-3.050966	-1.131578	0.466313

E (au) =-454.2178634
ZPVE (au) = 0.10658
solvated E (au) =-454.224379

B97D

Not found at this level of theory

ωB97XD

C	1.85829700	-1.40343700	-0.07057600
C	0.49681900	-1.13394500	-0.13828600
C	0.04922000	0.18828600	-0.06829200
C	0.96616900	1.23595300	0.06840600
C	2.32416500	0.95999500	0.13556600
C	2.76981900	-0.35936600	0.06616500
H	2.20882600	-2.42895300	-0.12687800
H	-0.21311500	-1.94677700	-0.25044000
H	0.59556400	2.25430800	0.12285000
H	3.03774900	1.77084800	0.24140200
H	3.83298100	-0.57352600	0.11962000
C	-1.38532500	0.53557800	-0.10510800
O	-1.86497300	1.63382800	-0.09254200
N	-2.29134100	-0.64155400	-0.31271200
N	-2.99683200	-1.11343400	0.49935900

E (au) =-454.372756
ZPVE (au) = 0.108216

MP2

C	1.83267600	-1.41702200	-0.03324400
C	0.46755500	-1.13632600	-0.07832800
C	0.04064700	0.19833200	-0.05156300
C	0.97246800	1.24410200	0.02964000
C	2.33213700	0.95086700	0.07477800
C	2.76406600	-0.37898000	0.04418400
H	2.17000900	-2.44991600	-0.05550500
H	-0.25376800	-1.94531400	-0.13983300
H	0.61370600	2.26945200	0.05495000
H	3.05768200	1.75793300	0.13473400
H	3.82686700	-0.60554700	0.07886500
C	-1.38746900	0.56947500	-0.06149400
O	-1.85843900	1.68319600	0.00810300
N	-2.31279500	-0.58632200	-0.34346000
N	-2.92712900	-1.22437300	0.38890700

E (au) =-453.2627405
ZPVE (au) = 0.109291

Transition structure from reaction coordinate P, Scheme 6.8

B3LYP

C	-4.96932600	0.50030100	0.15823500
C	-4.16490500	-0.63118300	0.27045100
C	-2.78434100	-0.56138900	0.01045000
C	-2.23527800	0.67593600	-0.36857800
C	-3.04250900	1.80557600	-0.48016700
C	-4.41436500	1.72701300	-0.21753900
H	-6.03545000	0.42654800	0.36484000
H	-4.57677200	-1.59256700	0.55974200
H	-1.17310600	0.73819100	-0.57754000
H	-2.59701300	2.75362700	-0.77436500
H	-5.04211600	2.61122900	-0.30520100
C	-1.98881000	-1.80930300	0.14992000
O	-2.50177100	-2.89956300	0.45579800
N	-0.62582200	-1.63607400	-0.10580500
N	0.25742300	-2.47203700	-0.07095900
S	2.15232500	-1.44512600	-0.66678600
O	3.39351000	-1.59934400	0.14703000
O	2.30518600	-1.62121500	-2.14510400
C	1.73915000	0.40872100	-0.53973900
C	1.69204000	1.17853900	0.62564800
C	1.60405600	1.07266000	-1.75936300
C	1.52400900	2.56413000	0.59043200
C	1.41473000	2.45438200	-1.81455800
H	1.66950500	0.47101200	-2.66109600
C	1.37367800	3.20339400	-0.63680800
H	1.50807200	3.11254900	1.52454800
H	1.30288900	2.94684800	-2.77773800
H	1.22674500	4.27966200	-0.66987000
N	1.79568800	0.57036300	1.96655600
O	2.19703100	1.29362700	2.88595200
O	1.45607400	-0.59769300	2.09712400

E (au) =-1439.521659
ZPVE (au) =0.208014
solvated E (au) =-1439.602672

M05

C	-3.834093	2.160497	-0.330209
C	-3.033411	1.068718	-0.013653
C	-3.528216	-0.236398	-0.161399
C	-4.837979	-0.415745	-0.629077
C	-5.634929	0.679430	-0.944270
C	-5.137067	1.974358	-0.797291
H	-3.437058	3.165627	-0.211095
H	-2.019828	1.210892	0.351361
H	-5.203481	-1.432089	-0.735706
H	-6.648499	0.524111	-1.307422
H	-5.758188	2.832206	-1.044550
C	-2.725443	-1.446012	0.148557
O	-3.152048	-2.600325	0.025220
N	-1.445636	-1.135497	0.596145
N	-0.509581	-1.826249	0.928781
S	1.087099	-0.340017	1.422226
O	0.489449	0.996651	1.215105
O	1.849562	-0.608641	2.660093
C	2.293029	-0.548035	0.022417
C	3.063814	0.448598	-0.578164
C	2.301123	-1.812418	-0.570307
C	3.802174	0.215796	-1.735718
C	3.066366	-2.073349	-1.703914

H	1.670598	-2.587456	-0.146953
C	3.814541	-1.056664	-2.293659
H	4.361072	1.034739	-2.174151
H	3.061876	-3.069062	-2.138224
H	4.400750	-1.248871	-3.187460
N	3.193187	1.804186	0.005153
O	3.242977	1.898723	1.211964
O	3.301800	2.733647	-0.781362

E (au) =-1438.849641
ZPVE (au) = 0.210234
solvated E (au) =-1438.93205

B97D

S	-2.32150600	-1.30850000	-0.50577300
O	2.11272600	-3.08642500	0.25902900
O	-2.68398600	-1.60548700	-1.93083900
O	-3.43199100	-1.29232400	0.49408000
O	-1.13203400	-0.36946800	2.16220900
O	-1.86963300	1.60248200	2.82269300
N	0.32061100	-1.59097300	-0.12064300
N	-0.60599000	-2.40424000	-0.03371600
N	-1.48849400	0.79576500	1.94778700
C	3.97040900	-0.93057000	0.15707400
H	4.32336700	-1.94442800	0.35020900
C	4.85885700	0.14918700	0.09293300
H	5.92970700	-0.02103000	0.23905200
C	4.38261000	1.44895300	-0.15584600
H	5.07695500	2.29243100	-0.20291900
C	3.00204900	1.65133900	-0.34165900
H	2.61356700	2.65501100	-0.53522500
C	2.11037800	0.57499400	-0.27786300
H	1.04540200	0.73861200	-0.42354700
C	2.57889600	-0.73809100	-0.02586200
C	1.68870800	-1.93253800	0.05867900
C	-1.62410400	0.46676900	-0.55923500
C	-1.45624700	1.01536000	-1.83756300
H	-1.64141100	0.37318700	-2.69925500
C	-1.06568800	2.35223200	-2.00690000
H	-0.91698900	2.75227900	-3.01258600
C	-0.86675100	3.17055200	-0.88278200
H	-0.56318000	4.21307700	-1.00154900
C	-1.05783400	2.64693300	0.40005100
H	-0.91635100	3.25588400	1.29169000
C	-1.41303600	1.29602500	0.55816100

E (au) =-1438.85147
ZPVE (au) = 0.202186

ωB97XD

S	-2.61893800	-0.79941100	-0.46956700
O	1.48568000	-3.14434500	0.11308600
O	-3.27432300	-0.57217800	-1.78175100
O	-3.50570900	-0.74940300	0.71502300
O	-0.86867200	-0.88568500	1.93860300
O	-0.70200200	0.90938600	3.13294900
N	-0.00657800	-1.62942900	-0.84052500
N	-1.03487000	-2.30534400	-0.77017400
N	-0.81780100	0.32098300	2.06218100
C	3.50103500	-1.19133800	0.21742800

H	3.66736200	-2.16615500	0.66449600
C	4.48442100	-0.20945700	0.22994000
H	5.44639900	-0.41187200	0.69406300
C	4.23664300	1.03532500	-0.34656200
H	5.00393100	1.80535900	-0.33458600
C	2.99996800	1.28731900	-0.93584600
H	2.79406900	2.25530100	-1.38509800
C	2.01566000	0.30482900	-0.94889000
H	1.05080000	0.49540300	-1.40539400
C	2.25665300	-0.94238700	-0.36750400
C	1.22026000	-2.02541900	-0.30762000
C	-1.53781000	0.73367900	-0.29733700
C	-1.51008200	1.57948100	-1.40163200
H	-2.05828700	1.26039600	-2.28313800
C	-0.81645300	2.78532900	-1.36946300
H	-0.80331000	3.42456300	-2.24837900
C	-0.14318100	3.17426800	-0.21441500
H	0.40536300	4.11092200	-0.18186300
C	-0.17615900	2.35616300	0.90626700
H	0.33020600	2.62888800	1.82388500
C	-0.86405200	1.14922600	0.84653500

E (au) =-1439.13098
ZPVE (au) =0.212362

MP2

Not found at this level of theory

H abstraction from anion 14

B3LYP

C	0.94436400	5.34916500	-0.34151000
C	0.64580600	4.01067300	-0.09235900
C	1.61028800	3.01318300	-0.30202800
C	2.87825800	3.38929100	-0.76498600
C	3.17806400	4.72909900	-1.01327500
C	2.21259500	5.71620900	-0.80359300
H	0.18635800	6.11198200	-0.17239400
H	-0.33235200	3.71388500	0.27076000
H	3.61077300	2.60359700	-0.91981600
H	4.16841400	5.00445400	-1.37157300
H	2.44461900	6.76183100	-0.99667200
C	1.33561000	1.55307000	-0.06276700
O	2.25644200	0.70843800	-0.27926100
N	0.11490200	1.28800500	0.39981200
N	-0.08789400	-0.08073300	0.52607700
S	-1.42701900	-0.41745600	1.48290900
O	-1.46858700	-1.87300400	1.67617700
O	-1.62448400	0.46644400	2.64342500
C	-2.78808200	0.02976300	0.34874800
C	-3.38934100	-0.83179500	-0.57482700
C	-3.31845700	1.31531900	0.49294400
C	-4.50873600	-0.44060900	-1.31005000
C	-4.40756000	1.73171900	-0.27029900
H	-2.86386200	1.96840200	1.22838700
C	-5.00943800	0.85075700	-1.16996400
H	-4.96427300	-1.15307000	-1.98867600
H	-4.79408800	2.74018100	-0.15029100
H	-5.86893600	1.16165100	-1.75747300
N	-2.89277400	-2.19216600	-0.87359300
O	-3.73573300	-3.09285200	-0.88297900

O	-1.71432600	-2.32289700	-1.17082300
H	0.88994000	-0.66537800	0.92936000
C	2.69471600	-2.22836200	0.29695000
C	2.01801400	-2.40905300	-0.91543000
C	3.80407100	-3.02858100	0.60677100
C	2.45583600	-3.38299400	-1.81218100
H	1.16419400	-1.78032600	-1.14090400
C	4.23713600	-4.00101300	-0.29173400
H	4.30996900	-2.87120000	1.55520900
C	3.56248700	-4.17855700	-1.50353000
H	1.92981800	-3.52361800	-2.75313500
H	5.09804800	-4.62142300	-0.05086700
H	3.89795800	-4.93957400	-2.20516200
C	2.20505000	-1.23038300	1.29784900
O	2.76818900	-0.97103700	2.33124400

E (au) =-1785.167607
ZPVE (au) = 0.317209
solvated E (au) =-1785.249977

M05

C	-4.91032200	-2.43077900	-0.28307700
C	-3.66206600	-1.87039500	-0.03109400
C	-3.42016500	-0.51748700	-0.29701500
C	-4.45876000	0.25888200	-0.81924400
C	-5.70922500	-0.29953400	-1.07201000
C	-5.94138400	-1.64797000	-0.80585300
H	-5.08344400	-3.48322800	-0.06838400
H	-2.85348700	-2.46515300	0.38019700
H	-4.25095100	1.30589100	-1.01579200
H	-6.50637000	0.31952500	-1.47782700
H	-6.91749100	-2.08652200	-1.00105400
C	-2.08586600	0.13449700	-0.05808000
O	-1.94757900	1.36120800	-0.29876300
N	-1.16297300	-0.68869200	0.44058100
N	0.05046200	-0.05826400	0.56065500
S	1.12144400	-0.90664800	1.50405400
O	2.28056400	-0.04987300	1.72075000
O	0.54102400	-1.62633100	2.63367200
C	1.61180200	-2.21222300	0.34640900
C	2.66566500	-2.12595700	-0.56335900
C	0.90523400	-3.41342300	0.42049300
C	3.03842300	-3.21282800	-1.34847900
C	1.23667100	-4.49043900	-0.39412100
H	0.10020600	-3.47957800	1.14302700
C	2.31024600	-4.39425500	-1.27619400
H	3.89031100	-3.11376200	-2.01201600
H	0.66357400	-5.41056400	-0.32888400
H	2.58765900	-5.23652500	-1.90314400
N	3.45268500	-0.89035900	-0.79635500
O	4.66462600	-1.00168400	-0.71911800
O	2.85272500	0.10798400	-1.12788100
H	-0.04032500	1.08721800	0.94792600
C	0.27104100	3.41976600	0.28406100
C	0.80681400	2.93902000	-0.91347800
C	0.32326400	4.78754600	0.57541900
C	1.38555600	3.82753800	-1.81476500
H	0.75857800	1.87756000	-1.12775300
C	0.90331900	5.67166300	-0.32721100

H	-0.09643800	5.13409500	1.51524100
C	1.43463600	5.19049200	-1.52447100
H	1.80350900	3.45266100	-2.74486500
H	0.94313600	6.73445500	-0.10057600
H	1.89077500	5.88032000	-2.23067200
C	-0.29881700	2.48286000	1.29624800
O	-0.84760300	2.81736300	2.31139800

E (au) =-1784.234096
ZPVE (au) = 0.319884
solvated E (au) =-1784.31645

B97D

C	-3.64548700	-4.02118200	-0.46651500
C	-2.68497800	-3.04110500	-0.18726300
C	-3.00084400	-1.66870700	-0.30495500
C	-4.30376300	-1.30930500	-0.70999200
C	-5.26513900	-2.29168500	-0.98850200
C	-4.94252800	-3.65310500	-0.86905600
H	-3.38407400	-5.07888200	-0.36800100
H	-1.67890500	-3.31776900	0.12832200
H	-4.53720200	-0.24769600	-0.79643500
H	-6.27062400	-1.99360400	-1.29977800
H	-5.69147100	-4.42002400	-1.08591500
C	-1.99830000	-0.58141400	-0.02717600
O	-2.35102100	0.64294700	-0.18722700
N	-0.80724600	-1.01768600	0.39869600
N	0.10495800	0.00170000	0.55892900
S	1.41679000	-0.45577800	1.57622700
O	2.17417100	0.77577800	1.87713600
O	1.05858900	-1.38748500	2.67331500
C	2.35113900	-1.46643300	0.36986400
C	3.33360200	-0.99139100	-0.52943100
C	2.07091300	-2.84696000	0.38726100
C	4.05148600	-1.88934100	-1.33953900
C	2.75073800	-3.73311200	-0.45408500
H	1.31695600	-3.20620100	1.08530200
C	3.75394100	-3.25436200	-1.31609000
H	4.82392800	-1.48822300	-1.99468100
H	2.50755700	-4.79735600	-0.42738200
H	4.29942700	-3.93843700	-1.96947100
N	3.65108200	0.43603100	-0.74490800
O	4.85834900	0.73154200	-0.84973200
O	2.71185700	1.22644600	-0.89034200
H	-0.39110800	0.98908800	0.95122200
C	-1.10929700	3.22079500	0.22923100
C	-0.31546400	2.96536300	-0.90684500
C	-1.59126600	4.52475500	0.47532400
C	-0.01612000	4.00844900	-1.79194000
H	0.06281800	1.95888400	-1.07425700
C	-1.29068900	5.56252600	-0.41575600
H	-2.19667700	4.69871100	1.36688400
C	-0.50278500	5.30569100	-1.55172600
H	0.60660200	3.81019200	-2.66714300
H	-1.66792200	6.57163900	-0.22719300
H	-0.26199700	6.11734800	-2.24365500
C	-1.35486600	2.14515700	1.23389800
O	-2.02560300	2.23410500	2.23851100

E (au) =-1784.24803
ZPVE (au) = 0.308069

ωB97XD

C	0.74160300	5.32670000	-0.30137800
C	0.49607300	3.98046300	-0.05559900
C	1.48368400	3.02315700	-0.30408500
C	2.71847500	3.44010100	-0.80226400
C	2.96545400	4.78724900	-1.04899900
C	1.97772500	5.73680800	-0.80011400
H	-0.03344000	6.06283000	-0.10042000
H	-0.45833900	3.64620800	0.33747800
H	3.47095600	2.67974900	-0.98545000
H	3.93267300	5.09790200	-1.43751100
H	2.16871300	6.79030900	-0.99053200
C	1.26340200	1.55329000	-0.06527300
O	2.20215400	0.74588400	-0.29997500
N	0.06797900	1.25125500	0.42131200
N	-0.07505800	-0.12092500	0.54383000
S	-1.38409300	-0.50382000	1.48414700
O	-1.40101200	-1.95441600	1.62579900
O	-1.58748700	0.32674700	2.66622400
C	-2.73302500	-0.04357800	0.37043500
C	-3.29649400	-0.89203100	-0.57681100
C	-3.27175600	1.23204900	0.52057900
C	-4.39462700	-0.50614200	-1.33576100
C	-4.34402800	1.64564400	-0.26071300
H	-2.83244400	1.88238400	1.26788900
C	-4.91110300	0.77410900	-1.18576100
H	-4.82500800	-1.21008900	-2.03932900
H	-4.74452500	2.64716900	-0.13733500
H	-5.75810900	1.08583400	-1.78925100
N	-2.77635400	-2.23917600	-0.87054200
O	-3.57620600	-3.16037900	-0.78453200
O	-1.63027400	-2.33270700	-1.26037700
H	0.94072100	-0.64876900	0.98511000
C	2.71270200	-2.12441600	0.30395100
C	1.93878500	-2.40138300	-0.82303500
C	3.90960000	-2.80897500	0.52387600
C	2.36779600	-3.36720300	-1.72735700
H	1.01488300	-1.85460400	-0.97896600
C	4.33658800	-3.76946400	-0.38496400
H	4.49007100	-2.57399300	1.41124500
C	3.56368700	-4.04904500	-1.51115900
H	1.76455500	-3.58840100	-2.60316700
H	5.27018300	-4.30080800	-0.21817200
H	3.89453600	-4.80220300	-2.22215200
C	2.24064000	-1.12689400	1.31052300
O	2.83570000	-0.81926800	2.30479500

E (au) =-1784.66422

ZPVE (au) = 0.32263

Transition Structure from reaction coordinate R, Scheme 6.8

B3LYP

C	-1.901416	-1.421996	-0.050010
C	-0.538222	-1.140956	-0.108716
C	-0.101720	0.192011	-0.056371
C	-1.036969	1.237599	0.055194
C	-2.394973	0.947287	0.116027
C	-2.827499	-0.382208	0.062682
H	-2.241938	-2.452239	-0.094619
H	0.187081	-1.940466	-0.205036

```
H    -0.678939    2.261484    0.095270
H    -3.118277    1.752921    0.203256
H    -3.889643   -0.606904    0.108228
C     1.321739    0.546491   -0.072099
O     1.842689    1.616441   -0.140692
N     2.331604   -0.848786   -0.166873
N     3.364762   -0.839168    0.358044
```

E (au) =-454.5411671
ZPVE (au) = 0.105151
solvated E (au) =-454.548298

M05

```
C    -1.874690   -1.432354   -0.067364
C    -0.520340   -1.128211   -0.130642
C    -0.105627    0.208179   -0.065891
C    -1.055571    1.233222    0.068255
C    -2.405979    0.919910    0.137181
C    -2.815676   -0.412051    0.067867
H    -2.198242   -2.466728   -0.125329
H     0.215105   -1.916389   -0.245611
H    -0.714486    2.261999    0.119221
H    -3.141043    1.712026    0.242129
H    -3.872869   -0.655148    0.117868
C     1.305699    0.592898   -0.049806
O     1.826933    1.655362   -0.166394
N     2.367832   -0.811024   -0.201318
N     3.336335   -0.913008    0.410642
```

E (au) =-454.2170755
ZPVE (au) = 0.105204
solvated E (au) =-454.223604

B97D

Not found at this level of theory

ωB97XD

```
C                 -1.91783100   -1.41606600   -0.01339000
 C                 -0.55471400   -1.14469700   -0.03129400
 C                 -0.11794500    0.18315800   -0.01676700
 C                 -1.04442300    1.23448000    0.01564300
 C                 -2.40223800    0.95429300    0.03437500
 C                 -2.83755000   -0.37111700    0.01976100
 H                 -2.26319000   -2.44480200   -0.02575800
 H                  0.17005800   -1.94938800   -0.05872000
 H                 -0.68224700    2.25753100    0.02686000
 H                 -3.12373200    1.76459200    0.05992700
 H                 -3.90143100   -0.58840600    0.03443900
 C                  1.30912300    0.52788800   -0.02607200
 O                  1.83670400    1.58829200   -0.04415900
 N                  2.32886800   -0.91277500   -0.04341900
 N                  3.45689900   -0.73772500    0.10384500
```

E (au) =-454.370008
ZPVE (au) = 0.10629

MP2

```
C                 -1.89819400   -1.42551900   -0.02297800
 C                 -0.53299700   -1.14533400   -0.06171000
 C                 -0.11153700    0.19154000   -0.03857400
 C                 -1.04447500    1.24071900    0.02774000
```

C	-2.40306200	0.94525400	0.06764300
C	-2.83039300	-0.38689500	0.04310500
H	-2.23634400	-2.45808300	-0.04317200
H	0.19742900	-1.94504300	-0.11946600
H	-0.68738500	2.26714900	0.04664000
H	-3.13149800	1.75029600	0.11882900
H	-3.89310500	-0.61474300	0.07338600
C	1.30857400	0.55385200	-0.05339900
O	1.83936200	1.62021300	-0.07330700
N	2.33128800	-0.87273200	-0.13369300
N	3.39849900	-0.81340900	0.23930400

E (au) =-453.2599558
ZPVE (au) = 0.107156

H abstraction from anion 9

B3LYP

C	-0.824266	2.295671	1.207647
O	-0.710904	2.549746	2.384600
H	-0.943814	0.926723	0.689508
O	-3.283613	0.580223	0.733203
C	-2.547142	-0.385211	0.474348
N	-1.202990	-0.186913	0.313129
N	-0.270582	-1.176635	0.511233
S	0.956134	-1.090936	-0.596574
O	0.789331	-0.023180	-1.606836
O	1.302375	-2.460399	-1.025258
C	-3.167625	-1.749687	0.256906
C	-2.514260	-2.878853	-0.261967
C	-4.533664	-1.846555	0.570537
C	-3.219073	-4.069402	-0.454987
H	-1.460219	-2.830667	-0.501469
C	-5.230086	-3.037920	0.386138
H	-5.024906	-0.959290	0.955217
C	-4.573096	-4.157934	-0.129953
H	-2.698329	-4.933200	-0.861800
H	-6.286349	-3.093058	0.642125
H	-5.113153	-5.091107	-0.278128
C	-0.989223	3.328715	0.140648
C	-1.239118	4.666883	0.484120
C	-0.872423	2.955620	-1.204736
C	-1.381329	5.626036	-0.513666
H	-1.320357	4.927211	1.535850
C	-1.004742	3.925229	-2.200523
H	-0.657427	1.920696	-1.458048
C	-1.263252	5.253895	-1.858168
H	-1.582114	6.662630	-0.251268
H	-0.906015	3.640641	-3.244832
H	-1.372097	6.004277	-2.638423
C	2.390772	-0.590496	0.455125
C	2.120416	0.035289	1.675295
C	3.732661	-0.856361	0.150407
C	3.146579	0.400866	2.546948
H	1.085745	0.207748	1.948223
C	4.765728	-0.534385	1.031845
C	4.473575	0.110758	2.229802
H	2.900204	0.899435	3.480419
H	5.782945	-0.789253	0.757725
H	5.277984	0.378088	2.909726
N	4.164136	-1.460222	-1.126204
O	3.632647	-1.071423	-2.157164

O 5.090568 -2.275273 -1.071211

E (au) =-1785.16403
ZPVE (au) = 0.317281
solvated E (au) =-1785.244783

M05

C -0.804817 2.252150 1.199012
O -0.620822 2.513967 2.362283
H -0.910265 0.902881 0.709360
O -3.240339 0.543799 0.730407
C -2.503740 -0.417732 0.484262
N -1.162057 -0.227479 0.335909
N -0.224323 -1.193748 0.511784
S 0.984897 -1.079706 -0.585379
O 0.789954 -0.031334 -1.592344
O 1.374271 -2.427008 -1.005502
C -3.114515 -1.785096 0.272913
C -2.459829 -2.906505 -0.252360
C -4.472990 -1.893921 0.600300
C -3.153995 -4.101337 -0.436288
H -1.409522 -2.852565 -0.506608
C -5.160140 -3.089419 0.427033
H -4.967928 -1.010184 0.987950
C -4.500318 -4.201597 -0.094615
H -2.630987 -4.959856 -0.849287
H -6.212053 -3.153415 0.695432
H -5.032688 -5.139583 -0.234951
C -1.058287 3.263801 0.133982
C -1.322886 4.594004 0.482352
C -1.010703 2.884167 -1.210578
C -1.549006 5.540280 -0.508724
H -1.348250 4.858555 1.535467
C -1.225557 3.840106 -2.200746
H -0.782852 1.853686 -1.470020
C -1.499217 5.161264 -1.852280
H -1.762322 6.572440 -0.241559
H -1.179958 3.550339 -3.246562
H -1.672144 5.902201 -2.629216
C 2.400403 -0.530380 0.447687
C 2.131017 0.097212 1.664011
C 3.741698 -0.765084 0.131138
C 3.156449 0.498484 2.515856
H 1.097264 0.244380 1.954904
C 4.775774 -0.413747 0.994667
C 4.483318 0.237704 2.186308
H 2.908675 1.000722 3.446192
H 5.795603 -0.651990 0.714583
H 5.288746 0.530624 2.853367
N 4.177163 -1.369524 -1.151101
O 3.678810 -0.951394 -2.173198
O 5.069238 -2.201005 -1.088234

E (au) =-1784.231343
ZPVE (au) = 0.320204
solvated E (au) =-1784.31192

B97D

C 0.55625900 -2.96972700 -1.09528600
O 0.58574700 -3.91592200 -1.86097500

H	-0.39742500	-1.86675800	-1.25004100
O	-2.07704800	-2.56744300	0.25993200
C	-2.19938900	-1.44430200	-0.27005200
N	-1.25793500	-1.00467100	-1.17914500
N	-1.02392600	0.24923000	-1.65056700
S	-0.48493400	1.33538500	-0.43963800
O	-0.78226300	0.87071500	0.94620500
O	-0.85504600	2.70413000	-0.87680400
C	-3.43703700	-0.61201200	-0.00735100
C	-3.89431700	0.41887200	-0.85299600
C	-4.20639300	-0.95891200	1.12263100
C	-5.08943600	1.09300600	-0.56212200
H	-3.30142000	0.70305300	-1.72098500
C	-5.39318000	-0.27661900	1.41732900
H	-3.85152400	-1.77213700	1.75606000
C	-5.84072400	0.75417600	0.57444000
H	-5.42893200	1.89303000	-1.22487400
H	-5.97008800	-0.54850100	2.30564600
H	-6.76565400	1.29081300	0.80362400
C	1.43792500	-2.80062000	0.09569100
C	2.68595300	-3.46397300	0.14088800
C	1.11013700	-1.85245000	1.08621200
C	3.60007200	-3.16669500	1.15808800
H	2.92010800	-4.19196100	-0.63895400
C	2.02372900	-1.56918000	2.10889000
H	0.15372300	-1.33599200	1.04662100
C	3.27064300	-2.21661600	2.14316000
H	4.57056900	-3.67027400	1.18685400
H	1.76530400	-0.82343500	2.86309900
H	3.99042500	-1.97702000	2.93029400
C	1.38311100	1.29885100	-0.57455700
C	1.96265200	0.22836600	-1.27304600
C	2.24646900	2.29744900	-0.08479200
C	3.35143900	0.12107200	-1.42695300
H	1.30561700	-0.51966700	-1.71153300
C	3.63630800	2.23003700	-0.27355100
C	4.19364700	1.12439500	-0.92493900
H	3.76836200	-0.74627900	-1.94205300
H	4.25761100	3.04202800	0.10315200
H	5.27669300	1.05553500	-1.04645300
N	1.76349100	3.47781700	0.68291200
O	0.92420300	3.29337500	1.56313000
O	2.29277600	4.56940300	0.41741900

E (au) =-1784.25002
ZPVE (au) = 0.307963

ωB97XD

C	-0.14015800	2.36242500	1.23392700
O	-0.05103600	2.68549200	2.38834800
H	-0.65246000	1.11932300	0.80152700
O	-2.92771000	1.59526200	0.60134200
C	-2.56760500	0.42425000	0.44412600
N	-1.24095100	0.12979300	0.39611400
N	-0.71127800	-1.10160400	0.67173200
S	0.45279000	-1.49478600	-0.40326600
O	0.47781400	-0.63919800	-1.59308500
O	0.46902200	-2.94910000	-0.54979700
C	-3.61561400	-0.64733100	0.22369100
C	-3.36929800	-1.98399900	-0.10697200
C	-4.94201700	-0.21579500	0.34164500
C	-4.43351100	-2.86014500	-0.30994200

H	-2.35196300	-2.34257200	-0.19090500
C	-5.99997200	-1.09334800	0.14457900
H	-5.11342100	0.82670700	0.58632700
C	-5.74809100	-2.42378900	-0.18320900
H	-4.22491500	-3.89522300	-0.56644600
H	-7.02268300	-0.73840000	0.24592000
H	-6.57203100	-3.11613500	-0.33938500
C	0.20438300	3.22915500	0.07268400
C	0.47832200	4.58683400	0.26808300
C	0.27947000	2.66577900	-1.20201400
C	0.82158000	5.38390700	-0.81473500
H	0.41235600	4.99547700	1.27219700
C	0.63798300	3.46928100	-2.28171200
H	0.07679600	1.60607100	-1.34390600
C	0.90356600	4.82198100	-2.09023700
H	1.02782200	6.44117700	-0.67027000
H	0.70976300	3.03166500	-3.27277400
H	1.17777100	5.44570200	-2.93750300
C	2.00522800	-1.13040200	0.49870800
C	1.92748800	-0.31852000	1.62847800
C	3.25915800	-1.64959200	0.17186500
C	3.05881600	0.00864200	2.36806800
H	0.95296200	0.03304300	1.94601800
C	4.39298100	-1.36743800	0.92531800
C	4.29790100	-0.51509100	2.01690500
H	2.95929400	0.66471400	3.22730100
H	5.33591500	-1.82024300	0.64203700
H	5.18615000	-0.27542200	2.59346100
N	3.48530000	-2.52489400	-0.99029400
O	2.95995700	-2.23081700	-2.04459000
O	4.24931100	-3.46953900	-0.82468800

E (au) =-1784.660903
ZPVE (au) = 0.322946